Recent Glacier Fluctuations In
Grand Teton National Park, Wyoming

Executive Summary : Recent Glacier Fluctuations In Grand Teton National Park, Wyoming

Author : Hazel A. Reynolds

Date : March 16, 2012

Abstract : This executive summary identifies major findings of a Master of Science thesis concerning recent glacier fluctuations in Grand Teton National Park, Wyoming, for the use of park resource managers and other personnel.

Keywords : summary, glacier fluctuations, Grand Teton National Park, thesis

Executive Summary : Recent Glacier Fluctuations In Grand Teton National Park, Wyoming

Reference: Reynolds, H.A., 2011, Recent Glacier Fluctuations In Grand Teton National Park, Wyoming, MS Thesis, Idaho State University, 225 p.

Overview

This MS thesis is a scientific document that reports the recent status of the modern glaciers within Grand Teton National Park. Unlike previous reports concerning these glaciers, this thesis studied more glaciers (seven) within the Park and incorporated more glacier observations (nine to eleven) from aerial and satellite imagery acquired between 1956 and 2010.

Problem

Previous reports concerning modern glaciers within the Teton Range studied a select few glaciers over varying time periods, using only a small number of glacier observations. With anticipated changes in climate conditions, weather patterns will also change, which will affect these glaciers. Conclusions from previous studies do not present either a time-detailed record of glacier area change or a determination of changes in temperature or precipitation that are the dominant cause of changes in glacier area. If a dominant weather parameter (temperature or precipitation) is identified with a specific glacier response (growth or shrinkage), then future resource management can be planned and implemented in anticipation of the identified dominant weather parameter changes.

Results

This thesis yielded three major findings:

1) Teton Glaciers experienced overall retreat from 1956-2010, which agrees with previous studies (Edmunds, 2010), but this trend of retreat has been punctuated by subdecadal-scale glacial ice growth and retreat.
   a) A dominant period of glacier growth occurred from 1975-1985.
   b) During 2006-2009, four of six glaciers (Schoolroom, Skillet, Falling Ice, and West Triple glaciers) grew in area while two of six glaciers (East and Middle Triple glaciers) shrank in area.
2) Spring precipitation appears to be the dominant influence on glacier area.
   a) Spring precipitation exhibits the best correlation with glacier area change at four of six glaciers (Schoolroom, Skillet, Falling Ice, and West Triple glaciers)

   b) Winter temperature exhibits the best correlation with glacier area change at East Triple Glacier and spring precipitation exhibits only a slightly weaker correlation.
   c) Fall temperature has the strongest correlation with glacier area change at Middle Triple Glacier.
3) Petersen Glacier, of the seven studied glaciers, exhibits little or no exposed ice. It is currently a debris-covered glacier, in which ice may persist but will likely diminish in volume and function.

Implications

Spring precipitation potentially affects glaciers a) by decreasing the length of the melting season; b) by adding snow to the glacier surface, which allows snowpack to persist into the summer, and/or c) by increasing cloud cover, thereby blocking sunlight and reducing melt rates. During dry spring seasons, the opposite is true, causing glacier retreat. The key to this effect is if the temperature is cool enough to create snow instead of rain.

Potential Points of Controversy

This thesis contains a number of potential points of controversy.

1) Weather records at glacier elevations are very limited. This study compared ice area changes to meteorological factors derived from the Parameter-elevation Regressions on Independent Slopes Model (PRISM). This model is dependent upon low-elevation, valley-based weather stations, and produces output at a course spatial scale (4 km^2) on a finer temporal resolution (monthly) than the glacial observations. Weather records from stations within the Teton Range at the elevations of the glaciers are of short duration (mainly summer and covering few years) and at a much finer temporal resolution (5 – 60 minutes).
2) The study utilized partial least squares regression analysis to determine statistical relationships between ice area change and meteorological fluctuations. Glacier area was compared to weather conditions over the preceding four water years to better represent likely glacier response time. An argument can be made that other values of time (three, five, ten years, etc.) of preceding water years could have been used.
3) The study reveals that the glaciers have, in specific time periods, grown in area during a period of generally rising average temperatures. These short periods of growth must be considered in the context of overall retreat since 1956 and in the context of the specific meteorological factors influencing growth and shrinkage. As noted, spring precipitation, rather than summer or average temperature, appears to be a dominant influence on glacier area change.

Recommendations

1) Continue to study these small mountain glaciers.
   a) The content of the second chapter of this thesis will be submitted to a peer reviewed journal.
   b) Collect snow, ice, stream, and weather data at or near these glaciers.
      i) Direct measurement of snow and glacier accumulation and melt.
      ii) Monitor glacier areas annually from air flights or Global Positioning System mapping.
      iii) Install and maintain stream gauges.
      iv) Install and maintain continuous, all season, high elevation weather stations.
   c) Researchers and other personnel within the Park, as well as cooperative researchers from outside the Park, should aide and facilitate the work outlined above.

For more information

Reynolds, H.A., 2011, Recent glacier fluctuations in Grand Teton National Park, Wyoming [M.S. Thesis]: Pocatello, Idaho State University, 225 p. (can be downloaded from http://geology.isu.edu/dml/thesis_index.htm)

Recent Glacier Fluctuations In Grand Teton National Park, Wyoming

by Hazel Arlette Reynolds

A thesis submitted in partial fulfillment
of the requirements for the degree of

Master of Science in
Geology

Department of Geosciences
Idaho State University
Pocatello, ID

September 2011

In presenting this thesis in partial fulfillment of the requirements for an advanced degree at Idaho State University, I agree that the Library shall make it freely available for inspection. I further state that my permission for extensive copying of my thesis for scholarly purposes may be granted by the Dean of the Graduate School, Dean of Science and Engineering, or by the University Librarian. It is understood that any copying or publication of this thesis for financial gain shall not be allowed without my written permission.

Signature ___________________________________

Date _______________________________________

To the Graduate Faculty:

The members of the committee appointed to examine the thesis of Hazel Arlette Reynolds find it satisfactory and recommend that it be accepted.

Glenn D. Thackray,
Principal Advisor

Benjamin T. Crosby,
Second Advisor

DeWayne Derryberry,
Graduate Faculty Representative

Acknowledgements

I wish to thank the following sources of funding: the National Science Foundation Idaho Experimental Program to Stimulate Competitive Research (EPSCoR) grant concerning the theme of Water Resources in a Changing Climate (grant #0814387); the Idaho State University Graduate Student Research and Scholarship Committee; the Idaho State University Department of Geosciences; and the J. David Love Field Geology Fellowship from the Wyoming Geological Association Scholarship Committee.

I also wish to thank the following for assistance with my thesis: Grand Teton National Park; Idaho State University Department of Geosciences; and many of the individuals that also helped such as Emily Baker, Emily Charaska, Craig Towery, Glenn Thackray, Ben Crosby, DeWayne Derryberry, Diana Boyack, Joe Wheaton, Colden Baxter, Mitch Plummer, Kathy Mellander, Sue O'Ney, Sue Consolo-Murphy, Jenni Corbin, Jake Edmunds, Ann Rowan, Katy Holm, Pat Calhoun, Nathan Hobbs, Kelly Whitehead, Kelsey Lanan, Mark Shapley, Chris Tennant, fellow graduate students, friends, and family.

Table of Contents

List of Figures

Chapter II

Chapter III

List of Tables

Chapter II

Chapter III

Abstract

Six glaciers in the Teton Range, Wyoming decreased in ice area from 1956-2010, with episodes of subdecadal-scale ice growth interrupting that trend. Periods of glacier growth include ca. 1974-1983 and 2006-2009. We compared ice area fluctuations to meteorological factors derived from the Parameter-elevation Regressions on Independent Slopes Model (PRISM). We used partial least squares regression analysis to determine statistical relationships between ice area change and meteorological fluctuations. Weather records were summarized as either seasons of water years or full water years (WY) and compared, in consecutive years, to ice area changes. We determined that spring precipitation and average annual temperature, averaged over four years, show the strongest correlation to glacier area change. Spring precipitation can affect growing glaciers by shortening the ablation season, adding mass, and providing clouds that reduce sun radiation and melting on the glacier surface. The opposite is true during dry springs, which correlate with smaller glacier area. The effect of spring precipitation on glacier area is dictated by the temperature of the precipitation at the glacier. We also found that the Teton glacier fluctuations do not clearly correspond with the El Niño-Southern Oscillation index.

We applied a two-dimensional numerical energy mass balance model to six of these glaciers. We conducted four tests with ten climate input files derived from PRISM and from weather station data, covering five time periods ranging in length from 1-54 water years. Using PRISM data output, the model failed to produce positive mass balance at the glaciers within observed weather conditions (WY 1956-2010). Using mean climatic variables from weather stations in the Teton Range (WY 1956-2010), the model also did

not produce positive modeled mass balance. Climate data from the weather stations during short periods with lower temperatures and higher precipitation produced positive modeled mass balance at Falling Ice, Middle Triple, and West Triple glaciers. Of these short periods, only modeled mass balance in 1982-1985 at the Mt. Moran glacier complex agreed with glacier area observations. We suggest the model overestimates melt at these glaciers, possibly influenced by model inputs that incorporate too much low-elevation weather station data. More data from high elevation stations will create a better understanding of energy mass balance at these glaciers.

Chapter I: Introduction

Introduction

The small glaciers of Grand Teton National Park, Wyoming (GTNP) occupy high elevation, east- and north-facing cirques in a semi-arid climate in the mid-latitudes. The setting of these glaciers makes them very sensitive to weather fluctuations (Arendt et al., 2002). Area fluctuation of glaciers in GTNP can be indicators not only of regional climate change, but also of the broader impacts of climate change on the region. Evaluating the historic behavior of these glaciers complements historical weather measurements by providing regionally specific data on landscape responses (Hall and Fagre, 2003).

Background and Importance

Mountain glaciers are important indicators of regional and global climate change (Barry, 2006), and glaciers in the GTNP are prime examples. Currently, at least ten named remote glaciers occupy the high alpine regions of the Teton Range. Remote glaciers tend to receive less attention than easily accessible glaciers, even though they may be more affected by climate fluctuations (Arendt et al., 2002). The glaciers in GTNP may be very sensitive to climate warming and/or drought due to their small size and their continental alpine environment. Long-term climate records are stored in glaciers by preservation of seasonal snowpack, which melts annually on non-glacier surfaces but is retained in glaciers as ice strata (Elder et al., 1994). Glaciers of GTNP can thus be indicators not only of global change in climate, but also of the regional impacts of climate change.

Glaciers affect the regions they occupy by storing large amounts of fresh water

(Fountain and Tangborn, 1985). Snowpack and glaciers are recognized as important agents in maintenance of summer streamflow across the western U.S. For example, the reduction of snowpack in the Sierra Nevada is projected to have extreme consequences for agricultural water storage and hydropower generation capacity in California, with projected streamflow declines of 25-30% (Cayan et al., 2006). A western U.S. coastal mountain study projects 70% annual snowpack reduction if the average regional temperature warms by 1 to 2.5˚C within 50 years (Leung et al., 2004).

Glacier ice can also be an important storage reservoir for water in western U.S. river systems, and can buffer river flows from extreme climatic shifts. For example, in the North Cascades, Washington, the largest proportions of glacier meltwater in late summer streamflow occur during warm and dry years and the smallest proportions occur during wet and cool years (Medley, 2008). Any loss in glacier area could lead to an increase in runoff variability because valuable freshwater storage would be unavailable in warm, dry years. Glacier area change is a time-delayed climate signal, as mountain glaciers respond to climate fluctuations on time scales from years to decades (Barry, 2006). These changes can be monitored over large areas and are very useful for regional scale studies (Medley, 2008).

For the Snake River, which drains the Teton Range on both the east and west sides, reductions in snow and ice storage are likely due to climate fluctuations. Jackson Lake, an agricultural water storage reservoir in GTNP, is primarily supplied by snowmelt and glacial meltwater. This reservoir is the first of several along the Snake River (Elder et al., 1994). These water containments are important for the water supply for local agriculture, human consumption, aquatic ecology, hydroelectric dams, and regulating the flow of the

Snake River to cushion the effects of floods and droughts.

The mass balance of glaciers also influences the mean sea level on a local or worldwide scale. The influence depends on the size of the glacier, but 9% of current global sea level change is caused by melting of mountain ice masses in Patagonia (Rignot et al., 2003). When a glacier grows, it retains fresh water (Fountain and Tangborn, 1985). When the glacier shrinks, it allows the stored water to return to the sea, reducing the amount of water in ice storage and adding more water to the ocean system. While the Teton glaciers are very small and will affect sea level only minimally if they melt completely, the lessons learned from these glaciers can be applied to other mountain glaciers in similar climatic and topographic settings.

As noted, this study documents glacier area change over a 60-year period and identifies the most likely meteorological variables responsible for that change. While this study does not directly address the volumes of glacier meltwater or their influence on overall streamflow, these findings may ultimately be applied to understanding those hydrologic influences. Documentation of glacier change is a first step in an overall analysis of hydrologic change attributable to climate fluctuations.

High elevation temperatures and precipitation

Mountains cause orographic uplift as they are physical barriers that force air parcels to move vertically (Dodson and Marks, 1997). Where the atmosphere is well mixed (e.g., summer days in inland areas), temperature often shows a strong and predictable decrease with elevation in the troposphere (Daly, 2006; Minder et al., 2010). Conversely, winter temperatures, and daily minimum temperatures in all seasons, have a more complex relationship with elevation (Daly, 2006; Minder et al., 2010). Without solar heating or significant winds to mix the atmosphere, temperatures stratify quickly, and cool, dense air drains into local valleys and depressions to create cold air pools that can be hundreds of meters thick. This process forms temperature inversions, in which temperature increases sharply, rather than decreasing, with elevation (Daly, 2006).

Precipitation has a spatially variable and complex relationship with elevation, but precipitation tends to increase with elevation due to orographic uplift and cooling of moisture-laden winds by terrain barriers (Daly, 2006; Hughes, 2008). However, when the terrain rises above the height of a moist boundary layer or trade wind inversion, lower slopes will have increased precipitation with elevation and upper slopes will have rapid drying as well as decreased precipitation with elevation. In these circumstances the elevation and location of maximum precipitation is variable, and depends on the depth of the moist boundary layer, wind speed and direction, terrain profile, and other factors (Leonard, 1989; Daly, 2006). Orographic processes amplify precipitation on windward slopes, and can sharply decrease it on leeward slopes downwind, causing the rain shadow effect common to many mountain ranges worldwide, and the effect is especially noticeable near major bodies of water (Daly, 2006). Thus, the relationships between temperature and elevation as well as precipitation and elevation can both vary spatially and temporally. However, temperature is generally easier to predict than precipitation at a given elevation or location.

Mass balance models

Glacial mass balance is often modeled because observational mass balance measurement programs, based on direct field measurement of accumulation and ablation, are too costly and difficult to maintain for the >160,000 glaciers on Earth (Arendt et al., 2002). Mass balance models are used to quantify and illustrate processes of glacier mass transport. Results of these models can be used to hindcast or forecast the status of a glacier, such as whether a glacier has or will actively advance or retreat.

Some glacial mass balance models that can be applied to terrestrial temperate alpine glaciers are highly simplified, while others are very complex and require many inputs and feedback loops. All models require input data (see below) to process through the model and produce mass balance outputs. The quality of the input data determines the quality of the results. Input data can vary from purely theoretical data to meticulously collected field data.

Input data collected in the field include meteorological data, such as air temperature, precipitation, air pressure, surface radiation budget (or net solar radiation), wind speed and direction, snow cover, snow depth, albedo, and water vapor (GCOS, 2003). Rates or quantities of ablation, snow density, snow water equivalent (SWE), bedrock abrasion, and river discharge may also be collected and/or calculated. The glacier geometry can be mapped and/or calculated as well. The glacier geometry includes a longitudinal profile of the bedrock surface and/or the ice surface, elevations of various points and features on and around the glacier such as moraine crests, and an ice surface survey once a year close to the start of the new water year to determine the ice elevation, thickness, and area. DEMs are commonly used with the advent of related computer analysis software. Thicknesses of accumulated snow layers can be obtained from snow pits. Basal shear can be calculated from components measured in the field (e.g., ice thickness). Few, if any, models require data for all of these variables.

There are two time systems of glacier measurement: the stratigraphic and the fixed-date systems. The stratigraphic system uses an observable summer glacier surface that is assumed to be formed at the time of minimum mass. A snow pit or ice core is used to study the subsurface in this system (ICSI, 1969). The summer surface can be identified by a number of criteria including a horizon of concentrated debris particles, a discontinuity between ice below and very young snow above, or isotopic evidence.

The alternative fixed-date system uses measurements that are taken at certain specific days or as close as possible to those dates. Winter and summer seasons are not defined under this system as these measurements are not necessarily related to any observable features in snow, firn, or ice (ICSI, 1969). Measurements taken at the end of the water year, or as close as possible to October 1 in the Northern Hemisphere, fall under the fixed-date system. These two systems cannot be combined in the same model without introducing errors (ICSI, 1969). The fixed-date system is often used due to field logistics.

Mass balance models can be categorized into numerical and physical models. Numerical models include data gathered from the field or calculated theoretical values and can quantify physical models for better analysis. Numerical models may be run through a computer program or software such as MATLAB (Matrix Laboratory), Excel (a Microsoft spreadsheet software) (Alexander, 2009), or ArcView (ESRI, Inc. software for models and Geographic Information Systems) (Plummer and Phillips, 2003; Plummer and Cecil, 2005). Physical models include glaciological models (Pelto, 2008), hydrological models (Fountain et al., 1997; Gray et al., 1999), topographical models such as survey comparisons (Gray et al., 1999; Sauber et al., 2005), and archival photo comparison (Chinn, 1999).

Numerical mass balance models in one, two, or three dimensions provide another means of testing hypotheses regarding mass balance (Alexander, 2009). Hubbard (1997) used a one-dimensional flowline model at two paleoglaciers in the Chilean Lake District. Hubbard determined that Puyehue Glacier had a response time of 1000 years after climatic fluctuations that occurred on a time-scale of 500-1000 years and Rupanco Glacier had a 2000 year response time. Plummer and Phillips (2003) and Plummer and Cecil (2005) used a two-dimensional numerical model to determine the balance and extent of paleoglaciers in Bishop Creek of the Sierra Nevada and modern the Teton Glacier, respectively. These two studies also used two-dimensional flow models that portrayed the accumulation and flow of ice in response to given patterns of accumulation and ablation (Plummer and Phillips, 2003). Gudmundsson (1999) developed a three-dimensional numerical model for the confluence area of Unteraargletscher, Bernese Alps, Switzerland. Gudmundsson determined a good overall agreement between measured and calculated 1) surface velocities and 2) vertical strain-rate variation with depth. The ice was about three times more rigid in the model than predicted from standard estimates of rheological parameters for glacier ice. The model helped to determine that differential ablation was more responsible than flow mechanics for forming an ice-cored medial moraine at the confluence area of Unteraargletscher.

Physical models such as glaciological models are considered to be a direct method of determining mass balance (Barry, 2006). The direct method involves repeated measurements at snow pits or ablation stakes on the glacier surface to ascertain the annual mass balance. The annual balance is calculated for the fixed dates of the annual water year. In the Northern Hemisphere, the water year begins on 1 October. The net balance is the minimum mass at the end of each summer. When surveying, the direct survey method is referenced to the previous balance year's summer surface (Barry, 2006). Fountain and Vecchia (1999) found that the number of mass balance measurements needed to determine the glacier balance appears to be scale invariant for small alpine glaciers (<10 km^2), and five to ten ablation stakes are sufficient. This allows the opportunity for more small glaciers to be accurately monitored.

The hydrological model is similar to the glaciological method in that they are both direct measurement methods. The hydrologic model uses precipitation as accumulation and runoff as ablation over the entire drainage basin (Fountain et al., 1997), but storage of water or ice is not measured directly. Results from hydrological models often do not correlate with results from other balance models (Fountain et al., 1997; Gray et al., 1999) and may be incorporated into other models (Kaser et al., 2002). Hydrological models can be measured by snow stakes, snow pillows, rain gauges, and stream gauges (Gray et al., 1999). Meier (1984) stated that hydrometeorological models are effective. Pelto (2008) used a simple statistical model developed from a sequence of measured balances combined with records at meteorological and hydrological stations. In hydro-meteorological models, glacier accumulation is approximated by winter precipitation and glacier ablation is approximated by summer air temperatures (Meier, 1984; Pelto, 2008). The annual balance is the difference between accumulation and ablation.

The topographical model is an indirect method to find mass balance. The fundamental premise is maintained that the glacier mass balance is determined by differences in topography over time. A topographical model involves geodetic survey methods that use nearby bedrock as a fixed reference surface and measures the glacier surface from boreholes in the glacier (Barry, 2006). Another example of an indirect method is the combination of a DEM and photogrammetric data with ice flow modeling to determine mass balance of a glacier (Barry, 2006). Sauber et al. (2005) used another topographical method as they determined surface ice elevation differences between a DEM and from Ice, Cloud, and land Elevation Satellite-derived elevations. Another example of an indirect method is a comparison of multiple oblique or corrected aerial photos of glaciers acquired at the end of every water year to assess glacier area change (Chinn, 1999). These topographical and indirect models are applied to more and different types of imagery data as technology advances.

Previous mass balance studies

The mass balance of a glacier is the relationship between ice accumulation, storage, and melting ice, and indicates whether a glacier should be expanding or contracting and whether those trends will persist (Sugden and John, 1976). Several studies (e.g., Bitz and Battisti, 1999; Nesje, 2005; Chueca et al., 2007; Hughes, 2008) have found that a combination of temperature and precipitation dominate glacier mass balance processes in contrasting proportions in mountain ranges of contrasting climatic regimes. In a study of glacier ice cores collected globally, Thompson et al. (2005) suggested the primary control driving the current large-scale glacier retreat is most likely the increase in the Earth's globally averaged air temperature. In a broad study of six glaciers world-wide, using a proposed seasonal sensitivity characteristic, Oerlemans and Reichert (2000) determined that summer temperatures dominate mass balance of glaciers in dry climates (~250 mm/yr) as the effect of temperature anomalies is limited to summer months and nearly all precipitation falls as snow. They also determined that spring and fall temperatures strongly affect glaciers in wetter climates. After looking for a relationship between annual temperature and precipitation, Oerlemans and Reichert (2000) acknowledged that wetter climates tend to have a smaller temperature range and concluded that as the climatic setting of a glacier increases in aridity, the sensitivity to temperature change is increasingly restricted to the summer months. The results of Oerlemans and Reichert (2000) are interesting in the context the present study, which determines that spring precipitation is a dominant influence on mass balance of glaciers in the semi-arid Teton Range.

It is unclear whether temperature or precipitation dominates mass balance in maritime glaciers. Alexander (2009) found that the maritime hyper-humid Franz Josef Glacier in the Southern Alps of New Zealand is sensitive to small temperature changes. Unfortunately, Alexander did not study the effects of precipitation domination on the glacier due to differences in precipitation curves in previous studies of the glacier. Oerlemans and Reichert (2000) determined the Franz Josef Glacier (~6000 mm/yr) experiences a reduced balance after an increase in winter temperature due to higher melt rates in the ablation area and a reduced proportion of snow in the accumulation area. Thus Oerlemans and Reichert (2000) strongly suggest that investigators look for correlations beyond the pairing of specific balance and summer temperature. In Northern Europe, Nesje (2005) could not discern if one climate factor dominated maritime glacier fluctuations in western Norway. Rather, he concluded that glacier variations not only are a response to ablation-season (summer) temperature, but are also highly dependent on accumulation-season (winter) precipitation.

Mass balance of maritime and continental glaciers in the Pacific Northwest of North America is dominated by either temperature or precipitation depending on geographic location. Bitz and Battisti (1999) examined the mass balance of maritime glaciers in northern Washington and British Columbia using published mass balance data with the stratigraphic system and fixed year system (1985-1995) as well as nearby weather station data anomalies (1959-1995). Bitz and Battisti (1999) determined these glaciers correlated positively with local precipitation anomalies and correlated negatively with local temperature anomalies. Medley (2008) used a precipitation temperature area-altitude balance model comparing modern glacier hypsometry to historic weather records (1935-2006) for selected glaciers in the southern Cascade Range of the Pacific Northwest. With sensitivity analysis, Medley determined that temperature changes have a stronger influence on glaciers than do changes in precipitation. Medley also pointed out that glaciers occupying peaks with lower elevations, such as in the North Cascades, are at higher risk of extinction than glaciers on higher peaks which may retreat to higher elevations. Hintereisferner (Austria) and Peyto Glacier (Canadian Rockies) are in moderately wet climates and Oerlemans and Reichert (2000) found that increased summer precipitation significantly contributed to the annual glacier balance with their proposed seasonal sensitivity characteristic. The accumulation areas of these glaciers cover a larger altitudinal range (Oerlemans and Reichert, 2000), allowing more precipitation to fall as snow at the highest elevations leading to an increased balance.

Small glaciers on massifs in Europe are sensitive to changes in both temperature and precipitation. A study by Chueca et al. (2007), mapped glacial margins from air photos and GPS measurements and compared digital elevation models (DEMs) to quantify observed extent and volume loss from 1981-2005 of cirque glaciers of Maladeta massif in the Spanish Pyrenees. These glaciers recently experienced both increased maximum temperatures and reduced snowfall (Chueca et al., 2007). Hughes (2008) studied the Debeli Namet cirque glacier on the Durmitor massif in Montenegro. He found that the small cirque glacier experienced rapid growth and decay within five years. An advance occurred due to much cooler summer temperatures and much higher winter precipitation. Retreats occurred during two of the warmest summers on record.

Small glaciers in the Rocky Mountains are dominated by both temperature and precipitation. Hoffman et al. (2007) studied glaciers in the northern Front Range of Colorado with historic air photos and maps as well as weather data from stations nearby. Hoffman found that both summer temperature and spring snowfall are good predictors of the Andrews Glacier mass balance. Hoffman also noted that these small glaciers are affected by avalanching and windblown snow accumulations in winter months. Edmunds (2010) attempted to identify a dominant climatic factor (temperature or April 1 snow water equivalent) for glacial area and volume loss in the Teton Range, with no satisfactory correlation.

In summary, changes in annual temperatures or precipitation vary in importance to glacier mass balance depending on the climatic setting, geographic setting, and size of the glacier. Seasonal changes in temperature and precipitation also affect glaciers depending on the glacier setting and character.

Glacier studies in the Teton Range

Surprisingly, most glaciers in GTNP have not been studied thoroughly. Fryxell (1935) reported that glaciers were first identified in the Teton Range during the summer of 1878, in the last season of the Hayden Survey. Fryxell (1935) also included a map with names and locations of seven glaciers (Falling Ice, Middle Teton, Skillet, Teton, and

Triple Glaciers). Decades later, the United States Geological Survey (USGS, 1968a & b) mapped three additional glaciers (Petersen, Schoolroom, and Teepe Glaciers).

Several studies measuring and monitoring mass balance of the Teton Glacier have been published within the last half-century. Reed (1967) and Elder et al. (1994) documented aspects of mass balance of the Teton Glacier from 1963 to 1966 and in 1993 respectively. Elder et al. (1994), measured winter mass balance on the Teton Glacier in mid-May 1993. The study's water year was considered just below normal for snow accumulation based on long-term measurements from stations in the region. Elder et al. (1994) dug snow pits on the glacier to determine snow density, snow temperature, and stratigraphy to develop an estimate of snow density as a function of snow depth. Snow depths were recorded with aluminum probes roughly 10 meters apart along four lateral transects and one longitudinal transect. After Elder et al. (1994) registered a DEM; they used a statistical binary regression tree method using elevation and an avalanche index as independent variables to determine the SWE over the Teton Glacier. Their study provided a mean SWE of 3.22 m. This SWE value is 2.7 times higher than the expected areal average Elder compared to Martner's (1986) Wyoming Climate Atlas. Elder et al., (1994) attribute the higher SWE value to a higher rate of orographic precipitation, leeward deposition of suspended snow by wind, and avalanches falling onto the glacier from adjacent slopes. This glacier is also protected from direct solar radiation by high, steep cirque walls. This study was one of the first to attempt a computational model for the complex setting of the Teton Glacier.

Gray et al. (1999) conducted a topographical study of the Teton Glacier with three datasets between the years of 1954 and 1994. Gray et al. (1999) used a map developed by

Reed (1964) who used aerial photos flown over the Teton Glacier in 1954 in conjunction with a plane table survey of the lower part of the glacier in 1963. Another topographical survey of the glacier was produced in 1994 by Elder, Greenwood, and others with an electronic total station and global positioning system. The 1994 survey used the same three control points from the 1963 survey. Gray et al. (1999) showed an average rate of loss of volume at 26,000 m^3/yr, or an average of -10 cm/yr depth loss, for the Teton Glacier. Although another modern surface survey is needed in order to compare rates of loss of mass since 1994, this study added another dataset towards understanding the balance characteristics of the Teton Glacier.

Adding to the list of studies on the Teton Glacier, Edmunds (2010) quantified the changes in glacial area and volume of the Teton, Middle Teton, and Teepe Glaciers from 1967 to 2006 and their effects on water resources in Wyoming. Edmunds (2010) used historic air photos and weather records from nearby stations. Edmunds determined that the Teton Glacier area decreased by 17%, Middle Teton Glacier decreased by 25%, and Teepe Glacier decreased by 60% from 1967 to 2006. With photogrammetry, Edmunds determined the volume of ice lost from 1967-2002 on Teton Glacier was 1.29 million m^3 for a rate of 36,900 ± 5,100 m^3/yr, Middle Teton Glacier lost 1.34 million m^3 of ice for a rate of 38,300 ± 5,700 m^3/yr, and Teepe Glacier lost 0.57 million m^3 of ice for a rate of 16,300 ± 2,300 m^3/yr. Edmunds (2010) found a much higher rate of ice loss at Teton Glacier than Gray et al. (1999).

Edmunds (2010) also determined ice loss on the Grand Teton contributed minimally to the Snake River. Edmunds came to this conclusion after comparing 1967-2002 Snake River streamflow data (just downstream of the Jackson Lake Dam) to the total estimated volume of glacier ice lost (3.2 million m^3) (assuming all ten named glaciers lost volume at the same rate as those on the east side of Grand Teton) over the same period of time. Edmunds also assumed all the volume lost flowed directly into the Snake River only during summer months of July August, and September. However, the flow of this stream gage has been regulated by the Jackson Lake Dam since 1906 (USGS, 2011) calling Edmunds' conclusions of glacier contributions into question.

Plummer and Cecil (2005) applied a numerical glacial mass balance model to predict future conditions of the Teton Glacier. Plummer and Cecil (2005) used historical photos of Teton Glacier and recent climate records from early 1900s to the present to calibrate their model. They used the Teton Glacier to develop the model and found that glacier size and aspect affected responses to temperature fluctuations and thus suggested that modern retreats may not directly reflect modern warming.

Other investigators also conducted studies in the Teton Range either directly or indirectly concerning these glaciers. With a goal of quantifying ice and snow in large regions, Krimmel (2002) determined the Teton Range contains 1.7 km^2 area of glacial ice. Fountain et al. (2006) determined the same mountain range has ~7 km^2 cumulative ice and snow. Edmund Williams and Mark Lovell (Brigham Young University-Idaho) conducted informal monitoring studies on student field trips spanning at least 20 years. Their unpublished results focus mainly on the Teton Glacier, but also include the Schoolroom Glacier. A recent study (Corbin, in progress) collected detailed data from a weather station installed near Petersen Glacier in the spring of 2006. Little detailed work has been done outside these time periods or on other glaciers in the range.

Study Area

This study looks at ice area changes of the Petersen, Schoolroom, Falling Ice, Skillet, and East Triple, Middle Triple, and West Triple glaciers in Grand Teton National Park, Wyoming. These glaciers are a subset of ten named glaciers in the Teton Range. The seven glaciers were studied via remote sensing techniques, and a limited number were studied in the field, dependent upon access and glacier character. These glaciers occupy high elevation (2865-3585 m) areas in semi-arid conditions (< 2000 mm annual precipitation) in the mid-latitude (43°40'-44°N) northern intermountain region of the Rocky Mountains.

The Teton Range is strongly affected by moisture-laden storms from the west. Storm systems from the Pacific Ocean funnel eastward to the end of the Snake River Plain. There they encounter the Teton Range, which is oriented NNE-SSW and is approximately 70 km long by 20 km wide. This is the first major orographic barrier for the moist Pacific westerlies (Meyer et al., 2004; Love et al., 2007). This orographic pattern leaves mountain ranges to the north and south of the Eastern Snake River Plain dry (mean annual precipitation 500-1300 mm) relative to the wetter (mean annual precipitation 1500-2000 mm) Teton Range and Yellowstone Highlands. Strong orographic effects within the Teton Range cause strongly contrasting climate niches in close proximity to one another.

Lithologically, the Teton Range is composed of a Precambrian crystalline basement of granites, pegmatites, and gneisses mainly exposed in the east, overlain unconformably by Paleozoic-Mesozoic sedimentary units and Neogene tuffs (Love et al., 2007; Foster et al., 2010). The Teton Range is in the northeastern Basin and Range Province. The two highest peaks (Grand Teton (4197 m) and Mt. Moran (3842 m)) are located on the eastern footwall of the east-dipping, normal Teton Fault bounding Jackson Hole basin and the Teton block. The peak of Grand Teton is approximately 2400 m above the floor of Jackson Hole. Since the initiation of displacement along the Teton Fault, (controversially argued to be between 13-5 Ma to 3-2 Ma (Hampel et al., 2007)) the watershed divide has migrated from a position adjacent to the range fault in the east to a position nearly 8 km westward. This westward migration was aided not only by tectonic uplift, but also by numerous glaciations. Dramatic U-shaped canyons carved between steep peaks with high relief (2065-4197 m) are landforms from the last two major glaciations. These canyons open to the east-facing range front. Much of the older Bull Lake (~160-130 ka) deposits remain exposed in the southern half of Jackson Hole whereas they were overridden by the younger Pinedale (~30-12 ka) in the northern half (Love et al., 2007). Large Bull Lake and Pinedale moraines capture modern runoff from the canyons, creating a number of lakes where the valley glaciers spilled into Jackson Hole. Glaciers persist in the Teton Range due to wet westerly winds, orography, aspect, and shading provided by steep, high peaks.

Focus of Current Study

This thesis determines the current status of the small alpine glaciers in the Teton Range by quantifying the areal extent of seven glaciers as named on USGS maps (USGS, 1968a & b) in GTNP over the past fifty years. Two questions are addressed, 1) whether these features are still glaciers or have degraded to snowfields or debris-covered glaciers and 2) whether temperature, precipitation, or an integration of both drive the areal changes in these glaciers. Consequently, this thesis uses a) statistical analysis of glacier area change and weather fluctuations and b) numerical mass balance modeling to determine the climatic causes of glacier area change if current global and regional climatic trends persist. Expected results are a net loss in mass balance due to climatic warming and/or drying.

This study focuses on temperature and precipitation variability. It deemphasizes relative humidity and aspects of wind for a number of reasons. Most importantly, other studies have found the highest correlations between change in mass balance and temperature and/or precipitation (Leonard, 1989; Meyer et al., 2004; Reynolds, 2006; Foster et al., 2010). Further, humidity and wind data are not available from many of the weather stations within the study area.

A number of climate variables affect the Teton Glaciers. We briefly introduce and discuss these variables. In colder non-winter months, cooler temperatures allow more accumulation than ablation to occur. In the winter, warmer temperatures associated with storms could provide heavier, water-rich snow. Cool spring temperatures can shorten the ablation season. Usually, warm summer temperatures are the primary control of the ablation season, dominating the cause of glacier ice loss.

Annual precipitation, mainly snow accumulation, is the primary control of glacier ice growth. Spring precipitation, especially when it falls as snow, can lengthen the glacial accumulation season and thus shorten the ablation season. As mentioned above, orographic precipitation can contribute larger amounts of snow to these glaciers. Higher precipitation is often accompanied by more storminess, and thus more clouds can provide both shade from direct sun (shortwave) radiation and retain reflected longwave radiation (Rupper and Roe, 2008). The former situation would retard ablation and the latter would not. Records of air pressure would help to constrain this factor.

Wind can contribute snow that was originally deposited upwind of the glacier. Wind can also enhance ablation through sublimation. High relative humidity can indicate that precipitation is deposited (as either snow leading to accumulation or liquid leading to ablation). Low relative humidity paired with high winds can lead to ablation. Aspect and shading can also affect the area changes of glaciers by controlling the amount of direct sun radiation daily and seasonally. Avalanches from steep slopes above or adjacent to the glacier will also contribute additional snow, ice, and debris.

Results of mass balance model tests can lead to an informed prediction of the future of glaciers within GTNP and can help the park plan for the future in respects of planning for water use, backcountry and rock climbing permits, and trail management within the Teton Range. Changes in these glaciers also affect safety hazards for park visitors and wildlife at the margins of the glaciers and within their glaciated basins. Hazards include rock avalanches, moraine dam failures (Moore et al., 2009), unstable and water-saturated slopes as meltwater infiltrates the ground, and flashier streamflow as snow and ice storage buffers are reduced in the headwaters. Additionally, this study will enhance the research of the changing ecology of basins occupied by glaciers. Finally, this study of Teton glaciers will impact future studies on the quality of nearby ecosystems, wildlife habitat, park visitor experience, and irrigators who rely upon the Snake River near the park and downstream.

Chapters II-IV

Chapter II of this thesis discusses changes in ice-covered areas within the Teton Range documented with archived aerial photos dating as early as 1956. These documented changes are compared to modeled weather records from weather stations in nearby lowland areas. We used the partial least squares regression technique to evaluate the dominant meteorological factor on these glaciers. When compared at one-year intervals, seasonal precipitation was found to be the dominant weather variable whereas annual temperature and precipitation are equally dominant weather variables at these glaciers when they are computed with no glacier response time. With an integrated four years of weather, spring precipitation and annual temperature are the dominant meteorological variables. Contents of Chapter II will be submitted to a peer-reviewed journal in the fall of 2011.

Chapter III of this thesis discusses the application and results of the glacier mass balance model developed by Plummer and Phillips (2003) to the small, remote glaciers of the Teton Range. Model inputs included DEMs of the target glaciers, PRISM output, and weather station data from locations in and around the Teton Range. We ran four tests and sensitivity analyses. Energy mass balance model results indicate that the PRISM data did not yield positive mass balance in glacier accumulation areas using reasonable climate fluctuations. The model produced positive mass balance at selected glaciers using the weather station data in short selected periods in the record that feature low temperature and high precipitation. We interpret that, given the coarse spatial resolution of PRISM and the small scale of these glaciers, the model more successfully calculates mass balance using the more numerous and mixed elevations of the weather station data. This model may overestimate melt at the glaciers, as ice growth observed in the air photos was reproduced as positive mass balance in model output of only one portion of one test. We conclude that wind is an important climatic influence on these glaciers, especially at the

Schoolroom Glacier, and that more data recorded by high elevation weather stations is needed to better understand the energy mass balance of glaciers in the Teton Range.

Chapter IV is a brief synthesis of this thesis. Future work and other thoughts are addressed in Chapter IV as well.

Appendix A

A discussion leading to the decision of using the PRISM output dataset is in Appendix A. Numerous sets of weather data from stations in and near the Teton Range were downloaded from online sources. Appendix A follows our methods and analysis of these datasets to determine a record of temperature and precipitation at the studied Teton glaciers over the last 60 years.

Appendix B

Due to a lack of publication space in Chapter II, reasonably large, corrected air photos and glacier images used in this study are presented in Appendix B. These are all of the images discussed in Chapter II. Most of these images are corrected and have superimposed minimum and maximum glacier margins.

Appendix C

Results of Pearson correlation coefficients and partial least squares regression analyses between glacier area and weather variables are in Appendix C. These are organized selections of outputs from statistical software (Minitab v.16).

Appendix D

A modern, high elevation weather station (2750 m) was established in spring 2006 near Lake Solitude (Corbin, in progress). However, our study has access to only two months of data collected over mid-July to mid-September 2010. Records from this station are a significant opportunity because these new weather data come from one of the first weather stations maintained in the Teton Range glaciers at high elevation. This station currently records air temperature, a rain gauge, relative humidity, wind speed, and net solar radiation. A second data logger (with records that are not available) is recording air temperature near the Petersen Glacier. All sets of data will allow the evaluation of glacier mass balance processes, and will maintain a collection of continuous data for future studies. The two-month portion of this station's record is included as Appendix D, as an avenue to provide access to one of the few weather records from the inner Teton Range.

Appendix E

Seasonal fluctuations of temperature and precipitation are presented in Appendix E. These complement the annual fluctuations of temperature and precipitation presented in Chapter III, which does not address seasonal fluctuations.

References

Alexander, D.J., 2009, Examining the response of Franz Josef Glacier to climate change and rock avalanches using a simple mass balance model [B.S. Thesis]: Christchurch, New Zealand, University of Canterbury, 54 p.

Arendt, A.A., Echelmeyer, K.A., Harrison, W.D., Lingle, C.S., and Valentine, V.B., 2002, Rapid wastage of Alaska glaciers and their contribution to rising sea level: Science, v. 297, no. 5580, p. 382-386, doi: 10.1126/science.1072497.

Barry, R.G., 2006, The status of research on glaciers and global glacier recession: A review: Progress in Physical Geography, v. 30, no. 3, p. 285-306, doi: 10.1191/0309133306pp478ra.

Bitz, C.M., and Battisti, D.S., 1999, Interannual to decadal variability in climate and the glacier mass balance in Washington, Western Canada, and Alaska: Journal of Climate, v. 12, p. 3181-3196.

Cayan, D., Luers, A.L., Hanemann, M., Franco, G., and Croes, B., 2006, Scenarios of climate change in California: An overview: California Climate Change Center Report Series, CEC-500-2005-186-SF, 53 p.

Chinn, T.J., 1999, New Zealand glacier response to climate change of the past 2 decades: Global and Planetary Change, v. 22, p. 155-168, doi: 10.1016/S0921-8181(99)00033-8.

Chueca, J., Julián, A., and López-Moreno, J.I., 2007, Recent evolution (1981–2005) of the Maladeta glaciers, Pyrenees, Spain: extent and volume losses and their relation with climatic and topographic factors: Journal of Glaciology, v. 53, no. 183, p. 547-557.

Corbin, J., in progress, The effects of recent watershed deglaciation, climate change, and microbial processes on nitrate loading and ecological response in high alpine aquatic systems of Grand Teton National Park [Ph.D. Thesis]: Missoula, University of Montana.

Daly, C., 2006, Guidelines for assessing the suitability of spatial climate data sets: International Journal of Climatology, v. 26, p. 707-721, doi: 10.1002/joc.1322.

Dodson, R., and Marks, D., 1997, Daily air temperature interpolated at high spatial resolution over a large mountainous region: Climate Research, v. 8, p. 1-20.

Edmunds, J.F., 2010, Glacier variability (1967-2006) in the Teton Range, Wyoming, U.S.A. [M.S. Thesis]: Laramie, University of Wyoming, 62 p.

Elder, K., Fullerton, S., and Tonnessen, K., 1994, Winter mass balance measurements on Teton Glacier begin to build basis for predicting seasonal melt and runoff: Park Science: A Resource Management Bulletin, v. 14, no. 3, p. 11-13.

Foster, D., Brocklehurst, S.H., and Gawthorpe, R.L., 2010, Glacial-topographic interactions in the Teton Range, Wyoming: Journal of Geophysical Research, v. 115, F01007, 20 p., doi: 10.1029/2008JF001135.

Fountain, A.G., Krimmel, R.M., and Trabant, D.C., 1997, A strategy for monitoring glaciers: U.S. Geological Survey Circular 1132, 16 p.

Fountain, A.G., Percy, Delaney, C., Ebnet, A., Basagic, H., Hoffman, M., Jackson, K., Nylen, T., Sniffen, P., Granshaw, F., and Ebnet, J., 2006, Glaciers online: Glaciers of the American West: Portland State University, http://glaciers.us, accessed 6 Jan 2009.

Fountain, A.G., and Tangborn, W.V., 1985, The effect of glaciers on streamflow variations: Water Resources Research, v. 21, no. 4, p. 579-586.

Fountain, A.G., and Vecchia, A., 1999, How many stakes are required to measure the mass balance of a glacier?: Geografiska Annaler, v. 81 A, no. 4, p. 563-573.

Fryxell, F.M., 1935, Glaciers of the Grand Teton National Park of Wyoming: Journal of Geology, v. 43, no. 4, p. 381-397.

Global Climate Observing System (GCOS), 2003, The second report on the adequacy of the Global Observing Systems for climate in support of the UNFCCC: GCOS – 82, World Meteorological Organization/TD no. 1143, 85 p.

Gray, M., Elder, K., Tonnesson, K., Ramirez, J., and Greenwood, R., 1999, Topographical mass balance determination of Teton Glacier, Wyoming: Western Snow Conference, South Lake Tahoe, CA, 12 p.

Gudmundsson, G.H., 1999, A three-dimensional numerical model of the confluence area of Unteraargletscher, Bernese Alps, Switzerland: Journal of Glaciology, v. 45, no. 150, p. 219-230.

Hall, M.H.P., and Fagre, D.B., 2003, Modeled Climate-Induced Glacier Change in Glacier National Park, 1850–2100: BioScience, v. 53, no. 2, p. 131-140.

Hampel, A., Hetzel, R., and Densmore, A.L., 2007, Postglacial slip-rate increase on the Teton normal fault, northern Basin and Range Province, caused by melting of the Yellowstone ice cap and deglaciation of the Teton Range?: Geology, v. 35, no. 12, p. 1107-1110, doi: 10.1130/G24093A.1.

Hoffman, M.J., Fountain, A.G., and Achuff, J.M., 2007, 20th-century variations in area of cirque glaciers and glacierets, Rocky Mountain National Park, Rocky Mountains, Colorado, USA: Annals of Glaciology, v. 46, p. 349-354.

Hubbard, A.L., 1997, Modelling climate, topography, and palaeoglacier fluctuations in the Chilean Andes: Earth Surface Processes and Landforms, v. 22, p. 79-92.

Hughes, P.D., 2008: Response of a Montenegro glacier to extreme summer heatwaves in 2003 and 2007: Geografiska Annaler, series A, v. 90, no. 4, p. 259-267, doi: 10.1111/j.1468-0459.2008.00344.x

International Commission of Snow and Ice (ICSI), 1969, Mass-balance terms: Journal of Glaciology, v. 8, no. 52, p. 3-7.

Kaser, G., Fountain, A., Jansson, P., 2002, A manual for monitoring the mass balance of mountain glaciers: UNESCO, International Hydrological Programme, Technical Documents in Hydrology, No. 59, 107 p.

Krimmel, R.M., 2002, Glaciers of the Conterminous United States: Glaciers of the Western United States, *in* Satellite image atlas of glaciers of the world: North America, Williams, R.S. Jr. and Ferrigno, J.G., eds., United States Geological Survey: Washington, D.C., p. J329-J377.

Leonard, E.M., 1989, Climatic change in the Colorado Rocky Mountains: Estimates based on modern climate at Late Pleistocene equilibrium lines: Arctic and Alpine Research, v. 21, p. 245-255.

Love, J.D., Reed, Jr., J.C., and Pierce, K.L., 2007, Creation of the Teton landscape: A geologic chronicle of Jackson Hole and the Teton Range: Moose, WY, Grand Teton Association, 132 p.

L. Ruby Leung, Yun Qian, Xindi Bian, Washington, W.M., Jongil Han, and Roads, J.O., 2004, Mid-century ensemble regional climate change scenarios for the western United States: Climatic Change, v. 62, no. 1-3, p. 75-113.

Martner, B., 1986, Wyoming climate atlas: Lincoln, NE, University of Nebraska Press, 432 p.

Medley, B., 2008, A method for remotely monitoring glaciers with regional application to the Pacific Northwest [M.S. Thesis]: Corvallis, Oregon State University, 85 p.

Meier, M.F., 1984, Contributions of small glaciers to global sea level: Science, v. 226, no. 4681, p. 1418-1421, doi: 10.1126/science.226.4681.1418.

Meyer, G.A., Fawcett, P.J., and Locke, W.W., 2004, Late Pleistocene equilibrium-line altitudes, atmospheric circulation, and timing of mountain glacier advances in the interior northwestern United States, *in* Haller, K.M., and Wood, S.H., eds., Geological field trips in southern Idaho, eastern Oregon, and northern Nevada: Reston, VA, USGS Open-File Report, 2004-1222, p. 63-68.

Minder, J.R., Mote, P.W., and Lundquist, J.D., 2010, Surface temperature lapse rates over complex terrain: Lessons from the Cascade Mountains: Journal of Geophysical Research, 115, D14122, 13 p., doi:10.1029/2009JD013493.

Moore, D., Fleming, S., Menounos, B., Wheate, R., Fountain, A., Stahl, K., Holm, K., Jakob, Matthias, 2009, Glacier change in western North America: Influences on hydrology, geomorphic hazards, and water quality: Hydrological Processes, v. 23, p. 42-61.

Nesje, A., 2005, Briksdalsbreen in western Norway: AD 1900-2004 frontal fluctuations as a combined effect of variations in winter precipitation and summer temperature: The Holocene, v. 15, no. 8, p. 1245-1252, doi: 10.1191/0959683605hl897rr.

Oerlemans, J., and Reichert, B.K., 2000, Relating glacier mass balance to meteorological data by using a seasonal sensitivity characteristic: Journal of Glaciology, v. 46, no. 152, p. 1-6, doi: 10.3189/172756500781833269.

Pelto, M.S., 2008, Glacier annual balance measurement, forecasting and climate correlations, North Cascades, Washington 1984-2006: The Cryosphere, v. 2, p. 13-21.

Plummer, M., and Cecil, L.D., 2005, Calibration of a glacier model to historic variations of the Teton Glacier to improve model-based inferences about glacier-climate relationships, *in* Proceedings, Geological Society of America, 2005 annual meeting, Salt Lake City, UT: Boulder, CO, Geological Society of America, v. 37, no. 7, p. 41.

Plummer, M.A., and Phillips, F.M., 2003, A 2-D numerical model of snow/ice energy balance and ice flow for paleoclimatic interpretation of glacial geomorphic features: Quaternary Science Reviews, v. 22, p. 1389-1406, doi: 10.1016/S0277-3791(03)00081-7.

Reed, Jr., J.C., 1964, Recent retreat of the Teton Glacier, Grand Teton National Park, Wyoming, *in* Geological Survey Research 1964: USGS Professional Paper 501-C, p. C147-C151.

Reed, Jr., J.C., 1967, Observations on the Teton Glacier, Grand Teton National Park, WY, 1965 and 1966 *in* Geological Survey Research 1967: USGS Professional Paper 575-C, p. C154-C159.

Reynolds, H., 2006, Effects of meteorological conditions on supraglacial stream discharge, Matanuska River discharge, and ablation rates at the Matanuska Glacier, Alaska [B.S. Thesis]: Beloit, WI, Beloit College, 49 p.

Rignot, E., Rivera, A. and Casassa, G., 2003, Contribution of the Patagonia Icefields of South America to sea level rise: Science, v. 302, no. 5644, p. 434-437.

Rupper, S., and Roe, G., 2008, Glacier changes and regional climate: a mass and energy balance approach: Journal of Climate, v. 21, p. 5384-5401, doi: 10.1175/2008JCLI2219.1.

Sauber, J., Molnia, B., Carabajal, C., Luthcke, S., and Muskett, R., 2005, Ice elevations and surface change on the Malaspina Glacier, Alaska: Geophysical Research Letters, v. 32, L23S01, 4 p., doi: 10.1029/2005GL023943.

Sugden, D.E., and John, B.S., 1976, Glaciers and landscape: A geomorphological approach: New York, NY, John Wiley, 376 p.

Thompson, L.G., Davis, M.E., Mosley-Thompson, E., Lin, P.-N., Henderson, K.A., and Mashiotta, T.A., 2005, Tropical ice core records: evidence for asynchronous glaciation on Milankovitch timescales: Journal of Quaternary Science, v. 20, p. 723-733, doi: 10.1002/jqs.972.

United States Geological Survey, 1968a, Grand Teton quadrangle, Wyoming, Teton County: U.S. Geological Survey Topographic Map, scale 1:24,000.

United States Geological Survey, 1968b, Mount Moran quadrangle, Wyoming, Teton County: U.S. Geological Survey Topographic Map, scale 1:24,000.

United States Geological Survey, 2011, National water information system: web interface: United States Geological Survey, http://waterdata.usgs.gov/usa/nwis/, accessed 21 April 2011.

Chapter II: Recent glacier fluctuations in Grand Teton National Park, Wyoming

Abstract

We document recent area changes (1956-2010) of seven glaciers within the Teton Range, Wyoming, USA. Teton Range glacier areas decreased from 1956-2010, an overall trend punctuated by subdecadal episodes of ice growth and shrinkage. Generally over that period, weather analysis products from the Parameter-elevation Regressions on Independent Slopes Model (PRISM) indicate that temperatures increased in both areas studied, while precipitation increased at Schoolroom Glacier and decreased at glaciers on Mt. Moran. Statistical comparison of glacier area and PRISM weather outputs suggests dominant meteorological influences on glacier area. When glacier area is compared with the weather conditions of a single preceding water year, partial least squares regression analysis indicates that spring, summer, and winter precipitation has the strongest correlation with glacier area, whereas annual temperature and precipitation are equally strong correlates. When glacier area is compared with weather conditions over the preceding four water years, to better represent likely glacier response time, spring precipitation and annual temperature display the strongest correlations to glacier area.

Introduction

Mountain glaciers are important indicators of regional and global climate change (Barry, 2006), and glaciers in Grand Teton National Park, Wyoming (GTNP) are prime examples. Currently, at least ten named glaciers occupy the high alpine regions of the Teton Range. As these remote glaciers are small (1.7 km^2 area; Krimmel, 2002) and occupy high elevation areas in a semi-arid, mid-latitude region, they are likely to be very sensitive to climatic fluctuations.

Remote glaciers tend to receive less attention than more easily accessible glaciers, even though they may be more strongly affected by climate warming (Arendt et al., 2002). Area fluctuation of glaciers in GTNP can be indicators not only of regional climate change, but also of the broader impacts of climate change on the region. Evaluating the historic behavior of these glaciers complements historical climate measurements by providing regionally specific information on landscape responses (Hall and Fagre, 2003).

We document Teton Range glacier area changes from 1956-2010 and determine the relationships of those changes to local meteorological fluctuations. We determined glacier area change from archived aerial photographs and utilized weather factors from the Parameter-elevation Regressions on Independent Slopes Model (PRISM) output to compare weather fluctuations with glacier area changes. We used partial least squares regression analysis to determine the dominant meteorological forcing of glacier areas, and isolate spring precipitation as a dominant meteorological influence on these glaciers.

Previous Work

Surprisingly, most glaciers in GTNP have not been studied thoroughly. Fryxell (1935) reported that glaciers were first identified in the Teton Range during the summer of 1878, in the last season of the Hayden Survey. Fryxell also included a map with names and locations of seven glaciers (Falling Ice, Middle Teton, Skillet, Teton, and Triple Glaciers). The United States Geological Survey (USGS, 1968a & b) mapped three additional glaciers (Petersen, Schoolroom, and Teepe Glaciers).

Five studies measuring and monitoring mass balance of the Teton Glacier have been published within the last half-century. Reed (1967) and Elder et al. (1994) documented aspects of mass balance of the Teton Glacier from 1963 to 1966 and in 1993 respectively. Elder et al. (1994), measured winter mass balance on the Teton Glacier in mid-May 1993; constructed a digital elevation model (DEM) so the snow water equivalent (SWE) at all points could be estimated as a function of elevation; and used four methods to interpolate between their depth and density measurements. Elder determined that the Teton Glacier received a mean SWE of 3.22 m, which is 2.7 times higher than the expected areal average of Martner's (1986) Wyoming Climate Atlas. Elder et al. (1994) attribute the higher SWE value to a higher rate of orographic precipitation, leeward deposition of suspended snow by wind, and avalanches falling onto the glacier from adjacent slopes. The Teton Glacier is also protected from solar radiation by high, steep cirque walls. Elder's study was one of the first to combine mass balance measurements with a computational model for the complex setting of the Teton Glacier, and the factors he identified likely influence most of the Teton Range glaciers.

Gray et al. (1999) added another dataset intended to improve understanding of the mass balance characteristics of the Teton Glacier. He conducted a topographical study of the Teton Glacier with three datasets between the years of 1954 and 1994. Results of Gray et al. (1999) show an average rate of volume loss of 26,000 m^3/yr or -10 cm/yr for the Teton Glacier.

Most recently, Edmunds (2010) quantified the changes in glacier area and volume of the Teton, Middle Teton, and Teepe Glaciers from 1967 to 2006 and their effects on water resources in Wyoming. Edmunds (2010) used historic air photos and weather records from nearby stations. Edmunds used air photo georeferencing methods to determine that the Teton Glacier area decreased by 17%, Middle Teton Glacier decreased by 25%, and Teepe Glacier decreased by 60% from 1967 to 2006. With photogrammetry, Edmunds determined the volume of ice lost from 1967-2002 on Teton Glacier was 1.29 million m^3 for a rate of 36,900 ± 5,100 m^3/yr, Middle Teton Glacier lost 1.34 million m^3 of ice for a rate of 38,300 ± 5,700 m^3/yr, and Teepe Glacier lost 0.57 million m^3 of ice for a rate of 16,300 ± 2,300 m^3/yr. Edmunds (2010) found a much higher rate of ice loss at Teton Glacier than did Gray et al. (1999), although the estimation uncertainties likely make the values indistinguishable. Notably, Edmunds' (2010) study covered a period roughly a decade later than the study by Gray et al. (1999).

Edmunds (2010) also determined ice loss on the Grand Teton contributed minimally to the Snake River. Edmunds came to this conclusion after comparing 1967-2002 Snake River streamflow data just downstream of the Jackson Lake to the total estimated volume of glacier ice lost (3.2 million m^3) over the same period of time. Edmunds assumed all the volume lost flowed directly into the Snake River only during summer months of July, August, and September. However, the flow at this stream gage has been regulated by the Jackson Lake Dam since 1906 (USGS, 2011), complicating interpretations of his results.

In a fifth study concerning Teton Glacier mass balance, Plummer and Cecil (2005) built upon a numerical mass balance model developed by Plummer and Phillips (2003), and applied the model to the Teton Glacier. Plummer and Cecil (2005) determined that glaciers of different size and aspect can have significantly different responses to temperature variations, to the extent that modern recessions may not, for example, reflect modern warming.

While the Teton Glacier has been studied repeatedly, the seven glaciers treated here have never been studied in detail nor have any Teton glaciers been studied using more than three observation years of past ice areas. We determined the recent and current status of these small alpine glaciers by quantifying the areal extent for 8-11 observation years spanning 1956-2010, for seven glaciers (Petersen, Schoolroom, Falling Ice, Skillet, and the Triple Glaciers). The seven glaciers were studied via remote sensing techniques mainly using archived aerial photographs, and two were studied in the field, dependent upon access and glacier character. We address two questions, 1) whether these features are still glaciers or have degraded to snowfields or debris-covered glaciers and 2) whether temperature, precipitation, or an integration of both drive the areal changes in these glaciers.

We focus on temperature and precipitation variability and acknowledge that other factors affect glacier area such as the specific conditions of local weather, wind speed, relative humidity, slope aspect, and seasonal storm tracks. These additional factors are beyond the scope of this paper. However, many studies have found the highest correlations between glacier change and temperature and/or precipitation (e.g., Benn and Evans, 1998; Plummer and Phillips, 2003; and Meyer et al., 2004).

Study Area

Regional physiography provides ideal conditions for the maintenance of small mountain glaciers in the Teton Range (Figure 1). The NNE-SSW trending Teton Range (~70 km long by 20 km wide) is strongly affected by moisture-laden storms from the west. Storm systems from the Pacific Ocean funnel eastward to the end of the Snake River Plain and into the Teton Range. The Teton Range is the first major orographic barrier for the moist Pacific westerlies in eastern Idaho and western Wyoming (Meyer et al., 2004; Love et al., 2007). Figure 2 illustrates this orographic pattern, which leaves

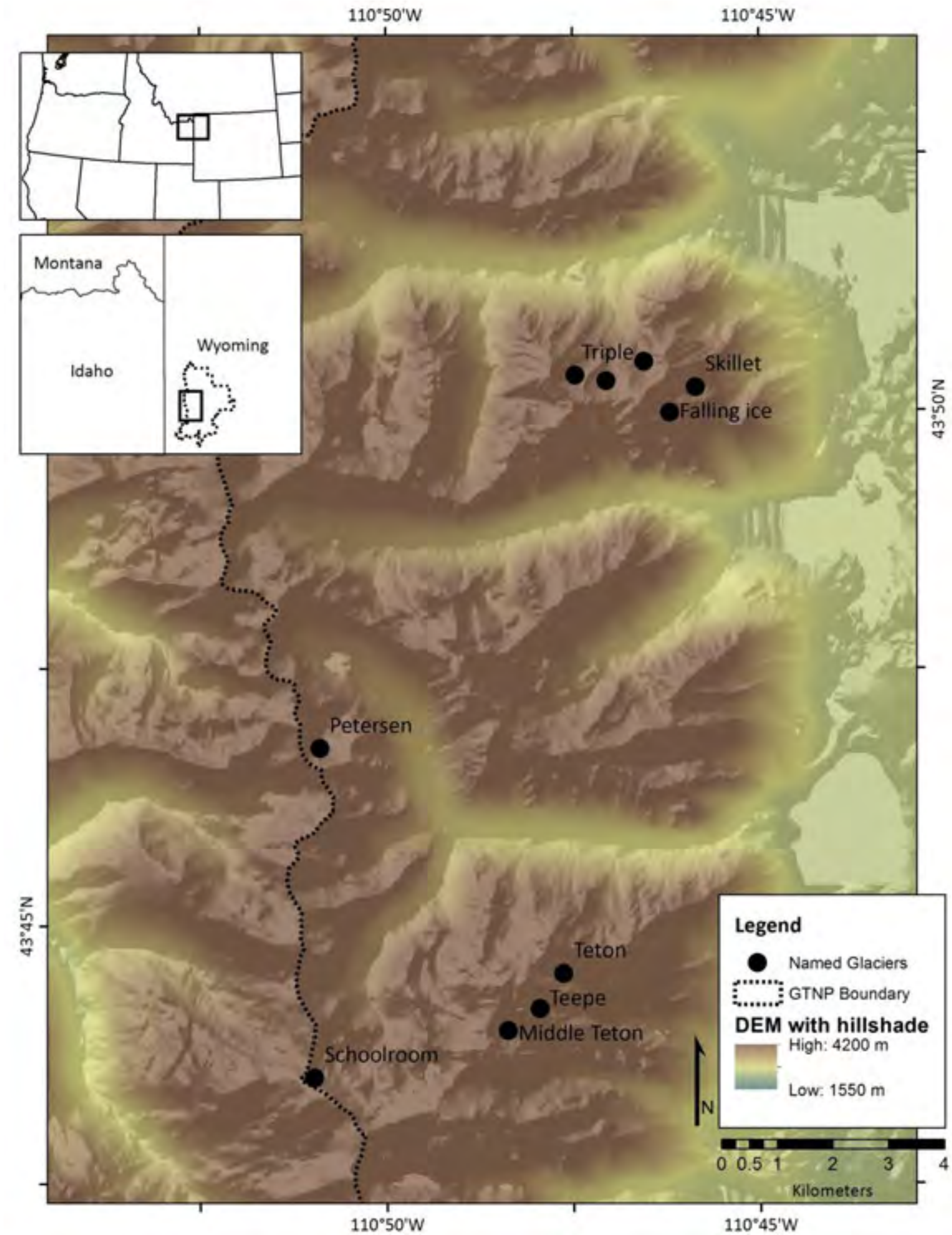

Figure 1. Topographic map of the field area. Black circles indicate the named glaciers. The Triple Glaciers are further named East, Middle, and West Triple Glacier. This study did not focus on the Teton, Teepe, or Middle Teton Glaciers. A dashed line is the park boundary, which is also the drainage divide in this portion of the park.

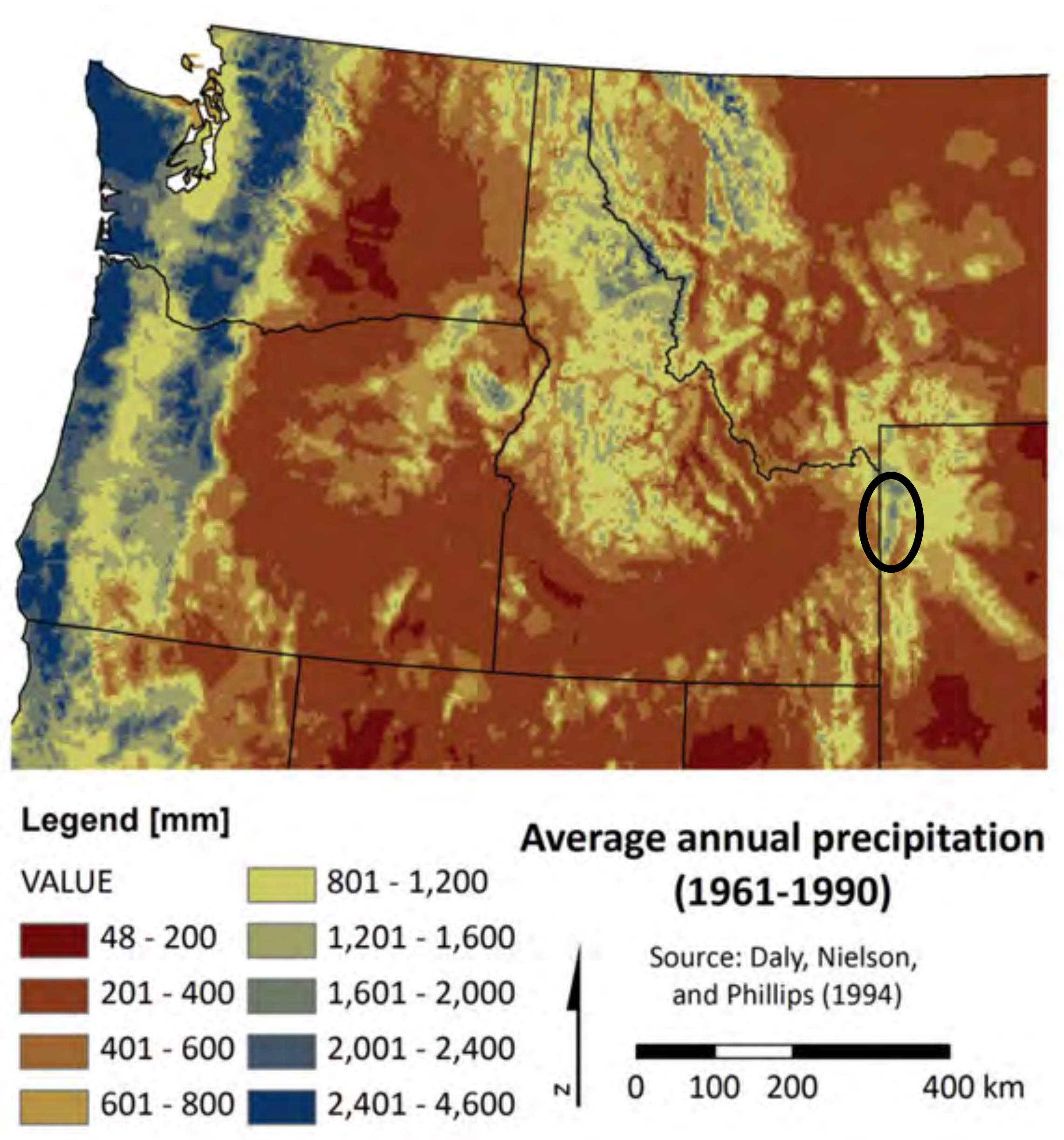

Figure 2. Map of average annual precipitation in western U.S. from Daly et al. (1994). An oval highlights the Teton Range.

mountain ranges to the north and south of the Eastern Snake River Plain dry (mean annual precipitation 500-1300 mm) relative to the wetter Teton Range and Yellowstone Highlands (mean annual precipitation 1500-2000 mm). At the studied glaciers, 1956-2010 PRISM output of average summer temperature and average annual precipitation is

9.8°C and 1715 mm at Schoolroom Glacier and 8.2°C and 1940 mm at Mt. Moran. Wise (2010) showed that streamflow in the region is strongly influenced by El Niño-Southern Oscillation (ENSO) cycles.

The Teton Range is in the northeastern Basin and Range Province. The two highest peaks (Grand Teton (4197 m) and Mt. Moran (3842 m)) are located on the eastern footwall of the east-dipping, normal Teton Fault bounding Jackson Hole basin and the Teton block. Since the initiation of displacement along the Teton Fault, the watershed divide has migrated from a position adjacent to the fault in the east to a position nearly 8 km westward. This westward migration was aided not only by tectonic uplift, but also by numerous glaciations (Love et al., 2007). Dramatic U-shaped canyons have been carved between steep peaks, generating high relief (2065-4197 m). Much of the older Bull Lake (~160-130 ka) deposits remain exposed in the southern half of GTNP, whereas they were overridden by the younger Pinedale glaciers (~30-12 ka) in the northern half (Love et al., 2007). Glaciers persist in the Teton Range due to wet westerly winds, orography, aspect, and shading provided by steep, high peaks. Currently all runoff from the west and east sides of the Teton Range drains into the Snake River system.

Methods

Glacier areas

We relied primarily on archived aerial photographs dating 1956-2009 to evaluate, qualitatively and quantitatively, recent changes in the ice area of seven of the Teton glaciers (Table 1). To achieve these goals, historic air photos, satellite imagery, and Geographic Information System (GIS) data were obtained from several sources (see Table 2).

Table 1. Characteristics of Teton glaciers in this study.

Teton glaciers	Maximum elevation [m]	Minimum elevation [m]	Aspect	Mean area [m^2]
Petersen	3190	2920	NE	---
Schoolroom	3180	3070	NE	28170
Falling Ice	3585	3210	SE	131840
Skillet	3410	2950	E	129510
East Triple	3300	2920	N	97260
Middle Triple	3420	2865	NE	199060
West Triple	3515	2920	N	164900

We created a base map by outlining glaciers with GIS software and digital USGS topographic maps. We built a glacier area inventory by analyzing time-successive corrected photos and adding glacial margins as layers within the GIS. To avoid mistaking seasonal snow patches as glacier ice, we used images from late August to October representing the end of the ablation season (Medley, 2008).

The ice margin inventory was built by tracing the glacier ice margins visually, instead of using a classification scheme. Due to problems with using a classification scheme in this situation, especially shadowing, we digitized the glacier ice margins by eye and included an estimation of debris-covered ice. We traced ice margins from images viewed at a zoom scale ranging from 1:300 to 1:1200, depending on the quality of the digital image.

Glacier ice margin minimum and maximum area values were entered in the inventory. Minimum and maximum values were used to capture uncertainty in classifying snowfields, nearby light-colored moraine material, shadows, and other questionable portions of the glacier that may or may not be an active part of the glacier. Areas of known bedrock were subtracted from both minimum and maximum glacier areas. Minimum glacier areas are used in the rest of this paper for simplification and

Table 2. Total glacier areas [m^2] of Teton glaciers determined from aerial imagery.

Year	1956	1967	1974	1979	1983	1989	1994	2001	2006	2009	2010
Date	2-Oct	3-Aug	18-Sep	12-Sep	15-Sep	6-Aug	25-Aug	25-Aug	11-Sep	11-Sep	5-Sep
Source*	DZT	USGS	TAR FS	NPS	NHAP	NAPP	DOQQ	DOQQ	NAIP	QB BW	Field trace
Falling Ice (max)	-----	135720	116187	138210	141328	137733	132338	129989	127845	131880	-----
(min)	-----	135031	114922	137459	138819	137321	131909	127772	126864	131765	-----
Schoolroom (max)	41261	39091	25601	32243	40973	27290	18979	21700	19806	26775	25047
(min)	40215	36444	22584	31062	36625	25429	15983	20645	17873	26708	-----
Skillet (max)	-----	147596	136190	137011	145156	131913	125426	120927	112871	123875	-----
(min)	-----	147146	130392	128906	145007	128944	122071	117054	108157	122524	-----
East Triple (max)	-----	115248	113803	100752	138852	109849	78592	75953	118315	96786	-----
(min)	-----	111321	85725	98783	113820	106503	55624	74383	85217	71148	-----
Middle Triple (max)	-----	204293	216911	203861	214574	214636	205442	190517	199603	184569	-----
(min)	-----	187872	210764	187613	192695	213332	198463	189334	184754	183819	-----
West Triple (max)	-----	222415	171127	166365	195797	209249	149640	108568	172043	175771	-----
(min)	-----	221144	163487	147307	178806	208126	106853	107120	106061	158370	-----
total area (max)	41261	864363	779819	778441	876680	830671	710417	647654	750483	739656	-----
(min)	40215	838958	727874	731130	805772	819654	630903	636308	628926	694334	-----
% of glacier snow-covered	115	115	66	66	33	66	50	25	75	110	105
% of ice on lake	0	90	0	0	40	0	0	0	0	0	0

*Source: DZT: Bridger-Teton National Forest Project DZT; USGS: United States Geological Survey; TAR: Targhee National Forest; NPS: National Park Service; NHAP: National High Altitude Program; NAPP: National Aerial Photography Program; DOQQ: Digitally orthorectified quarter quadrangles; NAIP: National Agriculture Imagery Program; QB BW: Digital panchromatic QuickBird satellite imagery.

consistency of figures, tables, and weather comparison calculations as well as to provide conservative ice area estimates. Findings would be similar if maximum areas were used instead.

To calibrate glacier ice positions and features in the images, we studied two glaciers in the field. Field investigation took place between mid-July and early-September 2009, and in early-September 2010. We recorded glacial features and nearby landforms to help interpret remotely sensed imagery, and documented glacier snow extent area and maximum ice margins using a global positioning system unit (Garmin GPSmap 60Csx; error <10 m; Garmin, 2006). We distinguished glacier ice from snowfields using evidence for active ice movement (crevasses, seracs, actively deposited end moraines, etc.) and evaluated ice morphology/hydrology for evidence of recent change. We added field results as another GIS layer to the inventory. Historic and recent ground-based photos were also used to help determine the ice margins and characteristics of the glaciers and nearby features.

We identified a number of sources of error associated with determining glacier area. These include 1) errors inherent to air photo georeferencing, 2) the uncertainty of definite ice margins when glaciers are obscured by snow cover, 3) the specific seasonality of eachimage, and 4) debris cover on the ice or dirty snow. Glacier margins are less clear and glacier areas are likely more error-prone on the larger, shaded glaciers carrying abundant rock debris. Finally, the aerial images may or may not have been taken at the extreme maximum or minimum of the glacier area trend in a given sequence of years.

Uncertainties in area estimation varied between glaciers. For examples, Schoolroom Glacier is a small, clean ice glacier with little or no debris cover, and thus there were smaller uncertainties with tracing margins or image quality. The uncertainties in area measurement for the Triple Glaciers, on the other hand, are greater because of significant debris cover on the margins of the ablation zone.

Weather records

We used the 103-year monthly temperature and precipitation values from the Parameter-elevation Regressions on Independent Slopes Model (PRISM) (Daly et al., 2002; Daly et al., 2010). PRISM is a well-reviewed model (Daly, 2006) that develops local weather-elevation regression functions for each DEM grid cell and calculates station weighting on the basis of a spatial climate knowledge base that assesses each station's physiographic similarity to the target grid cell. The knowledge base and resulting station weighting functions account for spatial variations in weather caused by elevation, terrain orientation or "topographic facets," effectiveness of terrain as a barrier to flow, coastal proximity, moisture availability, a two-layer atmosphere (to handle inversions), and topographic position (valley, mid-slope, ridge) (Daly, 2006). Minder et al. (2010) note that PRISM's approach allows surface lapse rates to vary seasonally, spatially, and to differ from the free air. Furthermore, the PRISM analysis methodology appears to capture much of the spatial and seasonal variability apparent in other data sets (Minder et al., 2010).

PRISM has several limitations. These include a large spatial resolution of grid cells of 2.5 arc minutes or 4 km^2. Furthermore, although PRISM uses data from all available observational networks, it has only monthly temporal resolution, may be subject to sizable errors where station observations are sparse, and relies on various assumptions in the interpolation procedure (Minder et al., 2010). Additionally, only weather records at low elevations have the longest records, and thus in a high relief mountain range such as the Tetons, uncertainties of weather conditions at high elevations bear substantial uncertainty.

Despite the limitations of the PRISM dataset, we decided to use PRISM output data because it provides a long record of weather conditions and is widely used in earth science studies. We tested numerous regressions of weather datasets to identify more reliable alternative approaches, and a discussion leading to this decision is in Appendix A. We obtained the PRISM output of precipitation as well as maximum and minimum temperature for each of the two pixels containing the target glaciers for water years 1949-2010. From the two temperature values, we calculated the mean monthly temperature.

Notably, we used single PRISM pixels to capture the modeled data over the specific areas occupied by the modern glaciers, rather than averaging several pixels. That is, our analysis of Schoolroom Glacier weather conditions is rooted in data from a single pixel, as is our analysis of weather conditions at the Mt. Moran glacier complex. A 4 km^2 PRISM pixels cover the small glaciers and their surroundings completely. While this procedure leaves our analysis prone to the uncertainties that may attend those individual pixels, we concluded that this was the best approach for specific reasons. First, the glaciers lie in rugged terrain. If we chose to average weather conditions from several pixels surrounding each glacier-occupied pixel, we would have incorporated modeled weather conditions over a wide range of elevations and aspects. Such a procedure would have introduced greater uncertainties than do the uncertainties attendant to a single pixel. Second, we might have chosen to average conditions from several pixels of similar elevation and aspect from across the range, to capture the range of variability inherent in the PRISM calculations. However, the distinct orographic barrier presented by the Teton Range precludes such an analysis. The NNE-SSW trending Teton Range lies directly across the path of the dominantly NW- and SW-traveling winter storms and wind flow directions. The E-W precipitation gradient is thus very strong, and the E-W and N-S locations within the range are very important in determining snowfall, and probably temperature as well. Therefore, averaging weather conditions from PRISM pixels with similar elevations and aspects from across the range would necessarily introduce a range of precipitation and temperature values related to that strong orographic effect. While the use of single PRISM pixels leaves our analysis subject to the model uncertainties associated with each single pixel, we concluded that these pixels represent the elevation, aspect, and orographic position most accurately.

We combined monthly PRISM temperature (means) and precipitation (sums) data for each pixel into seasonal and annual groups. Seasonal groups are: fall (Oct-Dec), winter (Jan-Mar), spring (Apr-Jun), and summer (Jul-Sep). Annual groups were compiled by water year (Oct-Sep). As the astronomical seasons change in the third week of the month (equinoxes and solstices), we assume the beginning of a season takes place the first day of the following month, which also agrees with water year quarters.

We examined statistical relationships between glacier area and PRISM variables in order to identify the weather factors influencing glacier size. We performed multiple regression analysis using partial least squares (PLS, Abdi, 2003) on each glacier, using temperature and precipitation variables to predict glacier area. PLS reduces the number of predictors (continuous or categorical) to a set of uncorrelated components and performs least squares regression on these components (Minitab, 2010). PLS is also useful in our situation where we have substantially more predictors (weather data) than observations (glacier areas) (Abdi, 2003; Minitab, 2010). We ran separate analyses for each glacier, as the glaciers are not necessarily correlated to each other and each glacier responded differently to the same weather variations. Each glacier was included in two analyses: 1) all eight seasonal weather variables (four seasons of temperature and precipitation) and 2) both annual weather variables. PLS analysis provides standardized regression coefficients of each weather variable that are comparable in strength at one glacier, but are not directly comparable to those of another glacier. With PLS we can assess two factors: 1) which meteorological variables are more influential than others for each glacier and 2) whether the pattern is the same for each glacier.

In order to determine effects of glacier response time, we conducted PLS analyses with single-year weather conditions, and with three- and four-year moving averages of weather conditions. We did so with the understanding that glaciers integrate several years of weather conditions into their area changes, and that three to four years is a reasonable time of glacier response for these small alpine glaciers (Paterson, 1994; Benn and Evans, 1998). We averaged the PRISM-generated weather conditions for the three- and four-year periods preceding each glacier area observation. We calculated these new averages both seasonally and annually and compared the weather data to the glacier area observations using PLS to determine the strongest meteorological influence on the area change of these glaciers. To simplify the discussion that follows, we focus only on the single-year and the four-year averaged weather conditions.

Results

Glacier area change

Glaciers in the Teton Range experienced overall reduction of area since 1956, punctuated by periods of subdecadal-scale ice growth and retreat (see Figure 3). Patterns of area change differed between glaciers, suggesting varied responses to weather forcing on variable meteorology between locations. We note both glacier area and terminus position on the date of observation (see Table 2 for image acquisition dates) and consider this day to be at the end of the water year. For example, we consider the image acquired on 6 August 1989 to be from 1989 water year and images acquired on 2 October 1956 to be from 1956 water year rather than the 1957 water year. Observations of glacier area are divided into three groups determined by the close spatial proximity of the glaciers (Schoolroom Glacier; Skillet and Falling Ice Glaciers; and Triple Glaciers). Figure 4 provides an example of the glacier area observations with traced ice margins at intervals from 1956 to 2010, and Appendix B includes all observations.

Petersen Glacier now exists only under debris cover. It is very difficult to determine where ice margins may lie, due to snow cover and rock debris cover for all images. Remnant ice and lobate features remain, suggesting that a debris-covered glacier currently occupies this basin. Field reconnaissance failed to find glacial ice in shallow holes in snow in July 2009. Corbin (pers. comm., 2009) did not find glacial ice during the summers of 2006-2008 in the Petersen Glacier basin. Therefore, we assume that the Petersen Glacier has ceased to exist without debris cover. We do not consider it further, as debris cover strongly modulates glacier response to climate change (Clark et al., 1994).

The Schoolroom Glacier is a clean ice glacier that lies below Hurricane Pass on the

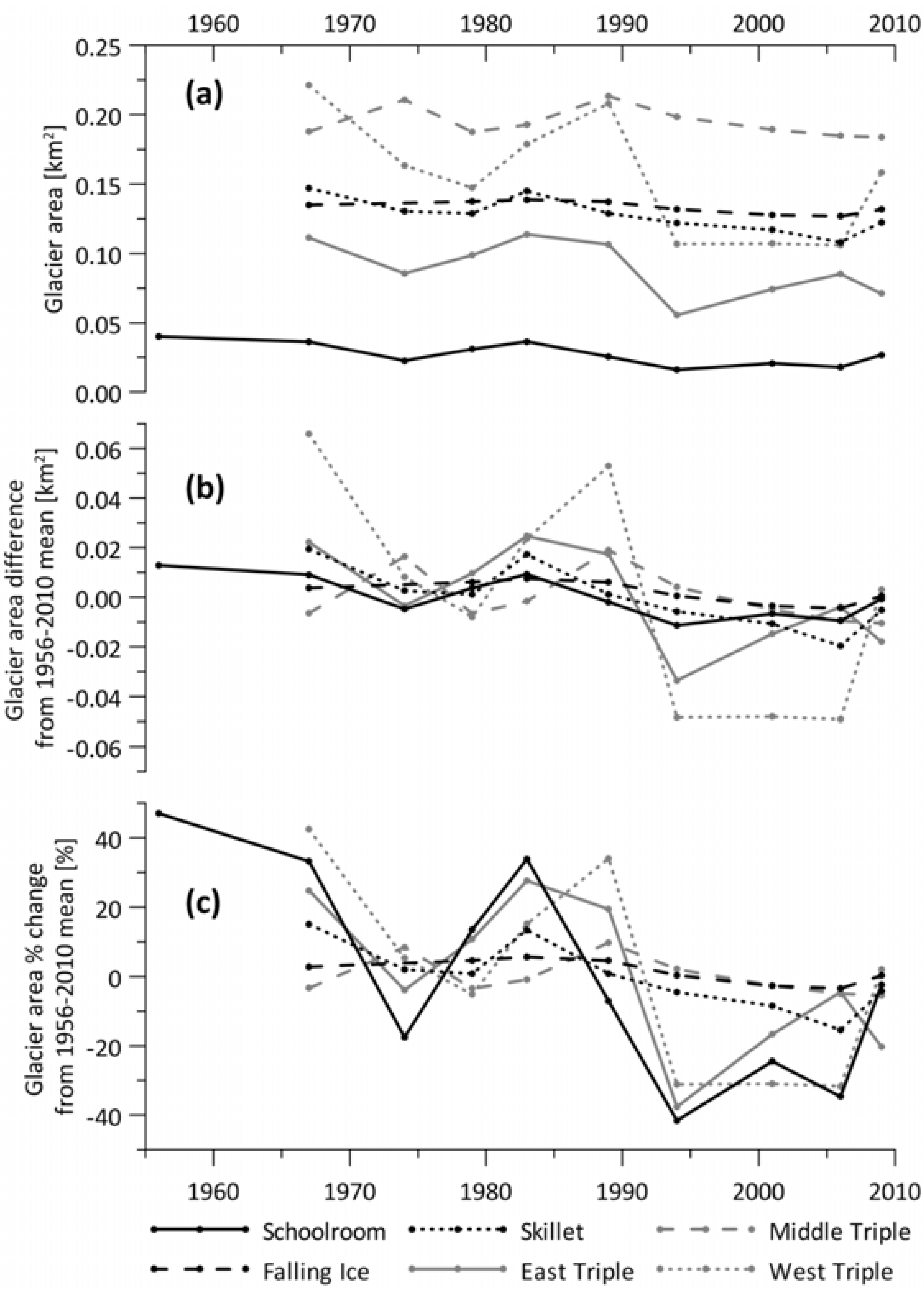

Figure 3. Plots of minimum (a) glacier area; (b) glacier area difference from the mean of the period of record; and (c) glacier area change from the mean of the period of record. Overall, there is a decline in glacier area punctuated by episodes of growth.

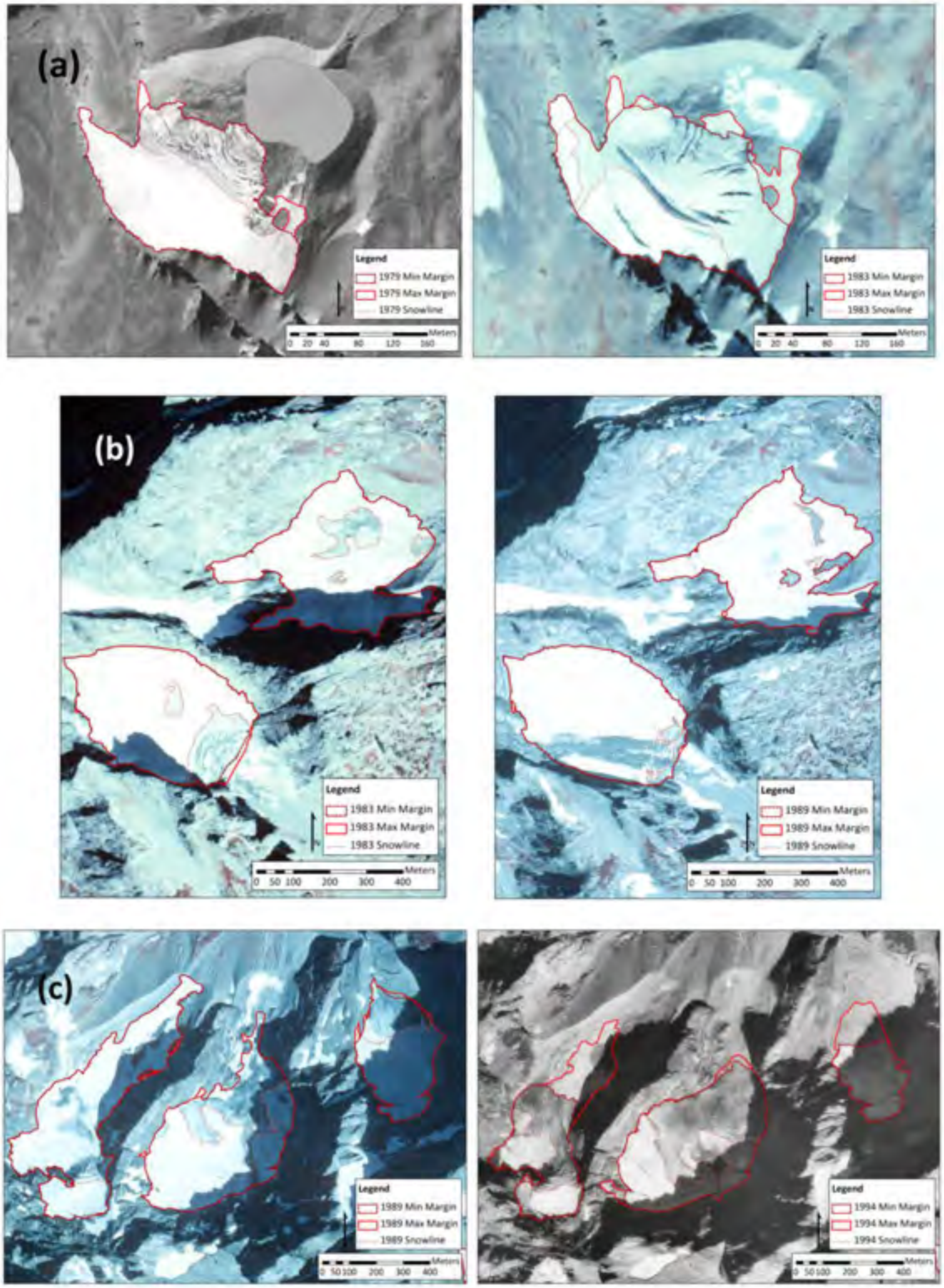

Figure 4. Examples of glacier area change in small periods of time for (a) Schoolroom Glacier, (b) Skillet (upper right) and Falling Ice (lower left) Glaciers, and (c) Triple Glaciers. Note the crevasse patterns in 3a, rockfall in 3b, and debris cover in 3c.

east side of the drainage divide in Cascade Canyon (Figures 1 & 4a). The accumulation area of the glacier is located on a west-dipping rock bench of Cambrian limestone (Love et al., 2007). This bench creates a bulge in the glacier as ice flows from the accumulation area to the ablation area. A proglacial lake captures most of the meltwater and likely obscures recessional moraines. A massive (as wide as 60 m and as tall as 7 m), arcuate, matrix-supported end moraine, presumed to have originated during the Little Ice Age, encircles the distal shore of the lake.

The Schoolroom Glacier experienced multiple episodes of growth and retreat since 1956, suggesting rapid responses to weather variations. Abundant snow obscured Schoolroom Glacier in 1956 and 1967; however, the glacier terminus retreated and area diminished from 1956-1974. A pronounced advance was notable between 1974-1979 and further ice advance occurred by 1983. By 1989, the Schoolroom Glacier terminus retreated and glacier area diminished. The smallest Schoolroom Glacier area was observed in 1994 followed by a small advance by 2001 and another retreat by 2006. The glacier advanced by 2009 followed by a small retreat by 2010, though these latter observations are complicated by snow cover, which obscured all glaciers during the entire ablation season in 2009, and likely in 2010. Field observations of Schoolroom Glacier demonstrated that glacial ice has been covered by snow through the 2009 and 2010 ablation season, following cool, wet spring weather, suggesting that spring weather may be a strong influence.

Crevasse pattern observations document changes in stresses within the glacier ice. Radial crevasses at the glacier terminus may belie glacier mass spreading laterally (Bennett and Glasser, 1996; Benn and Evans, 1998). These may be caused by an increase in mass input. Transverse crevasses are indicative of longitudinal, extending flow (Bennett and Glasser, 1996; Benn and Evans, 1998). These may be caused by a large increase in longitudinal glacier flow near the terminus. Near its terminus, Schoolroom Glacier displayed concentric transverse crevasses in 1979, radial crevasses in 1983, 1994, and 2001, and small transverse crevasses in 2006. These crevasse patterns did not consistently occur with either larger or smaller glacier areas, but they do indicate that Schoolroom Glacier continues to be an active glacier, with changing crevasses patterns suggesting mass flux variability over the period of observation since 1956.

Skillet and Falling Ice Glaciers (Figure 4b) are on the northeast and southeast slopes of Mt. Moran, respectively. Mt. Moran consists of Precambrian crystalline basement of granite, gneiss, and schist (Love et al., 2007). Transverse crevasses are seen at the top of the largest portion of Skillet Glacier in every image, suggesting a small rock bench at depth. Falling Ice Glacier terminates at a prominent rock ledge with concentric crevasses, and the resulting ice fall exerts a dynamic control on glacier area and likely complicates glacier-climate relationships. This glacier is confined between two mountain peaks (horns) that also provide shade.

Falling Ice Glacier area barely fluctuated while Skillet Glacier area generally decreased from 1967-2009. In the 1967 aerial photo, both Skillet and Falling Ice Glaciers were covered by snow. These glaciers maintained similar areas in 1979 as in 1967, following a small area decrease in Skillet Glacier and slight area increase in Falling Ice Glacier. Both glaciers grew slightly by 1983. By 1989, bedrock was first observed at Skillet Glacier near the middle of the glacier, and glacier area was smaller. Falling Ice Glacier advanced and transported debris from a rock fall on the southern right lateral portion of the glacier. Both glaciers diminished from 1989-2006. Bedrock was observed near the middle of Skillet Glacier from 1989-2009. Snow obscured ice margins on these glaciers in 2009, but both appeared to have expanded. As discussed briefly below, Falling Ice Glacier appears to have a dynamic ice limit in the form of an ice fall.

Three glaciers collectively called the Triple Glaciers (Figure 4c) are located on the north slope of Mt. Moran. West Triple Glacier displays transverse crevasses over a narrow rock bench near the top of the glacier's accumulation area. The Middle Triple Glacier displays transverse crevasses throughout the glacier and in all images. East Triple Glacier has several large transverse crevasses near the top of the accumulation area.

Areas of the Triple Glaciers fluctuated with dissimilar temporal patterns from 1967-2009. All three glaciers decreased in area from 1967-2009. The Triple Glaciers had small patches of melted snow in 1967. By 1974, West and East Triple Glacier areas diminished slightly while Middle Triple Glacier increased slightly. By 1979, West and Middle Triple Glaciers' termini retreated and areas were smaller. The Triple Glaciers' termini advanced and glacier area increased by 1983. West and Middle Triple Glacier termini advanced by 1989 while East Triple Glacier retreated. The Triple Glaciers notably retreated and diminished between 1989 and 2001. Only East Triple Glacier advanced from 1994-2001. The Triple Glaciers advanced from 2001-2006. West Triple Glacier terminus advanced and area increased while Middle and East Triple Glaciers retreated by 2009.

To summarize these changes in glacier area, Table 2 reports the glacier areas through time. To summarize these changes visually, Figure 3a is a plot of the minimum glacier areas, Figure 3b is a plot of minimum glacier area difference from 1956-2010 mean, and Figure 3c is a plot of the glacier area percent change from 1956-2010 mean. Between

1956 and 2010, Teton Range glacier areas decreased, but this overall decrease was punctuated by subdecadal episodes of growth. In particular, 1974-1983 was a general period of ice growth for all glaciers, with individual glaciers displaying additional periods of ice growth during the period of observation.

Weather fluctuations

Records of annual and seasonal temperatures and precipitation from 1949-2010 were compared at the two PRISM pixels covering the glacier locations (Figures 5 & 6, Table 3). In Table 3, we assumed that a linear temperature trendline slope $< |0.005|$ and precipitation slope of $< |0.0005|$ indicate a lack of discernible trends. Annual and all seasonal temperatures increased at Mt. Moran glaciers with the highest magnitude of change, 9.9°C, observed over Mt. Moran during the winter. Annual and winter temperatures increased at Schoolroom Glacier and the highest magnitude of change (6.9°C) occurred in the winter. Over the studied period, no trends were observed at the Schoolroom Glacier in fall, spring, or summer temperature. Annual and seasonal precipitation decreased at Mt. Moran except in fall, when no discernable trend was observed. Schoolroom Glacier experienced increased annual, fall, and winter precipitation. Spring precipitation showed no trend at Schoolroom Glacier and summer precipitation decreased.

Figures 7 and 8 display four-year averages of seasonal and annual PRISM output at the Schoolroom and Mt. Moran pixels. In both Figures 7 and 8, the patterns of temperature and precipitation of Schoolroom and Mt. Moran pixels change in character ca. 1999-2010. For example, fall, spring and summer temperatures shifted upward as spring and summer precipitation displayed lower magnitudes of interannual fluctuation.

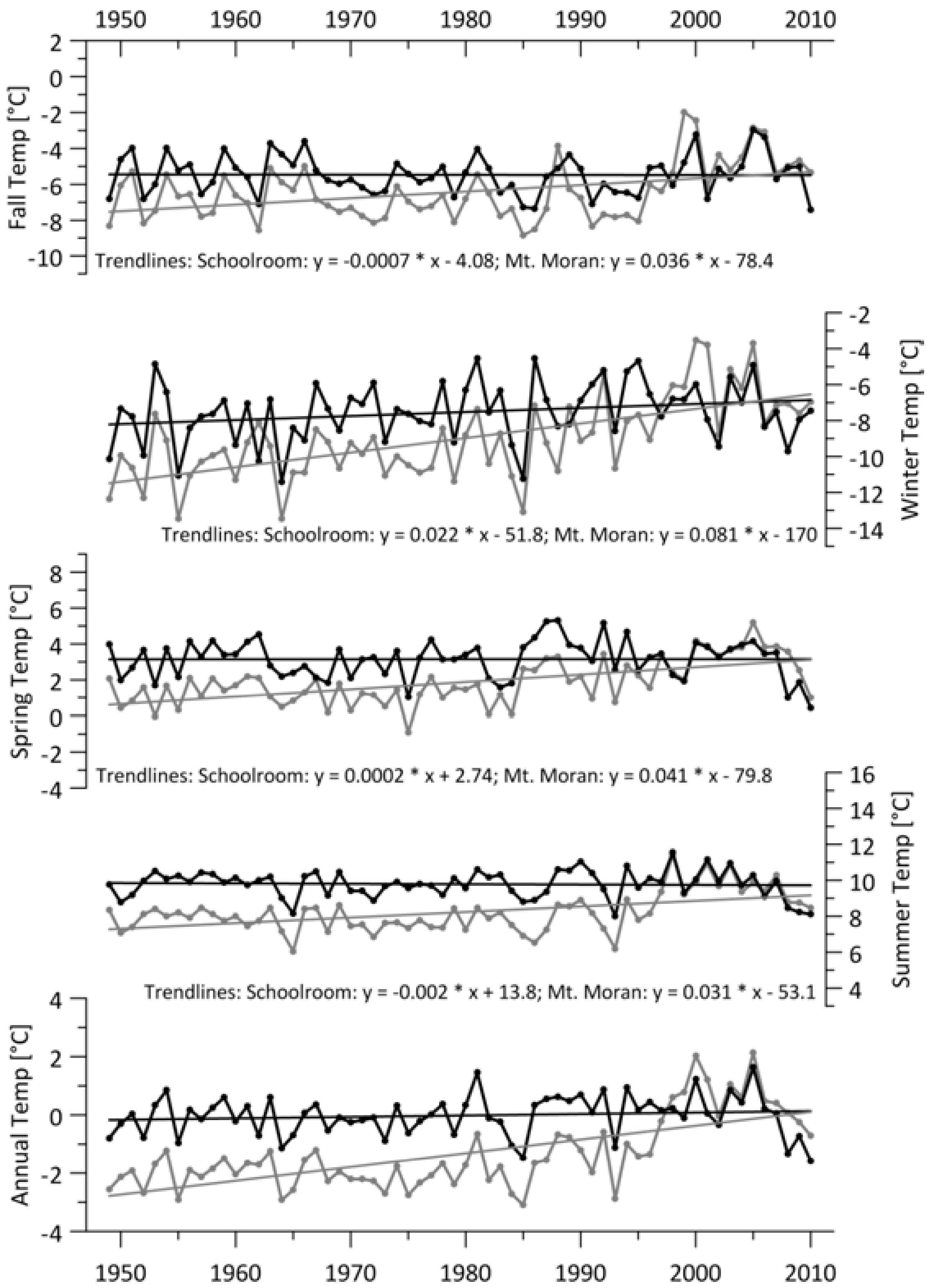

Figure 5. Seasonal and annual average temperature PRISM output at the Schoolroom (black line) and Mt. Moran (grey line) PRISM pixels. Annual temperature trendlines are positive (Schoolroom: y = 0.005 * x - 9.84; Mt. Moran: y = 0.047 * x - 95.2).

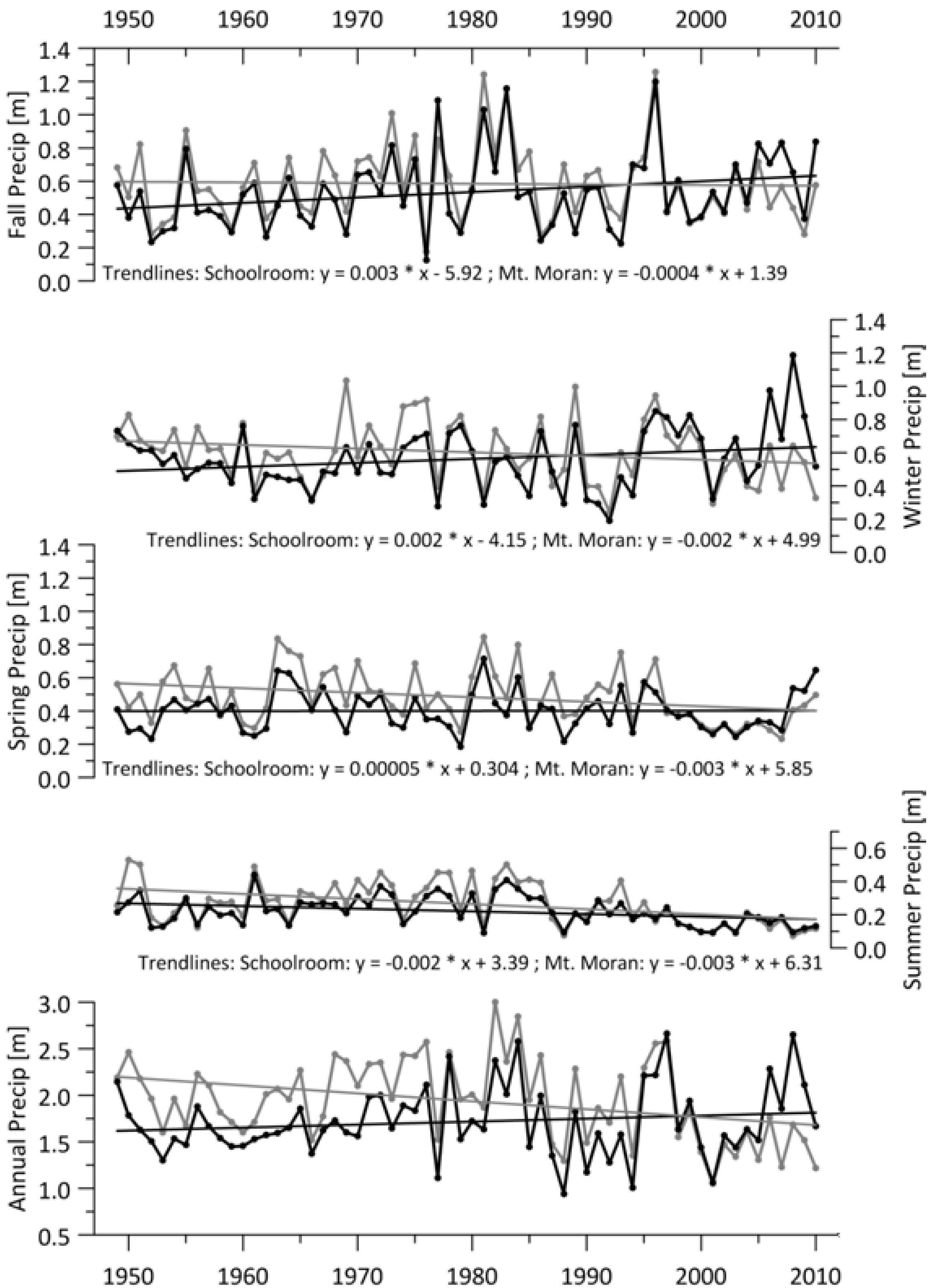

Figure 6. Seasonal and annual sums of precipitation PRISM output at the Schoolroom (black line) and Mt. Moran (grey line) PRISM pixels. Annual precipitation trendlines are mixed (Schoolroom: y = 0.003 * x - 4.64; Mt. Moran: y = -0.009 * x + 18.8).

Table 3. Trends of seasonal weather variables at two PRISM pixels where + denotes positive trend, - denotes negative trend, and x denotes no trend.

		Schoolroom	Mt. Moran
Temperature	Annual	+	+
	Fall	x	+
	Winter	+	+
	Spring	x	+
	Summer	x	+
Precipitation	Annual	+	-
	Fall	+	x
	Winter	+	-
	Spring	x	-
	Summer	-	-

We attribute this change to a data shift as more high-elevation weather stations were installed in the Teton Range and were incorporated into PRISM calculations. The four-year moving average of annual temperature increased over the period of record in both pixels. Annual precipitation increased over the period of record at the Schoolroom pixel whereas at Mt. Moran, annual precipitation decreased over the period of record.

Observations and statistical correlations of glacier area – weather relationships

There were notable changes in the studied weather variables in relation to glacier observations. Five glaciers increased in area between 1974 and 1983, when annual temperatures were relatively low and annual precipitation was relatively high. Most glaciers decreased in area between 1983-1994 when annual, winter, and spring temperatures increased and annual precipitation decreased. The period 1994-2010 showed mixed responses. Some glaciers (Schoolroom, East Triple, and West Triple glaciers) increased in area while others (Falling Ice, Skillet, and Middle Triple glaciers) decreased between 1994-2010, when annual temperature increased and then subsequently

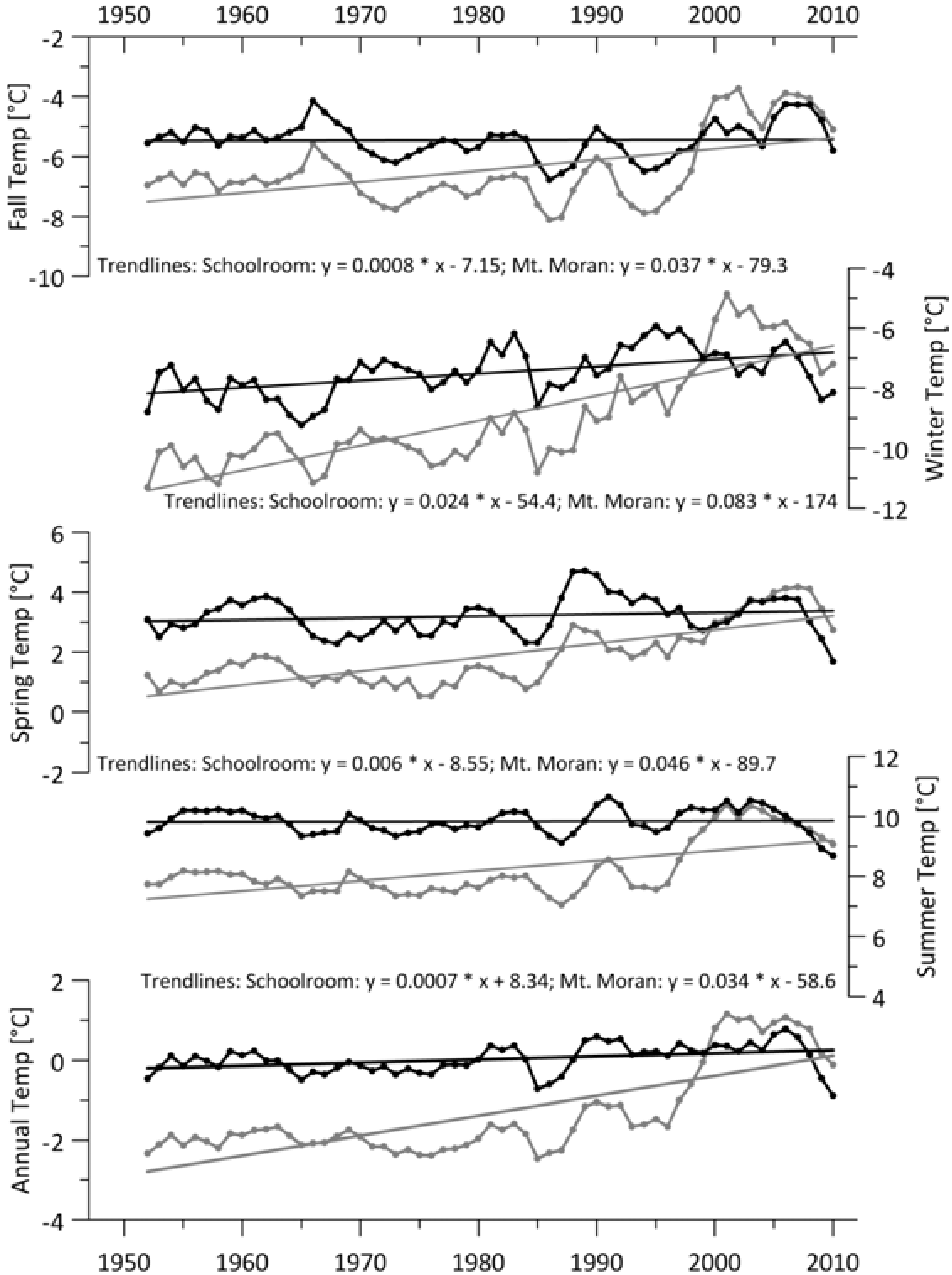

Figure 7. Seasonal and annual four-year moving average temperature PRISM output at the Schoolroom (black line) and Mt. Moran (grey line) PRISM pixels. Annual temperature trendlines are positive (Schoolroom: y = 0.008 * x - 15.4; Mt. Moran: y = 0.050 * x - 100.3).

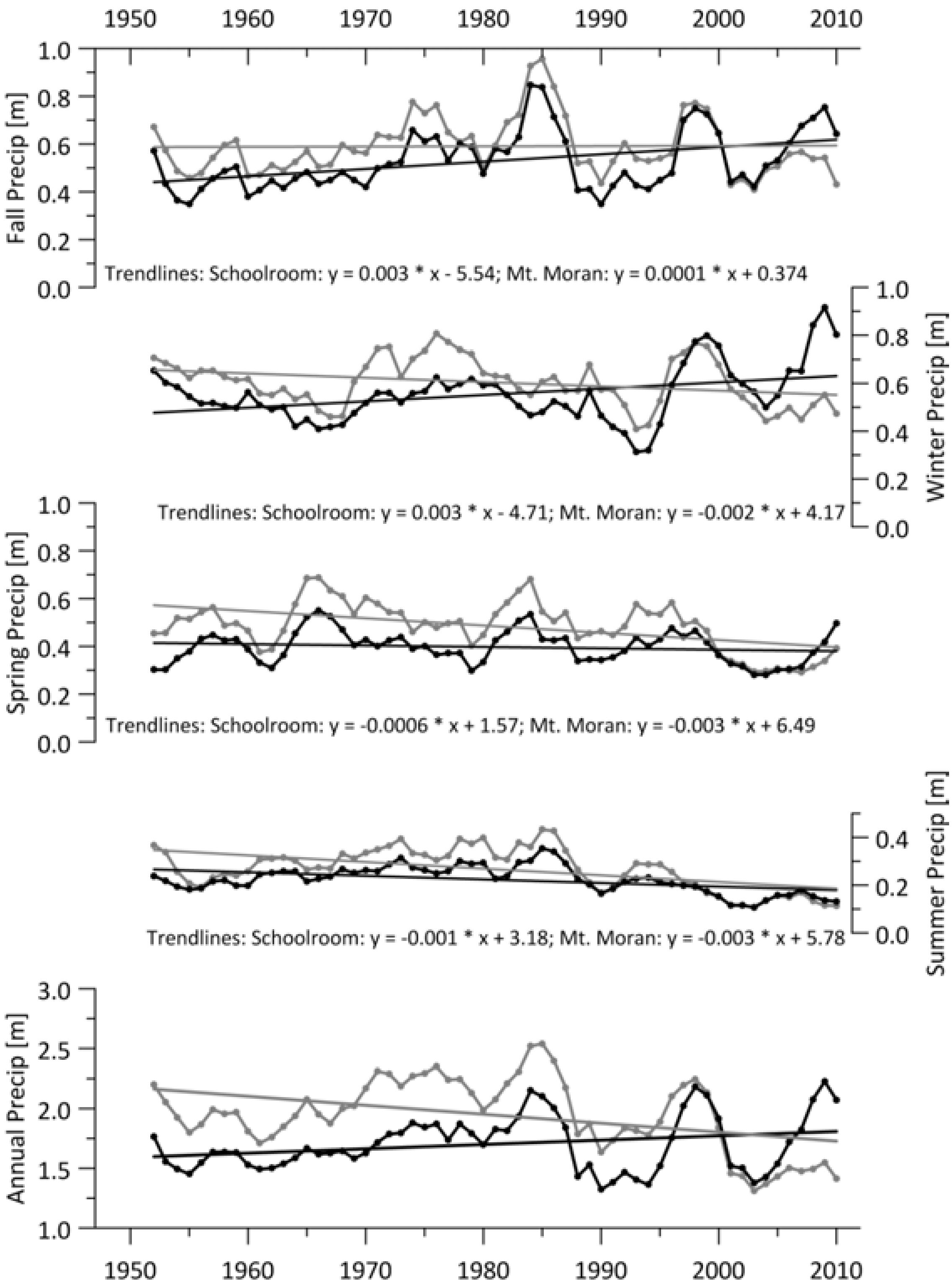

Figure 8. Seasonal and annual four-year moving average sums of precipitation PRISM output at the Schoolroom (black line) and Mt. Moran (grey line) PRISM pixels. Annual precipitation trendlines are mixed (Schoolroom: y = 0.004 * x - 5.49; Mt. Moran: y = -0.008 * x + 16.8).

decreased, and while annual precipitation rapidly increased and decreased from about 1.4 m/yr to 2.7 m/yr to 1.4 m/yr again within seven years and increased again by 2010. Thus, the glacier area changes appear to bear an observational relationship to weather changes during specific, several year-long periods.

In order to provide a rigorous analysis of these observed relationships, we performed statistical analyses of glacier areas and weather conditions. Partial least squares (PLS) regression analyses elucidate the relative strengths of correlations between glacier area and selected weather variables. We analyzed variables with one- and four-year averages. Note that we compared both quarterly and whole water year temperatures and precipitation to glacier area observations considered to be at the end of the water year. Standardized regression coefficients from analyses of the same water year are displayed in both Figure 9 and Table 4. Extended results from PLS are displayed in Appendix C. Pearson correlation coefficients (Appendix C) produce broadly similar results to those of PLS, and we decided to continue with the stronger statistical approach of PLS.

Glacier area and temperature are negatively correlated, as expected: as temperatures rise, glacier area decreases. Glacier area and precipitation are positively correlated: as precipitation increases, glacier area increases. We did not consider any situations in which these relationships are reversed because reversed relationships, usually small in magnitude, commonly occur about half of the time when a relationship is not statistically significant.

With one water year of weather data compared with glacier area, PLS analysis indicates that the dominant seasonal weather variable was precipitation at Skillet and Triple glaciers. The strongest seasonal correlates were winter, spring, and summer

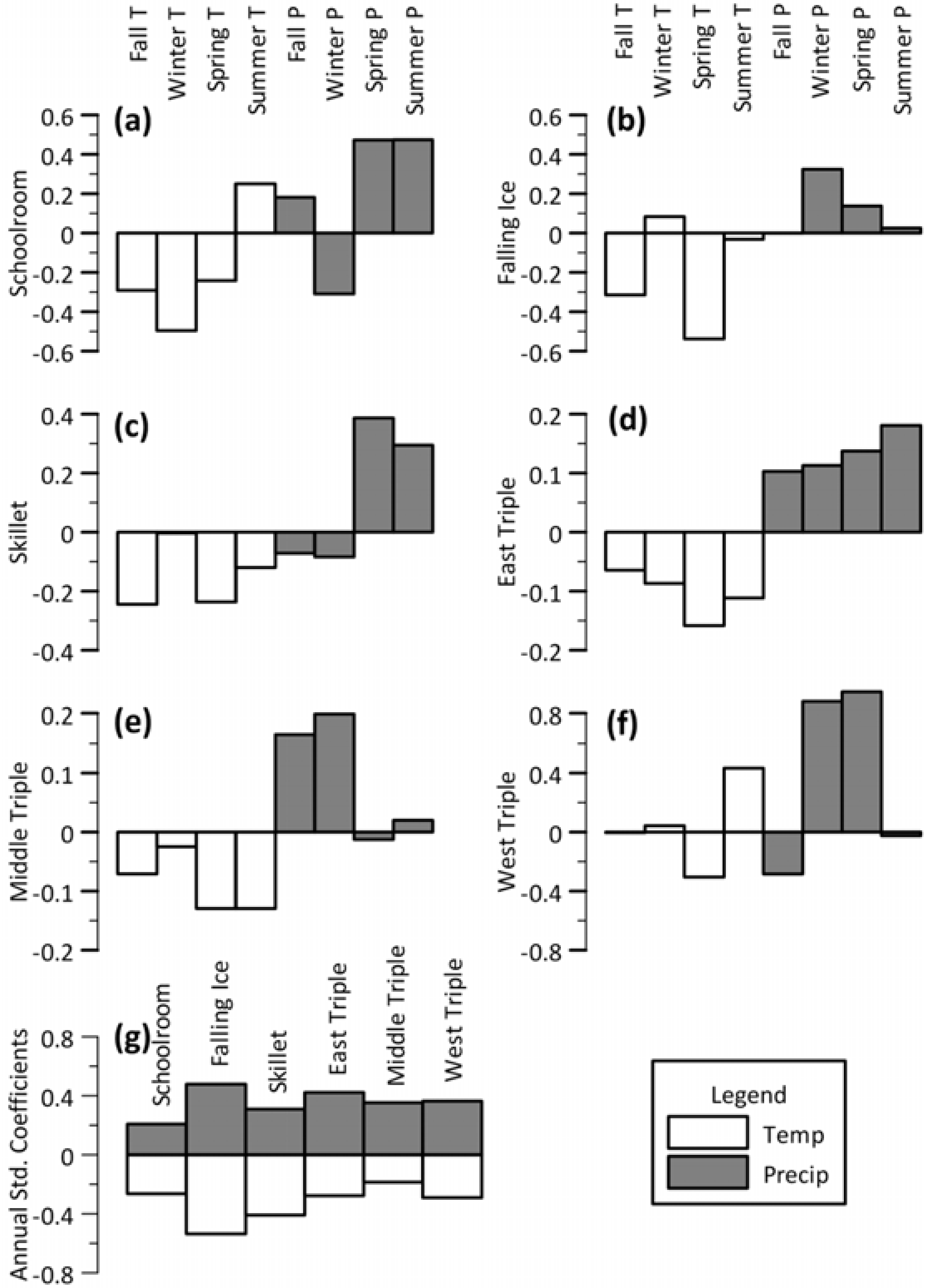

Figure 9. Standardized regression coefficients of Teton glaciers of the same water year seasonal and (g) annual temperature and precipitation. Seasonal plots are for (a) Schoolroom, (b) Falling Ice, (c) Skillet, (d) East Triple, (e) Middle Triple, and (f) West Triple.

Table 4. Highest ranked partial least squares regression standardized regression coefficients of weather variables for Teton glaciers, averaged in one water year only.

Seasonal

rank	**School-room**	Std. coeff.	**Falling Ice**	Std. coeff.	**Skillet**	Std. coeff.	**East Triple**	Std. coeff.	**Middle Triple**	Std. coeff.	**West Triple**	Std. coeff.
1	Winter T	-0.496	Spring T	-0.537	Spring P	0.387	Summer P	0.181	Winter P	0.199	Spring P	0.945
2	Summer P	0.474	Winter P	0.325	Summer P	0.295	Spring T	-0.158	Fall P	0.165	Winter P	0.881
3	Spring P	0.473	Fall T	-0.315	Fall T	-0.244	Spring P	0.137	Summer T	-0.130	Summer T*	0.434
											Spring T	-0.305

Annual

rank	**School-room**	Std. coeff.	**Falling Ice**	Std. coeff.	**Skillet**	Std. coeff.	**East Triple**	Std. coeff.	**Middle Triple**	Std. coeff.	**West Triple**	Std. coeff.
1	Temp	-0.264	Temp	-0.535	Temp	-0.409	Precip	0.423	Precip	0.353	Precip	0.364
2	Precip	0.208	Precip	0.479	Precip	0.310	Temp	-0.277	Temp	-0.185	Temp	-0.291

* denotes opposite correlation than expected.

precipitation. Summer and winter precipitation were the second strongest correlates for the remaining two glaciers (Schoolroom and Falling Ice glaciers). PLS analysis indicates that dominant annual weather variable was temperature at Schoolroom, Falling Ice, and Skillet. The dominant one-year annual weather variable was precipitation at the Triple Glaciers. Overall, annual temperature and annual precipitation are equally dominant weather variables at these glaciers, when considering only the water year preceding an observation. The three-year PLS analysis did not produce clearer results and is included in Appendix C but not discussed further.

Figure 10 and Table 5 present partial least squares regression standardized regression coefficients of four-year moving averages of weather variables for Teton glaciers. Weather conditions were averaged over the four years preceding each glacier area observation. Four of six glaciers (all but East and Middle Triple Glaciers) correlate most strongly with the four-year moving average of precipitation in the spring, and for the East Triple Glacier spring precipitation is the second strongest correlate, only slightly less strong than winter temperature. As discussed below, this correlation is consistent with recent glacier observations. With annual averages over four-year intervals, all but East and Middle Triple Glaciers correlate most strongly with temperature.

Discussion

Glaciers in the Teton Range experienced overall retreat from 1956-2010, punctuated by episodes of subdecadal-scale ice growth and retreat. The period 1974-1973 was a general period of ice growth. We find that all of the glaciers on Mt. Moran retreated and diminished between 1989 and 1994, and those on the east face (Falling Ice and Skillet glaciers) continued this trend into 2006. Schoolroom Glacier also followed a trend of

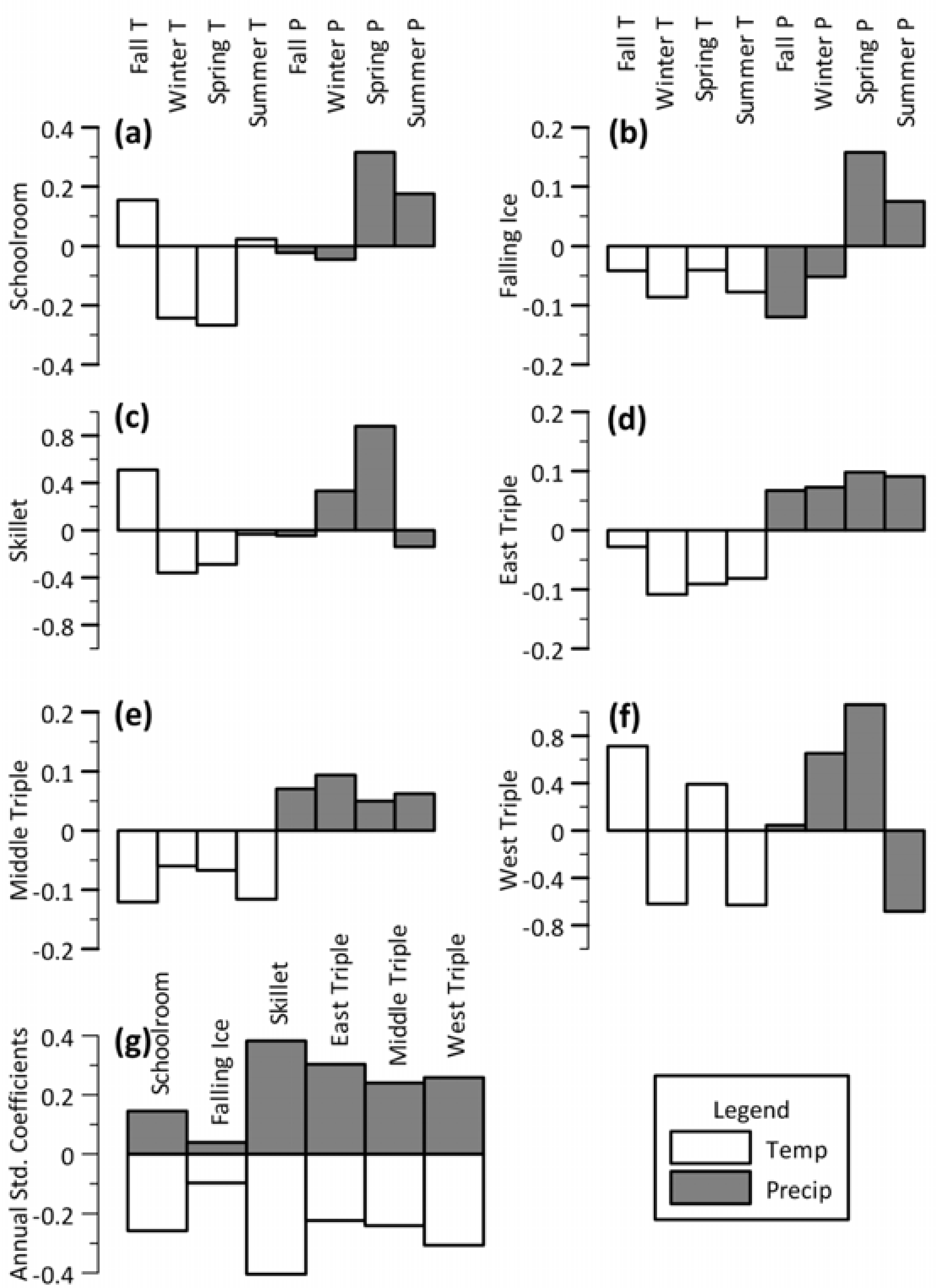

Figure 10. Standardized regression coefficients of Teton glaciers with four-year moving averages of seasonal and (g) annual temperature and precipitation. Seasonal plots are for (a) Schoolroom, (b) Falling Ice, (c) Skillet, (d) East Triple, (e) Middle Triple, and (f) West Triple.

Table 5. Highest ranked partial least squares regression standardized regression coefficients of four-year moving averages of weather variables for Teton glaciers.

Seasonal

rank	**School-room**	Std. coeff.	**Falling Ice**	Std. coeff.	**Skillet**	Std. coeff.	**East Triple**	Std. coeff.	**Middle Triple**	Std. coeff.	**West Triple**	Std. coeff.
1	Spring P	0.316	Spring P	0.158	Spring P	0.879	Winter T	-0.108	Fall T	-0.121	Spring P	1.060
2	Spring T	-0.267	Fall P*	-0.120	Fall T*	0.510	Spring P	0.098	Summer T	-0.116	Fall T*	0.713
3	Winter T	-0.243	Winter T	-0.086	Winter T	-0.359	Summer P	0.091	Winter P	0.094	Summer P*	-0.682
			Summer T	-0.077	Winter P	0.333					Winter P	0.652
											Summer T	-0.629

Annual

rank	**School-room**	Std. coeff.	**Falling Ice**	Std. coeff.	**Skillet**	Std. coeff.	**East Triple**	Std. coeff.	**Middle Triple**	Std. coeff.	**West Triple**	Std. coeff.
1	Temp	-0.257	Temp	-0.097	Temp	-0.404	Precip	0.304	Precip	0.241	Temp	-0.306
2	Precip	0.145	Precip	0.040	Precip	0.383	Temp	-0.223	Temp	-0.240	Precip	0.259

* denotes opposite correlation than expected.

retreat from 1983-1994. We also found that temperature generally increased at these glaciers during the past 60 years while precipitation generally increased at Schoolroom Glacier and decreased at Mt. Moran. The strongest one-year seasonal weather variable was precipitation and the strongest four-year seasonal variable was spring precipitation. Annual temperature was the dominant one-year influence on three glaciers and annual precipitation was the dominant influence on the remaining three glaciers while the four-year interval displayed temperature as the dominant annual weather influence. Additionally, the Petersen Glacier has ceased to exist without debris cover.

Glacier area fluctuations

Glacier areas in the Teton Range declined over the past half century, with short periods of growth. Schoolroom Glacier lost 49% of ice area from 1956-2010 (Figure 3) and fluctuated as much as 89%. Meanwhile, glaciers on Mt. Moran lost 2-45% of ice from 1967-2009 and fluctuated 9-74%. The general glacier area decline has been punctuated by short, subdecadal periods of growth such as an increase of 31% ice area at Schoolroom Glacier between 1974-1979 and 17% ice area increase at East Triple Glacier from 1979-1983. The six glaciers collectively displayed a period of overall ice growth from 1974-1983.

Our finding of periods of subdecadal ice growth contrast with conclusions of other studies in the Teton Range. Previous studies compared glacier area or volume changes between three to five dates of glacier observation (Gray et al., 1999; Edmunds, 2010). We compared glacier area changes between nine to eleven dates of glacier observation, depending on the glacier and available aerial photos. Gray et al. (1999) determined retreat at the Teton Glacier between 1954, 1963, and 1994. Edmunds (2010) determined overall retreat at the Teton, Middle Teton, and Teepe Glaciers between 1967, 1983, 1994, 2002, and 2006. Both investigators missed periods of ice growth. With our larger number of glacier observations, which include observations in the 1970s, we were able to capture these subdecadal periods of ice area growth.

Other modern glaciers in nearby western U.S. mountain ranges have exhibited episodes of ice growth during this period of time, amongst overall retreat, but the timing of ice growth has differed by region. We compared studies of western U.S. mountain glaciers (Hall and Fagre, 2003; Granshaw and Fountain, 2006; Hoffman et al., 2007; Jackson and Fountain, 2007; Josberger et al., 2007; Cheesbrough et al., 2009; Thompson, 2009) and their reports of glacier area increase, decrease, or short periods of both (Figure 11). We generalized Teton glacier advances and retreats for use in Figure 11 (see Figure 3c). Although all glaciers in western U.S. experienced decreased area over the 60 year period, some mountain ranges had periods of glacier area increase, similar to observations in the Teton Range. Notably, Teton Range glaciers exhibited growth later than those in most areas, excepting Rocky Mountain National Park. There, Hoffman et al. (2007) attributed ice advance between 1953 and 1999 to redistribution of snow by wind and avalanches.

The main period of ice growth in the Teton Range was later than periods of ice growth observed at other glaciers in the Pacific Northwest. We found that most of the Teton glaciers increased in area between 1974-1983 when annual temperatures were relatively low and annual and spring precipitation were relatively high. Conversely, most Teton glaciers decreased in area between 1983-1994 when annual temperatures increased and annual precipitation decreased. The period of ice growth in Teton glaciers is contrary

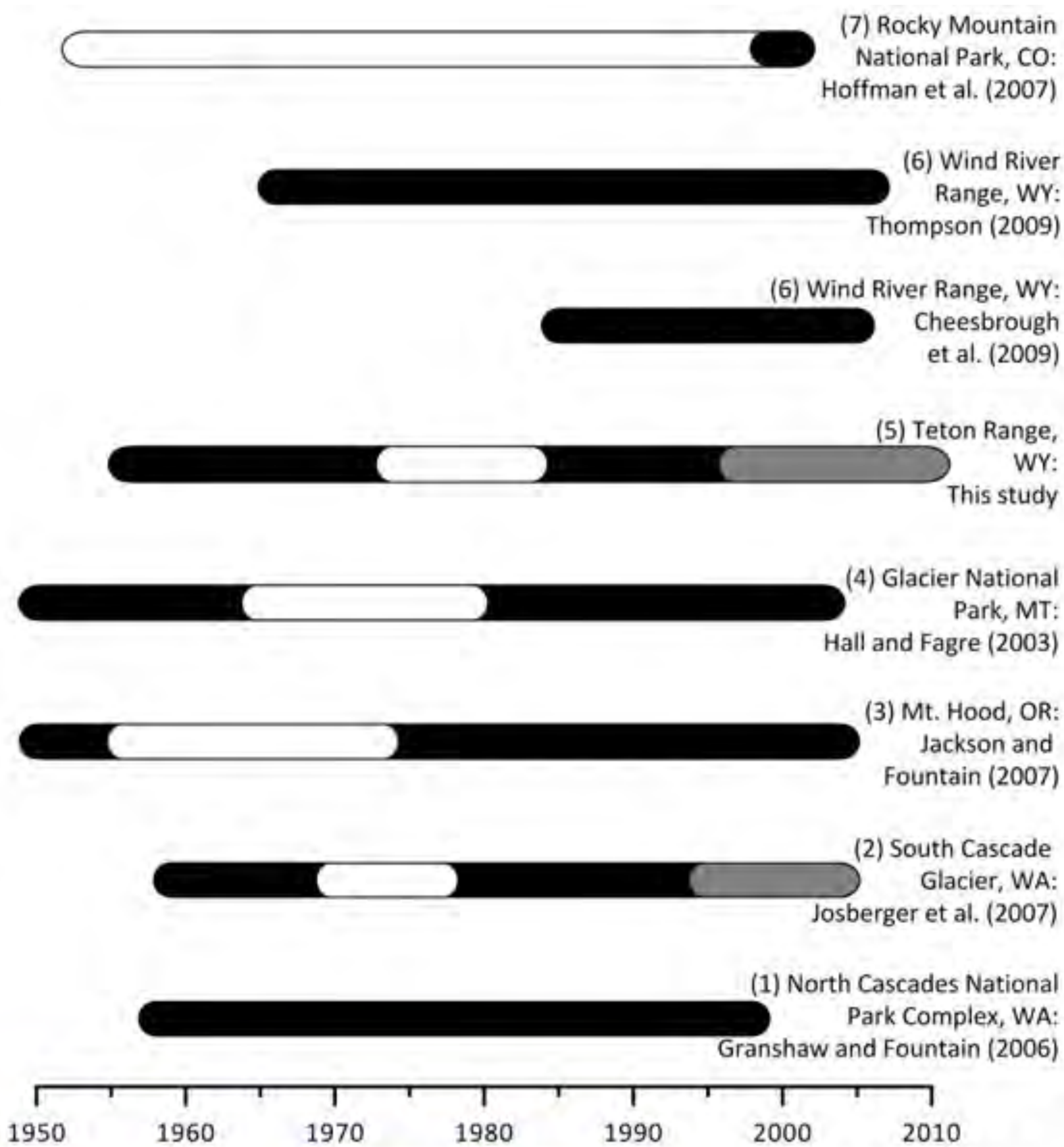

Figure 11. Comparision of periods of modern glacier growth in western U.S. (see map). The number and frequency of observations vary between studies. Most glaciers decreased in area (black). Some grew (white) between 1955-1985 and gray indicate short periods of both growth and retreat. Note that Teton Range glaciers exhibited growth later than those in most areas, excepting Rocky Mountain National Park.

to a general expectation of coincident ice fluctuation at all regional mountain ranges. This period of growth likely reflects a glacier response to a combination of regional atmospheric forcings beyond the scope of this thesis (e.g., Pacific Decadal Oscillation).

Glacier area – weather relationship implications

Partial least squares analysis (PLS) determined the strongest correlations between meteorological variables and glacier area. The strongest one-year seasonal weather variable was precipitation, while annual average precipitation and temperature were equally influential. The strongest four-year averaged variables, which likely reflect glacier response more accurately, are spring precipitation and annual temperature. We also determined that the patterns of response to these weather variables are not the same for each glacier.

Falling Ice Glacier is strongly correlated with spring and annual temperature, as the area changes of the glacier are generally linear. This result suggests that higher spring and annual temperatures lead to smaller glacier areas. If mean spring temperatures remain above freezing and/or if they are coincident with storms, they would contribute to glacier loss through ablation. Conversely, spring temperatures occasionally dip below freezing and, if coincident with precipitating storms, would contribute to increasing glacier mass.

We suggest that smaller temperature variability forces this glacier, which has limited area variability due to a dynamic terminus control in the form of a calving ice fall. Annual temperatures at Mt. Moran tended to remain below freezing until 1998, after which they remained above freezing until 2009.

PLS determined the strongest one-year variable for the Schoolroom Glacier was winter temperature followed closely by summer precipitation. These two weather variables operate in opposite seasons to produce typical annual glacier area fluctuations. That is, glacier area increases in winter as cooler temperatures allow more accumulation than ablation to occur, though this factor is eliminated and perhaps controverted, if temperatures remain below freezing all winter. Alternatively, as summer precipitation decreases, glacier area decreases. However, this issue may not be directly caused by reduced precipitation input as much as by reduced cloudiness or shade from direct sun (Rupper and Roe, 2008).

Schoolroom Glacier is heavily influenced by wind. The glacier is located on the immediate eastern slope of the watershed divide for the Teton Range and below a trail pass aptly named Hurricane Pass. This pass is often windy with high gusts. A high, low-relief surface is located to the southwest and upwind of the glacier. It is highly likely that snow deposited on this surface and further upwind is redeposited onto the glacier by wind, and may be a primary factor for the continued existence and area fluctuations of this clean-ice glacier.

The strongest one-year weather-ice area relationships with the remaining four glaciers are with different seasonal precipitation values. Skillet Glacier and West Triple Glacier exhibited the strongest correlations with spring precipitation. Winter and summer precipitation are the strongest weather variables for East and Middle Triple Glaciers, respectively. Spring precipitation, especially when it falls as snow, can lengthen the glacial accumulation season and thus shorten the ablation season, as discussed below. Spring precipitation may also correlate with cloudiness, which will also reduce ablation. As mentioned above, orographic precipitation can contribute larger amounts of mass to these glaciers than are likely captured by the PRISM outputs. Higher precipitation in any season is often accompanied by more storminess and thus more clouds can provide both shade from shortwave radiation and retain reflected longwave radiation (Rupper and Roe, 2008). The former situation would retard ablation and the latter would not. Records of air pressure would help to constrain this factor.

The four-year moving average PLS results are different from those found with one water year. As is discussed in detail below, spring precipitation was the strongest seasonal factor at four glaciers and a close second strongest factor at a fifth. We find the dominant annually averaged weather variable is temperature at four of six glaciers from the four-year moving average analysis and a very close second strongest factor at another glacier.

Spring precipitation produces more consistent results than the other variables. It is the strongest seasonal variable at four glaciers in the four-year analysis. Figure 8 shows that spring and annual precipitation increased during 1979-1984 as these glaciers increased in ice area. The importance of this variable is further reinforced by glacier observations in 2009 and 2010, which revealed larger glacier areas coincident with cold, wet spring weather (see below).

These four-year results better represent the glaciological response to the meteorological influences than does the simple year-by-year comparison. Results from the four-year time interval converge on a specific variable and season as well as an annual weather variable. However, we are concerned that different weather variables were determined to be the dominant weather influences for these glaciers at different time-averaged intervals.

There are at least three possible causes for this divergence in dominant seasonal and annual variables. One may be that more frequent additional glacier observations are needed to determine the natural response time and thus the appropriate analysis interval. A second possible cause for the difference could be the averaging of the coarse spatial resolution PRISM data (4 km^2) and the artifacts associated with such large topographic relief. A third cause may be that a cold, dry winter would lower the annual temperature, but would not necessarily increase ice area, as the air temperature is likely below freezing most of the winter. A subsequent cold, wet spring could then increase the glacier area while further reducing the low annual temperature. This new determination of spring precipitation and annual temperature as dominant weather variables from the four-year analysis indicates that these glaciers are influenced by both temperature and precipitation. The more detailed seasonal analysis suggests that comparing annual temperature to ice fluctuations may blur important relationships, as the annual temperature may be reduced by colder winter temperatures, which are not necessarily influential in the glacier mass balance.

Existing observations confirm the statistical findings. Specifically, the four-year averaged weather conditions indicate that spring precipitation is the dominant influence on glacier area for four of the six glaciers and is only a slightly weaker second strongest influence for a fifth glacier. Thus, for five of the six glaciers, spring precipitation bears a strong statistical relationship to glacier area. This effect appears to have been operative during the period 1974-1983, which saw glacier growth in a period with above-normal spring (and fall) precipitation (Figure 6). The water years 2009-2011 are also instructive in terms of direct observation of glacier mass balance. Both 2009 and 2011 were above-normal water years, while 2010 was below normal. However, all three water years experienced cool, wet springs. Quickbird satellite imagery showed snow cover on all glaciers in September 2009, near the end of the water year. For the 2009 and 2010 water years, at least, fresh snow mantled the entire Schoolroom Glacier into September, indicating positive mass balance for those water years. This pattern appears to have continued into 2011. Thus, while glacier expansion has not yet been documented for these years, spring precipitation correlates observationally with positive mass balance. The actual influence may be through multiple influences. First, high spring precipitation may add snow to the glacier, if air temperature is sufficiently low. Second, high spring precipitation implies cloudiness, which reduces incident infrared radiation and can reduce melting. Third, wetter spring conditions tend to occur in concert with cooler temperatures. Both the second and third influences would effectively reduce the length of the ablation season. Thus, the correlation of spring precipitation and glacier area may reflect glacier mass balance through mass addition or reduced mass loss in wetter spring conditions.

The contrasting relationships of seasonally and annually averaged weather conditions are also instructive. We infer that seasonally averaged weather conditions are likely to reflect weather-glacier relationships than are annually averaged weather conditions. For example, annually averaged weather conditions mask important variables such as spring precipitation and the contrast between winter and summer temperatures. A dry water year overall, such as 2010, may have a wet spring that begets positive glacier mass balance, as observed at the Schoolroom Glacier, but will be missed if only annually averaged weather conditions are used in statistical tests. Similarly, a cold winter may be very dry, with little mass added to glaciers, but may reduce the annually averaged temperature despite an ensuing anomalously warm summer that melts snow and ice quickly. For these reasons and others, we conclude that seasonally averaged weather conditions more effectively predict glacier response.

Notably, these statistical relationships suggest, rather than prove, glacier-weather relationships. Direct mass balance measurements spanning several years will be necessary to firmly demonstrate these relationships.

El Niño-Southern Oscillation

The El Niño-Southern Oscillation (ENSO) index does not appear to correspond to the observed changes in glaciers in the Teton Range. Periods of glacier advance and retreat have corresponded with periods of dominant El Niño phases. In contrast, Wise (2010) used Snake River streamflow to determine that this region has a strong precipitation response to ENSO conditions, similar to the Pacific Northwest. Drier years are coincident with El Niño phases and the warm phase of the Pacific Decadal Oscillation. Wise (2010) also determined that precipitation in this region is strongly affected by slight shifts in storm track position. Wet years are coincident with more southerly storm tracks across the U.S. and dry years occur with storm tracks shifted over northwestern U.S.

We compared the multivariate ENSO index from Wolter (2011) to glacier area (Figure 12). Generally, there is a weak correspondence between glacier area and the ENSO index. We observed glacier retreat during strong La Niña phases and some glacier growth during strong El Niño phases.

Conclusions

Teton Range glacier areas decreased from 1956-2010, punctuated by episodes of

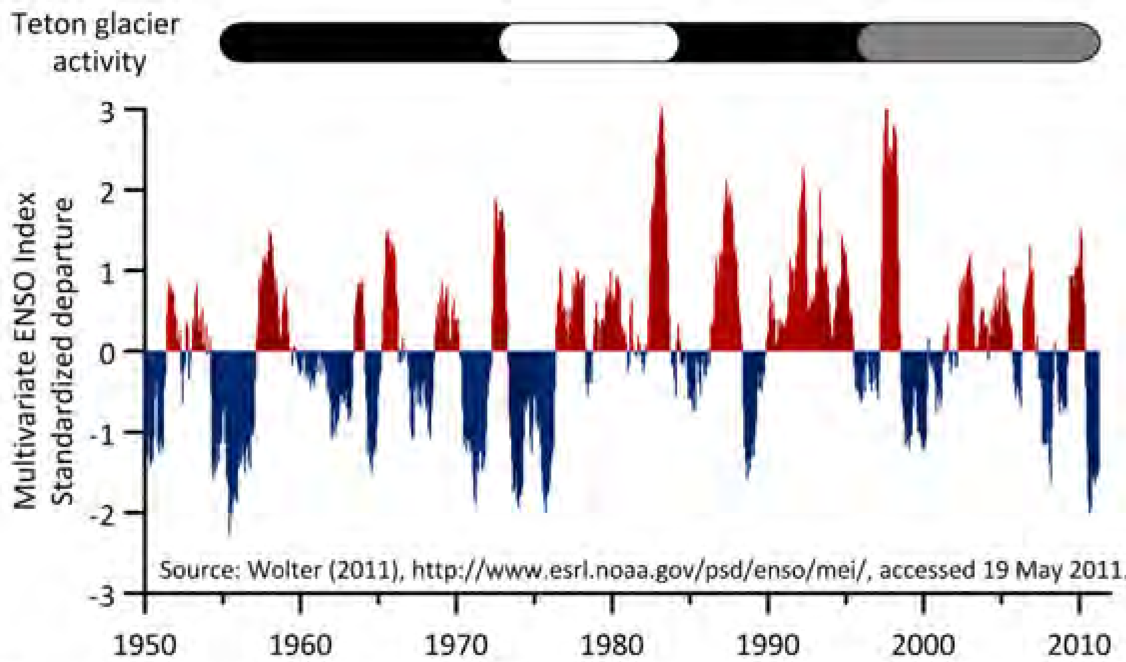

Figure 12. Comparision of El Niño Southern Oscillation (ENSO) index to Teton glacier retreat (black), growth (white), and periods of mixed activity (gray). Negative ENSO values denote the cold ENSO phase (La Niña) and positive values denote the warm ENSO phase (El Niño). Teton glaciers generally do not follow the index.

subdecadal-scale ice growth and retreat. A dominant period of ice growth occurred ca. 1974-1983, and this period of advance occurred later than did advances of glaciers in mountain ranges closer to the Northwest Pacific Coast. We also determined that the Petersen Glacier is no longer a clean ice glacier, but is currently a debris-covered glacier.

We found that temperature generally increased at these glaciers during the past 60 years while precipitation generally increased at Schoolroom Glacier and decreased at Mt. Moran. The strongest correlations to weather variables averaged over four years, which we consider to best represent the glacier response time, is with spring precipitation and annual temperature. The correlation between spring precipitation and glacier area at five of the six glaciers corresponds with recent observations. This strong correlation is a novel finding of this study, and deserves further examination.

References

Abdi, H., 2003, Partial least squares (PLS) regression, *in* Lewis-Beck, M., Bryman, A., and Futing, T., eds., 2003, Encyclopedia for research methods for the social sciences: Thousand Oaks, CA, Sage, p. 792-795.

Arendt, A.A., Echelmeyer, K.A., Harrison, W.D., Lingle, C.S., and Valentine, V.B., 2002, Rapid wastage of Alaska glaciers and their contribution to rising sea level: Science, v. 297, no. 5580, p. 382-386, doi: 10.1126/science.1072497.

Barry, R.G., 2006, The status of research on glaciers and global glacier recession: A review: Progress in Physical Geography, v. 30, no. 3, p. 285-306, doi: 10.1191/0309133306pp478ra.

Benn, D.I., and Evans, D.J.A., 1998, Glaciers and Glaciation: London, England, Arnold, 734 p.

Bennett, M.R., and Glasser, N.F., 1996, Glacial geology: Ice sheets and landforms: Chichester, England, John Wiley and Sons, 364 p.

Cheesbrough, K., Edmunds, J., Tootle, G., Kerr, G., and Pochop, L., 2009, Estimated Wind River Range (Wyoming, USA) glacier melt water contributions to agriculture: Remote Sensing, v. 1, p. 818-828, doi: 10.3390/rs1040818.

Clark, D.H., Clark, M.M., and Gillespie, A.R., 1994, Debris-covered glaciers in the Sierra Nevada, California, and their implications for snowline reconstructions: Quaternary Research, v. 41, no. 2, p. 139-153, doi: 10.1006/qres.1994.1016.

Corbin, J., 2009, personal communication in person on 4 September 2009.

Daly, C., 2006, Guidelines for assessing the suitability of spatial climate data sets: International Journal of Climatology, v. 26, p. 707-721, doi: 10.1002/joc.1322.

Daly, C., Gibson, W., Doggett, M., Smith, J., and Taylor, G., 2010, Near-real-time monthly high-resolution precipitation climate [and average maximum/minimum temperature] data set for the conterminous United States: Corvallis, Oregon, PRISM Climate Group, http://prismmap.nacse.org/nn/, accessed January 2011.

Daly, C., Gibson, W., and Taylor, G., 2002, 103-Year high-resolution precipitation [and temperature] climate data set for the conterminous United States: Corvallis, Oregon, PRISM Climate Group, http://prismmap.nacse.org/nn/, accessed January 2011.

Daly, C., Neilson, R.P., and Phillips, D.L., 1994, A statistical-topographic model for mapping climatological precipitation over mountainous terrain: Journal of Applied Meteorology, v. 33, p. 140-158.

Edmunds, J.F., 2010, Glacier variability (1967-2006) in the Teton Range, Wyoming, U.S.A. [M.S. Thesis]: Laramie, University of Wyoming, 62 p.

Elder, K., Fullerton, S., and Tonnessen, K., 1994, Winter mass balance measurements on Teton Glacier begin to build basis for predicting seasonal melt and runoff: Park Science: A Resource Management Bulletin, v. 14, no. 3, p. 11-13.

Fryxell, F.M., 1935, Glaciers of the Grand Teton National Park of Wyoming: Journal of Geology, v. 43, no. 4, p. 381-397.

Garmin, 2006, GPSMAP 60Cx and 60CSx: Garmin International Inc., 2 p., http://www8.garmin.com/specs/GPSMAP60CSx0206.pdf, accessed November 2009.

Granshaw, F.D., and Fountain, A.G., 2006, Glacier change (1958-1998) in the North Cascades National Park Complex, Washington USA: Journal of Glaciology, v. 52, no. 177, p. 251-256.

Hall, M.H.P., and Fagre, D.B., 2003, Modeled climate-induced glacier change in Glacier National Park, 1850–2100: BioScience, v. 53, no. 2, p. 131-140.

Hoffman, M.J., Fountain, A.G., and Achuff, J.M., 2007, 20th-century variations in area of cirque glaciers and glacierets, Rocky Mountain National Park, Rocky Mountains, Colorado, USA: Annals of Glaciology, v. 46, p. 349-354.

Jackson, K.M., and Fountain, A.G., 2007, Spatial and morphological change on Eliot Glacier, Mount Hood, Oregon, USA: Annals of Glaciology, v. 46, no. 1, p. 222-226, doi: 10.3189/172756407782871152.

Josberger, E.G., Bidlake, W.R., March, R.S., and Kennedy, B.W., 2007, Glacier mass-balance fluctuations in the Pacific Northwest and Alaska, USA: Annals of Glaciology, v. 46, p. 291-296.

Krimmel, R.M., 2002, Glaciers of the Conterminous United States: Glaciers of the Western United States, *in* Satellite image atlas of glaciers of the world: North America, Williams, R.S. Jr. and Ferrigno, J.G., eds., United States Geological Survey: Washington, D.C., p. J329-J377.

Love, J.D., Reed, Jr., J.C., and Pierce, K.L., 2007, Creation of the Teton landscape: A geologic chronicle of Jackson Hole and the Teton Range: Moose, WY, Grand Teton Association, 132 p.

Medley, B., 2008, A method for remotely monitoring glaciers with regional application to the Pacific Northwest [M.S. Thesis]: Corvallis, Oregon State University, 85 p.

Meyer, G.A., Fawcett, P.J., and Locke, W.W., 2004, Late Pleistocene equilibrium-line altitudes, atmospheric circulation, and timing of mountain glacier advances in the interior northwestern United States, *in* Haller, K.M., and Wood, S.H., eds., Geological field trips in southern Idaho, eastern Oregon, and northern Nevada: Reston, VA, USGS Open-File Report, 2004-1222, p. 63-68.

Minder, J.R., Mote, P.W., and Lundquist, J.D., 2010, Surface temperature lapse rates over complex terrain: Lessons from the Cascade Mountains: Journal of Geophysical Research, 115, D14122, 13 p., doi: 10.1029/2009JD013493.

Minitab, 2010, Partial least squares, Regression, Statistics, Help, 16.1.1.0

Paterson, W.S.B., 1994, The physics of glaciers (3d ed.): Oxford, England, Elsevier, 480 p.

Plummer, M., and Cecil, L.D., 2005, Calibration of a glacier model to historic variations of the Teton Glacier to improve model-based inferences about glacier-climate relationships, *in* Proceedings, Geological Society of America, 2005 annual meeting, Salt Lake City, UT: Boulder, CO, Geological Society of America, v. 37, no. 7, p. 41.

Plummer, M.A., and Phillips, F.M., 2003, A 2-D numerical model of snow/ice energy balance and ice flow for paleoclimatic interpretation of glacial geomorphic features: Quaternary Science Reviews, v. 22, p. 1389-1406, doi: 10.1016/S0277-3791(03)00081-7.

Reed, Jr., J.C., 1967, Observations on the Teton Glacier, Grand Teton National Park, WY, 1965 and 1966 *in* Geological Survey Research 1967: USGS Professional Paper 575-C, p. C154-C159.

Rupper, S., and Roe, G., 2008, Glacier changes and regional climate: a mass and energy balance approach: Journal of Climate, v. 21, p. 5384-5401, doi: 10.1175/2008JCLI2219.1.

Thompson, D.R., 2009, Glacier variability (1966-2006) in the Wind River Range, Wyoming, U.S.A. [M.S. Thesis]: Laramie, University of Wyoming, 75 p.

United States Geological Survey, 1968a, Grand Teton Quadrangle, Wyoming, Teton County: U.S. Geological Survey Topographic Map, scale 1:24,000.

United States Geological Survey, 1968b, Mount Moran Quadrangle, Wyoming, Teton County: U.S. Geological Survey Topographic Map, scale 1:24,000.

United States Geological Survey, 2011, National water information system: web interface: United States Geological Survey, http://waterdata.usgs.gov/usa/nwis/, accessed April 2011.

Wise, E.K., 2010, Climate-streamflow linkages in the North-Central Rocky Mountains: implications for a changing climate: Annals of the Association of American Geographers, v. 100, no. 4, p. 806-817.

Wolter, K., 2011, Multivariate ENSO index (MEI): National Oceanic and Atmospheric Administration Physical Sciences Division, http://www.esrl.noaa.gov/psd/enso/mei/, accessed May 2011.

Chapter III: Modeling small glaciers in the Teton Range, Wyoming

Abstract

Two-dimensional numerical glacier energy mass balance modeling was employed in an attempt to explain observed glacier area changes in terms of mass balance processes. Energy mass balance model inputs included digital elevation models of the target glaciers, temperature and precipitation output from the Parameter-elevation Regressions on Independent Slopes Model (PRISM), and weather station data from locations in and around the Teton Range. We ran four tests and associated sensitivity analyses. The energy mass balance model does not yield positive mass balance in glacier accumulation areas using reasonable magnitudes of weather fluctuations based on the PRISM output. Using the actual weather station data for selected short periods in the record that feature low temperature and high precipitation, the energy mass balance model produced positive mass balance at three glaciers on Mt. Moran. We interpret that the energy mass balance model more successfully calculates mass balance using the more numerous and mixed elevations of the weather station data. However, this model may overestimate melting at the glaciers, as ice expansion observed in archival aerial photographs was reproduced as positive mass balance in only one portion of one model test at one glacier. We conclude that wind redistribution of snow is an important weather influence on these glaciers, especially at the Schoolroom Glacier, and that more data recorded by high elevation weather stations are needed to better understand the energy mass balance of glaciers in the Teton Range.

Introduction

Mountain glaciers are important indicators of regional and global climate change

(Barry, 2006), and glaciers in Grand Teton National Park, Wyoming (GTNP) are prime examples. Currently, at least ten named glaciers occupy the high alpine regions of the Teton Range. As these remote glaciers are small (1.7 km^2 area; Krimmel, 2002) and occupy high elevation areas in a semi-arid, mid-latitude region, they are likely to be very sensitive to climatic fluctuations.

Remote glaciers tend to receive less attention than more easily accessible glaciers, even though they may be more strongly affected by climate warming (Arendt et al., 2002). Area fluctuation of glaciers in GTNP can be indicators not only of regional climate change, but also of the broader impacts of climate change on the region. Evaluating the historic behavior of these glaciers complements historical climate measurements by providing regionally specific information on landscape responses (Hall and Fagre, 2003). In a companion study, we documented fluctuations of seven glaciers in GTNP using archived aerial photographs and satellite data, during the period 1956-2010.

Our goal of this study is to model glacier mass balance in the period 1956-2010, in order to explain climatic influences on observed glacier area fluctuations. We use an energy balance inclusive glacier mass balance model for six of the Teton Glaciers (Table 1). We used model hind-casting to explore the mass balance processes in these glaciers. We conducted four tests, which consisted of multiple simulations using the mass balance model developed by Plummer and Phillips (2003), and performed sensitivity analyses to determine the required magnitudes of altered climate conditions to produce positive mass balance on the Schoolroom, Falling Ice, Skillet, and the Triple Glaciers.

Previous Work

Plummer and Phillips (2003) developed a two-dimensional numerical energy mass

Table 1. Characteristics of Teton glaciers in this study. Petersen Glacier is included in the PRISM climate data set as four points are considered to be better than three and some small discontinuous accumulation areas are visible in some air photos (Appendix B), thus we include Petersen Glacier characteristics here.

Teton glaciers	Maximum elevation [m]	Minimum elevation [m]	Aspect	Mean area [m^2]
Petersen	3190	2920	NE	---
Schoolroom	3180	3070	NE	28170
Falling Ice	3585	3210	SE	131840
Skillet	3410	2950	E	129510
East Triple	3300	2920	N	97260
Middle Triple	3420	2865	NE	199060
West Triple	3515	2920	N	164900

balance model, to determine the balance and extent of paleoglaciers in Bishop Creek of the Sierra Nevada. Plummer and Phillips (2003) also used two-dimensional flow models that portrayed the accumulation and flow of ice in response to given patterns of accumulation and ablation. They used sensitivity analysis to determine that secondary influences such as wind speed and cloudiness affect glacier mass balance.

Plummer and Cecil (2005) applied the model developed in Plummer and Phillips (2003) to predict future conditions of the Teton Glacier. Plummer and Cecil (2005) used historical photos of Teton Glacier and weather records from early 1900s to the present to calibrate their model. They found that glacier size and aspect affected responses to temperature fluctuations and thus suggested that modern retreats may not wholly reflect modern warming.

Laabs et al. (2006) applied the model developed in Plummer and Phillips (2003) to paleoglaciers at the time of the last glacial maximum (LGM) in the Wasatch and southern Uinta Mountains to constrain paleoclimatic conditions. Laabs et al. (2006) assumed that modern temperature and precipitation lapse rates represent those during the LGM. They determined that the Little Cottonwood glacier in the Wasatch Mountains required more precipitation to grow to its LGM limits than did glaciers in the Uinta Mountains. They attributed the increased precipitation to moisture derived from the surface of glacial Lake Bonneville, a relationship similarly documented through equilibrium line altitude patterns around the LGM.

In Chapter II, we document the current status of the small alpine glaciers in the Teton Range by quantifying the areal extent of seven glaciers named on U.S. Geological Survey maps (USGS, 1968a & b) (Petersen, Schoolroom, Falling Ice, Skillet, and Triple Glaciers) in GTNP over the past fifty years. These glaciers are a subset of ten named glaciers in the Teton Range. We determined that 1) Six of the seven named glaciers are still clean-ice glaciers. The seventh named glacier, Petersen Glacier, has degraded to a debris-covered glacier. 2) Glacier ice area decreased from 1956-2010, but this decrease was interrupted by subdecadal periods of ice growth and shrinkage (see below). 3) Seasonal precipitation (three-month sums for a seasonal quarter of a water year) is the dominant influence for five of the glaciers in the Teton Range while annual water year temperature strongly influences areal changes in three glaciers and annual water year precipitation strongly influences the areal changes in the other three glaciers. When weather conditions are averaged over the four years prior to each glacier observation, spring precipitation emerges as the dominant correlate with glacier area.

Study Area

Regional physiography provides ideal conditions for the maintenance of small mountain glaciers in the Teton Range (Figure 1). The NNE-SSW trending Teton Range (~70 km long by 20 km wide) is strongly affected by moisture-laden storms from the west. Storm systems from the Pacific Ocean funnel eastward to the end of the Snake River Plain and into the Teton Range. The Teton Range is the first major orographic barrier for the moist Pacific westerlies in eastern Idaho and western Wyoming (Meyer et al., 2004; Love et al., 2007). Figure 2 illustrates this orographic pattern, which leaves mountain ranges to the north and south of the Eastern Snake River Plain dry (mean annual precipitation 500-1300 mm) relative to the wetter Teton Range and Yellowstone Highlands (mean annual precipitation 1500-2000 mm).

The Teton Range is in the northeastern Basin and Range Province. The two highest peaks (Grand Teton (4197 m) and Mt. Moran (3842 m)) are located on the eastern footwall of the east-dipping, normal Teton Fault bounding Jackson Hole basin and the Teton block. Since the initiation of displacement along the Teton Fault, the watershed divide has migrated from a position adjacent to the fault in the east to a position nearly 8 km westward. This westward migration was aided not only by tectonic uplift, but also by numerous glaciations. Dramatic U-shaped canyons have been carved between steep peaks with high relief (2065-4197 m). Much of the older Bull Lake (~160-130 ka) deposits remain exposed in the southern half of GTNP whereas they were overridden by the younger Pinedale (~30-12 ka) in the northern half (Love et al., 2007). Glaciers persist in the Teton Range due to wet westerly winds, orography, aspect, and shading provided by steep, high peaks. Currently all runoff from the west and east sides of the Teton Range drains into the Snake River system.

In Chapter II, we observed glaciers ice fluctuations within the Teton Range. Generally, glacier ice area decreased from 1956-2010, but this was interrupted by subdecadal periods of ice growth and shrinkage. Most glacier ice areas declined from

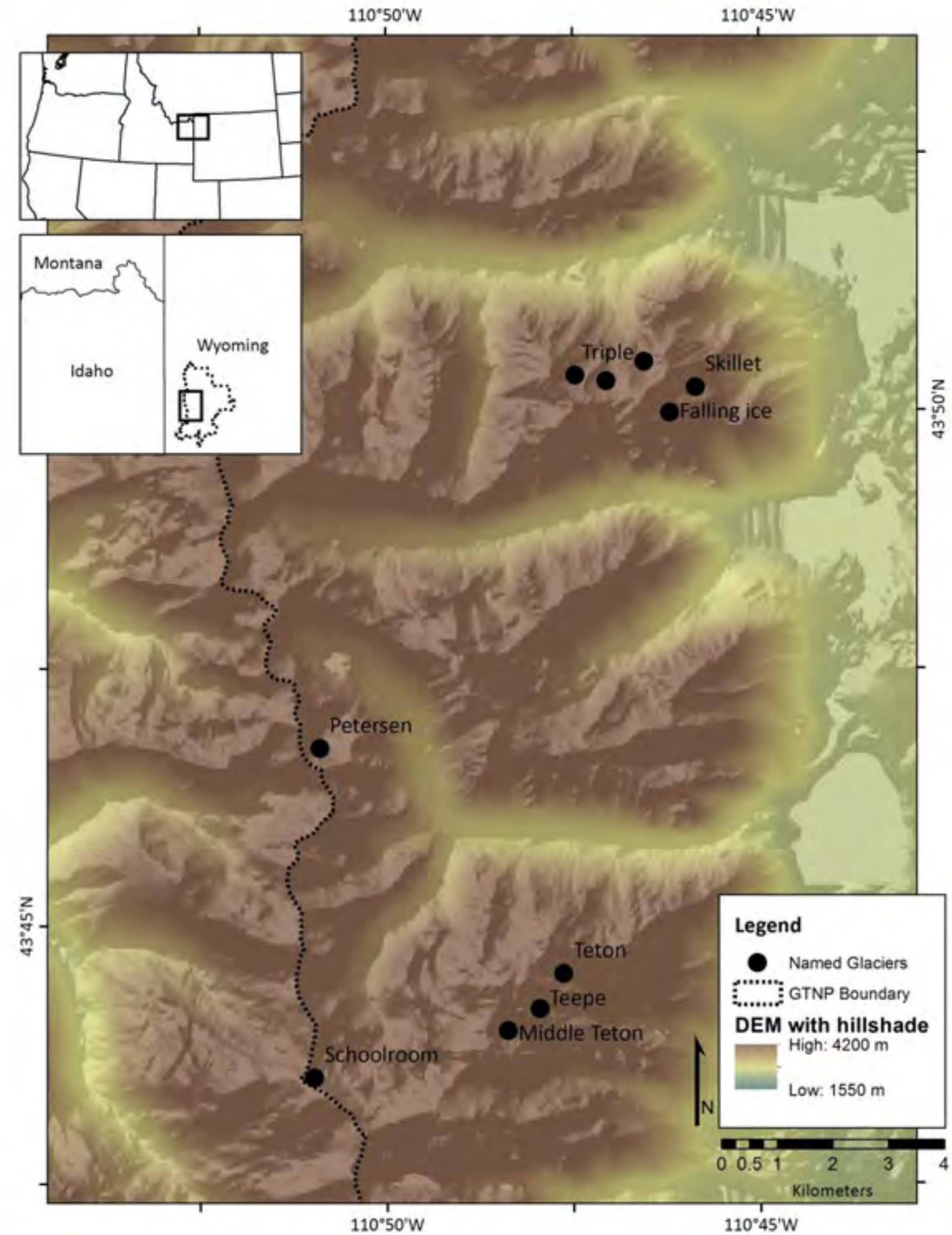

Figure 1. Topographic map of the field area. Black circles indicate the named glaciers. The Triple Glaciers are further named East, Middle, and West Triple Glacier. This study did not focus on the Petersen, Teton, Teepe, or Middle Teton Glaciers. A dashed line is the park boundary, which is also the drainage divide in this portion of the park.

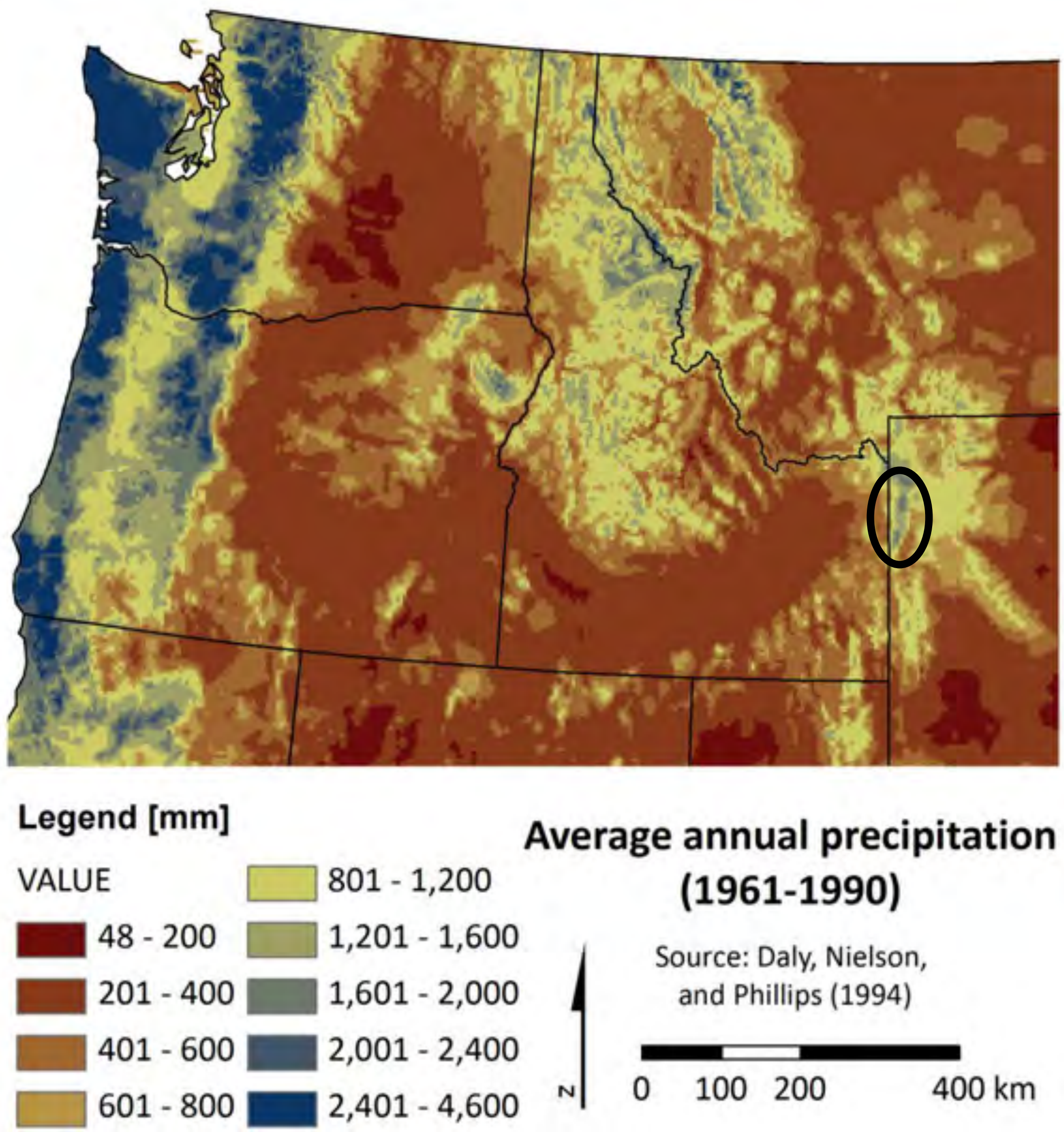

Figure 2. Map of average annual precipitation in western U.S. from Daly et al. (1994). An oval highlights the Teton Range.

1956-1974 (except at Falling Ice and Middle Triple glaciers). Most of the glaciers grew from 1974-1983, while a couple of others (Middle and West Triple Glaciers) grew from 1979-1989. All glaciers retreated from 1989-1994 and a few (Falling Ice, Skillet, and Middle Triple glaciers) continued to retreat by 2006 while two (Schoolroom and East Triple glaciers) advanced from 1994-2006. Four glaciers increased in ice area from 2006-

2009 (all but Middle and East Triple glaciers). Clearly, the episodic growth of these glaciers requires positive mass balance, and the energy mass balance model should reproduce positive mass balance using the weather conditions during those periods of growth.

Methods

The mass balance of a glacier is the relationship between ice accumulation, storage, and melting, and indicates whether a glacier should be expanding or contracting and whether those trends will persist (Sugden and John, 1976). Mass balance is often modeled because conventional mass balance measurement programs, based on direct field measurement of accumulation and ablation, are too costly and difficult to maintain for the >160,000 glaciers on Earth (Arendt et al., 2002). Mass balance models are used to quantify and illustrate processes of glacier mass transport. Results of these models can be used to describe the status of a glacier, such as whether a glacier is actively advancing, retreating, or stagnant.

Model

The model developed by Plummer and Phillips (2003) is a two-dimensional glacier model that may be applied to determine steady-state glacier shapes and distributions for a broad range of climatic conditions. The model operates in the ESRI ArcView v3.x GIS computer software environment and requires a digital elevation model (DEM) and solar angles input file to produce a viewfactor or insolation grid for each month (used for incoming shortwave radiation calculations). A climate input file of monthly means for a water year is required to produce an annual energy mass balance grid of snow for the same water year. The model produces a mass balance grid by calculating two-dimensionally, in the horizontal-plane, distribution of snow accumulation using a surface mass and energy balance approach. This approach uses a relatively accurate representation of the effects of topography on shortwave radiation, which is the largest component of the surface energy balance (Plummer and Phillips, 2003). This new grid can be used as an input file along with the DEM in a 2-D flow model (based in the FORTRAN software environment) for any given amount of time to “grow” the glacier in ice thickness (ultimately ending at steady-equilibrium), assuming the mass balance grid has some quantity of positive values.

The energy mass balance model can run multiple climate scenario simulations. Climate fluctuations from the climate input file can be applied as additive changes to temperature and multiplicative changes to precipitation (Plummer and Phillips, 2003). That is, a change to temperature of -2°C would subtract 2°C from every month in the climate input file and a change to precipitation of 2 times would multiply the precipitation value of every month in the climate input file by 2 times.

We used only the energy mass balance portion of the Plummer and Phillips (2003) model, and did not use the ice flow model portion. As most of these glaciers are unlikely to attain steady-state equilibrium within a small number of years (such as the several year time periods between glacier observations in Chapter II), applying the flow model to a transient state situation would not be productive. Additionally, most of our model simulations do not yield positive mass balance at the target glaciers within reasonable or observed meteorological conditions. For simplicity, we will refer to the energy mass balance model (Plummer and Phillips, 2003) in this chapter as “the model.”

Model inputs

We applied information from a number of sources to the model. We used two 10 m DEMs, one over Schoolroom Glacier (384 rows by 401 columns) and another over Mt. Moran covering the area of the five glaciers in that complex (275 rows by 399 columns). We used insolation grids from Plummer (pers. comm., 2011).

We used two forms of climate input. First, we used output from the Parameter-elevation Regressions on Independent Slopes Model (PRISM, Daly et al., 2002; Daly et al., 2010) to compile climate input files. Strengths and weaknesses of PRISM data are discussed in Chapter II, and that discussion pertains to this chapter as well. We used four grid cells of monthly PRISM output located over the target glaciers and applied a similar naming scheme to the pixels: Petersen, Schoolroom, Mt. Moran, and Teton. We included the Petersen pixel in the PRISM climate input file as we considered four data points to be better than three and small, discontinuous accumulation areas are visible in some air photos (Appendix B) at the Petersen Glacier. See Figure 3 for the variability of these data. We compiled linear monthly temperature and precipitation lapse rate slopes and y-intercepts as well as monthly temperature means from PRISM data. We compiled the daily standard deviation of temperature from weather stations in and near the Teton Range (see below, hereafter referred to as stations or station data), as PRISM data are monthly and draw information from these stations. We also compiled monthly wind speed and relative humidity from high elevation stations (2569-3585 m, see Table 2) as these are closest to glacier-occupied elevations. We used values of cloudiness from Plummer (pers. comm., 2011). Monthly mean values for an average water year (WY) were compiled for the period of record for glacier observations (1956-2010) and selected

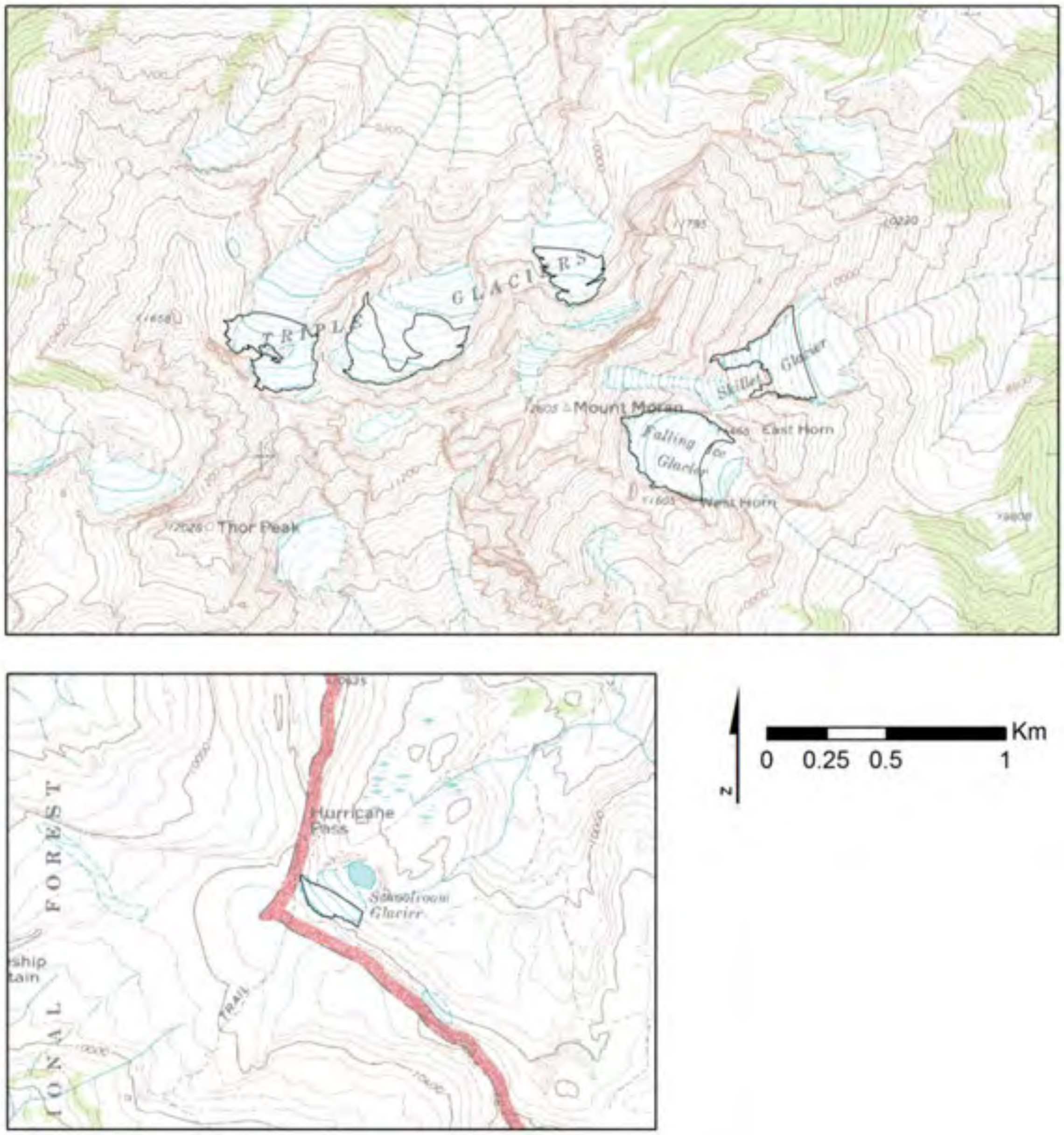

Figure 3. Glacier accumulation areas outlined in black and placed on top of 7.5 minute topographic maps (USGS, 1968 a &b).

periods of low temperature and high precipitation (1968-1976, 1982-1985, 1993, and 2008-2010) that we consider most favorable for positive glacier mass balance. During these shorter time periods, we used temperature and precipitation lapse rates, mean temperature, and standard deviation of daily temperature from the specific time period.

Table 2. Characteristics of weather stations near and within the Teton Range.

Common name	Station Type	Latitude [decimal degrees]	Longitude [decimal degrees]	Altitude [m]	Beginning (nearly) continuous record	Measurement frequency
Driggs, ID	COOP	43.73	-111.12	1865.4	1 Jun 1930	daily
Alta, WY	COOP	43.77	-111.03	1962.0	1 Jan 1948	daily
Moose, WY	COOP	43.65	-110.72	1964.1	14 Dec 1958	daily
Grand Teton	RAWS	43.72	-110.71	2039.0	1 Jan 1997	daily
Moran, WY	COOP	43.86	-110.59	2072.0	1 Mar 1911	daily
Grassy Lake	SnoTel	44.13	-110.83	2214.4	1 Oct 1980	daily
Phillips Bench	SnoTel	43.52	-110.91	2499.4	1 Oct 1980	daily
Teton Pass	WY DOT	43.50	-110.96	2569.0	5 Oct 2006	5 mins
Lake Solitude	N/A	43.79	-110.85	2778.3	11 Jul 2010	15 mins
Grand Targhee	SnoTel	43.78	-110.93	2822.4	18 Aug 2006	daily
Jackson Hole Summit	BTAVAL	43.59	-110.85	3145.0	5 Dec 1999	15 mins
Teton Saddle	SnowNET	43.73	-110.81	3539.0	25 Jun 2006	15 mins

As an alternative approach, we also constructed climate lapse rates from raw weather station data to derive high-elevation temperatures and to compare to mass balance model results using PRISM-weather data. We compiled data from 12 stations in and around the Teton Range for the period October 1955 – September 2010 (Table 2). COOPerative station data were downloaded from National Climatic Data Center website (NCDC, 2010). These stations are located in Idaho (Driggs) and Wyoming (Alta, Moose, and Moran). Snowpack Telemetry (SnoTel) station data were downloaded from Natural Resources Conservation Service's National Weather and Climate Center website (NWCC, 2010). These stations are located near Grassy Lake, Grand Targhee, and Phillips Bench. Remote Automatic Weather Station data were downloaded from the Western Regional Climate Center website (WRCC, 2010). This station is named Grand Teton and is located near Moose, Wyoming. Other weather station data were downloaded from

MesoWest (MesoWest, 2010), associated with the University of Utah. These stations include the high altitude Grand Teton Saddle station that collects data between the mid-June to mid-September, the station at the top of the gondola on Jackson Hole Summit, and Wyoming Dept. of Transportation station located at the summit of Teton Pass (Route 22).

We also used data from a modern, high elevation weather station established in spring 2006 near Lake Solitude and Petersen Glacier (Corbin, in progress). However, we have access to only two months of collected data over mid-July to mid-September 2010. The two-month portion of this station's record available to this study is included as Appendix D.

Station data were compiled into monthly data. Sub-daily data were averaged (temperature) and summed (precipitation) and converted to metric units. These were further averaged and summed into monthly data.

We compiled linear monthly temperature and precipitation lapse rate slopes and y-intercepts as well as monthly temperature means from station data. We also compiled the daily standard deviation of temperature from station data. We used monthly wind speed and relative humidity from high elevation stations (2569-3585 m). We used values of cloudiness from Plummer (pers. comm., 2011). Monthly mean values for an average water year were compiled for the period of record for glacier observations (1956-2010) and selected periods of low temperature and high precipitation (1968-1976, 1982-1985, 1993, and 2008-2010).

Tests

We performed four tests with the energy mass balance model (Plummer and Phillips,

2003) to determine the change in temperature and precipitation values required to produce positive mass balance on the target glaciers. As noted above and discussed in detail in Chapter II, we documented episodic increases in glacier ice area during the period 1956-2010, and weather conditions during those times of growth should yield positive mass balance in the energy mass balance model. In the first test (A), we used average monthly mean values in the climate file from 1956-2010 PRISM output at the Schoolroom Glacier and at the Mt. Moran glacier complex. We ran sensitivity analyses for all of the tests at stepped increments of either temperature or precipitation at both locations. In the second test (B), we used the average monthly mean values from PRISM output in the climate file from short periods (1968-1976, 1982-1985, 1993, and 2008-2010) of the most favorable weather conditions for glacier growth (low temperature and high precipitation) at the two areas of interest. The third test (C) used average monthly mean values in the climate file from regressions of the 1956-2010 station data at the two areas. The fourth test (D) used the same short periods of most favorable weather conditions (see test B) using station data at the two locations. Thus, we performed two similar tests using each source of weather time series.

Model sensitivity analysis

We ran sensitivity analyses of the mass balance of the glaciers at incremental changes in temperature (0 to -5°C) and precipitation (0.5 to 5 times) from the 1956-2010 average or from averages of the short periods of most favorable weather conditions. We determined the quantity of glacier mass balance from a model simulation output grid by first creating a polygon shapefile of each glacier's accumulation area (Figure 3). Glacier termini were approximated from glacier observations in aerial photographs (Chapter II) whereas upper ice margins were traced from the glacier's largest minimum area. For example, Middle Triple Glacier's largest minimum area was observed in 1989. To draw the accumulation area, we traced the headwall margins from 1989 and approximated the lower terminus of the accumulation area from air photos from 1967-2009. Once these accumulation area shapefiles were created, we added the mass balance grid to the ArcGIS workspace. The output grid area covered the DEM areas. We created a second shapefile to isolate the grid values to the area of the accumulation of the target glacier by extracting values from the grid using a mask of the first shapefile. From the second shapefile's layer properties, we found the mean value of the shapefile and thus of the mean mass balance over the accumulation area of the target glacier. We extracted mass balance grids for each glacier for each of the model simulation mass balance output grids.

We ran incremental changes to temperature and precipitation between reasonable ranges for each variable to determine reasonable thresholds for the tests. We determined the reasonable ranges for PRISM outputs by looking at the recent variability as seen in Figure 4. In the past half-century, temperature has fluctuated from -2 to 3.4°C and precipitation has fluctuated from -0.90 to 1.1 m or -55 to 66% from the mean. We studied seasonal weather factors in Chapter II and, as the energy mass balance model deals only with annual change, we include seasonal fluctuations in Appendix E. Figure 5 displays the annual weather variability recorded by the stations from water years 1956-2010. Fluctuations in temperature and precipitation are differences from the mean (1956-2010). From the station data, temperature varied by -2 to 1.5°C about the mean and precipitation varied -40 to 60% about the mean.

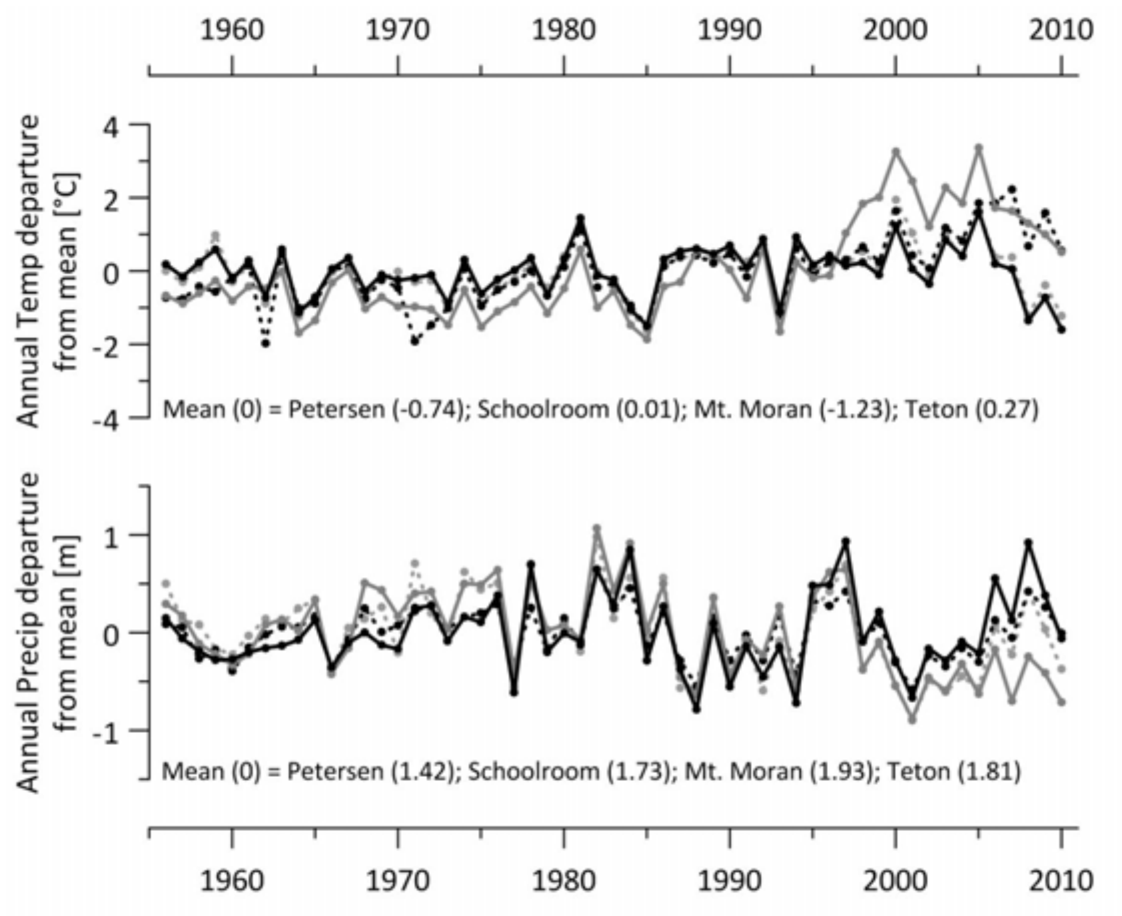

Figure 4. Annual temperature and precipitation differences from mean (1956-2010) PRISM output (labeled as zero) at the Petersen (dotted black line), Schoolroom (black line), Mt. Moran (grey line), and Teton (dotted gray line) PRISM pixels. Annual temperature range -2 to 3.4°C and preciptation range -0.90 to 1.1 m (or -55 to 66%).

Results

Using 1956-2010 conditions, the mass balance model did not produce positive mass balance. To determine the hypothetical climate conditions that would produce positive mass balance within the accumulation areas of the glaciers (Figure 3), we ran the energy mass balance model incrementally for all four tests.

From Test A, we determined that the PRISM climate input file (1956-2010) requires climate fluctuations beyond the variability in the meteorological record. Therefore, we conducted model tests using incremental departures from the actual temperature and

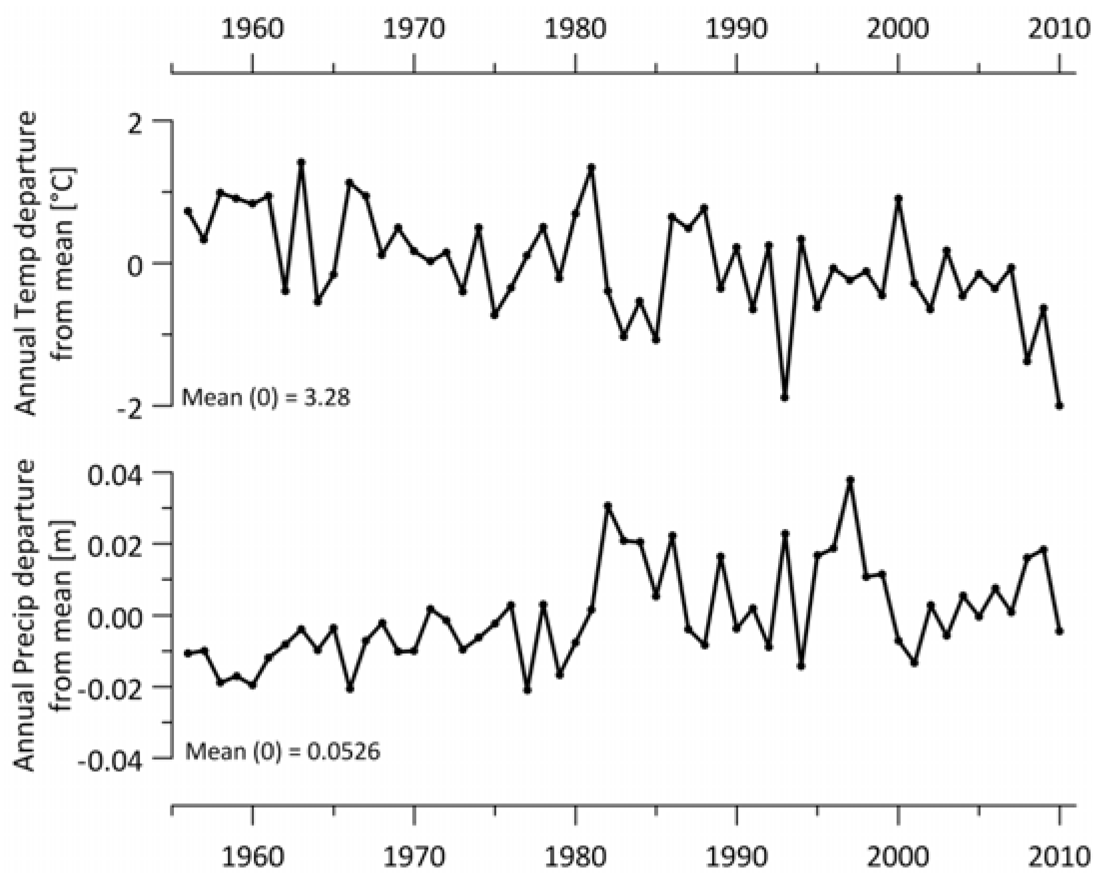

Figure 5. Mean annual temperature and precipitation differences from mean (1956-2010) (labeled as zero) at stations in and around the Teton Range. Sources of data for these stations are: COOP, RAWS, SnoTel, WY DOT, BTAVAL, and SnowNET. These stations are located at elevations of 1865-3539 m. Annual temperatures range 1.3 to 4.8°C and precipitation range 0.032 to 0.090 m (or -40 to 80%). The negative trend in temperature and the positive trend in precipitation may be attributed to the addition of higher elevation weather stations beginning in 1958.

precipitation values. A temperature decrease of more than 4.5°C below the 1956-2010 PRISM mean (holding precipitation at the mean of the record) and over 4.5 times the average precipitation (holding temperature at the mean of the record) are required in this test to produce positive mass balance at the Schoolroom Glacier (Table 3 and Figure 6). At Mt. Moran, this test required a temperature decrease of more than 4°C and more than 4 times the average precipitation at all five glaciers to yield positive mass balance (Table 4 and Figure 7).

Table 3. Results from Test A for Schoolroom Glacier with mean PRISM data (water year (WY) 1956-2010).

Change in Temperature [°C]	Precipitation multiplication factor	Schoolroom mass balance [m]
0	1	-7.11996
0	2	-4.69926
0	3	-2.7397
0	4	-0.99452
0	5	0.454816
0	1	-7.11996
-1	1	-4.98723
-2	1	-3.61187
-3	1	-2.57997
-4	1	-0.74413
-5	1	0.28747

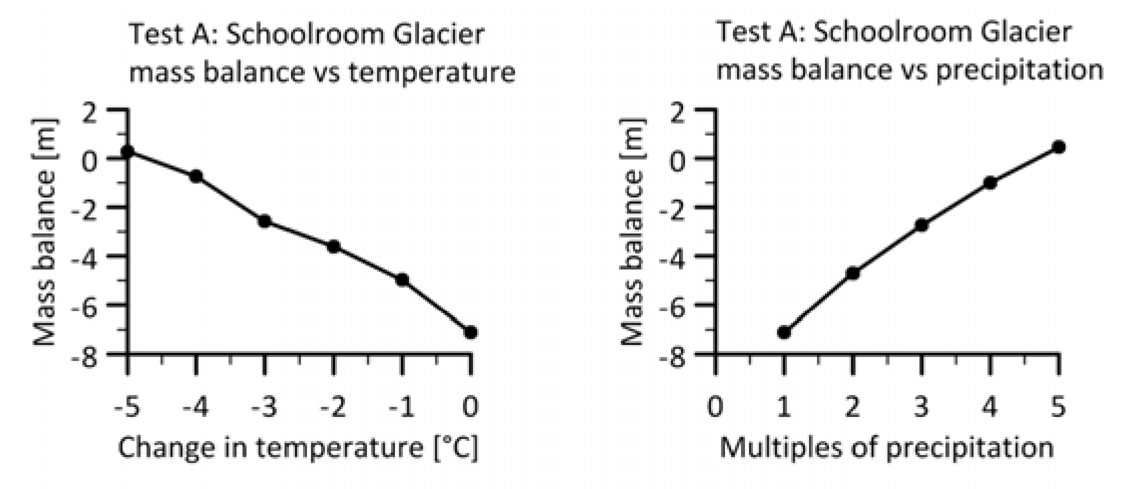

Figure 6. Results of Test A for Schoolroom Glacier versus PRISM mean (WY 1956-2010). Note that modeled mass balance does not produce positive mass balance unless temperature is reduced by 5ºC or precipitation is multiplied by 5 times.

From Test B, we determined that PRISM output for the periods of most favorable conditions for ice growth (see Methods section) also require adjustments beyond the variability in the record. At Schoolroom Glacier, the model required a decrease of more than 4°C and more than 5 times the average precipitation (Table 5 and Figure 8) for all four time periods to calculate positive mass balance. At Mt. Moran, these thresholds

Table 4. Results from Test A for Mt. Moran glacier complex with mean PRISM data (WY 1956-2010).

Change in Temperature [°C]	Precipitation multiplication factor	Skillet mass balance [m]	West Triple mass balance [m]	Falling Ice mass balance [m]	East Triple mass balance [m]	Middle Triple mass balance [m]
0	1	-7.8183474	-6.54797	-8.09295	-5.96629	-5.78679
0	2	-5.4190121	-4.03523	-5.33477	-3.72244	-3.57551
0	3	-3.3254697	-1.903	-3.00281	-1.89474	-1.65558
0	4	-1.9856546	-0.03303	-0.68093	-0.37939	-0.01077
0	5	0.00777296	1.424138	0.854448	0.877607	1.353935
0	1	-7.8183474	-6.54797	-8.09295	-5.96629	-5.78679
-3	1	-3.0822572	-1.7647	-2.84641	-1.6039	-1.39343
-4	1	-1.1535251	-0.36652	-1.02871	-0.26101	-0.18636
-5	1	0.14201648	0.501443	0.294337	0.405889	0.53301

required a temperature decrease of more than 4°C and more than 3 times the average precipitation.

From Test C, we determined that input of station data (1956-2010) into the model produced positive mass balance, but only near the extremes of the variability of the record. At Schoolroom Glacier, at a modeled decrease of 4°C and 4 times the average precipitation did not produce modeled positive mass balance in the accumulation area (Table 6 and Figure 9). At Mt. Moran (Table 7 and Figure 10), a decrease of 3°C did not produce positive mass balance in the model output grid; however a decrease of 4°C from the average temperature produced positive mass balance at Falling Ice, Middle Triple, and West Triple glaciers. A decrease of 4.5°C from the average temperature produced positive mass balance at East Triple Glacier as well. At 3 times the average precipitation, all glaciers at Mt. Moran had negative mass balance. At 4 times the average precipitation, all glaciers except Skillet Glacier have positive mass balance. Skillet Glacier required more than 4.5 times the average precipitation to produce positive mass balance in the

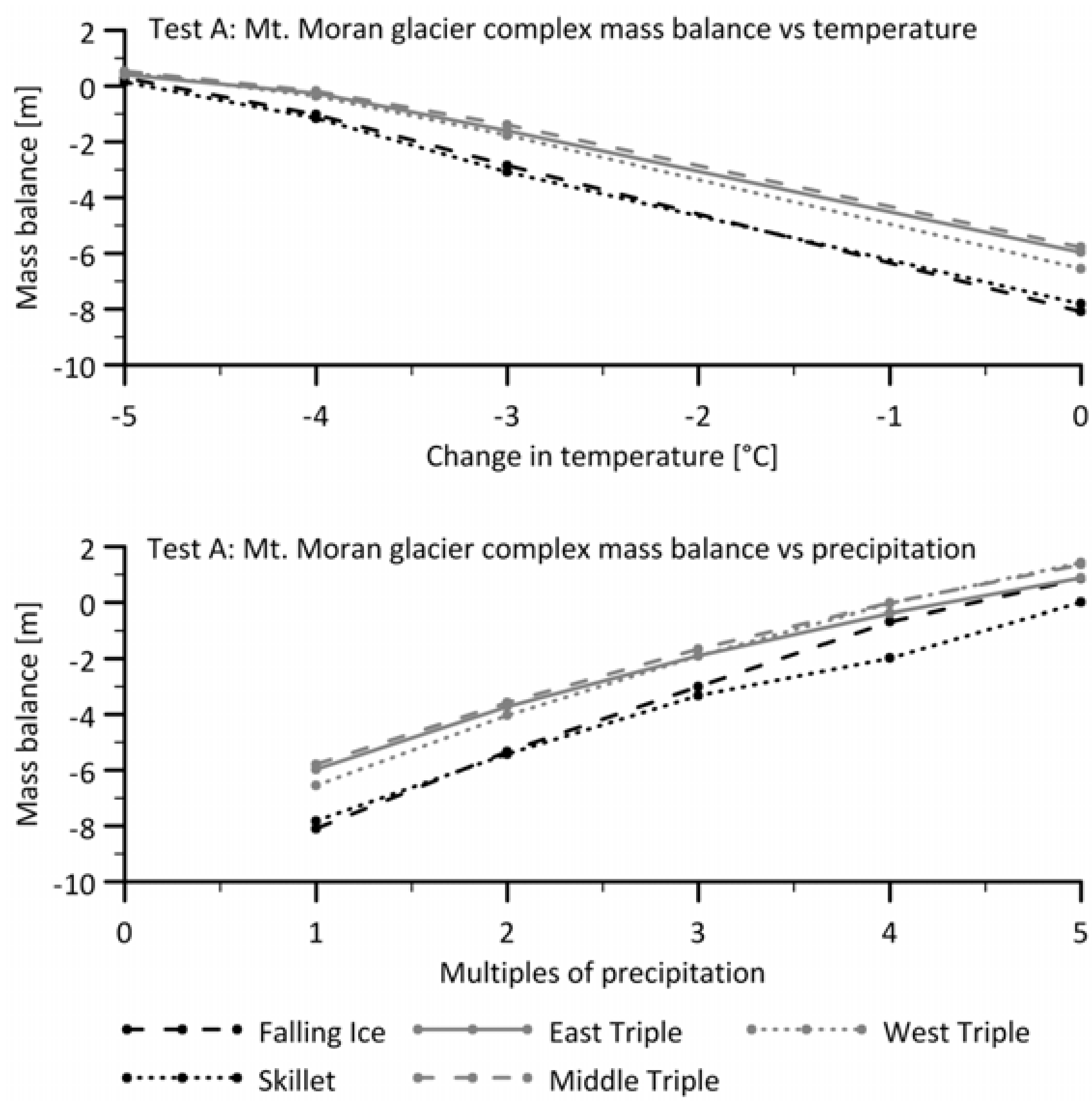

Figure 7. Results of Test A for Mt. Moran glacier complex versus PRISM mean (WY 1956-2010). Note that modeled mass balance does not produce positive mass balance unless temperature is reduced by 5ºC or precipitation is multiplied by 5 times.

accumulation area. Clearly, these adjustments to the averages are well beyond the range of variability observed in the meteorological record.

From Test D, we determined that station data for periods in the record most favorable for ice growth produced positive mass balance at selected glaciers within weather conditions from the record (as modified using our lapse rate calculations). At the

Table 5. Results from Test B for Schoolroom Glacier.

Change in Temperature [°C]	Precipitation multiplication factor	WY 1968-1976 Schoolroom mass balance [m]	WY 1982-1985 Schoolroom mass balance [m]	WY 1993 Schoolroom mass balance [m]	WY 2008-2010 Schoolroom mass balance [m]
0	2	-6.6796			
0	4	-4.622001	-4.455137		
0	5	-4.039366	-3.921829	-2.0841	-5.304714
-4	1			-0.3938	-2.003222
-5	1	-0.886847	-0.712068	0.1896	-1.361659

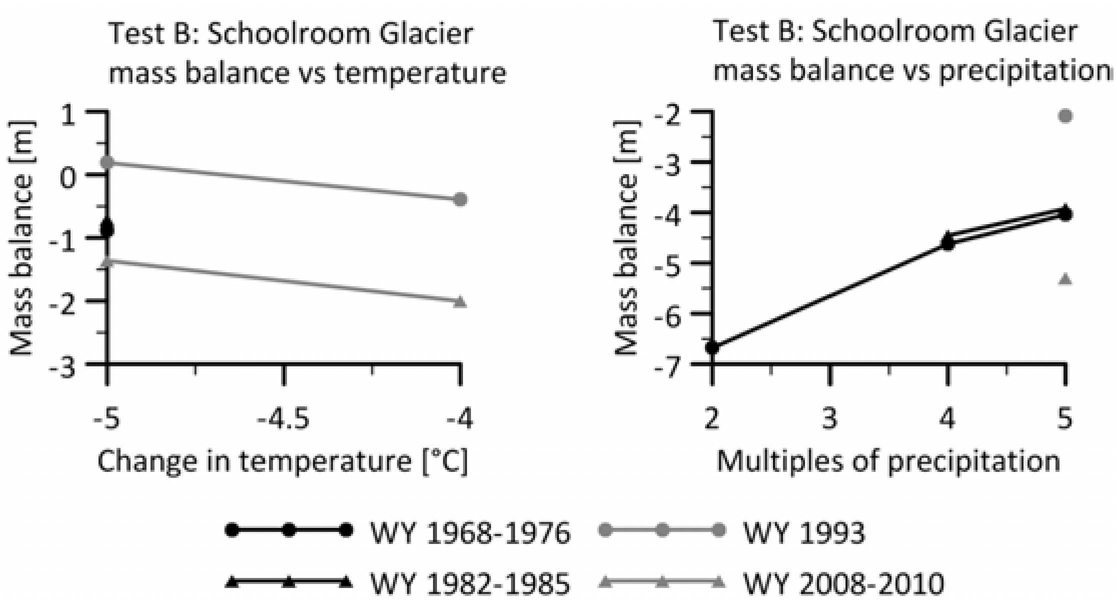

Figure 8. Results of Test B for Schoolroom Glacier versus PRISM means of short periods of favorable glacier ice growth (WY 1968-1976, WY 1982-1985, WY 1993, and WY 2008-2010). Similar results were found for Mt. Moran. Note that modeled mass balance does not produce positive mass balance unless temperature is reduced by 5ºC for the WY 1993 simulation or >5ºC for the other three simulations or precipitation is multiplied by >5 times.

Table 6. Results from Test C for Schoolroom Glacier with mean station data (WY 1956-2010).

Change in Temperature [°C]	Precipitation multiplication factor	Schoolroom mass balance [m]
0	1	-6.039
0	4	-0.42087
0	1	-6.039
-4	1	-0.63619

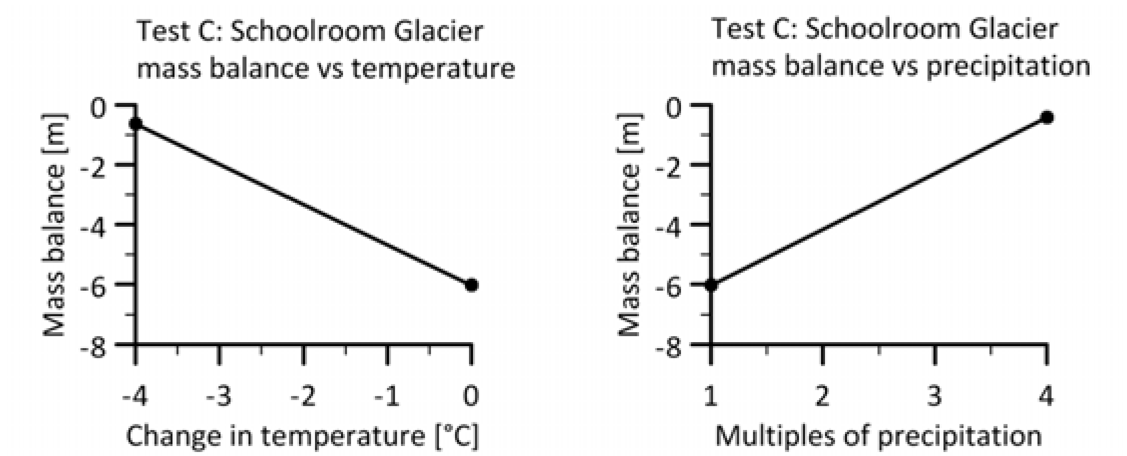

Figure 9. Results from Test C for Schoolroom Glacier versus weather station mean (WY 1956-2010). Note that modeled mass balance does not produce positive mass balance unless temperature is reduced by >4ºC or precipitation is multiplied by >4 times.

Table 7. Results from Test C for Mt. Moran glacier complex with mean station data (WY 1956-2010).

Change in Temperature [°C]	Precipitation multiplication factor	Skillet mass balance [m]	West Triple mass balance [m]	Falling Ice mass balance [m]	East Triple mass balance [m]	Middle Triple mass balance [m]
0	3	-2.76455	-0.09593	-0.25405	-1.42955	-0.50946
0	4	-0.91806	1.499145	1.251513	0.10194	0.972048
0	4.5	-0.06568	2.242615	1.995707	0.795788	1.662543
-3	1	-2.64091	-0.20279	-0.53913	-1.13896	-0.37931
-4	1	-0.98797	0.43666	0.331446	-0.12695	0.247929
-4.5	1	-0.5402	0.690875	0.584436	0.146319	0.504499
-5	1	-0.07795	0.904006	0.838167	0.388323	0.752074

Schoolroom Glacier (Table 8 and Figure 11), the model did not produce positive mass balance from the measured climatic conditions for any of the most favorable periods. The model requires Schoolroom Glacier during 1968-1976 to have experienced a temperature decrease of more than 3.5°C lower and precipitation more than 2.5 times the average conditions from the record (as modified using our lapse rate calculations). At the Schoolroom Glacier (Table 8 and Figure 11), the model did not produce positive mass

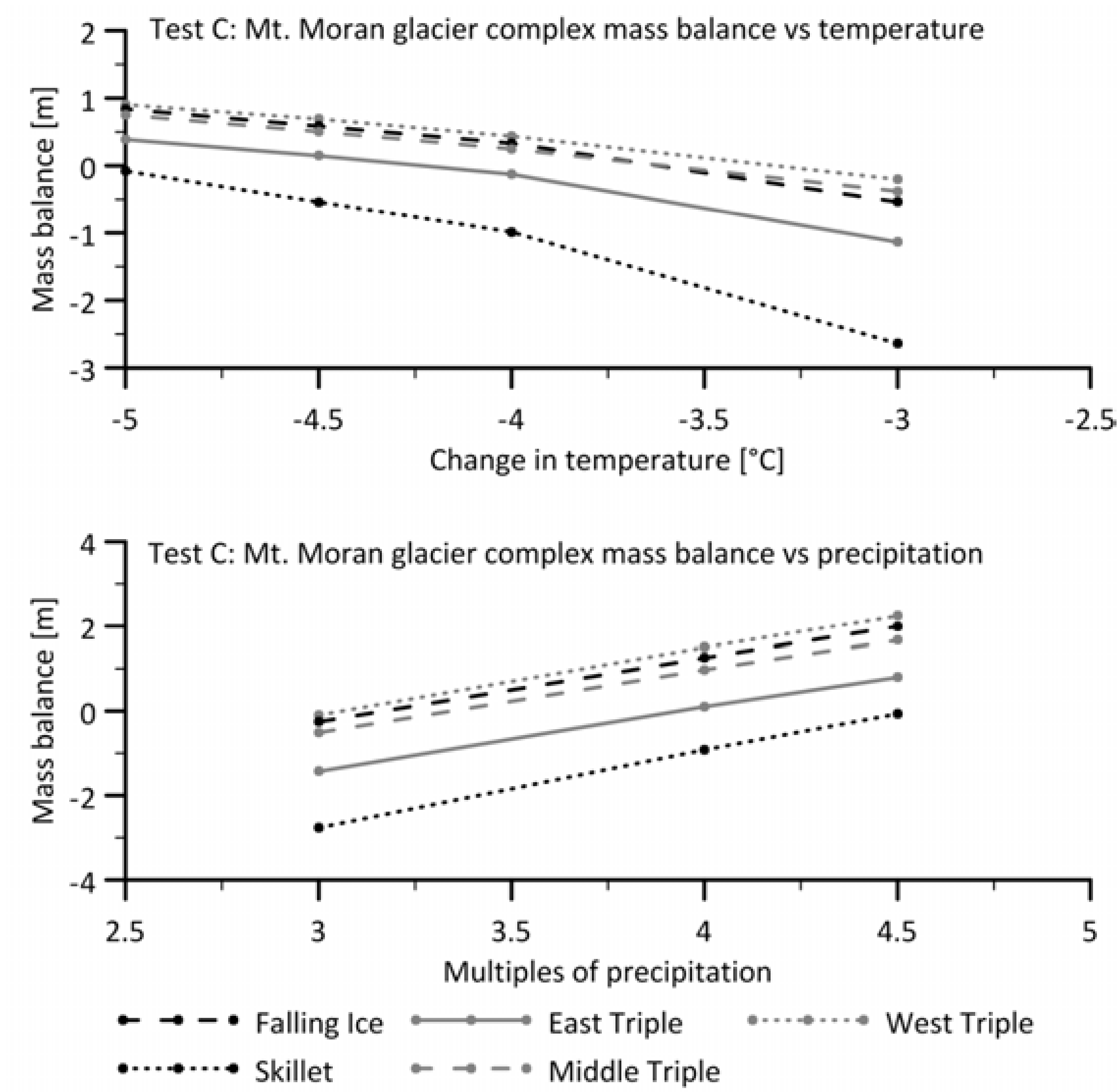

Figure 10. Results from Test C for Mt. Moran glacier complex versus weather station mean (WY 1956-2010). Note that modeled mass balance does not produce positive mass balance unless temperature is reduced by 4°C for three glaciers or precipitation is multiplied by 3.5 times at the same three glaciers.

balance from the measured climatic conditions for any of the most favorable periods. The model requires Schoolroom Glacier during 1968-1976 to have experienced a temperature decrease of more than 3.5°C lower and precipitation more than 2.5 times the average precipitation to yield positive mass balance in the accumulation area. During 1982-1985, the model required air temperatures at the Schoolroom Glacier to be decreased by 2°C

Table 8. Results from Test D for Schoolroom Glacier.

Change in Temperature [°C]	Precipitation multiplication factor	WY 1968-1976 Schoolroom mass balance [m]	WY 1982-1985 Schoolroom mass balance [m]	WY 1993 Schoolroom mass balance [m]	WY 2008-2010 Schoolroom mass balance [m]
0	1	-1.016092	-1.625689	-0.6513	-7.188037
0	1.5	-1.004773	-0.981199	-0.4825	-6.999503
0	2	-0.993484	-0.017375	-0.1676	-6.813634
0	2.5	-0.982166	0.4071077	0.0849	-5.891579
0	3			0.26858	-5.587237
0	1	-1.016092	-1.625689	-0.6513	-7.188037
-0.5	1	-0.873906	-1.381638	-0.385	
-1	1	-0.625809	-1.143016	-0.1366	
-1.5	1	-0.450737	-0.626805	0.03678	
-2	1	-0.336816	0.0732744		
-2.5	1	-0.241149	0.2911643		
-3	1	-0.108718			
-3.5	1	-0.002828			
-4	1	0.0225076			-3.929918

and 2.5 times the average precipitation. For 1993, the model required Schoolroom Glacier a temperature decrease of 1.5°C from the average period temperature and 2 times the average period precipitation to produce positive mass balance. During 2008-2010, a period during which snow has not melted completely from the Schoolroom Glacier ablation area, modeled positive mass balance requires climate conditions to have been far more than the meteorological record shows in the past 50 years.

At Mt. Moran during the period of 1968-1976 (Table 9 and Figure 12), the model required all five glaciers to have decreased air temperature of more than 1°C from the period average to produce positive mass balance. At a temperature decrease of 2°C from the average, Falling Ice and West Triple glaciers had modeled positive mass balance. At a temperature decrease of 2.5°C from the average, Middle Triple Glacier also had modeled positive mass balance. All five glaciers required a change of precipitation greater than 2.5

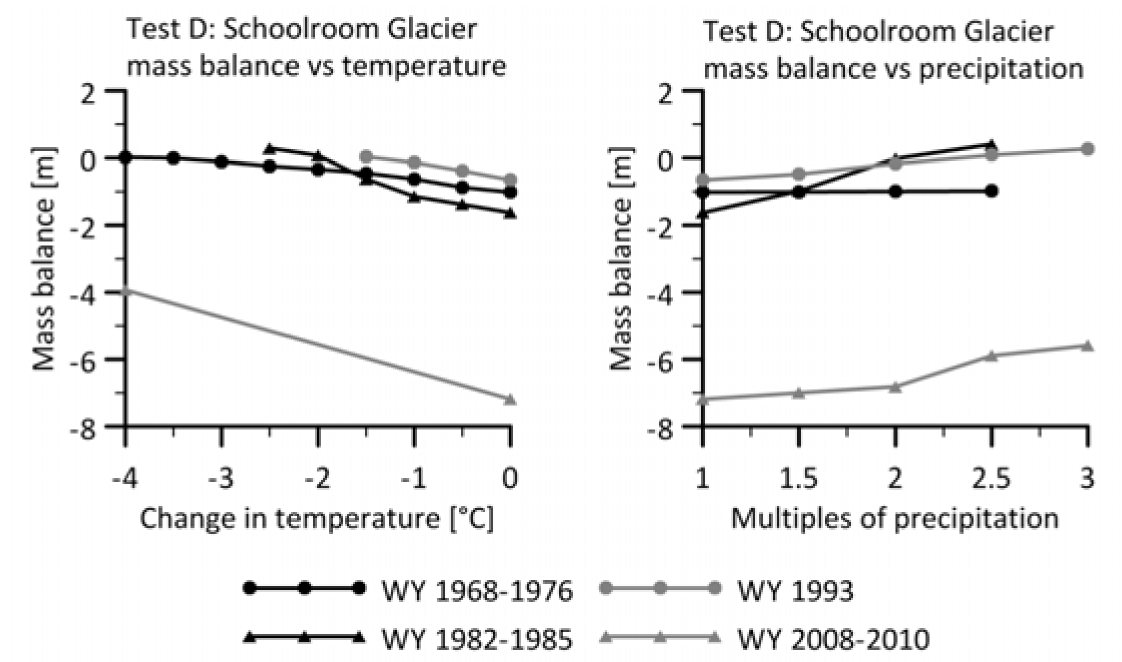

Figure 11. Results from Test D for Schoolroom Glacier versus weather station means of short periods of favorable glacier ice growth (WY 1968-1976, WY 1982-1985, WY 1993, and WY 2008-2010). Note that modeled mass balance does not produce positive mass balance unless temperature is reduced by >1.5ºC for the WY 1993 period, 2ºC for the WY 1982-1985 period, and >3.5ºC for the WY 1968-1976 and 2008-2010 periods. Precipitation must be multiplied by >2 times to produce modeled positive mass balance during all four periods.

Table 9. Results from Test D for Mt. Moran glacier complex.

Climate conditions Change in Temperature [°C]	WY 1968-1976 Precipitation multiplication factor	Skillet mass balance [m]	West Triple mass balance [m]	Falling Ice mass balance [m]	East Triple mass balance [m]	Middle Triple mass balance [m]
0	0.5	-1.55347	-0.20033	-0.22474	-0.73682	-0.23329
0	1	-1.30372	-0.18851	-0.20007	-0.56873	-0.22215
0	1.5	-1.10939	-0.17642	-0.17449	-0.55765	-0.21069
0	2	-1.10002	-0.16392	-0.14373	-0.54656	-0.19917
0	2.5	-1.1028	-0.14702	-0.11469	-0.50543	-0.18513
0	1	-1.30372	-0.18851	-0.20007	-0.56873	-0.22215
-1	1	-0.79806	-0.04807	-0.00028	-0.23466	-0.1053
-2	1	-0.42956	0.017116	0.023375	-0.10814	-0.01858
-3	1	-0.17306	0.023443	0.023422	-0.0271	0.022107

Climate conditions Change in Temperature [°C]	WY 1982-1985 Precipitation multiplication factor	Skillet mass balance [m]	West Triple mass balance [m]	Falling Ice mass balance [m]	East Triple mass balance [m]	Middle Triple mass balance [m]
0	0.5	-2.23329	-0.75811	-0.98131	-1.52408	-0.99275
0	1	-1.79966	-0.13117	0.154384	-1.12709	-0.38216
0	1.5	-1.21448	0.701814	0.779809	-0.31139	0.414307
0	2	-0.16818	1.234895	1.331229	0.294636	0.899165
1	1	-2.33845	-0.73598	-1.05202	-1.62309	-1.06929
0	1	-1.79966	-0.13117	0.154384	-1.12709	-0.38216
-1	1	-1.24246	0.494125	0.499728	-0.45237	0.265895
-2	1	-0.38834	0.755528	0.787182	0.282869	0.566483
-2.5	1	0.153929				

Climate conditions Change in Temperature [°C]	WY 1993 Precipitation multiplication factor					
0	0.5	-1.76232	-0.11949	-0.18488	-0.46838	-0.1526
0	1	-1.18874	0.069381	0.095819	-0.18997	0.024088
0	1.5	-0.854	0.261668	0.288801	-0.0129	0.205477
0	2	-0.58951	0.451847	0.48277	0.148978	0.383412
0	2.5	-0.33043	0.641918	0.676688	0.311237	0.561308
1	1	-3.03078	-0.14734	-0.37199	-0.91911	-0.26655
0	1	-1.18874	0.069381	0.095819	-0.18997	0.024088
-1	1	-0.39468	0.168624	0.185469	0.036966	0.11306
-2	1	0.067595	0.256751	0.274367	0.120448	0.183121
-2.5	1	0.133088	0.312982	0.340853	0.15527	0.225433

Climate conditions Change in Temperature [°C]	WY 2008-2010 Precipitation multiplication factor					
0	1	-7.64261	-5.00397	-6.06104	-5.95521	-5.28705
0	2	-7.18132	-3.85938	-4.88376	-5.21892	-4.22833
0	1	-7.64261	-5.00397	-6.06104	-5.95521	-5.28705
-3	1	-3.13839	-1.46425	-2.07703	-1.80759	-1.48194

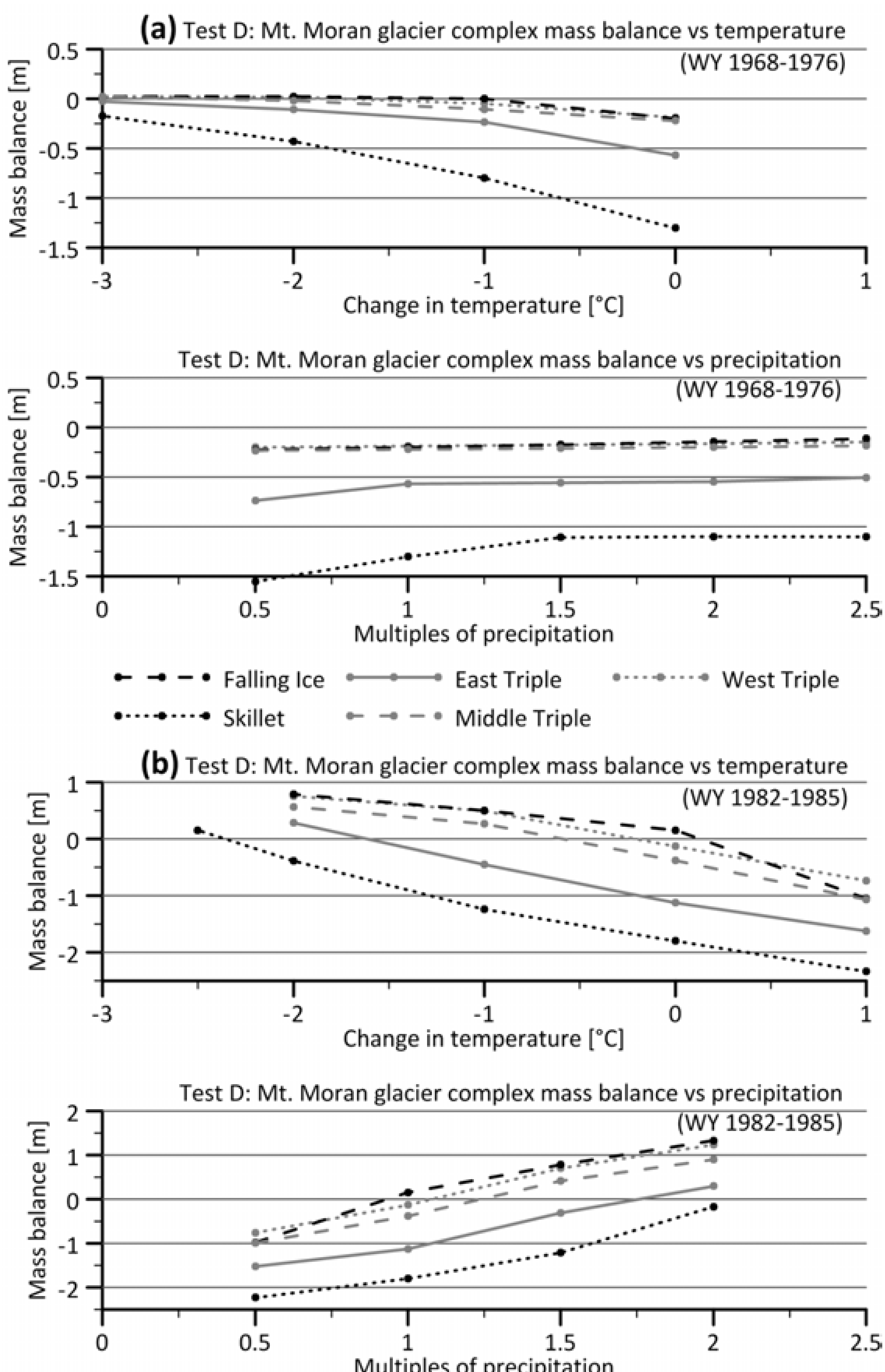
(a) Test D: Mt. Moran glacier complex mass balance vs temperature
(WY 1968-1976)
Mass balance [m]
0.5
0
-0.5
-1
-1.5
-3
-2
-1
0
1
Change in temperature [°C]
Test D: Mt. Moran glacier complex mass balance vs precipitation
(WY 1968-1976)
Mass balance [m]
0.5
0
-0.5
-1
-1.5
0
0.5
1
1.5
2
2.5
Multiples of precipitation
Falling Ice
East Triple
West Triple
Skillet
Middle Triple
(b) Test D: Mt. Moran glacier complex mass balance vs temperature
(WY 1982-1985)
Mass balance [m]
1
0
-1
-2
-3
-2
-1
0
1
Change in temperature [°C]
Test D: Mt. Moran glacier complex mass balance vs precipitation
(WY 1982-1985)
Mass balance [m]
2
1
0
-1
-2
0
0.5
1
1.5
2
2.5
Multiples of precipitation

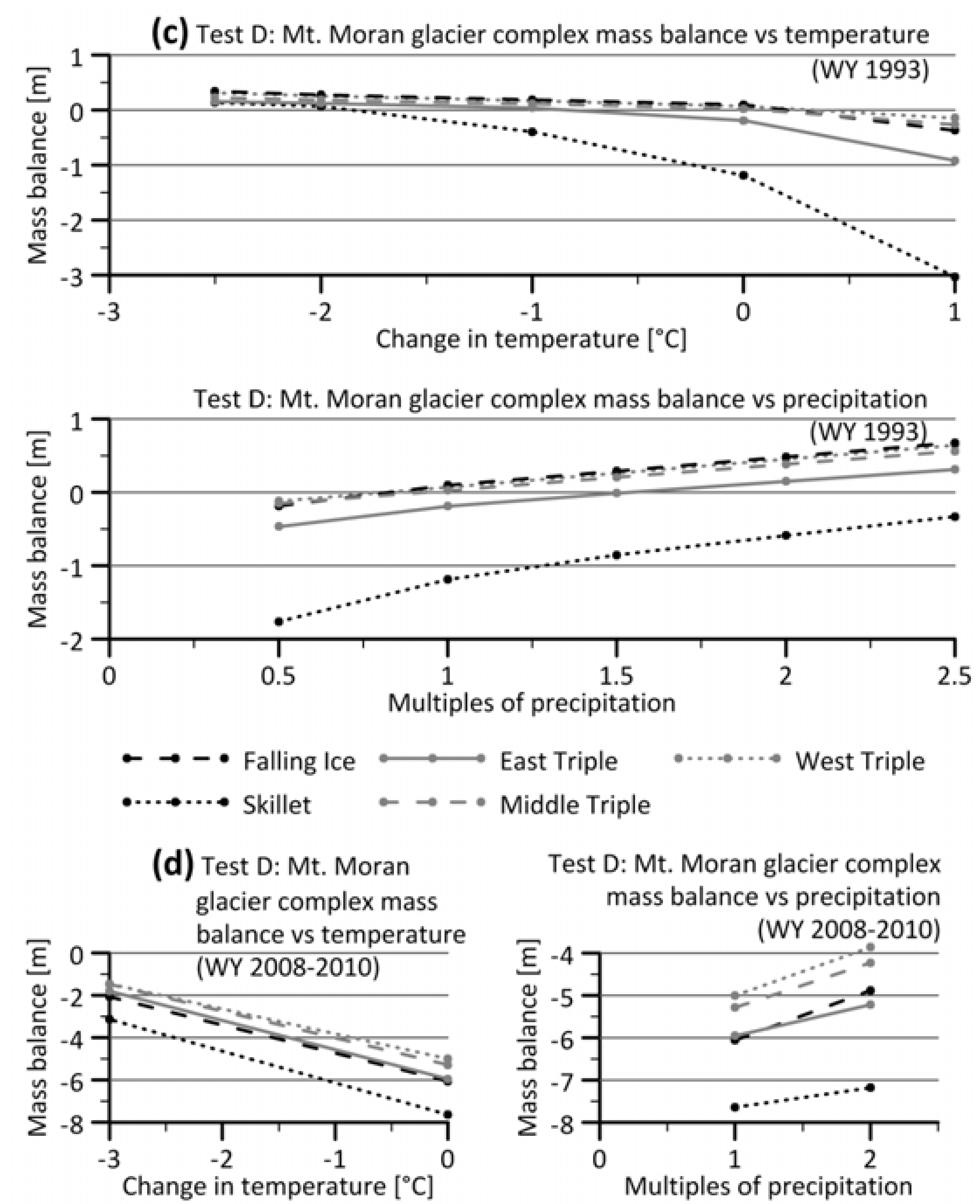

Figure 12. Results from Test D for Mt. Moran glacier complex versus weather station means of short periods of favorable glacier ice growth ((a) WY 1968-1976, (b) WY 1982-1985, (c) WY 1993, and (d) WY 2008-2010). Note that modeled mass balance does not produce positive mass balance unless temperature is reduced by 2°C for the WY 1968-1976 period at two glaciers, 0°C for the WY 1982-1985 period at one glacier, 0°C for the WY 1993 period at three glaciers, and >3°C for the WY 2008-2010 periods. Precipitation must be multiplied by >2.5 times to produce modeled positive mass balance during WY 1968-1976 and WY 2008-2010, 1 time for one glacier during WY 1982-1985, and 1 time for three glaciers during WY 1993.

times the average of the 1968-1976 record.

During the period of 1982-1985 at Mt. Moran (Table 9 and Figure 12), with no change to the mean monthly period weather, the energy mass balance model yielded positive mass balance at Falling Ice Glacier. A decrease in temperature of 1°C from the period average yielded modeled positive mass balance at Middle and West Triple Glaciers. The model required East Triple Glacier to have had a temperature decrease of 2°C from the period average, whereas Skillet Glacier needed a decrease of 2.5°C from the period average to produce positive mass balance. The model produced no positive mass balance when 0.5 times the average period precipitation was imposed on the glaciers. At 1.5 times the average precipitation, there was positive mass balance at Falling Ice, Middle Triple, and West Triple glaciers. East Triple required 2 times the period average precipitation, while Skillet Glacier required more than 2 times the period average precipitation.

For weather conditions from the water year of 1993, when anomalously low temperatures and high precipitation occurred (Table 9 and Figure 12), the model produced positive mass balance for Falling Ice, Middle Triple, and West Triple glaciers with no change to the actual measured values. East Triple Glacier required a temperature decrease of 1°C and Skillet Glacier required a temperature decrease of 2°C beyond the record to produce positive mass balance on East Triple Glacier was 2 times the mean and Skillet Glacier required more than 2.5 times the mean precipitation in 1993.

During the period of 2008-2010 (Table 9 and Figure 12), modeled mass balance for all six glaciers required weather fluctuations beyond the observed variability. Decreased air temperatures of more than 3°C and precipitation above 2 times were needed to produce modeled positive mass balance at the six studied Teton glaciers.

In summary, using PRISM climate input data in Tests A and B, the model required cooler and wetter conditions than have been observed in the past 50 years to produce positive mass balance at the target glaciers. Using station-derived climate input data in Test C, the model also required conditions colder and wetter than observed in the past 50 years to produce positive mass balance at the Teton glaciers. Station-derived climate input data in Test D produced positive mass balance at certain glaciers in the Mt. Moran glacier complex during the short time periods favorable for glacier growth of 1982-1985 and 1993. The model produced positive mass balance for a greater number of glaciers when using the most favorable short term meteorological conditions in the record. In general, the model appears to underrepresent glacier mass balance. As these glaciers persist and have, in fact, grown during specific subdecadal time periods over the 1956-2010 period, they have clearly experienced periods of positive mass balance that are not represented in the model output.

Discussion

The model does not produce positive mass balance in the accumulation areas of the Teton glaciers within reasonable ranges of climatic conditions, based on the last half-century of weather records, excepting the use of weather station-derived data of short periods of climate that favored glacier growth. The station data from various elevations only produce positive mass balance accumulations at a few glaciers during times of low temperature and high precipitation, the most favorable conditions for ice growth. These model results contrast with the periods of glacier area expansion during the study period observed from aerial photographs, which clearly require positive mass balance to occur.

Why does the energy mass balance model not produce positive mass balance using actual climate conditions from the period of interest? Here we discuss four possibilities: 1. Overestimation of high elevation temperatures, 2. Influences of glacier characteristics on modeling, 3. Wind redeposition of snow at Schoolroom Glacier, 4. Possible model biases.

1. Overestimation of high elevation temperatures

The model temperature inputs require temperature records from low elevation stations, applied to the glacier elevations using simple and complex lapse rate models, yet the use of low elevation records in this fashion may well overestimate the temperature at the elevations of the glaciers. Easily accessible low elevation stations have longer records, can be maintained more often, and collect data that are considered to be more reliable. These low elevation stations are also located in the valleys where, for instance, summer temperatures are far warmer than those at the glaciers. Both PRISM and the station climate input files draw from data collected at low elevation stations and the lapse rates may not be reasonable and may cause the model to overheat the glaciers artificially, as the model did not yield positive mass balance within reasonable meteorological conditions. One strategy would be to include only temperature records from high elevation stations in the climate input file; however, this process would limit the study period to 1989-2010.

We conducted a test of whether PRISM climate input data caused overheating in the energy mass balance model at the glacier elevations. We ran a model simulation at the Schoolroom Glacier with PRISM climate input data (1956-2010), with temperature at 0°C change and precipitation at 1 times the average precipitation. Instead of requesting an output grid of mass balance, we requested an output grid of temperature of the last month in the water year. From this simulation, we determined that temperature decreased with elevation, agreeing with the fact that the environmental lapse rate also causes decreased temperature with increasing elevation. When we ran a second model simulation with the same climate input file, but at -5°C and 1 times the average precipitation, the resulting temperature grid of the last month of the water year displayed the opposite relationship. From the second temperature grid, we determined that temperature increased with increasing elevation, suggesting both an inverted environmental lapse rate and providing a means for more melting at higher elevations, such as those occupied by glaciers in the Teton Range. This could be due to biases in PRISM output as discussed above and below.

With respect to precipitation, low elevations stations may bias the record toward lower values. An argument can be made that the station precipitation data record should not include the low elevation stations; however, doing so would limit the station data record to 1980-2010. Station data may have underestimated precipitation at the glaciers, as they did not yield positive mass balance at all of the glaciers that advanced (see Chapter II).

Another source of error may be influences changes of high elevation weather measurement. The second half of weather timeseries records (Figures 4 & 5) display greater fluctuations of weather conditions. The PRISM output pattern changed in the 1980s due to the introduction of data from SnoTel stations to the north and south of the focus PRISM pixels as these new data from SnoTel elevations helped to better constrain the modeled data at the highest elevations. Weather station data also change in pattern due to the addition of higher elevation stations recording lower temperatures and higher precipitation.

2. Influences of glacier characteristics on modeling

Modeling of Skillet Glacier mass balance may require more extreme climate fluctuations than do other glaciers on Mt. Moran for two reasons. We do not include the “handle” portion of Skillet Glacier in our ice areas as it is not attached to the “pan” of the glacier in air photos (1974-2009) (Figure 3). This glacier would understandably lose ice mass from the detachment between the two glacier portions and the unique characteristics of this glacier are not fully reproduced by the model. In eliminating this “handle” we may have underestimated the accumulation area, which would lower the mean value of mass balance over the accumulation area. Another possibility is that this east-facing glacier is exposed to the sun for a portion of the day and lies at a lower elevation than other glaciers on the mountain, the solar angles input file (and subsequent insolation files) may ablate more snow from the surface of Skillet Glacier in the model.

Additionally, the energy mass balance model requires colder temperatures and higher precipitation at East Triple Glacier than other glaciers on Mt. Moran to produce modeled positive mass balance. East Triple Glacier occupies the lowest elevations of any glaciers in the Mt. Moran glacier complex. While it is a clean ice glacier on a north slope and protected from direct short-wave radiation by shading and solar angles, it is compromised in model output grids as it occupies lower elevations. The model relies upon components of monthly lapse rates (slopes and y-intercepts), which are linear with an independent variable of elevation. As the East Triple Glacier is located at lower elevations than other glaciers on Mt. Moran, it experiences warmer temperatures and less precipitation in any given model simulation and thus requires greater adjustments of climate conditions to produce positive mass balance in the model output.

3. Wind redeposition of snow at Schoolroom Glacier

Schoolroom Glacier is heavily influenced by wind. Schoolroom Glacier is located just east of the watershed divide for the Teton Range and directly below a trail pass aptly named Hurricane Pass. This pass is often windy, with high gusts. A high, broad, low-relief surface lies southwest of and upwind of the glacier. It is highly likely that snow deposited on this surface and further upwind is re-deposited onto the glacier, and may be a primary factor for the continued existence and occasional ice growth of this clean-ice glacier. If this wind-throw is significant, it would require a higher precipitation multiple in the model to produce positive mass balance. Otherwise, modeled positive mass balance is not possible at this glacier within the snowfall values estimated by the PRISM model.

4. Possible model biases

The model may bias melting at the glaciers. When temperatures are above 0°C, ten melting components are calculated and used in the energy mass balance model. These components are turbulent heat exchange (which takes relative humidity into account); latent heat (which takes air vapor pressure into account); sensible heat (which takes wind into account); advective heat component from precipitation (assuming the snow temperature is at 0°C); longwave radiation (which takes cloudiness and the viewfactor grid into account); ground heat; shortwave radiation (which takes cloudiness and insolation grids into account); liquid precipitation; melt season albedo, backscattered radiation (which takes elevation, optical paths, and dewpoint into account). With so many components, there are numerous opportunities for more melt at the glaciers when data from lower elevation stations are imposed upon high elevations (such as higher summer air temperatures, differences in cloudiness, lower precipitation, differences in relative humidity, higher ground temperature, higher dewpoint, etc.). We suggest that if more high elevation stations collect weather parameters, such as those listed above, the model would likely produce a better representation of the energy mass balance for glaciers and snow fields in the Teton Range.

Conclusions

Energy mass balance model simulations of six Teton glaciers do not produce positive mass balance consistent with observations of episodic ice growth during the 1956-2010 period of record. We conducted four tests with contrasting climate input files. Only Test D produced glacier mass balance scenarios that agreed with glacier observations in 1982-1985. Climate files generated with PRISM output did not produce modeled positive mass balance in the accumulation areas of Teton glaciers, unless climate fluctuations far beyond the weather conditions observed in the last half-century were imposed in model simulations. This also leads us to believe the spatial resolution of 4 km^2 of PRISM pixels and an over-extrapolation of low elevation temperatures and precipitation do not allow the mass balance model to simulate energy mass balance accurately on these small glaciers.

Climate files generated with data from weather stations within and near the Teton Range produced positive mass balance at some of the glaciers in specific circumstances. These results were produced from climate input files derived from short periods of time when both annual temperatures were low and annual precipitation was high.

None of these short time periods of extreme weather produced positive mass balance at the Schoolroom Glacier with a reasonable temperature or precipitation change. This suggests that wind redistribution of snow greatly affects the mass balance of this glacier beyond our model simulations. The magnitude of wind redistribution could be hidden by the larger magnitude of modeled precipitation needed to produce positive mass balance in the model.

Glaciers at Mt. Moran had positive mass balance during the short periods of favorable weather for glacier growth recorded at weather stations in Test D. With a decrease of 2°C from the average temperature during 1968-1976, Falling Ice and West Triple Glaciers had positive mass balance. The weather conditions of 1982-1985 produced positive mass balance at Falling Ice Glacier. Imposing a temperature decrease of 1°C from 1982-1985 mean climate produced positive mass balance at Middle and West Triple Glacier as well. When precipitation was increased to 1.5 times the period average, the same three glaciers (Falling Ice, Middle Triple and West Triple glaciers) also yielded positive mass balance. In 1993, the model produced positive mass balance at these same three glaciers. These weather fluctuations are at or near the extremes of observed weather at the stations from 1956-2010.

The station data record may be strongly affected by high elevation stations (with lower temperatures and higher precipitation) that were installed much later than the low elevation stations. However, the large number of stations at different elevations contributes more data points to construct the lapse rates used for climate input files for the model, in contrast to the four PRISM pixels. Additionally, some temperature lapse rates for PRISM climate input files produced higher temperatures at higher elevations, allowing for additional artificial melting at the glaciers. Thus, the station data may indeed be more robust.

While station data climate input files capture some of the positive mass balance accumulation at some of the glaciers within observed weather conditions, the other glaciers would not have existed under these conditions. Ice expansion observed in air photos over the glaciers was captured in the model output during one portion of Test D, in 1982-1985. Thus, we suggest that the model overestimates melting at the glaciers because the temperature inputs are biased by too much data collected at lower elevations. Additionally, as the model was developed for modeling larger glaciers over longer time periods it may be unable to represent all of the unique characteristics of these small alpine glaciers. Wind and avalanching also affect these glaciers, providing and moving snow onto or off of the glacier surface. We did not adjust these parameters in the model and future work may refine these model components. If more high elevation station data of more weather parameters were collected on a continual basis, the model should be able to produce a more accurate representation of the energy mass balance with this model for glaciers and snow fields in the Teton Range.

References

Arendt, A.A., Echelmeyer, K.A., Harrison, W.D., Lingle, C.S., and Valentine, V.B., 2002, Rapid wastage of Alaska glaciers and their contribution to rising sea level: Science, v. 297, no. 5580, p. 382-386, doi: 10.1126/science.1072497.

Barry, R.G., 2006, The status of research on glaciers and global glacier recession: A review: Progress in Physical Geography, v. 30, no. 3, p. 285-306, doi: 10.1191/0309133306pp478ra.

Corbin, J., in progress, The effects of recent watershed deglaciation, climate change, and microbial processes on nitrate loading and ecological response in high alpine aquatic systems of Grand Teton National Park [Ph.D. Thesis]: Missoula, University of Montana.

Daly, C., Gibson, W., Doggett, M., Smith, J., and Taylor, G., 2010, Near-real-time monthly high-resolution precipitation climate [and average maximum/minimum temperature] data set for the conterminous United States: Corvallis, Oregon, PRISM Climate Group, http://prismmap.nacse.org/nn/, accessed January 2011.

Daly, C., Gibson, W., and Taylor, G., 2002, 103-Year high-resolution precipitation [and temperature] climate data set for the conterminous United States: Corvallis, Oregon, PRISM Climate Group, http://prismmap.nacse.org/nn/, accessed January 2011.

Daly, C., Neilson, R.P., and Phillips, D.L., 1994, A statistical-topographic model for mapping climatological precipitation over mountainous terrain: Journal of Applied Meteorology, v. 33, p. 140-158.

Hall, M.H.P., and Fagre, D.B., 2003, Modeled Climate-Induced Glacier Change in Glacier National Park, 1850–2100: BioScience, v. 53, no. 2, p. 131-140.

Krimmel, R.M., 2002, Glaciers of the Conterminous United States: Glaciers of the Western United States, *in* Satellite image atlas of glaciers of the world: North America, Williams, R.S. Jr. and Ferrigno, J.G., eds., United States Geological Survey: Washington, D.C., p. J329-J377.

Laabs, B.J.C., Plummer, M.A., and Mickelson, D.M., 2006, Climate during the last glacial maximum in the Wasatch and southern Uinta Mountains inferred from glacier modeling: Geomorphology, v. 75, p. 300-317, doi: 10.1016/j.geomorph.2005.07.026.

Love, J.D., Reed, Jr., J.C., and Pierce, K.L., 2007, Creation of the Teton landscape: A geologic chronicle of Jackson Hole and the Teton Range: Moose, WY, Grand Teton Association, 132 p.

MesoWest, 2010, Station search: Salt Lake City, Utah, University of Utah, http://mesowest.utah.edu/index.html, accessed September 2010.

Meyer, G.A., Fawcett, P.J., and Locke, W.W., 2004, Late Pleistocene equilibrium-line altitudes, atmospheric circulation, and timing of mountain glacier advances in the interior northwestern United States, *in* Haller, K.M., and Wood, S.H., eds., Geological field trips in southern Idaho, eastern Oregon, and northern Nevada: Reston, VA, USGS Open-File Report, 2004-1222, p. 63-68.

National Climatic Data Center (NCDC), 2010, Station locator: Asheville, North Carolina, National Oceanic and Atmospheric Administration, http://www.ncdc.noaa.gov/oa/climate/stationlocator.html, accessed October 2010.

National Weather and Climate Center (NWCC), 2010, SNOTEL data and products: Portland, Oregon, Natural Resources Conservation Service, http://www.wcc.nrcs.usda.gov/snow/, accessed October 2010.

Plummer, M.A., 2011, personal communication in person on 20 May 2011.

Plummer, M., and Cecil, L.D., 2005, Calibration of a glacier model to historic variations of the Teton Glacier to improve model-based inferences about glacier-climate relationships, *in* Proceedings, Geological Society of America, 2005 annual meeting, Salt Lake City, UT: Boulder, CO, Geological Society of America, v. 37, no. 7, p. 41.

Plummer, M.A., and Phillips, F.M., 2003, A 2-D numerical model of snow/ice energy balance and ice flow for paleoclimatic interpretation of glacial geomorphic features: Quaternary Science Reviews, v. 22, p. 1389-1406, doi: 10.1016/S0277-3791(03)00081-7.

Sugden, D.E. and John, B.S., 1976, Glaciers and landscape: A geomorphological approach: New York, NY, John Wiley, 376 p.

United States Geological Survey, 1968a, Grand Teton quadrangle, Wyoming, Teton County: U.S. Geological Survey Topographic Map, scale 1:24,000.

United States Geological Survey, 1968b, Mount Moran quadrangle, Wyoming, Teton County: U.S. Geological Survey Topographic Map, scale 1:24,000.

Western Regional Climate Center (WRCC), 2010, RAWS USA climate archive: Reno, Nevada, Desert Research Institute, http://www.raws.dri.edu/, accessed October 2010.

Chapter IV: Conclusions

Teton Range glacier areas decreased from 1956-2010 with episodes of subdecadal-scale ice growth and retreat. Six glaciers in this study are currently clean ice glaciers mantled by varying but minimal debris. A seventh named glacier, Petersen Glacier, is no longer a clean ice glacier, but is rather a debris-covered glacier.

Glaciers in the Teton Range experienced a main period of advance (ca. 1974-1983) later than other glaciers in mountain ranges closer to the Northwest Pacific Coast. The period of ice growth in Teton glaciers is contrary to expectations of coincident ice growth at all regional mountain ranges. This period of growth likely reflects a glacier response to a combination of regional atmospheric forcings beyond the scope of this thesis (e.g., Pacific Decadal Oscillation). Glaciers in the Teton Range do not clearly correlate with the El Niño-Southern Oscillation (ENSO) index. Wise (2010) showed a correlation between streamflow and the ENSO index in this region and thus a correlation to glacier fluctuations might be expected. However, glacier responses integrate several years of weather fluctuations and are thus not clearly correlated to the ENSO index. It is likely that these glaciers response to Pacific Ocean meteorological forcing on longer time scales and may be influenced by the Pacific Decadal Oscillation and other processes.

Our study is the first to find that the Teton glaciers have experienced short-term episodes of growth during the past five decades, while experiencing overall decline. Previous studies compared glacier area or volume changes between fewer and more widely spaced observation dates and determined only retreat at the Teton, Middle Teton, and Teepe Glaciers (Gray et al., 1999; Edmunds, 2010). We compared glacier area changes between nine to eleven observation dates. With our higher temporal resolution, including glacier observations in the 1970s, we were able to capture short periods of ice area growth that punctuate the long-term glacier decline documented in previous studies.

We determined glacier area-weather relationships by comparing meteorological Parameter-elevation Regressions on Independent Slopes Model (PRISM) output of 1956-2010 to observed glacier ice fluctuations from air photos of the same time span. PRISM model temperatures generally increased at these glaciers during the past 50 years while PRISM model precipitation generally increased at Schoolroom Glacier and decreased at Mt. Moran. This result indicates that these glaciers experienced short periods of growth during an overall period of warming. This result is counter-intuitive only if temperature is assumed to be the dominant driver of glacier growth and retreat. However, glaciers integrate changes in both temperature and precipitation, and our results show that these small mountain glaciers are particularly sensitive to precipitation as well as temperature.

When we compare glacier area to the weather conditions of a single preceding water year, partial least squares (PLS) regression analysis indicates that spring, summer, and winter precipitation have the strongest correlation with glacier area whereas annual temperature and precipitation are equally strong correlates. Using the average of the four water years of precipitation and temperature conditions preceding each glacier area observation, in order to better represent likely glacier response time, PLS results indicate that spring precipitation and annual temperature have the strongest correlations to glacier area.

With one exception, energy mass balance model simulations of six Teton glaciers do not produce positive mass balance consistent with observations of ice persistence and episodic ice growth during the 1956-2010 period of record (Chapter III). Of four tests conducted with contrasting climate input files, only one test, using climate derived from weather stations in and around the Teton Range produced glacier mass balance scenarios that agreed with glacier observations in 1982-1985 at the Mt. Moran glacier complex.

The weather station record used for tests C and D in Chapter III may be strongly affected by high elevation stations (with lower temperatures and higher precipitation) that were installed much later than the low elevation stations. However, we incorporated weather stations in the Teton Range that were not incorporated in the PRISM model outputs. These include the station at Lake Solitude and likely the SnowNET station on the Teton Saddle. Additionally, some temperature lapse rates for PRISM climate input files produced higher temperatures at higher elevations, allowing for greater modeled melting at the glaciers in the energy mass balance model, and thus the station data may be more robust. This leads us to believe the PRISM output is biased toward higher temperatures at the glacier elevations, and thus does not allow the model to simulate energy mass balance accurately on these small glaciers.

While station data climate input files allow the mass balance model to produce positive mass balance at some of the glaciers within short periods of the most favorable observed weather conditions, the other glaciers would not have existed under these conditions. Ice expansion observed in air photos was captured in the mass balance model output in only one portion of one test on one glacier. We suggest above that the model overestimates melting at the glaciers by utilizing too much data collected at lower elevations. We also note that this model was originally constructed for larger Pleistocene glaciers, and may need further adaptation for application to short-term fluctuations of small glaciers.

None of the climate input files from short time periods of recorded weather conditions most favorable for ice growth produced positive mass balance at the Schoolroom Glacier within reasonable temperature or precipitation ranges. This result, coupled with the unique setting of this glacier below Hurricane pass, suggests that wind redistribution of snow greatly affects the mass balance of this glacier beyond our model simulations. The magnitude of wind redistribution could be hidden by the larger magnitude of modeled precipitation needed to produce positive mass balance in the model.

From both Chapters II and III, it is clear that the actual meteorological influences that cause these glaciers to advance and retreat are difficult to determine. Many meteorological factors influence glaciers and we chose to study the two most influential – temperature and precipitation. We utilized only two of the many possible records of weather and compare them to the greatest number of glacier observations possible. Statistical analysis can highlight the most important glacier area-weather relationships, but accurate, high-elevation weather records and frequent glacier observations are needed to link glacier fluctuations firmly with weather conditions.

Future work

This was a baseline study and we implore other researchers to continue to study these small mountain glaciers. Suggestions of future work include measuring mountain weather and climate with a greater number of high-elevation stations recording a greater number of meteorological parameters in the Teton Range, conducting in-depth mass balance measurement studies on the Teton glaciers, and continuing adjustments of parameters within the energy mass balance model such as wind and avalanches. Other future work might include annual monitoring of glacier margins from aerial flights or GPS mapping at the end of ablation seasons. Further monitoring of these glaciers would highlight the intricacies of how they operate, their hydrologic contributions to the Snake River system, and other geomorphologic and ecologic processes. We strongly encourage the National Park Service and other investigators of the geomorphology community to carry out these future studies.

Appendix A: Weather record analyses

The steps taken to determine temperature and precipitation data that will be used in this study are outlined below.

Temperature:

Station data were obtained from online and field sources.

Daily COOP station data from COOP NCDC online source for the following stations: Driggs, ID, 1865.4 m; Alta, WY, 1962 m; Moose, WY, 1964.1 m; Moran, WY, 2072 m. http://lwf.ncdc.noaa.gov/oa/climate/stationlocator.html

Monthly COOP station data from WRCC for the following stations: Driggs, ID, 1865.4 m; Alta, WY, 1962 m; Moose, WY, 1964.1 m; Moran, WY, 2072 m. http://www.wrcc.dri.edu/

Daily RAWS station data from RAWS online source for Grand Teton RAWS station near Moose, WY, 2039 m. http://www.raws.dri.edu/

Daily SNOTEL station data from SNOTEL online source for Grassy Lake, 2214.4 m; Phillips Bench, 2499.4 m; and Grand Targhee, 2822.4 m. http://www.wcc.nrcs.usda.gov/snow/

Daily Wyoming DOT station at Teton Pass, data provided by MesoWest, 2569 m. http://mesowest.utah.edu/index.html

Daily Climate station at Lake Solitude, 2778.3 m, data collected by this study, station established by Jenni Corbin in spring 2006

Daily Jackson Hole Summit at the top of the tram at Jackson Hole Ski Resort, data provided by MesoWest, 3145 m. http://mesowest.utah.edu/index.html

Daily Teton Saddle seasonal station between Middle and Grand Teton peaks data provided by MesoWest, 3539 m. http://mesowest.utah.edu/index.html

Modeled data were obtained from online sources for sets of data over the 4 targets of interest (Petersen Glacier, Schoolroom Glacier, Mt Moran, and Teton Glacier):

Monthly Parameter-Elevation Regressions on Independent Slopes Model (PRISM) dataset for monthly MaxT and monthly MinT from PRISM Climate group website, from the Monthly Products Analysis (1985-Present) dataset. For each grid cell I calculated the monthly mean. http://www.prism.oregonstate.edu/

Determination steps:

1. I attempted to find monthly lapse rates from WY2009, the year with the most stations at the most elevations. I plotted the 15th day of each month in Matlab.

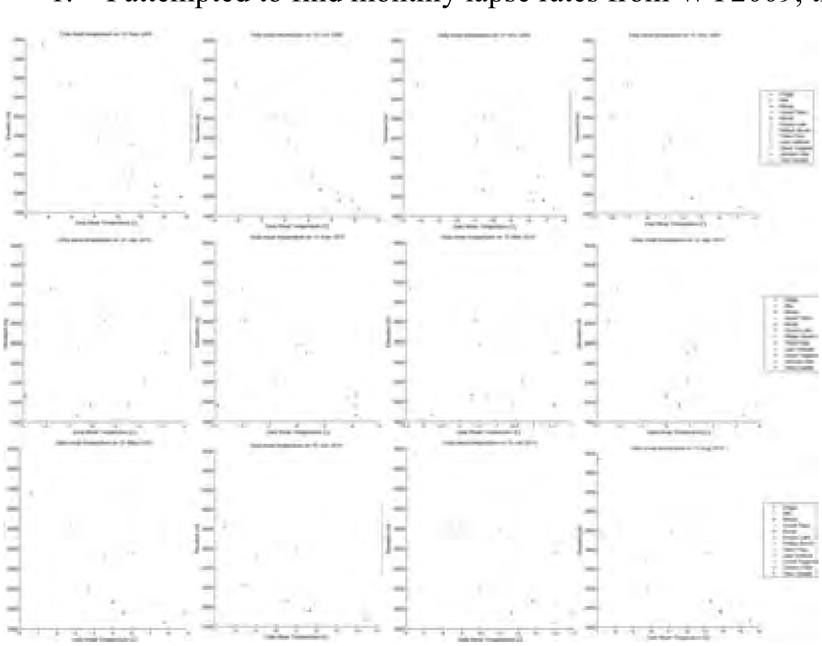

Step 1 wouldn't work well because these are noisy plots with poorly constrained lapse rates.

2. I attempted to find monthly lapse rates from WY2009. I plotted the day with the best visual linear relationship lapse rate of each month in Matlab.

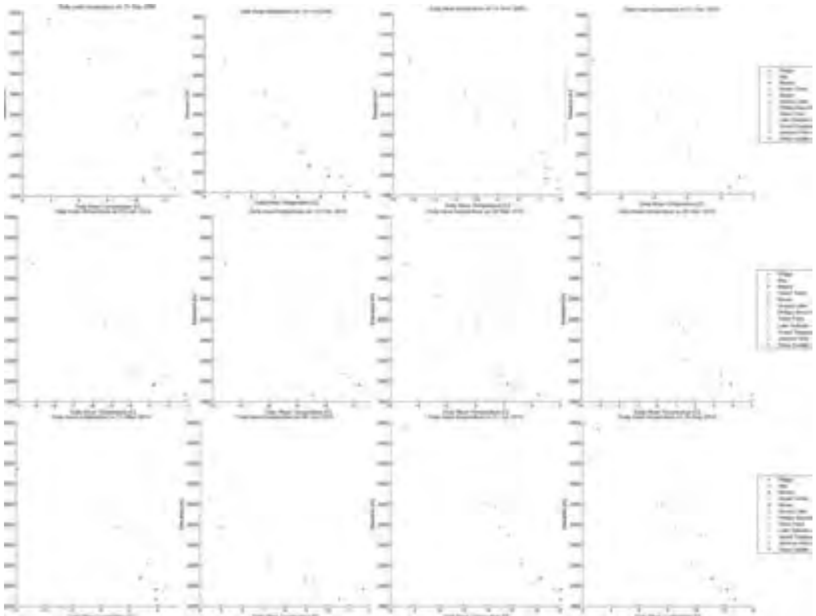

I selected the best days from Step 2 and determined the R^2 values in Excel of each plot. I also determined the slope, or lapse rate and y-intercept of each monthly plot. I omitted a few data points from a few plots to see a clearer plot. I compared relative humidity, dew point, and lapse rate to each other and over time. From this I determined these lapse rates were environmental lapse rates and fell between the limits of dry and saturated adiabatic lapse rates. From this, I also determined an average environmental lapse rate for cold months (Oct-Apr, -6.51 °C/km) and warm months (May-Sep, -6.22 °C/km).

Step 2 wouldn't work well because these are ideal days from each month. I know there are stormy days and days with inversions, but these lapse rates do not reflect this.

3. I attempted to find daily lapse rates from WY2009. I used Excel to develop a linear relationship for each day (daily lapse rate) based on the temperatures recorded for that day at the different stations to determine temperatures at high elevations such as the glaciers. I calculated the slope, y-intercept, and R^2 of each daily lapse rate and found temperatures over the middle of the glaciers.

date	Driggs	Alta	Moose	Grand Teto	Moran	Grassy Lake	Phillips Bench	Teton Pass	Lake Solitude	Grand Targhee	Jackson Hole Summit	Teton Saddle	slope	y-intercept	R^2	Petersen	Schoolroom	Mt Moran	Teton
	1865.4	1962.0	1964.1	2036.0	2072.0	2214.4	2499.4	2569.0	2778.3	2822.4	3145.0	3519.0				2960	3140	3180	3270
8/28/2010	15.0	15.0	18.3	11.7	13.3	15.8	15.1	8.9	8.3	13.3		4.1	-0.00647	28.0887685	0.652	8.94	7.78	7.52	6.94
8/27/2010	22.2	18.3	21.7	19.1	18.8	15.9	17.4	15.7	13.7	17.2		7.5	-0.00713	34.074626	0.823	12.96	11.68	11.40	10.75
8/26/2010	19.4	19.4	15.6	16.9	15.0	12.7	14.9	19.0	16.0	14.7		11.1	-0.00509	23.3084105	0.352	14.16	13.60	13.48	13.20
8/25/2010	17.2	17.2	12.8	14.7	15.8	9.6	11.0	16.1	13.6	10.4		9.6	-0.00354	21.9065459	0.175	11.43	10.79	10.65	10.33
8/24/2010	12.8	13.3	9.4	11.6	11.1	6.8	7.4	11.1	9.3	5.0		5.9	-0.00393	18.8511361	0.506	7.22	6.51	6.35	6.00
8/23/2010	11.7	10.6	14.4	5.2	9.4	11.8	12.6	7.0	4.7	8.9		-1.1	-0.00718	26.1814258	0.706	4.92	3.63	3.34	2.70
8/22/2010	15.0	14.4	20.6	15.9	14.4	15.4	17.7	13.6	10.3	16.4		5.6	-0.00556	27.7030541	0.523	11.24	10.24	10.02	9.52
8/21/2010	22.8	21.1	16.1	18.2	16.1	13.8	15.3	18.8	16.4	13.1		11.0	-0.00489	26.3077281	0.518	13.81	12.95	12.76	12.32
8/20/2010	20.0	17.8	15.6	18.3	14.4	13.5	15.1	16.0	13.2	12.6		7.1	-0.00567	28.2789452	0.767	11.49	10.47	10.25	9.73
8/19/2010	17.8	17.2	18.3	16.6	15.0	13.9	16.5	14.9	13.0	15.1		6.6	-0.00557	28.3174303	0.769	11.84	10.83	10.61	10.11
8/18/2010	19.4	17.8	16.7	16.9	14.4	13.6	15.0	18.1	15.0	14.2		9.7	-0.00399	25.0766204	0.583	13.27	12.55	12.39	12.03
8/17/2010	19.4	17.2	14.4	15.9	15.0	15.5	12.2	16.1	13.4	13.9		8.1	-0.00475	26.0404798	0.750	11.98	11.13	10.94	10.51

Step 3 produced temperature ranges well beyond reasonable limits at high elevations, occasional positive slopes, and the full range of R^2 values.

4. I attempted to use the average environmental lapse rate from Step 2 for cold months and simulate the daily high elevation temperature record using a linear relationship. If Y=mx+b, Y is the temperature at high elevation, m is the lapse rate from Step 2, x is the high elevation, and b is the y-intercept. I had a difficult time determining what the y-intercept would be, so I used the average of the two low elevation stations with long records that had the best R^2 values with similarly high elevation stations. Thus, b = mean daily temperature of Alta and Moose.

Step 4 produced more temperature ranges well beyond reasonable limits at high elevations and far values recorded at nearby high elevation stations on the same day. I am also uncomfortable with the y-intercept for this step. This method underestimates high elevation temperatures.

5. I attempted to simplify data and determine temperatures at high elevations by using monthly values from WRCC and mean monthly temperatures at the other stations. Similar to Step 3, I computed monthly temperatures at high elevations using monthly values, slopes, y-intercepts, and also computed R^2 values.

Month, Year	Driggs	Alta	Moose	RAWS	Moran	Grassy Lake	Phillips Bench	Teton Pass	Lake Solitude	Grand Targhee	JHS	Teton Saddle	slope	y-intercept	R^2	Petersen	Schoolroom	Mt Moran	Teton
	1865.4	1962.0	1964.1	2039.0	2072.0	2234.4	2499.4	2569.0	2779.3	2822.4	3145.0	3559.0				2960	3140	3180	3270
Oct-10	10.17	9.88	8.60										-0.0098	28.40	0.434	-0.50	-2.26	-2.65	-3.51
Sep-10	12.46	13.04	9.00	10.27		8.10	10.07	4.20	7.18	8.65		2.90	-0.0052	21.19	0.670	5.74	4.80	4.59	4.12
Aug-10	16.71	15.74	14.15	14.58		12.81	13.05	13.08	11.15	11.94		6.16	-0.0053	25.66	0.904	10.11	9.16	8.95	8.48
Jul-10	16.84	16.42	16.32	16.07	14.81	13.86	14.38	14.58	12.88	12.34	13.59	6.93	-0.0045	25.12	0.796	11.82	11.01	10.85	10.40
Jun-10	12.58	12.51	12.02	11.11	10.23	8.24	8.90	8.52		6.74		5.55	-0.0043	19.69	0.838	7.01	6.24	6.06	5.68
May-10	4.91	4.61	4.83	4.27	2.78	2.20	2.63	1.78		-0.11	-2.86		-0.0055	15.35	0.958	-1.07	-2.07	-2.30	-2.79
Apr-10	2.67	2.04	1.89	0.74	0.54	0.47	0.78	-0.76		-1.74	-4.69		-0.0048	11.20	0.887	-2.87	-3.73	-3.92	-4.34
Mar-10	-1.88	-1.64	-2.08	-1.81	-3.03	-2.53	-1.57	-3.65		-3.82	-6.77		-0.0031	4.35	0.701	-4.89	-5.45	-5.58	-5.88
Feb-10	-7.52	-5.97	-8.96	-7.28	-8.99	-7.18	-6.15	-7.90		-8.04	-10.53		-0.0015	-4.47	0.205	-8.79	-9.06	-9.11	-9.25
Jan-10	-6.73	-4.79	-9.58	-8.46	-10.48	-7.42	-5.57	-8.64		-5.93	-8.75		0.0005	-8.49	0.011	-7.14	-7.06	-7.04	-7.00
Dec-09	-9.43		-10.52	-10.09		-11.05	-9.55	-11.47		-11.05	-14.14		-0.0026	-4.56	0.625	-12.39	-12.87	-12.98	-13.2[illegible]
Nov-09	-0.96	-0.56	-1.84	-2.43	-2.88	-3.86	-1.91	-2.99		-3.06	-6.59		-0.0032	4.83	0.611	-4.72	-5.29	-5.41	-5.70
Oct-09	2.82	2.17	1.34	1.22	-0.99	-0.17	-0.06	-1.65		-2.46	-5.74		-0.0058	[illegible]	[illegible]	[illegible]	[illegible]	[illegible]	[illegible]

Step 5 produced temperature ranges well beyond reasonable limits at high elevations, occasional positive slopes, and the full range of R^2 values. This method both under- and overestimates temperatures at high elevations.

When I consolidated the daily temperatures calculated for high elevations from Step 3 into monthly values and compared them to results in Step 5, I found similar temperatures.

Month, Year	y-intercept	R^2	Petersen	Schoolroom	Mt Moran	Teton	Mean A	Peterse	Schoolr	Mt Mora	Teton	Cold Lapse rate (Oct-Apr)	Warm Lapse rate (May-Sep)			
			2960	3140	3180	3270	1963.1	2960	3140	3180	3270	-0.0065	-0.00622			
Feb-51	29.34	0.634	-23.10	-26.28	-26.99	-28.59	-3.811	10.098	8.9278	8.6678	8.08281					
Jan-51	25.30	0.771	-27.92	-31.16	-31.88	-33.49	-8.806	6.0623	4.8923	4.6323	4.04734					
Dec-50	43.62	0.685	-28.90	-33.31	-34.29	-36.50	-2.472	24.378	23.208	22.948	22.3625	daily LR mean T into monthly avg from AvgTC sheet				
Nov-50	39.00	0.841	-20.07	-23.66	-24.46	-26.26	0.8778	19.755	18.585	18.325	17.7401					
Oct-50	48.93	0.837	-13.96	-17.78	-18.63	-20.55	8.3611	29.685	28.515	28.255	27.6704	Average of Pet	Average of Scho	Average (	Average of Teton	
Sep-50	46.19	0.966	-8.00	-11.29	-12.03	-13.67	10.678	26.946	25.776	25.516	24.9315	-7.98	-11.29	-12.03	-13.69	Sep-50
Aug-50	50.60	0.818	-4.26	-7.59	-8.34	-10.00	15.278	31.356	30.186	29.926	29.3407	-5.06	-8.55	-9.33	-11.07	Aug-50
Jul-50	44.76	0.871	-1.03	-3.82	-4.44	-5.83	15.117	25.518	24.348	24.088	23.5031	-1.08	-3.90	-4.53	-5.94	Jul-50
Jun-50	30.93	0.674	0.70	-1.14	-1.55	-2.47	11.739	11.694	10.524	10.264	9.67942	0.74	-1.11	-1.52	-2.45	Jun-50
May-50	33.54	0.826	-8.90	-11.48	-12.05	-13.34	6.1944	14.299	13.129	12.869	12.284	-8.80	-11.39	-11.97	-13.26	May-50
Apr-50	40.46	0.950	-17.83	-21.38	-22.17	-23.94	2.3611	21.216	20.046	19.786	19.2011	-17.62	-21.15	-21.93	-23.70	Apr-50
Mar-50	44.11	0.949	-27.91	-32.29	-33.27	-35.46	-2.956	24.87	23.7	23.44	22.8551	-27.43	-31.75	-32.71	-34.87	Mar-50
Feb-50	58.40	0.836	-38.24	-44.11	-45.42	-48.36	-3.928	39.164	37.994	37.734	37.1491	-35.96	-41.42	-42.64	-45.37	Feb-50
Jan-50	20.03	0.990	-22.96	-25.57	-26.15	-27.46	-8.289	0.7879	-0.382	-0.642	-1.22712	-21.87	-24.30	-24.84	-26.05	Jan-50
Dec-49	24.81	0.924	-22.18	-25.03	-25.67	-27.10	-5.789	5.5735	4.4035	4.1435	3.55845	-22.11	-24.98	-25.62	-27.05	Dec-49
Nov-49	47.67	0.870	-20.42	-24.56	-25.48	-27.55	3.6	28.428	27.258	26.998	26.4129	-20.38	-24.54	-25.47	-27.55	Nov-49
Oct-49	22.76	0.913	-7.04	-8.85	-9.25	-10.16	3.3778	3.5165	2.3465	2.0865	1.50155	-6.92	-8.74	-9.14	-10.05	Oct-49
Sep-49	44.97	0.929	-5.62	-8.70	-9.38	-10.92	12	25.729	24.559	24.299	23.7143	-5.51	-8.59	-9.28	-10.82	Sep-49
Aug-49	67.75	0.828	-10.31	-15.06	-16.11	-18.48	17.444	48.513	47.343	47.083	46.4983	0.54	-2.38	-3.03	-4.50	Aug-49
Jul-49	48.01	0.887	-0.24	-3.17	-3.82	-5.29	16.722	28.766	27.596	27.336	26.7506	2.72	0.26	-0.29	-1.52	Jul-49
Jun-49	34.04	0.958	0.74	-1.28	-1.73	-2.74	12.25	14.797	13.627	13.367	12.782	0.84	-1.19	-1.64	-2.66	Jun-49
May-49	31.78	0.895	-2.41	-4.49	-4.95	-5.99	9.5889	12.538	11.368	11.108	10.5229	-2.28	-4.37	-4.84	-5.88	May-49
Apr-49	43.04	0.824	-15.52	-19.08	-19.87	-21.65	5.3167	23.802	22.632	22.372	21.7873	-15.65	-19.26	-20.07	-21.87	Apr-49
Mar-49	36.04	0.641	-20.88	-24.34	-25.11	-26.84	0.0278	16.796	15.626	15.366	14.7812	-20.62	-24.06	-24.83	-26.54	Mar-49
Feb-49	32.50	0.775	-29.16	-32.91	-33.74	-35.62	-7.033	13.257	12.087	11.827	11.2417	-29.01	-32.75	-33.59	-35.46	Feb-49
Jan-49	79.78	1.000					-13.76	60.541	59.371	59.111	58.5257	-60.81	-69.31	-71.20	-75.45	Jan-49
Dec-48	34.14	0.782	-32.36	-36.41	-37.30	-39.33	-8.522	14.903	13.733	13.473	12.8884	-32.34	-36.40	-37.30	-39.33	Dec-48
Nov-48	14.41	0.977	-14.81	-16.59	-16.98	-17.87	-4.778	-4.83	-6	-6.26	-6.84488	-14.80	-16.60	-17.00	-17.90	Nov-48
Oct-48	40.19	0.813	-11.20	-14.32	-15.02	-16.58	7.1222	20.95	19.78	19.52	18.9351	-11.19	-14.35	-15.05	-16.62	Oct-48

6. I attempted to find temperatures at high elevations using monthly values and an averaged environmental lapse rate. Using a similar process as in Step 4, I calculated for monthly values instead of daily values.

As in the results for Step 4, Step 6 also did not predict reasonable temperatures at high elevations as compared to values recorded at nearby high elevation stations. This method strongly underestimates temperatures at high elevations.

7. I attempted to find temperatures at high elevations using monthly values, an averaged environmental lapse rate, and a monthly y-intercept. The y-intercept is the same y-intercept from Step 5.

Step 7 also produced temperature ranges well beyond reasonable limits at high elevations.

To decide which simulated dataset I should use, I ran a few analyses.
First, I plotted the temperature record from Step 5.

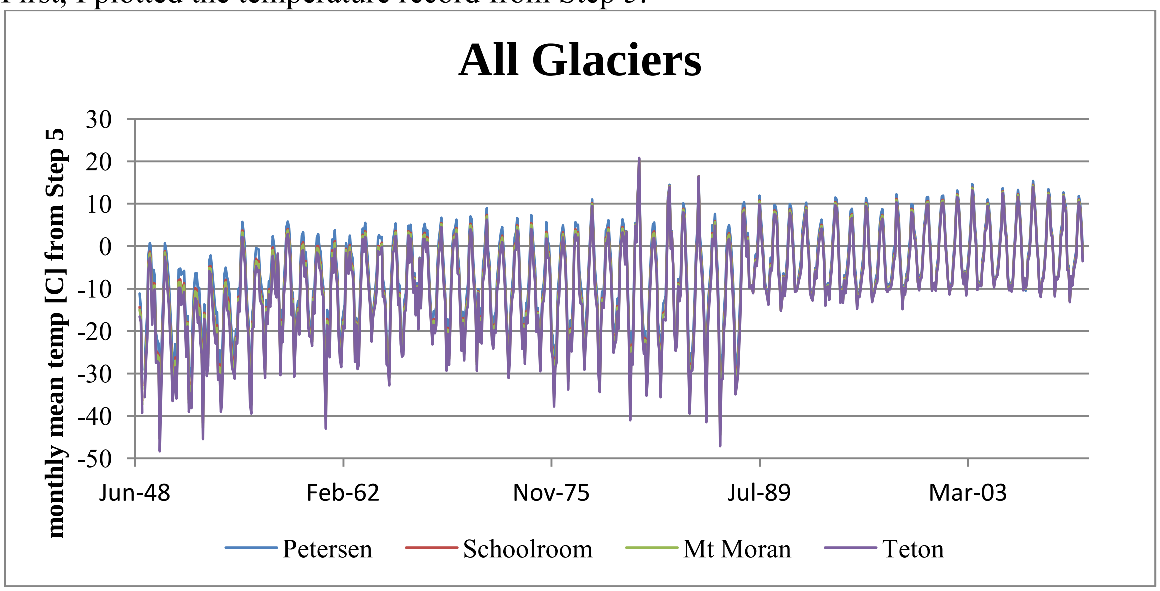

Few stations are at high elevations and these stations have short periods of record. There are more long periods of record at the low elevation stations. With 2-3 stations at low elevations contributing to the linear relationship, the oldest temperatures are progressively underestimating values at high elevations. With fewer stations involved in calculating the lapse rate, these values are poorly constrained and highly variable compared with the most recent values from 2006 to 2010. Recall that SNOTEL stations in this area began recording temperature in 1988. If I want to continue with this dataset, I must correct for this artifact that falsely indicates a large regional warming.

Then I plotted the R^2 values of the temperature record from Step 5.

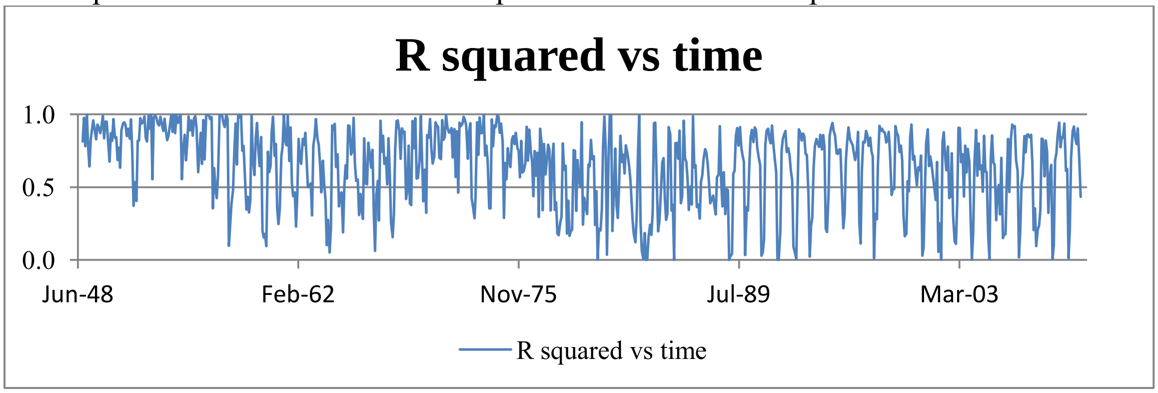

Generally, fewer stations allows for a better prediction of a linear line. As more stations are included in the plot, more variation from the line is possible.

Then, I plotted the slope of the temperature record from Step 5.

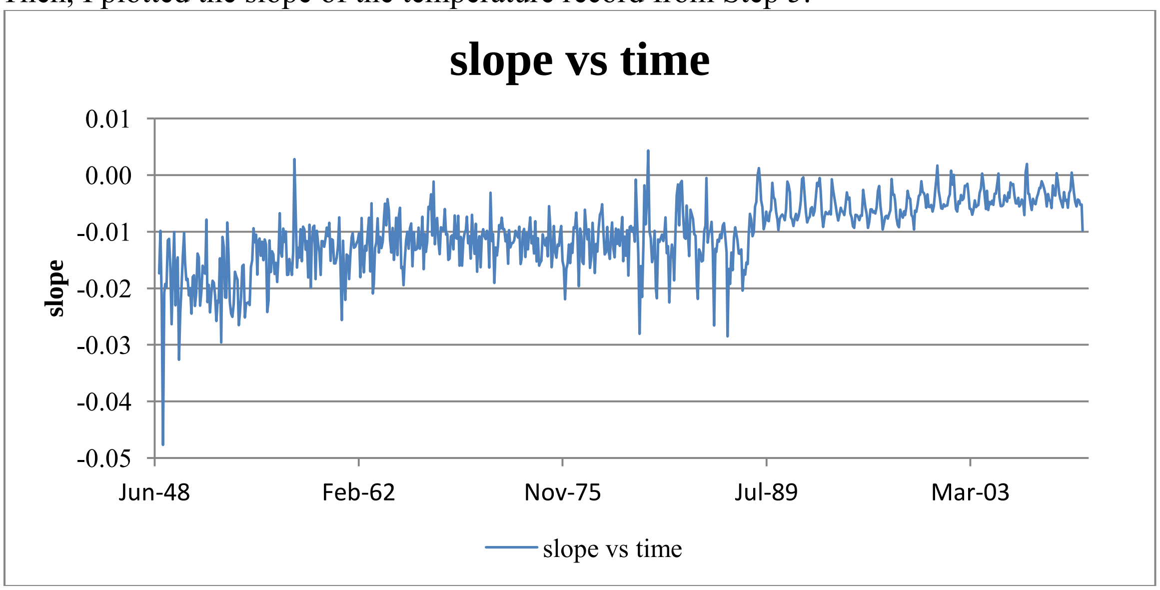

The calculated slope really affects my monthly lapsed temperatures from Step 5.

8. Then I looked at PRISM temperature data. I calculated the R^2 values of the modeled PRISM pixels over the glaciers (high elevations) compared to the recorded station data at a monthly resolution. I also compared PRISM data and station data to the dataset from Step 5.

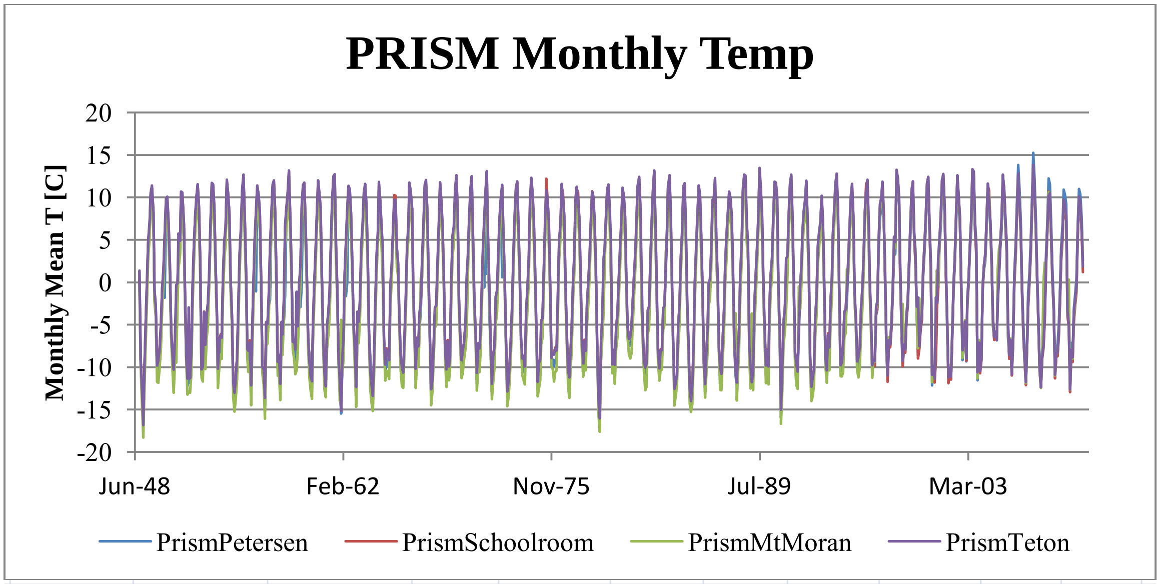

		Rsquared table								
			prismT				MonthlyLapseRates			
			2898	3192	3219	3153	2960	3140	3180	3270
			Petersen	Schoolroom	Mt Moran	Teton	Petersen	Schoolroom	Mt Moran	Teton
StationData	1865.4	Driggs	0.967	0.984	0.955	0.976	0.673	0.595	0.578	0.542
	1962.0	Alta	0.965	0.978	0.954	0.970	0.682	0.605	0.589	0.554
	1964.1	Moose	0.964	0.975	0.950	0.973	0.770	0.705	0.691	0.659
	2039.0	RAWS	0.977	0.978	0.940	0.971	0.948	0.924	0.918	0.903
	2072.0	Moran	0.961	0.977	0.953	0.971	0.732	0.659	0.643	0.608
	2214.4	Grassy Lake	0.986	0.978	0.948	0.973	0.969	0.949	0.944	0.931
	2499.4	Phillips Bench	0.983	0.965	0.946	0.960	0.986	0.974	0.970	0.961
	2569.0	Teton Pass	0.943	0.947	0.935	0.940	0.961	0.956	0.954	0.950
	2778.3	Lake Solitude	0.987	0.997	0.981	0.987	0.999	1.000	1.000	1.000
	2822.4	Grand Targhee	0.986	0.987	0.934	0.982	0.985	0.980	0.978	0.974
	3145.0	JHS	0.887	0.892	0.782	0.858	0.972	0.976	0.976	0.975
	3539.0	Teton Saddle	0.722	0.745	0.729	0.753	0.883	0.896	0.899	0.905
MonthlyLapse	2960	Petersen	0.710	0.682	0.743	0.686				
Rates	3140	Schoolroom	0.638	0.608	0.674	0.612				
	3180	Mt Moran	0.623	0.592	0.659	0.596				
	3270	Teton	0.589	0.557	0.627	0.562				

Green cells are the 3 best or highest R^2 values in each column. Pink cells are the 3 worst or lowest values. From this table, temperatures derived from Step 5 are better predictors of temperatures at high elevation stations and glacier elevations than PRISM. PRISM data and values from Step 5 do not agree.

Precipitation:

Station data were obtained from online and field sources.

Daily COOP station data from COOP NCDC online source for the following stations: Driggs, ID, 1865.4 m; Alta, WY, 1962 m; Moose, WY, 1964.1 m; Moran, WY, 2072 m. These are daily values summed into monthly values. http://lwf.ncdc.noaa.gov/oa/climate/stationlocator.html

Daily RAWS station data from RAWS online source for Grand Teton RAWS station near Moose, WY, 2039 m. http://www.raws.dri.edu/

Daily SNOTEL station data from SNOTEL online source for Grassy Lake, 2214.4 m; Phillips Bench, 2499.4 m; and Grand Targhee, 2822.4 m. http://www.wcc.nrcs.usda.gov/snow/

Daily Climate station at Lake Solitude, 2778.3 m, data collected by this study, station established by Jenni Corbin in spring 2006

Modeled data were obtained from online sources for sets of data over the 4 targets of interest (Petersen Glacier, Schoolroom Glacier, Mt Moran, and Teton Glacier):

Daily SNODAS dataset for precipitation and SWE from NSIDC and converted English units to metric. http://nsidc.org/data/g02158.html

Monthly Parameter-Elevation Regressions on Independent Slopes Model (PRISM) dataset for precipitation from PRISM Climate group website, from the Monthly Products Analysis (1985-Present) dataset. http://www.prism.oregonstate.edu/

Determination steps:

1. I attempted to determine the amount of winter precipitation that fell from the sky on top of the glaciers. Assuming the maximum snow-water equivalent (SWE) of each year would quantify the positive contribution of the mass balance equation of glaciers, I used SNOTEL stations and 3 of the SNODAS pixels that included glaciers in them to find the day of maximum SWE in each water year and that value.

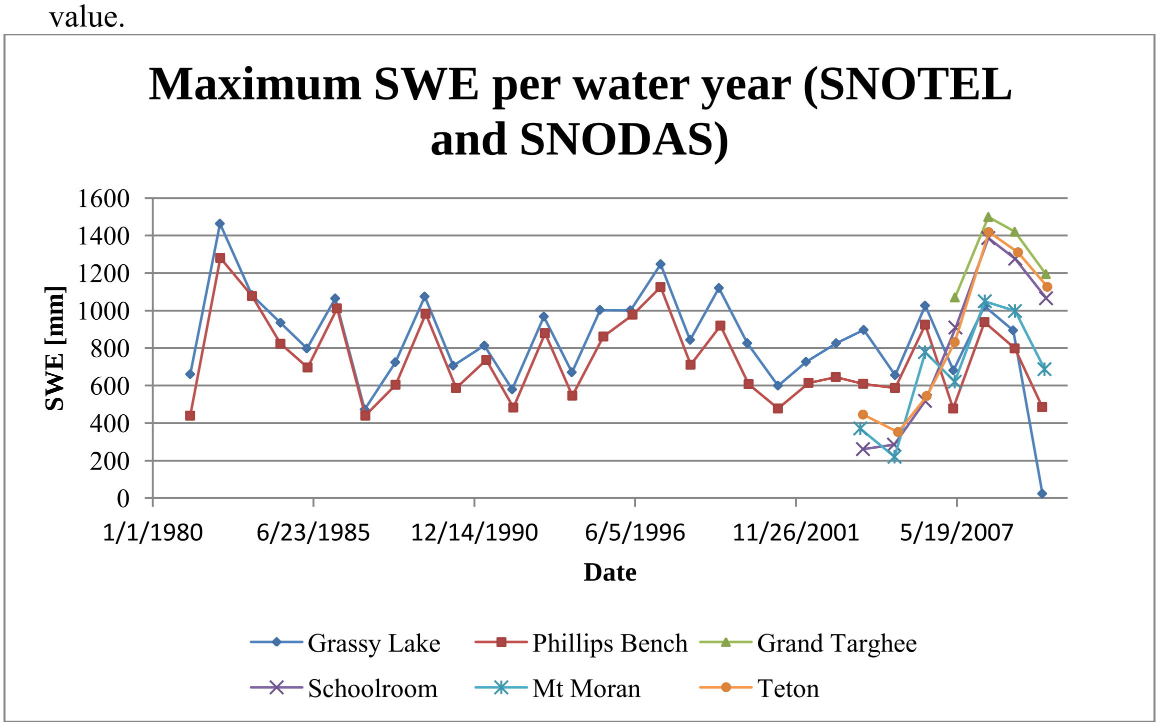

Then I compared R^2 values of the different maximum SWE records.

R^2		Snotel [y]		
		Gl	PB	GT
Snodas [x]	Sch	0.1095	0.0746	0.9953
	MtMo	0.4506	0.4165	0.9782
	Teton	0.1637	0.0867	0.9478
	Rand	0.9345	0.7359	0.9856

I chose a SNODAS pixel near the Phillips Bench SNOTEL station (named random or rand). When I ran this modeled pixel against the SNOTEL stations, I found there is a strong relationship between Grand Targhee and all 3 glacier pixels. There are very poor relationships between GL and PB stations and southern glacier pixels. There is also a poor/moderate relationship between GL and PB stations with the northern glacier pixel. The random pixel near Phillips Bench correlates best with the two stations farther away, leading to the idea that nearest neighbor is not a strong factor in SNODAS data.

2. I attempted to compare winter precipitation at COOP stations (sum Oct-May) and maximum SWE per water year from Step 1. I also looked at different periods of record, so I created a couple of R^2 matrices.

stats	2004-present							1981-present	
R^2		Snotel [y]			lowland				
		Gl	PB	GT	Alta	Driggs		GL	PB
Snodas [x]	Sch	0.1095	0.0746	0.9953	0.1671	0.5227	Alta	0.6529	0.6083
	MtMo	0.4506	0.4165	0.9782	0.5066	0.2641	Driggs	0.4416	0.3234
	Teton	0.1637	0.0867	0.9478	0.2383	0.6477			
	Rand	0.9345	0.7359	0.9856	0.8662	0.0566			
lowland	Alta	0.7554	0.6563	0.8991					
	Driggs	0.0646	0.0003	0.4464					

Step 2 revealed that Sch and Teton modeled pixels correlate more strongly with Driggs. MtMo and Rand modeled pixels correlate more strongly with Alta. Short term correlations (2004-2010) are best between Alta and all three SNOTEL stations. Long term correlations (1981-2010) are also best with Alta and all two SNOTEL stations.

3. I attempted to compare PRISM data of winter precipitation (Oct-May) to the data compared in Step 2 to determine which dataset would be the best predictor of winter precipitation record over the glaciers for the last 60 years. An additional R^2 matrix compared the longest term records (1949-2010).

	1992	579	1992	483			Long-term (1981-2010)			
	1991	813	1991	737			GL	PB	Alta	Driggs
	1990	706	1990	587		Alta	0.6529	0.6083		
	1989	1074	1989	983		Driggs	0.4416	0.3234		
	1988	724	1988	605		PSch	0.5260	0.4884	0.6330	0.2558
	1987	472	1987	439		PMtMo	0.7068	0.7491	0.6820	0.1649
	1986	1064	1986	1011		PTet	0.7426	0.7601	0.7056	0.3390
	1985	798	1985	696		PPet	0.6850	0.6303	0.7480	0.3783
	1984	935	1984	823						
	1983	1082	1983	1077			Longest-term (1949-2010)			
	1982	1463	1982	1280			PSch	PMtMo	PTet	PPet
	1981	660	1981	439		Alta	0.5550	0.4311	0.3267	0.6694
						Driggs	0.3073	0.3067	0.3885	0.4436
	Short-term (2004-2010)									
		Snotel [y]			lowland		PRISM			
		Gl	PB	GT	Alta	Driggs	PSch	PMtMo	PTet	
SNODAS	Sch	0.1095	0.0746	0.9953	0.1671	0.5227	0.3401			
	MtMo	0.4506	0.4165	0.9782	0.5066	0.2641	0.0029	0.2404		
	Teton	0.1637	0.0867	0.9478	0.2383	0.6477	0.4402		0.4150	
	Rand	0.9345	0.7359	0.9856	0.8662	0.0566				
Lowland	Alta	0.7554	0.6563	0.8991						
	Driggs	0.0646	0.0003	0.4464						
PRISM	PSch			0.6354						
	PMtMo			0.8263						
	PTet			0.6748						
	PPet			0.8367						

Results from Step 3 revise an observation from Step 2 about long term correlations. Long term correlations are best with Alta, all two SNOTEL stations, and all 4 PRISM pixels. Thus, PSch is best with Alta; PMtMo is best with PB; PTet is best with PB; and PPet is best with Alta.

Additionally, the two models do not agree very well, though there is a difference in pixel size and model inputs. Shortest term correlations are best for SNOTEL Grand Targhee with all modeled pixels. Long term correlations for PRISM data are moderate-best with both SNOTEL stations. Long term correlations for PRISM data are better with Alta COOP station than Driggs. Longest term correlations are better between PRISM pixels and Alta COOP station.

So to answer the question of what is the winter precipitation record over the glaciers for the last 60 years, I decided to use PRISM winter precipitation data since it's highly regarded and has R^2 values of 0.33 to 0.67 for the closest COOP station over 60 years of data. I do not need to include Teton Glacier in this study anyway, which is the weakest correlation with Alta COOP anyway.

Strengths of PRISM (Parameter-elevation Regressions on Independent Slopes Model) include that it is vetted. It is less variable/reliant upon how many stations are contributing to the linear relationship for temperature. It does not show a pronounced artificial warming trend in the region either. PRISM does not assume a strictly linear relationship, as my method does. PRISM has a moderate-good correlation with a lowland station for a long period of record of precipitation, and has a moderate-best correlation with precipitation at mid-elevation stations.

PRISM is a model configured and evaluated by experienced climatologists (Daly, 2006). It develops local climate-elevation regression functions for each DEM grid cell and calculates station weights on the basis of a spatial climate knowledge base that assesses each station's physiographic similarity to the target grid cell. The knowledge base and resulting station weighting functions currently account for spatial variations in climate caused by elevation, terrain orientation or "topographic facets", effectiveness of terrain as a barrier to flow, coastal proximity, moisture availability, a two-layer atmosphere (to handle inversions), and topographic position (valley, midslope, ridge) (Daly, 2006). Topographic "facets" are used to identify sharply defined climate regimes delineated by terrain features (e.g., rain shadows or orographic regimes); this prevents mixing data from stations with windward and leeward exposures (Daly et al., 1994; Simpson et al., 2005). Minder et al. (2010) note that PRISM's approach allows surface lapse rates to vary seasonally, spatially, and to differ from the free air. Furthermore, the PRISM analysis methodology appears to capture much of the spatial and seasonal variability apparent in other data sets (Minder et al., 2010).

Limitations of PRISM include that PRISM data output have large spatial resolution of grid cells of 2.5 arc minutes or 4 km square. PRISM data do not have some of the information from stations I used, such as the temperature from the Climate station near Lake Solitude. Although PRISM uses data from all available observational networks, it has only monthly temporal resolution, may be subject to sizable errors where station observations are sparse, and relies on various assumptions in the interpolation procedure (Minder et al., 2010).

Models such as PRISM cannot account for daily variations in vertical or spatial temperature as they use monthly resolution inputs (Lundquist and Cayan, 2007). Some models use a linear lapse rate derived from available nearby surface measurements, but this method is limited by the number of surface measurements available and cannot account for nonlinear variations (Lundquist and Cayan, 2007). Lundquist and Cayan

(2007) call for work to bridge the gap between spatially dense short-term observations and a sparse network of longer-term observations such as descriptions of how fine-spatial-scale variations evolve in time. Lundquist and Cayan also note that the gap between scales is particularly evident in studies of long-term temperature trends, which demonstrate threats to snow and regional water supplies.

Despite the weaknesses of the PRISM dataset, I decided to continue this project using PRISM output data. Perhaps future studies in this region that downscale PRISM data will benefit from this document.

References Cited:

Daly, C., Neilson, R.P., and Phillips, D.L., 1994, A statistical-topographic model for mapping climatological precipitation over mountainous terrain: Journal of Applied Meteorology, v. 33, p. 140-158.

Daly, C., Gibson, W.P., Doggett, M., Smith, J., and Taylor, G., 2004, Up-to-date monthly climate maps for the conterminous United States, *in* Proceedings, 14th American Meteorological Society Conference on Applied Climatology, 84th American Meteorological Society Annual Meeting Combined Preprints, American Meteorological Society, Seattle, WA, January 13-16, 2004, Paper P5.1, CD-ROM.

Daly, C., 2006, Guidelines for assessing the suitability of spatial climate data sets: International Journal of Climatology, v. 26, p. 707-721, doi: 10.1002/joc.1322.

Lundquist, J.D., and Cayan, D.R., 2007, Surface temperature patterns in complex terrain: Daily variations and long-term change in the central Sierra Nevada, California: Journal of Geophysical Research, v. 112, D11124, 15 p., doi: 10.1029/2006JD007561.

Minder, J.R., Mote, P.W., and Lundquist, J.D., 2010, Surface temperature lapse rates over complex terrain: Lessons from the Cascade Mountains: Journal of Geophysical Research, 115, D14122, 13 p., doi: 10.1029/2009JD013493.

Simpson, J.J., Hufford, G.L., Daly, C., Berg, J.S., and Fleming, M.D., 2005, Comparing maps of mean monthly surface temperature and precipitation for Alaska and adjacent areas of Canada produced by two different methods: Arctic, v. 58, no. 2, p. 137-161.

Appendix B: Air Photos of Glacier Area Change

The corrected and traced air photos of glacier area change used in this study are displayed below.

Petersen Glacier:

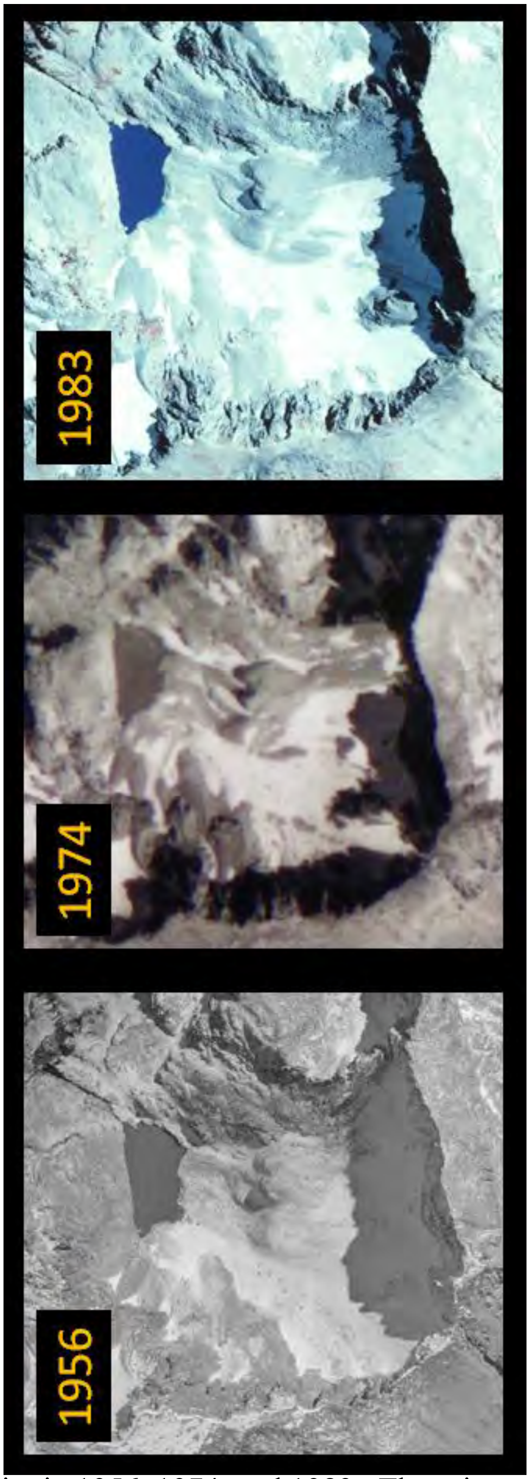

Figure 1. Petersen Glacier in 1956, 1974, and 1983. These images are cropped and uncorrected.

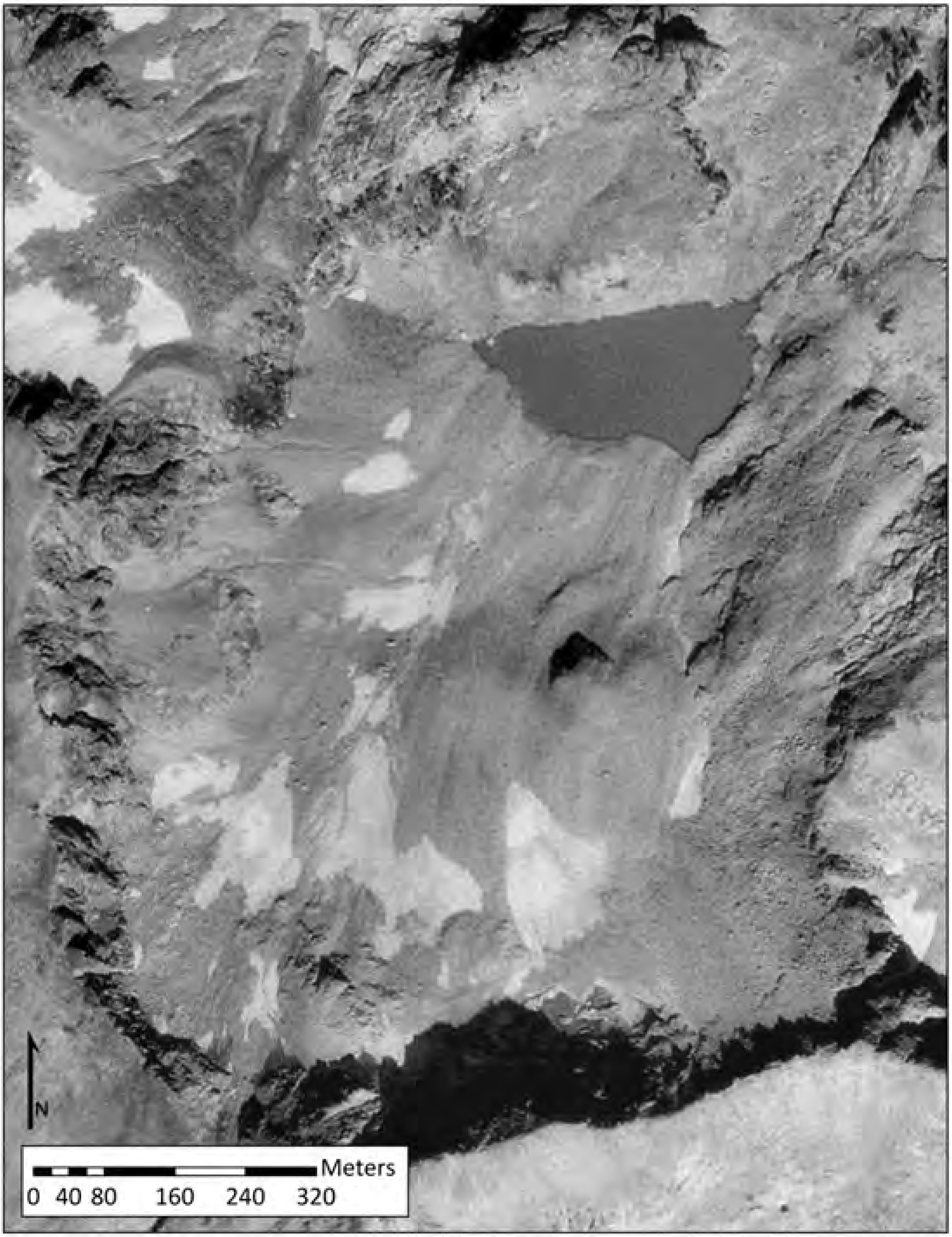

Figure 2. Petersen Glacier in 1994.

Figure 3. Petersen Glacier in 2001.

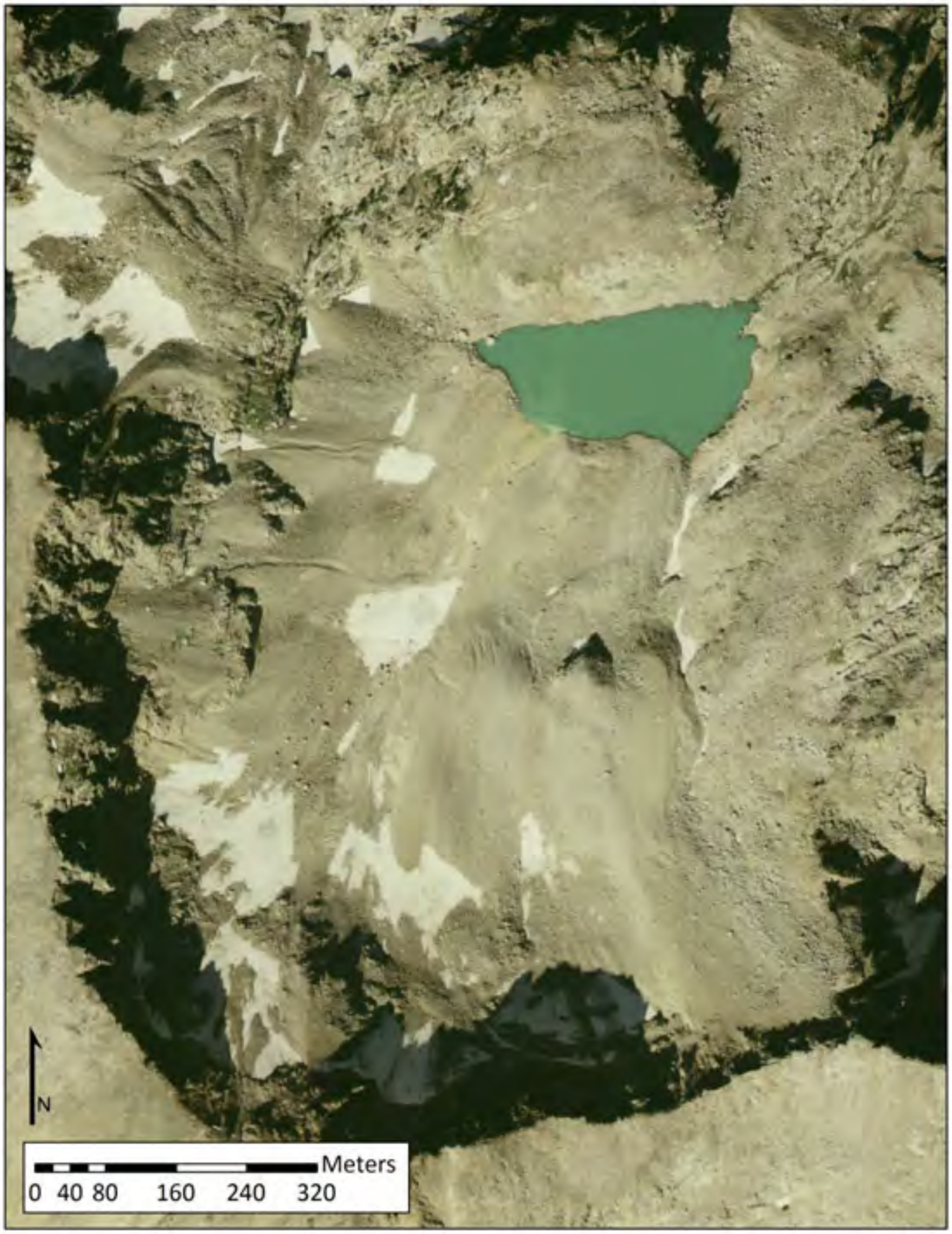

Figure 4. Petersen Glacier in 2006.

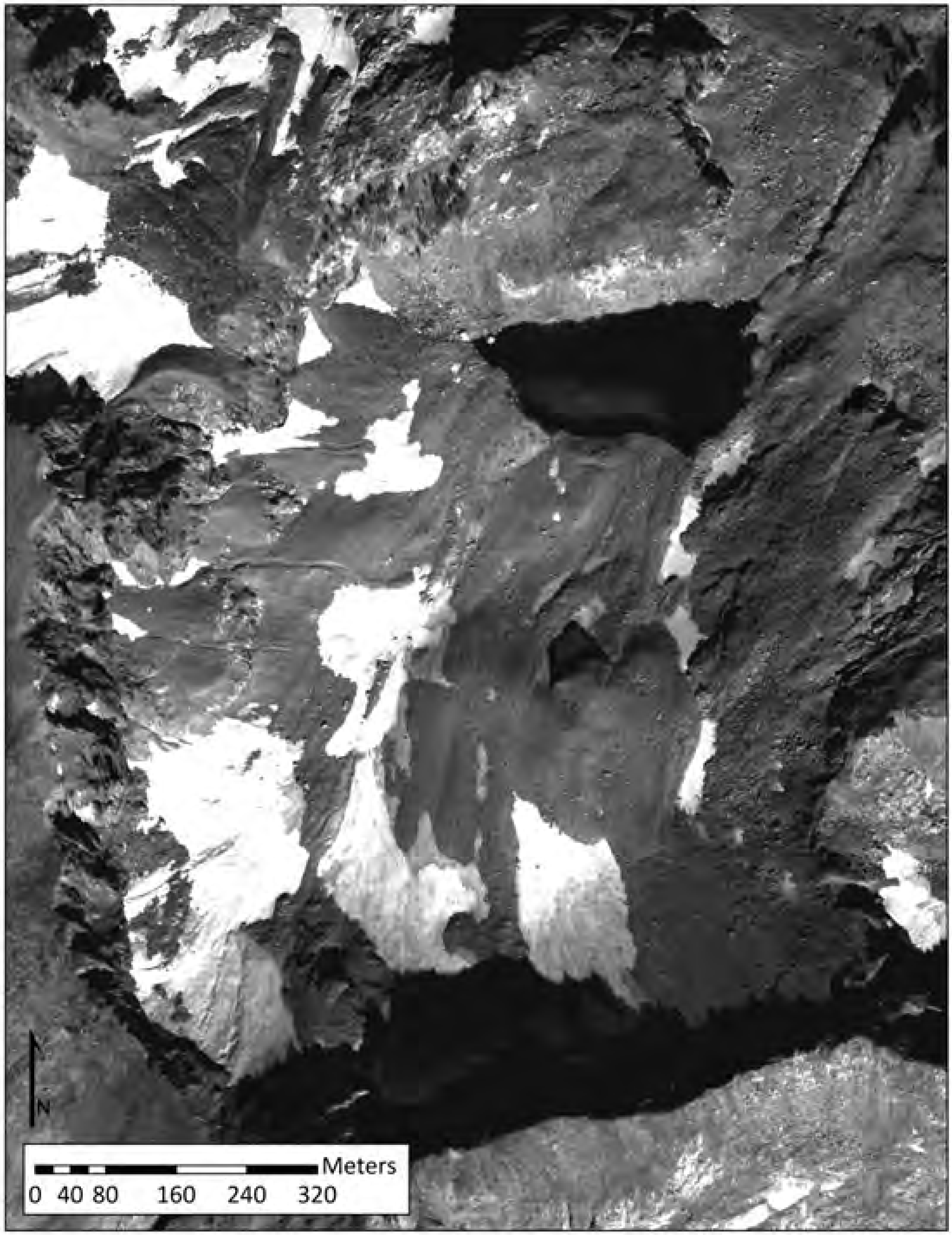

Figure 5. Petersen Glacier in 2009.

Schoolroom Glacier:

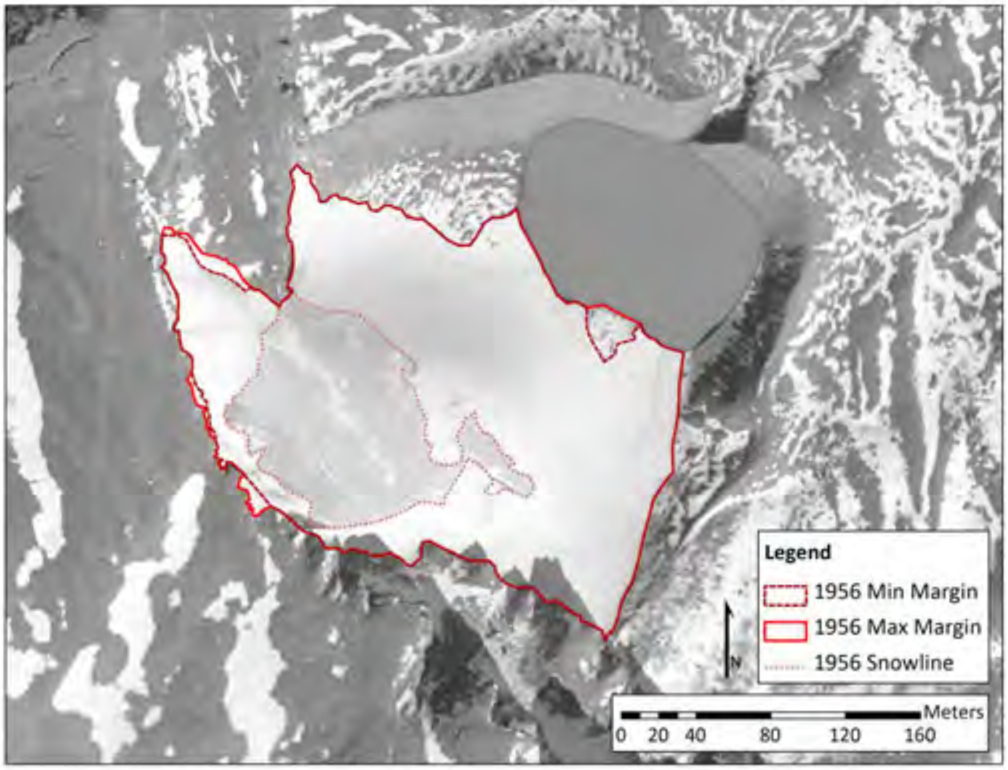

Figure 6. Schoolroom Glacier in 1956.

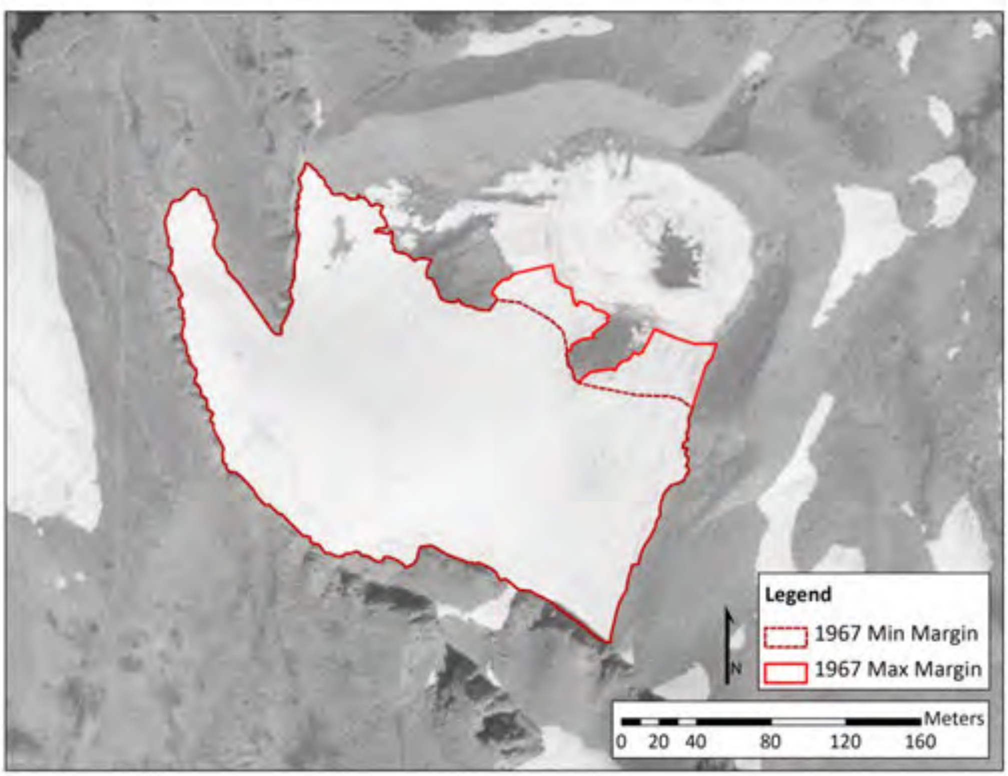

Figure 7. Schoolroom Glacier in 1967.

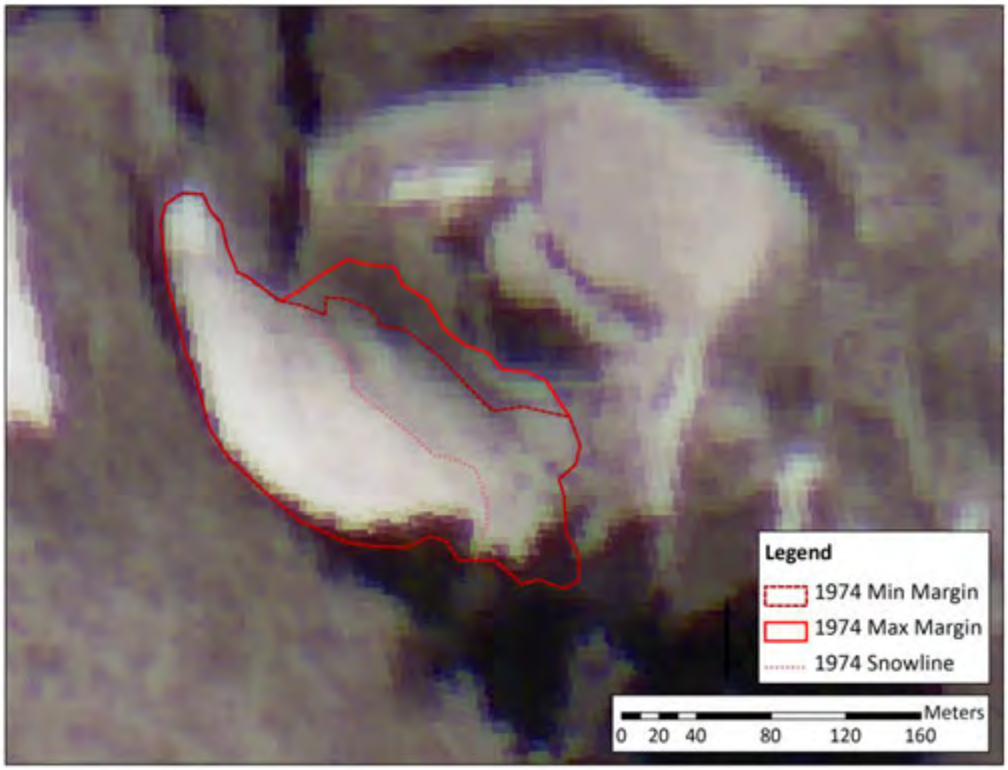

Figure 8. Schoolroom Glacier in 1974.

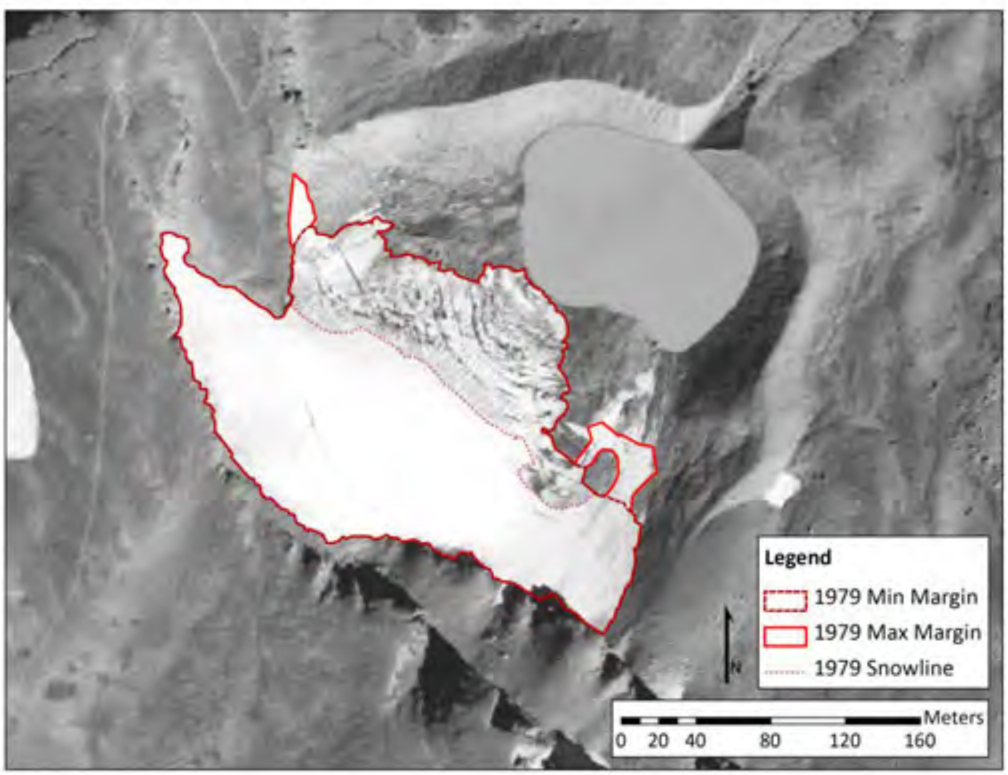

Figure 9. Schoolroom Glacier in 1979.

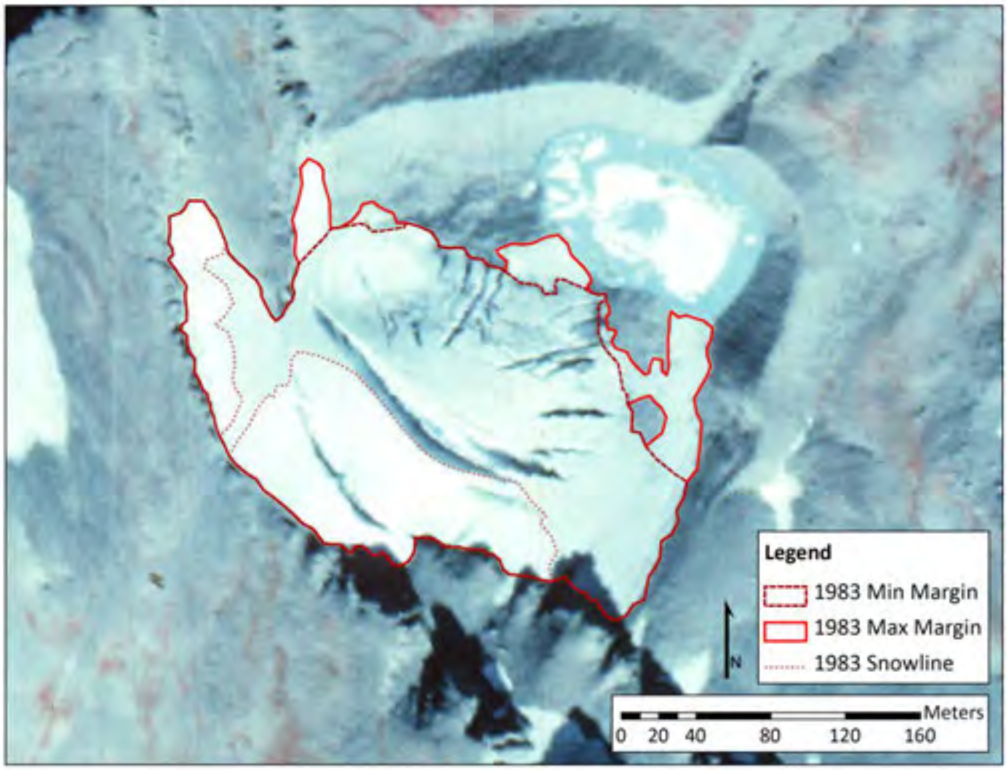

Figure 10. Schoolroom Glacier in 1983.

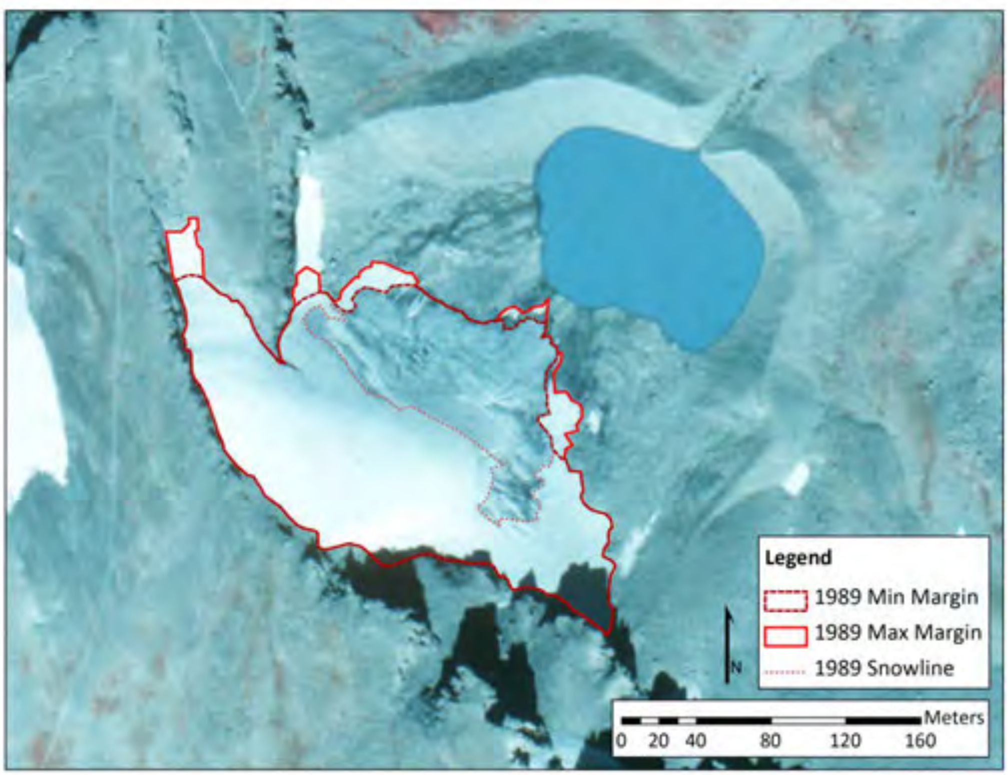

Figure 11. Schoolroom Glacier in 1989.

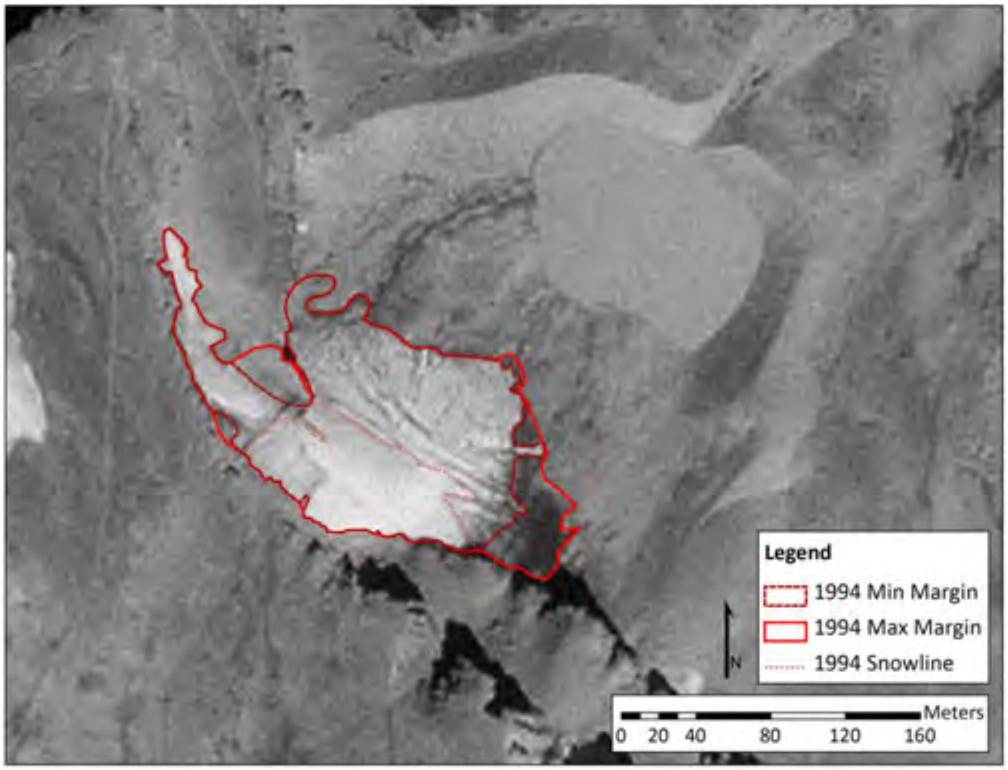

Figure 12. Schoolroom Glacier in 1994.

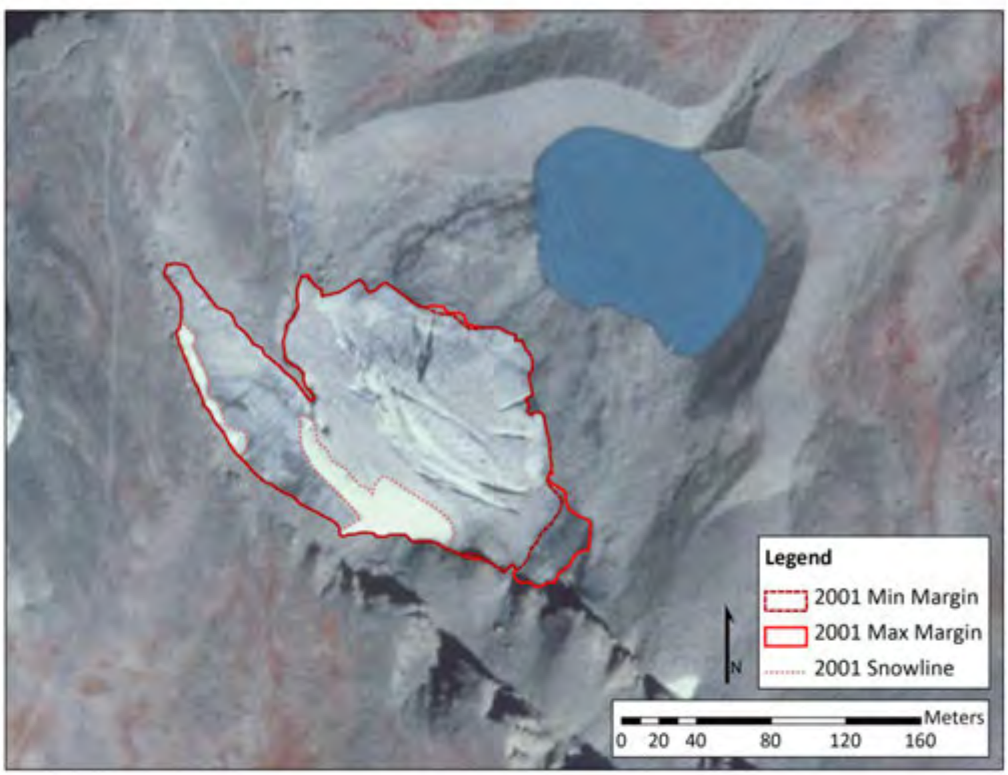

Figure 13. Schoolroom Glacier in 2001.

Figure 14. Schoolroom Glacier in 2006.

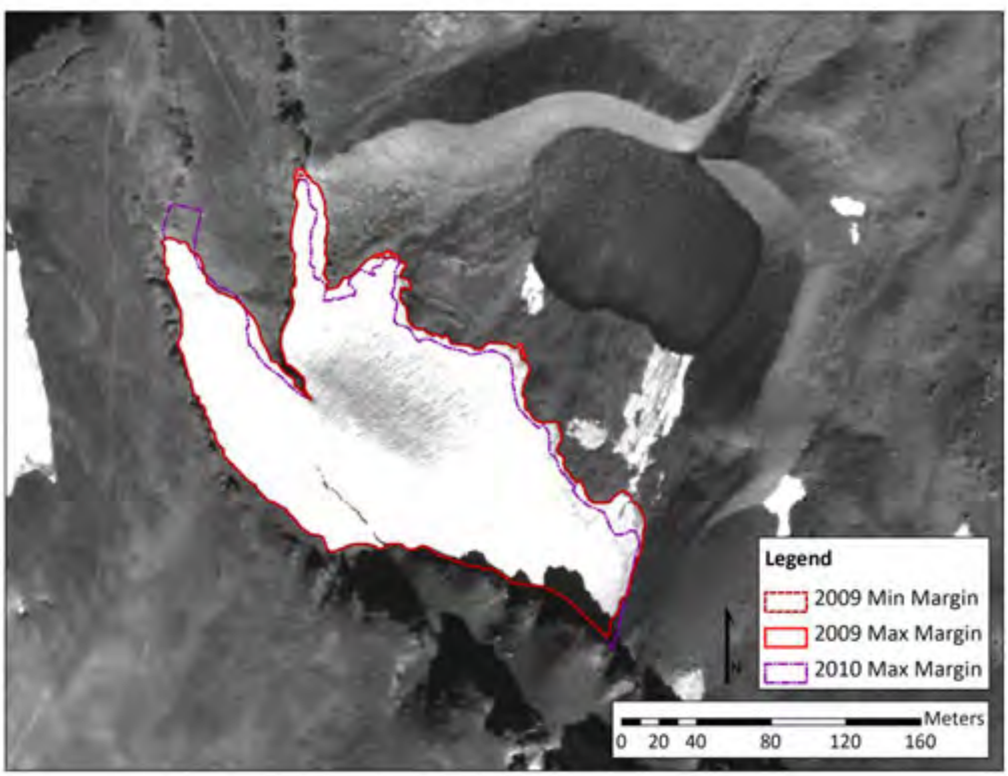

Figure 15. Schoolroom Glacier in 2009 and 2010.

Skillet and Falling Ice Glaciers:

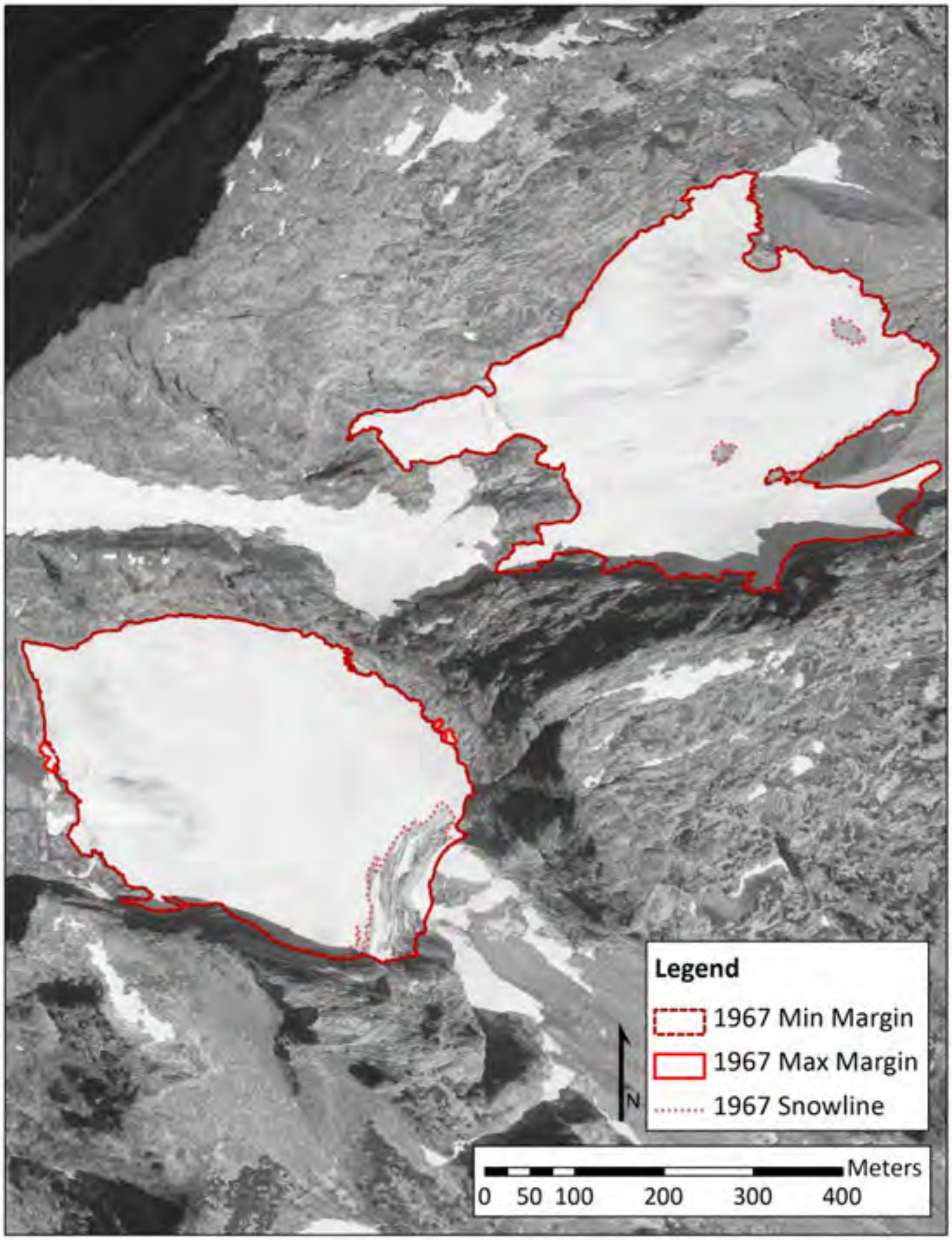

Figure 16. Skillet and Falling Ice Glaciers in 1967.

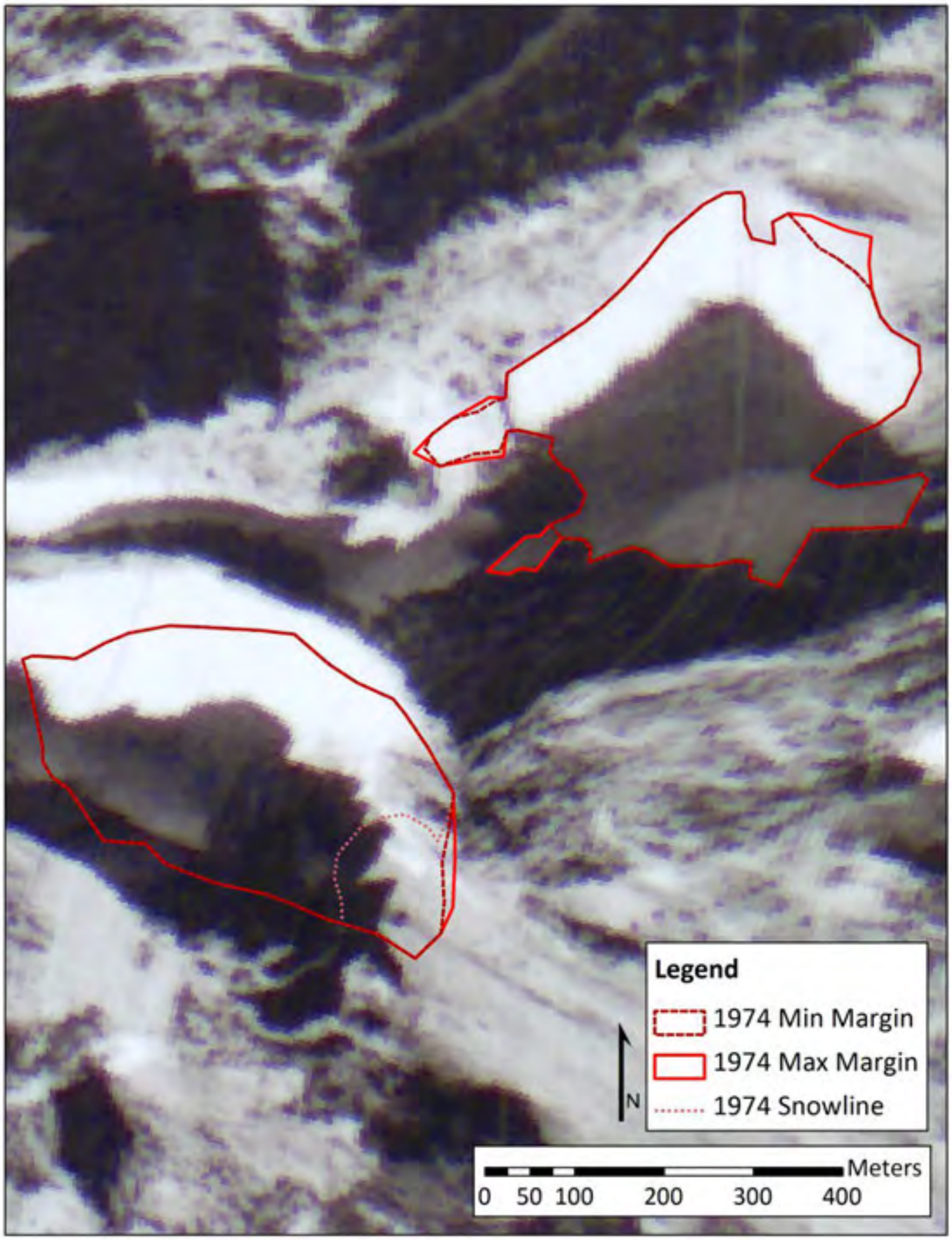

Figure 17. Skillet Glacier in 1974.

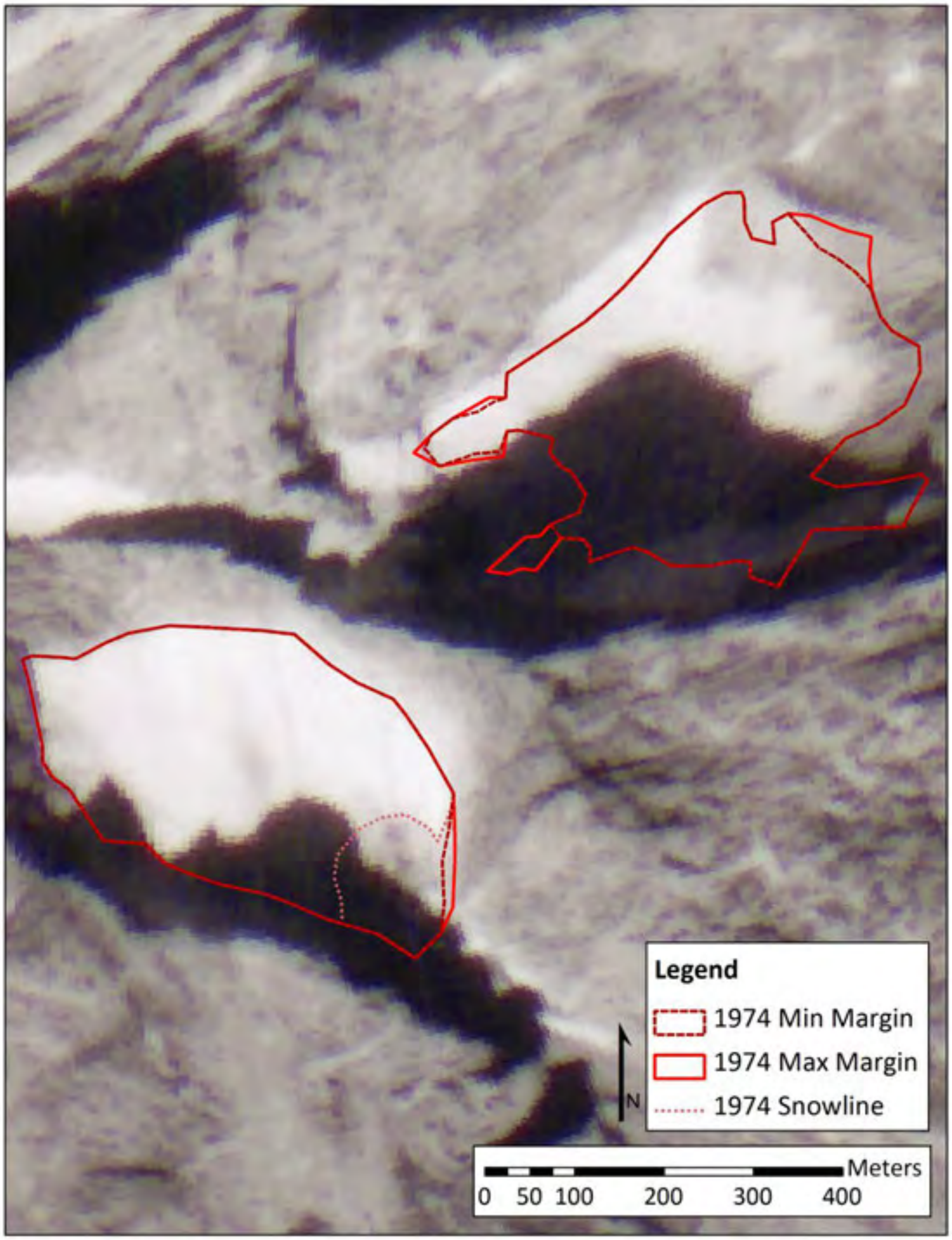

Figure 18. Falling Ice Glacier in 1974.

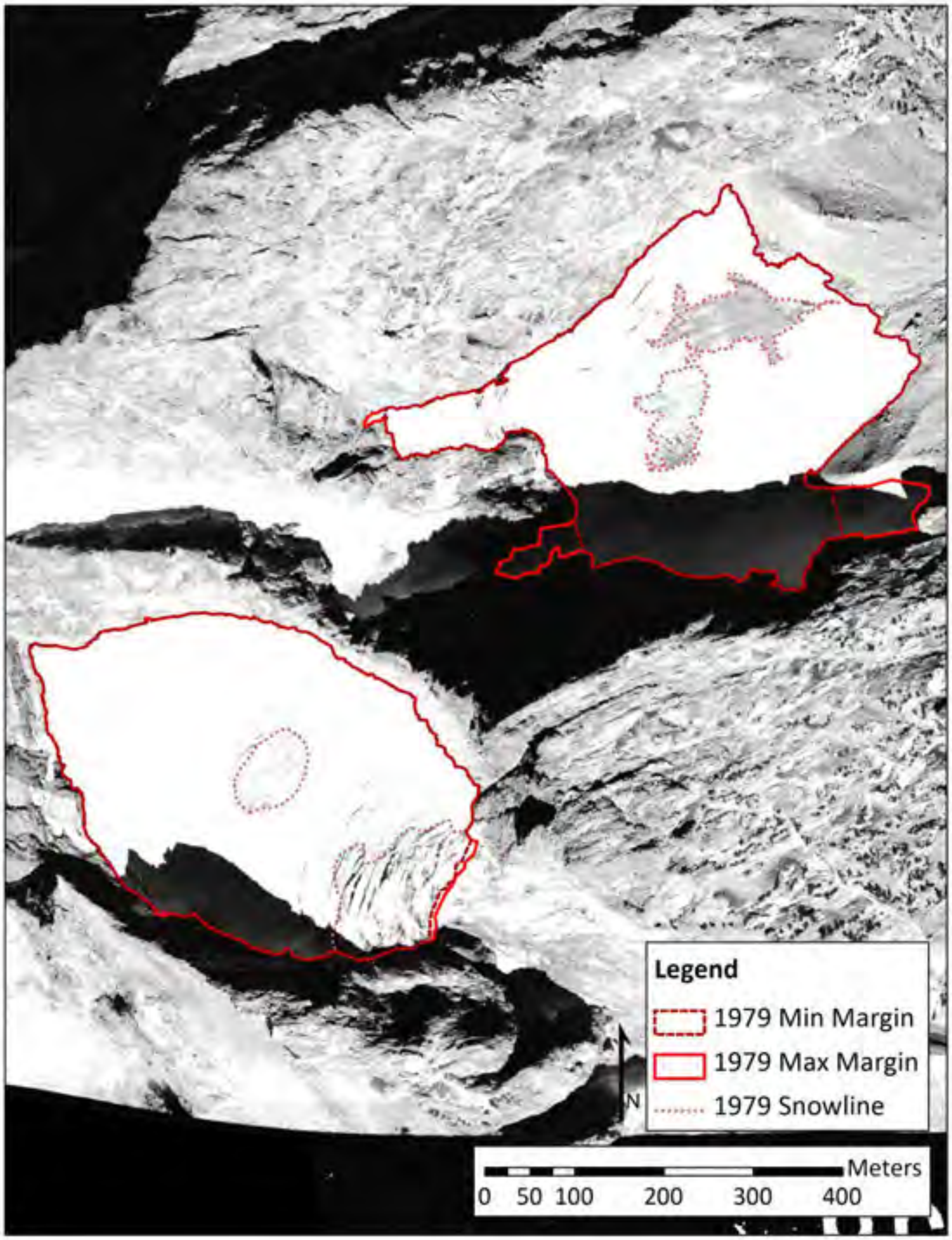

Figure 19. Skillet and Falling Ice Glaciers in 1979.

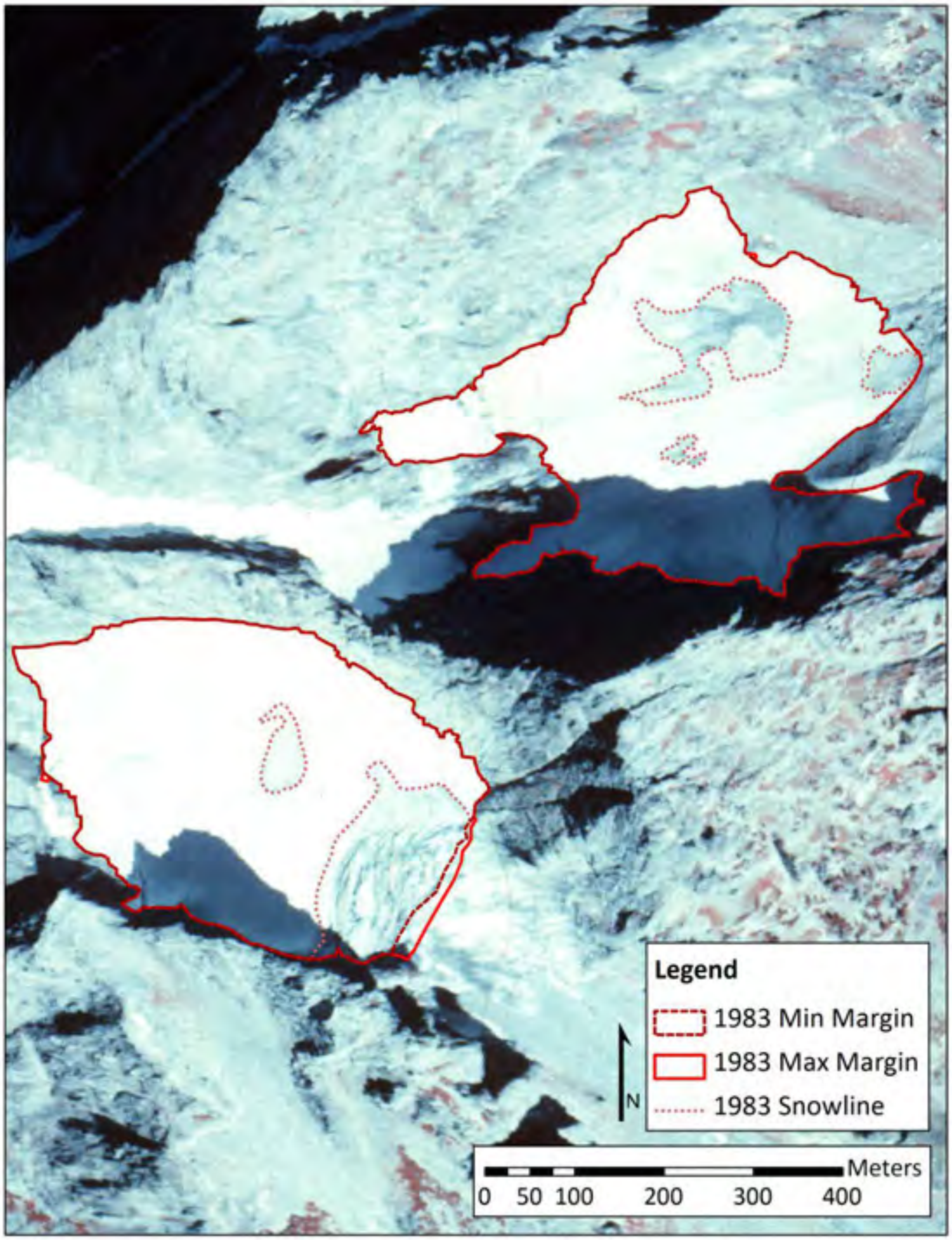

Figure 20. Skillet and Falling Ice Glaciers in 1983.

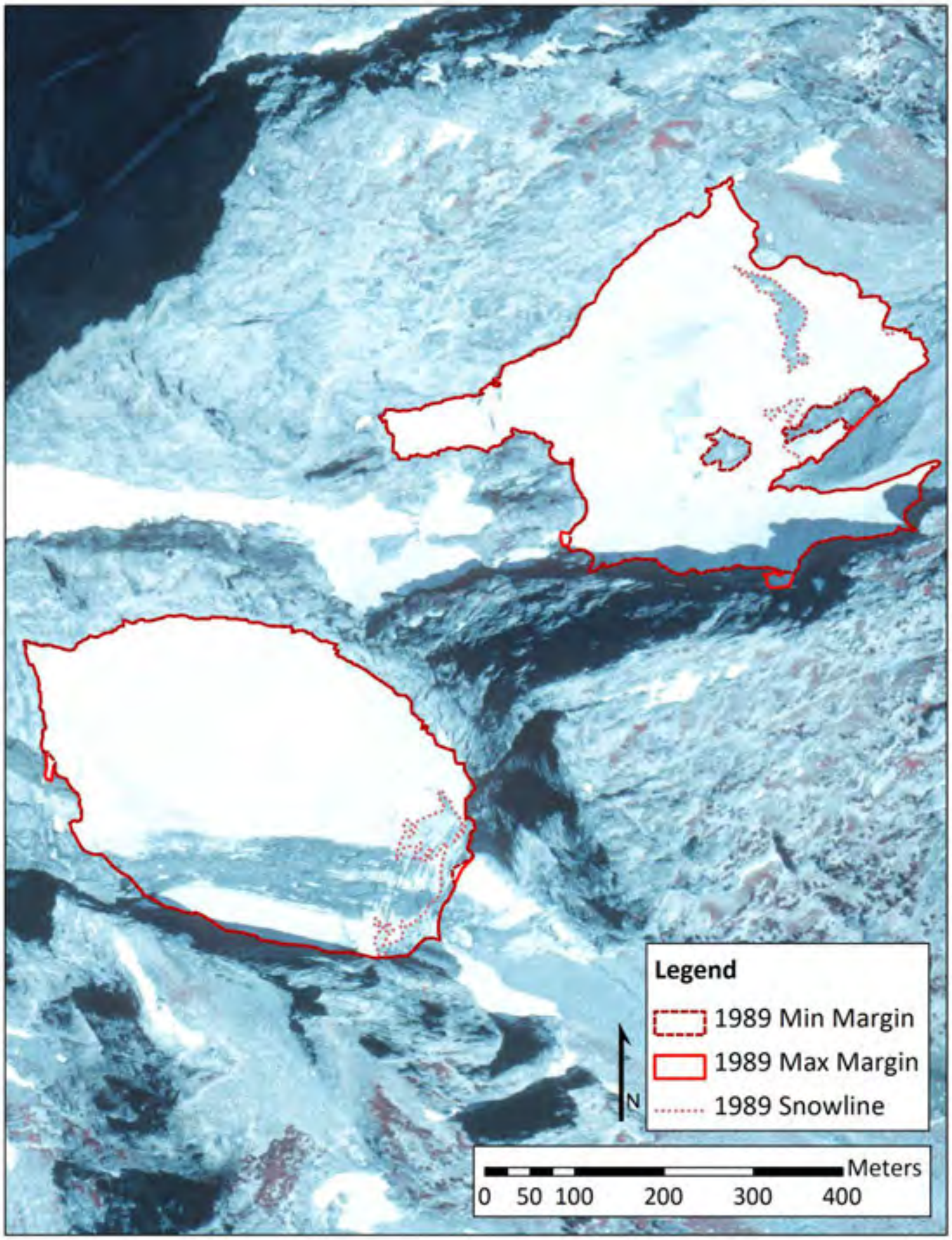

Figure 21. Skillet and Falling Ice Glaciers in 1989.

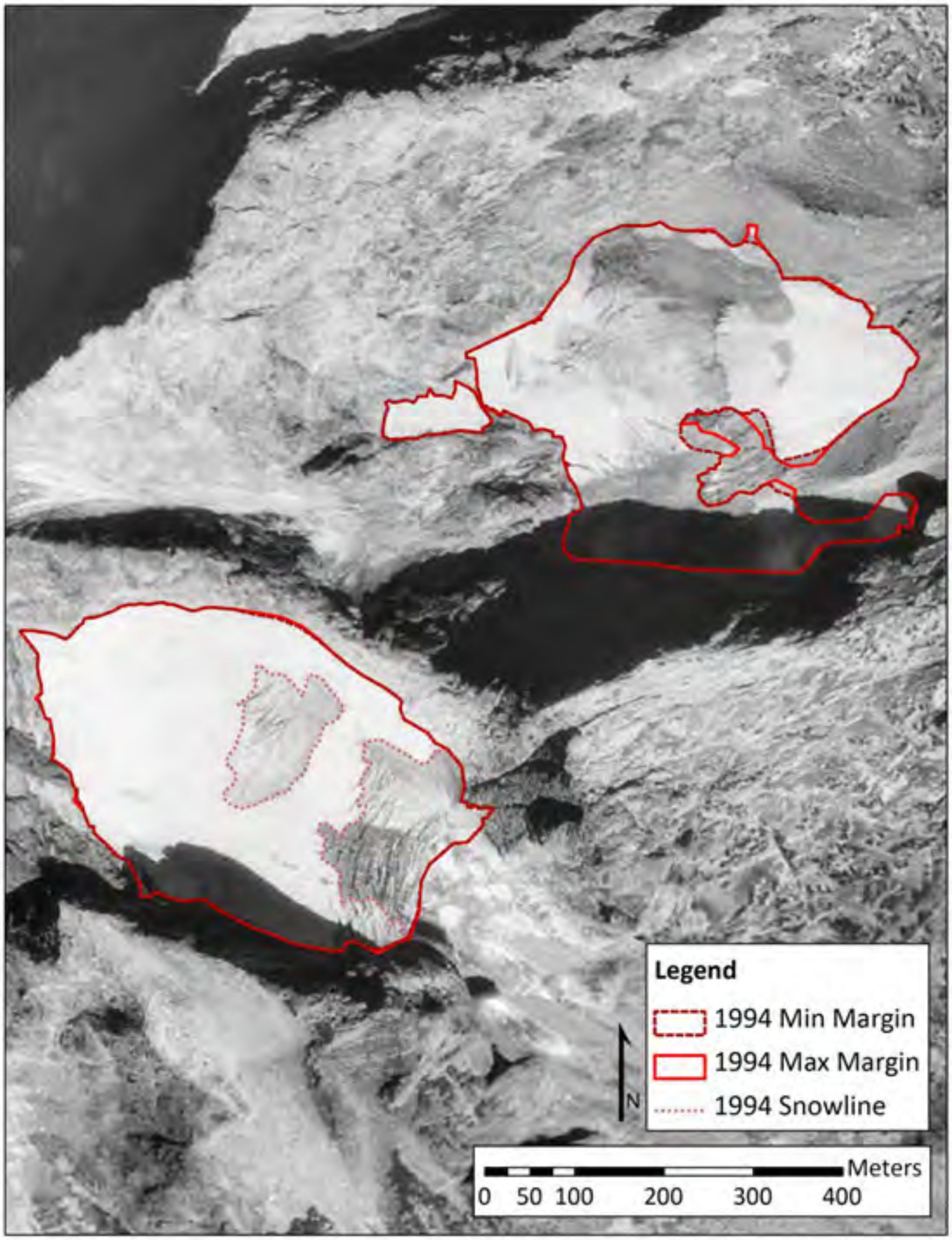

Figure 22. Skillet and Falling Ice Glaciers in 1994.

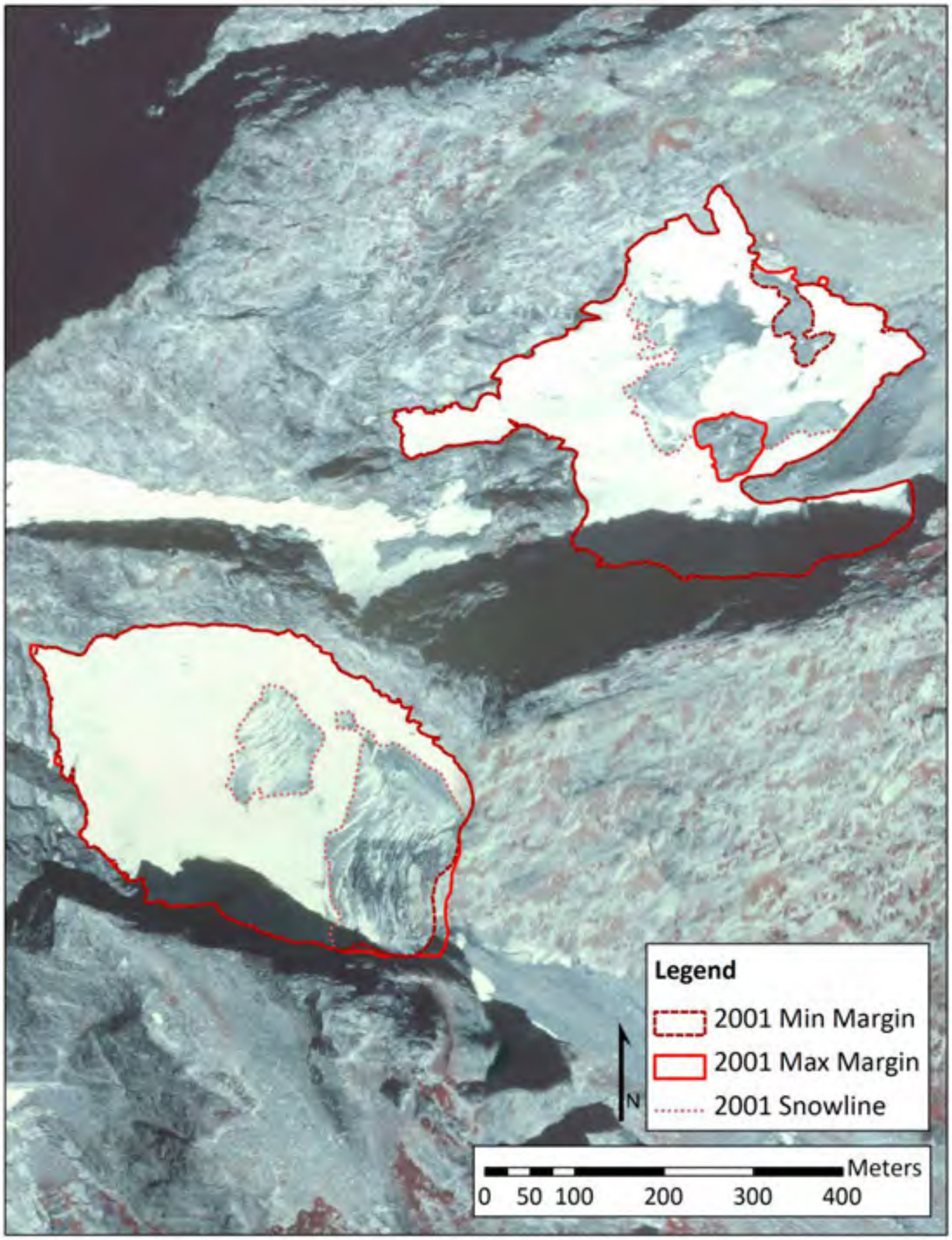

Figure 23. Skillet and Falling Ice Glaciers in 2001.

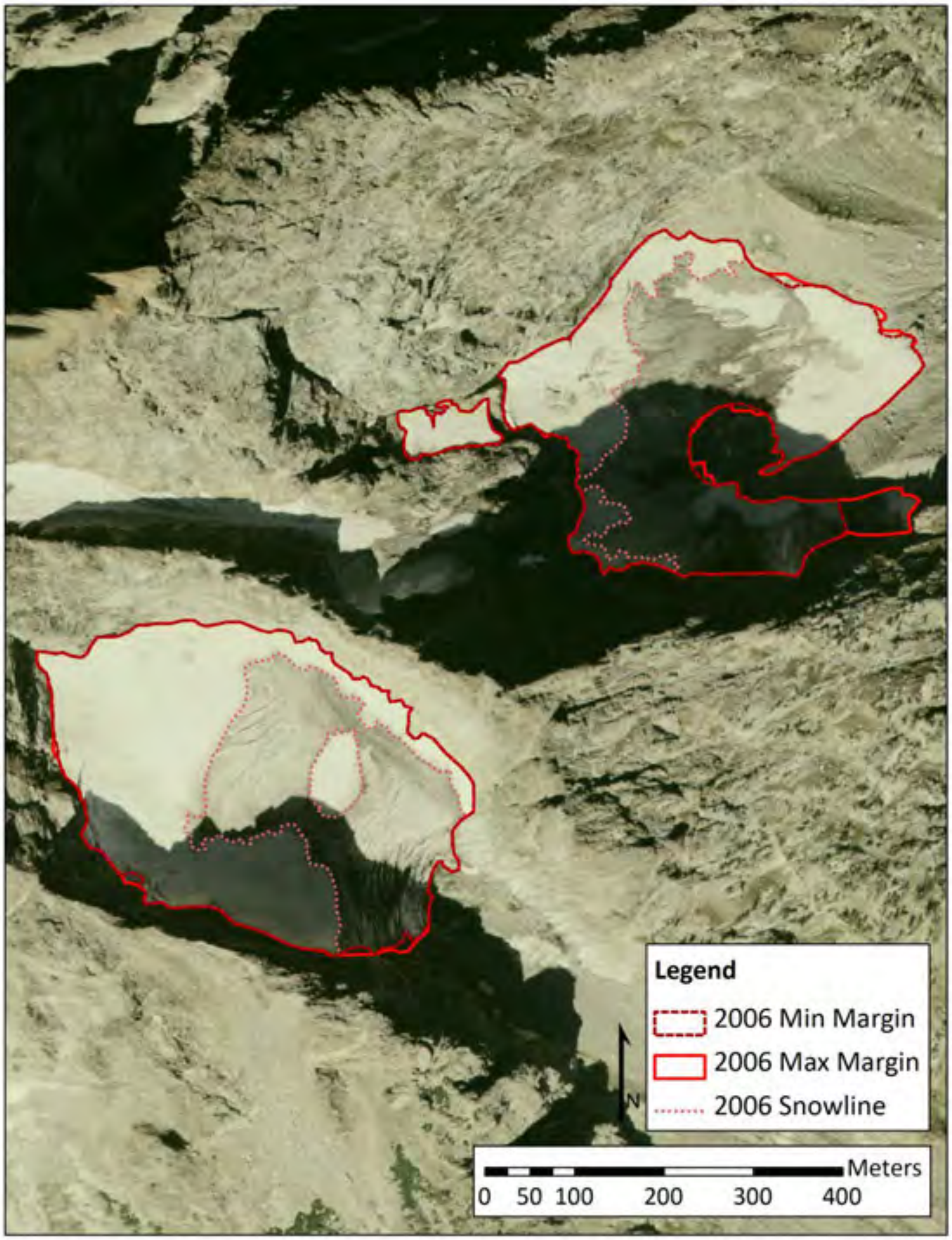

Figure 24. Skillet and Falling Ice Glaciers in 2006.

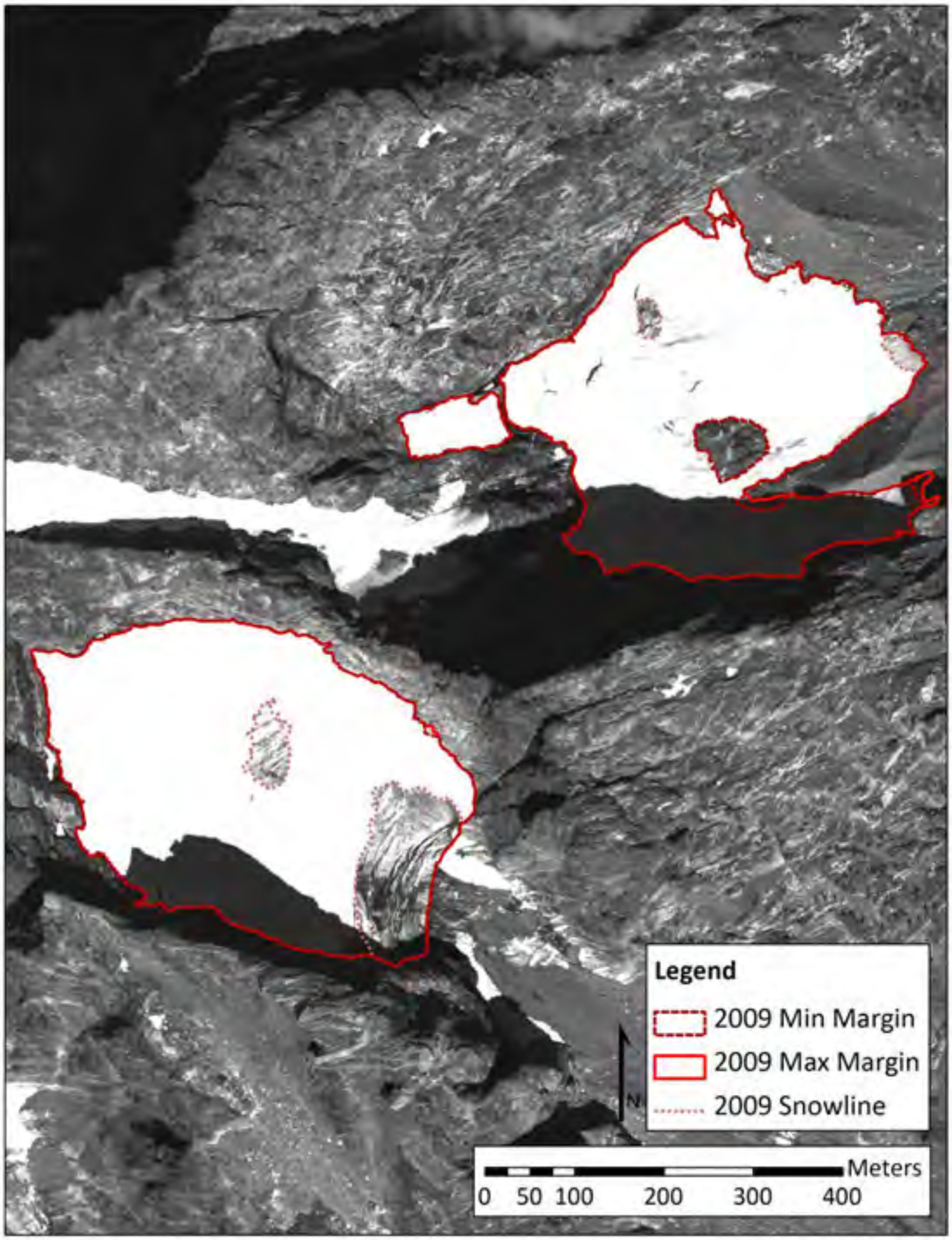

Figure 25. Skillet and Falling Ice Glaciers in 2009.

Triple Glaciers:

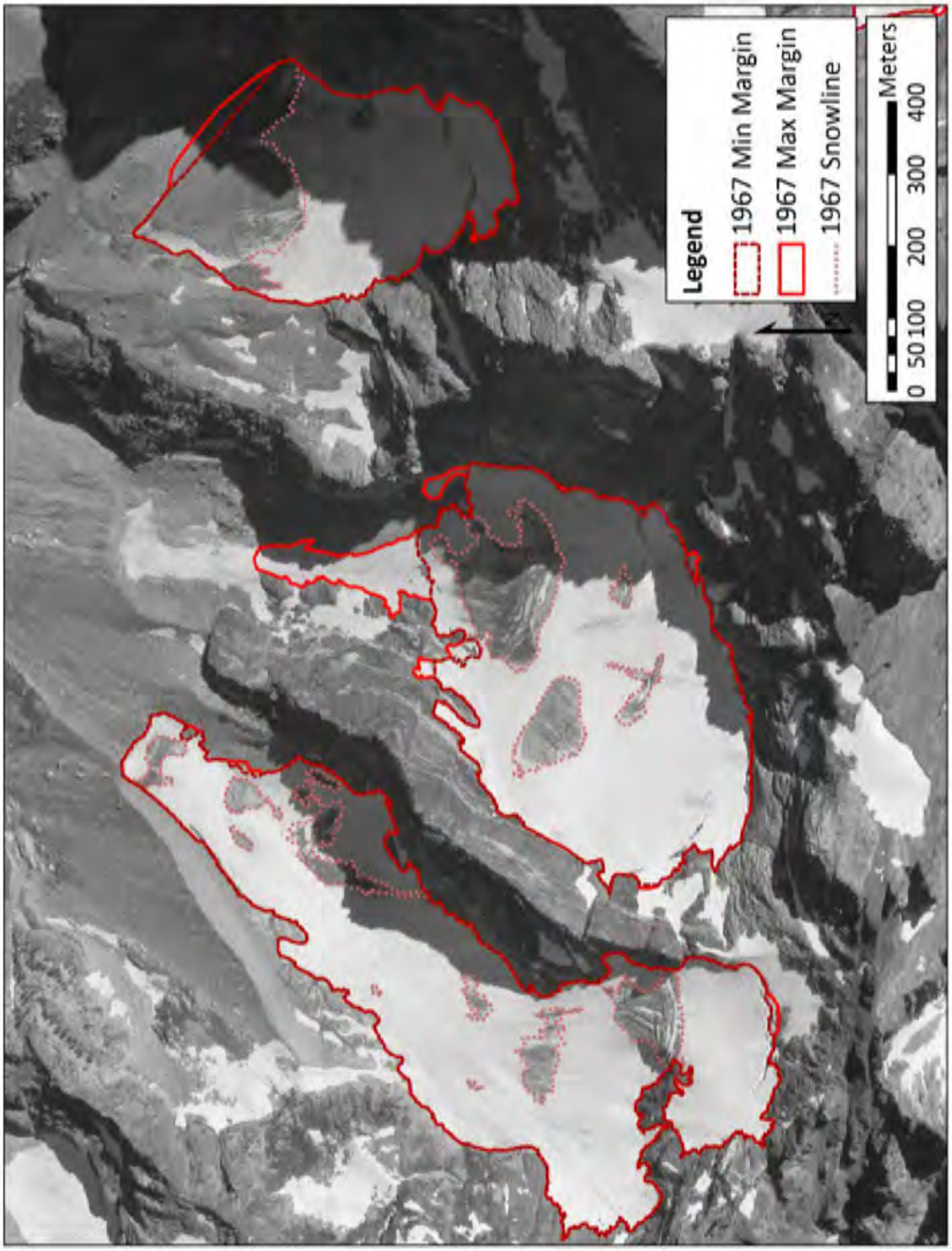

Figure 26. Triple Glaciers in 1967.

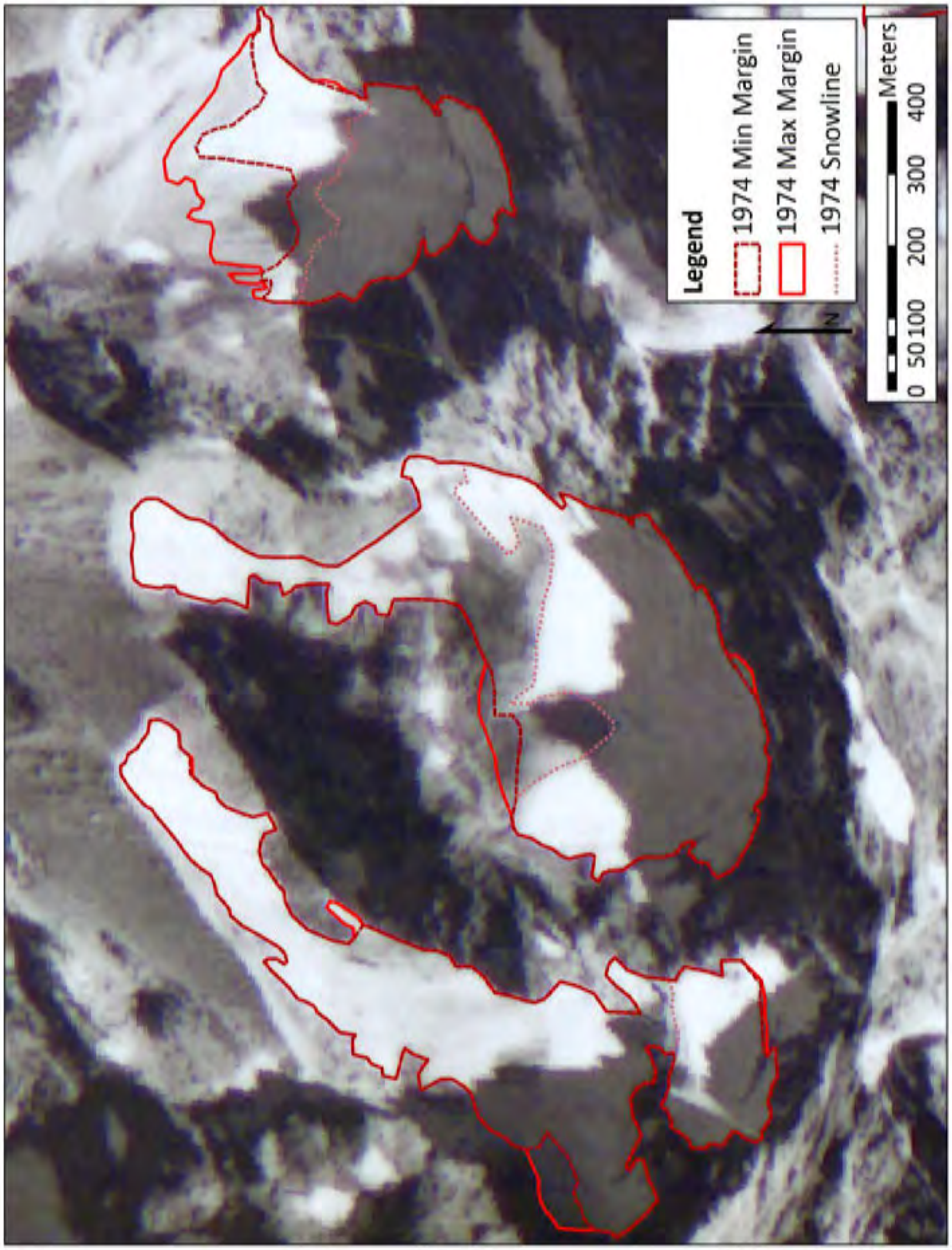

Figure 27. Triple Glaciers in 1974.

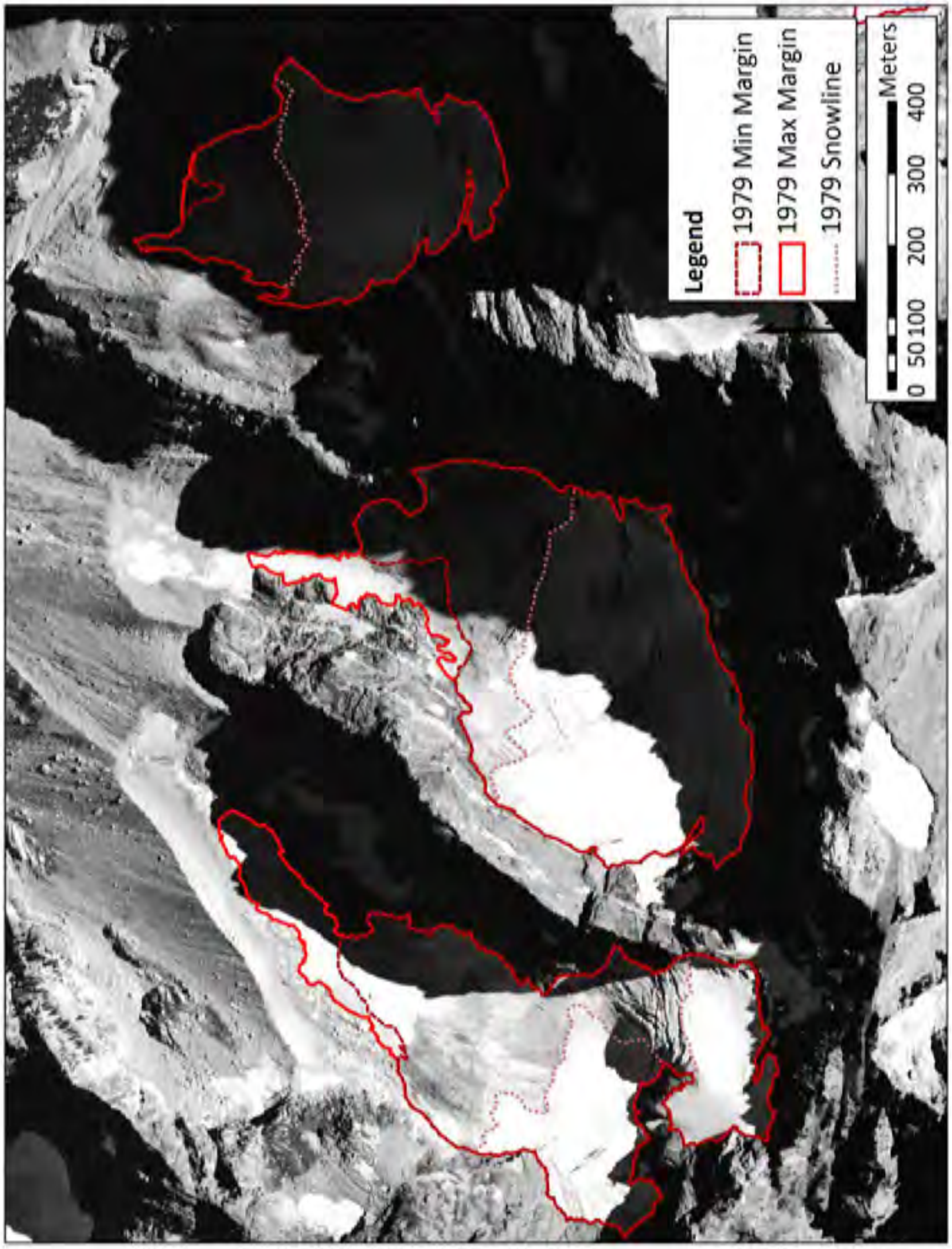

Figure 28. Triple Glaciers in 1979.

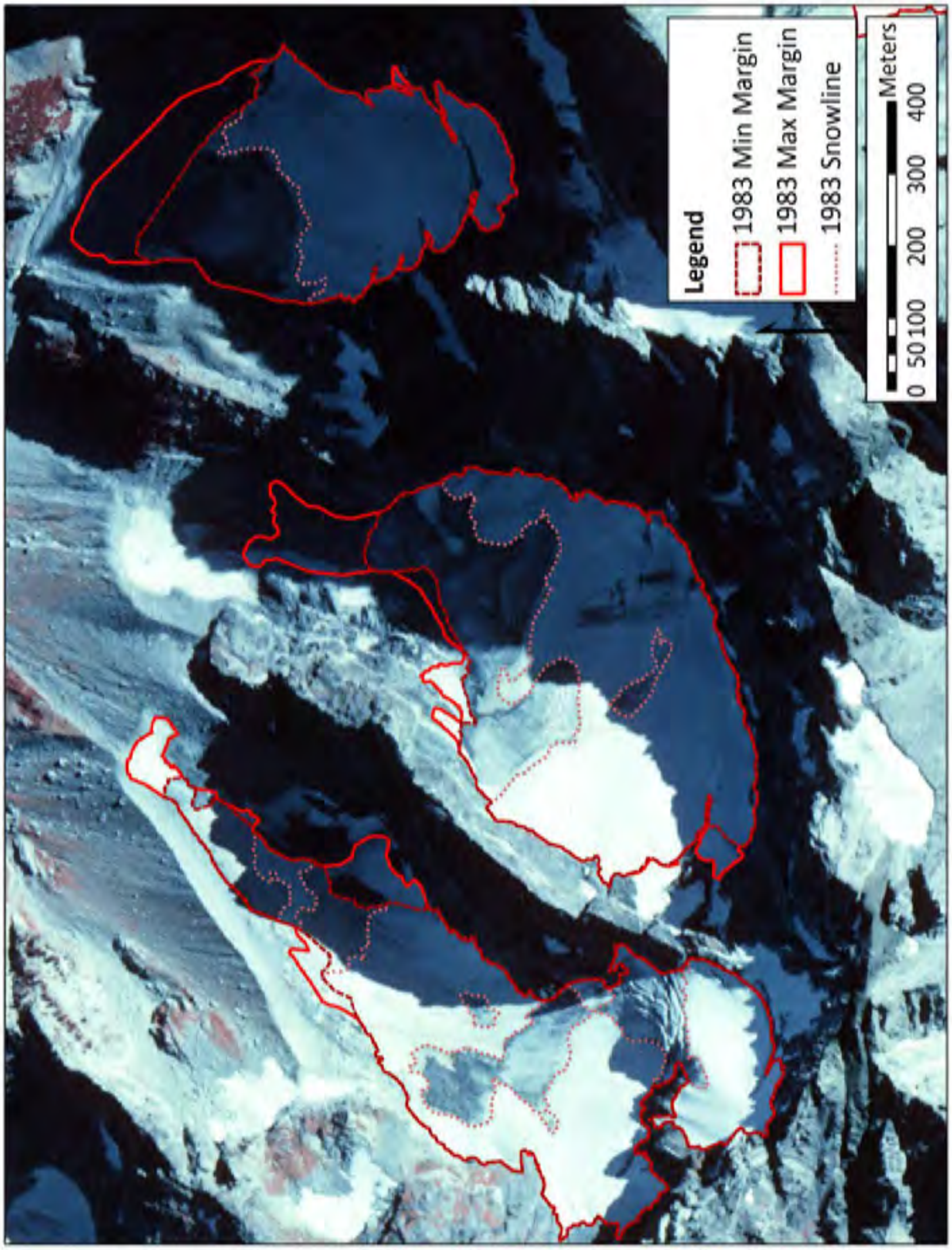

Figure 29. Triple Glaciers in 1983.

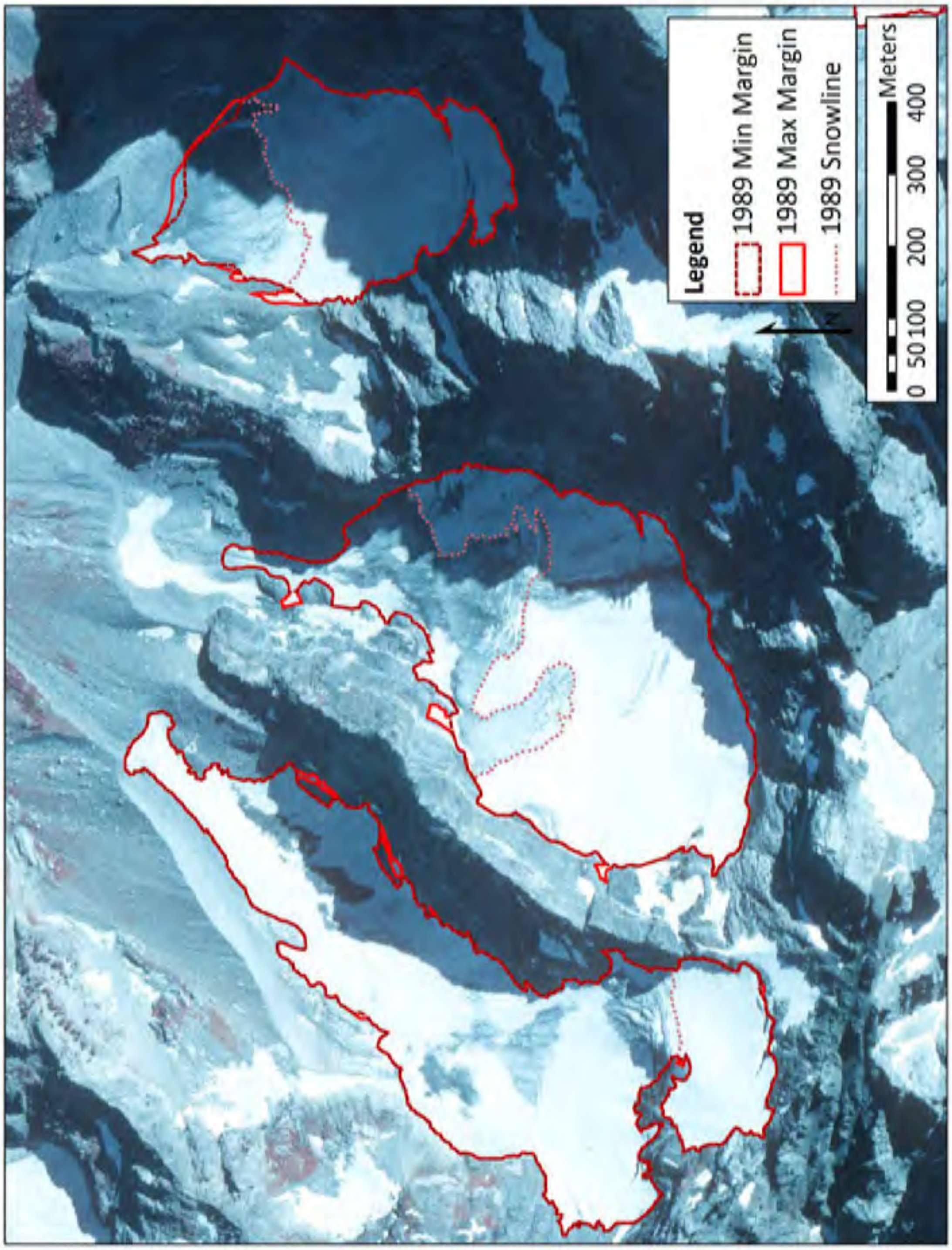

Figure 30. Triple Glaciers in 1989.

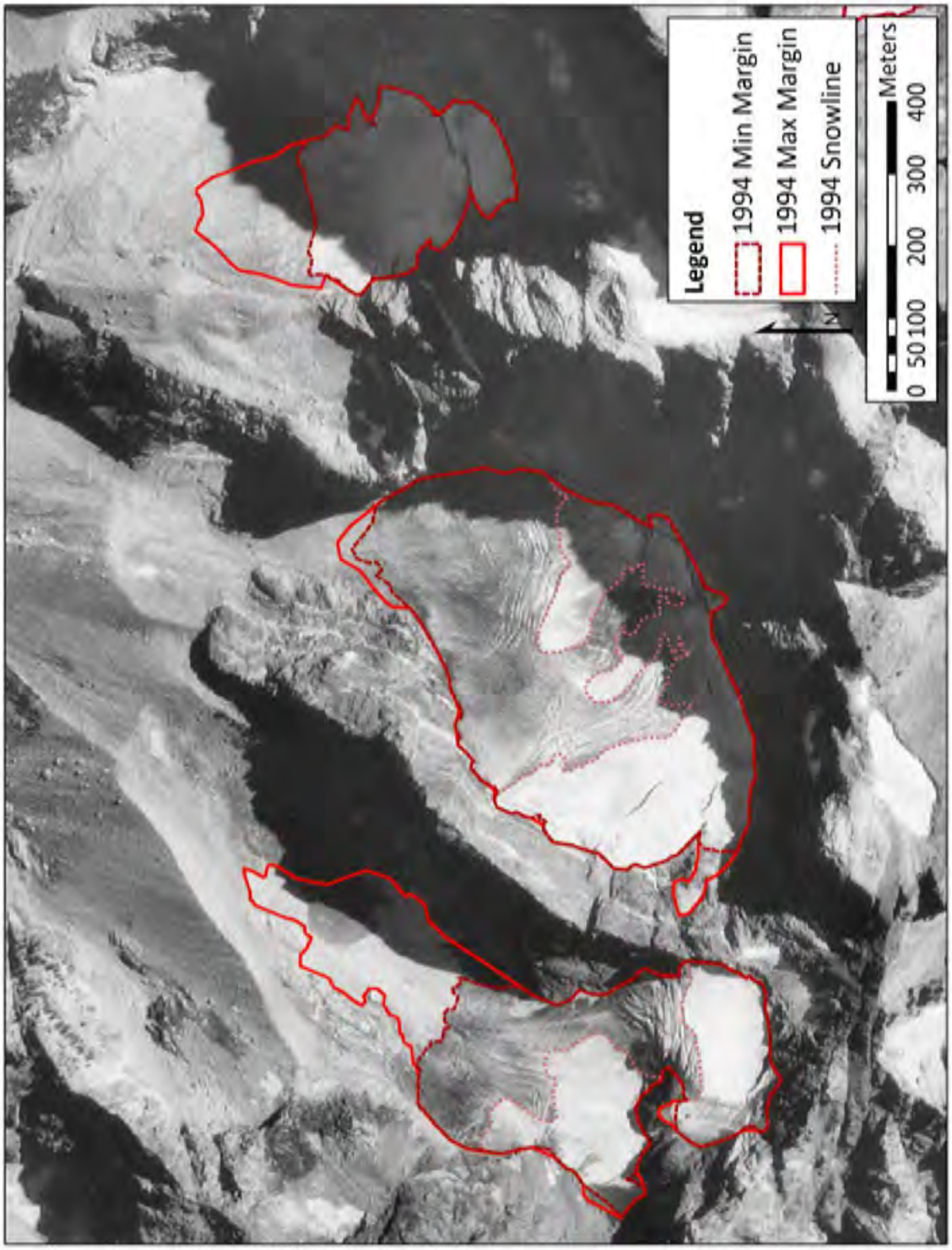

Figure 31. Triple Glaciers in 1994.

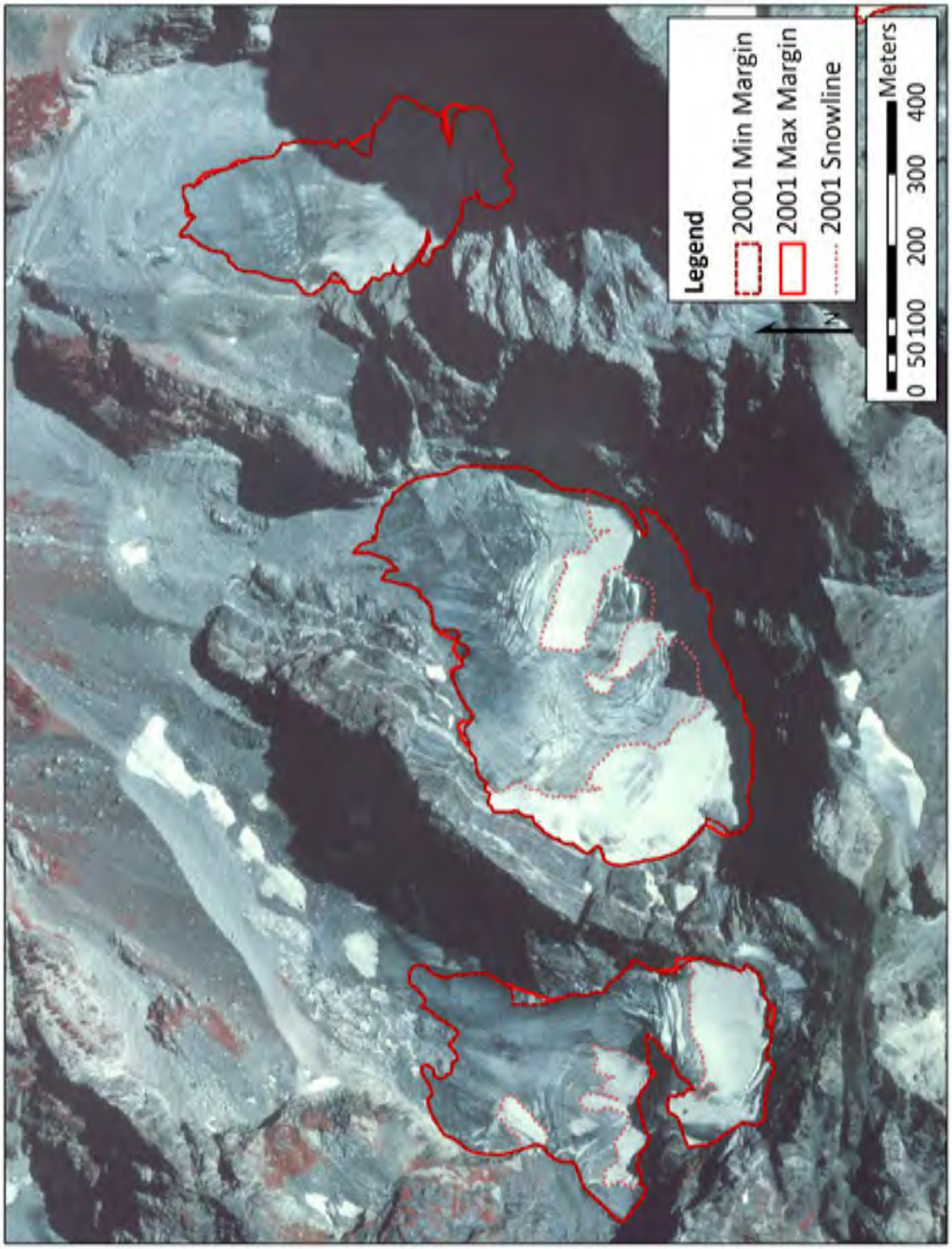

Figure 32. Triple Glaciers in 2001.

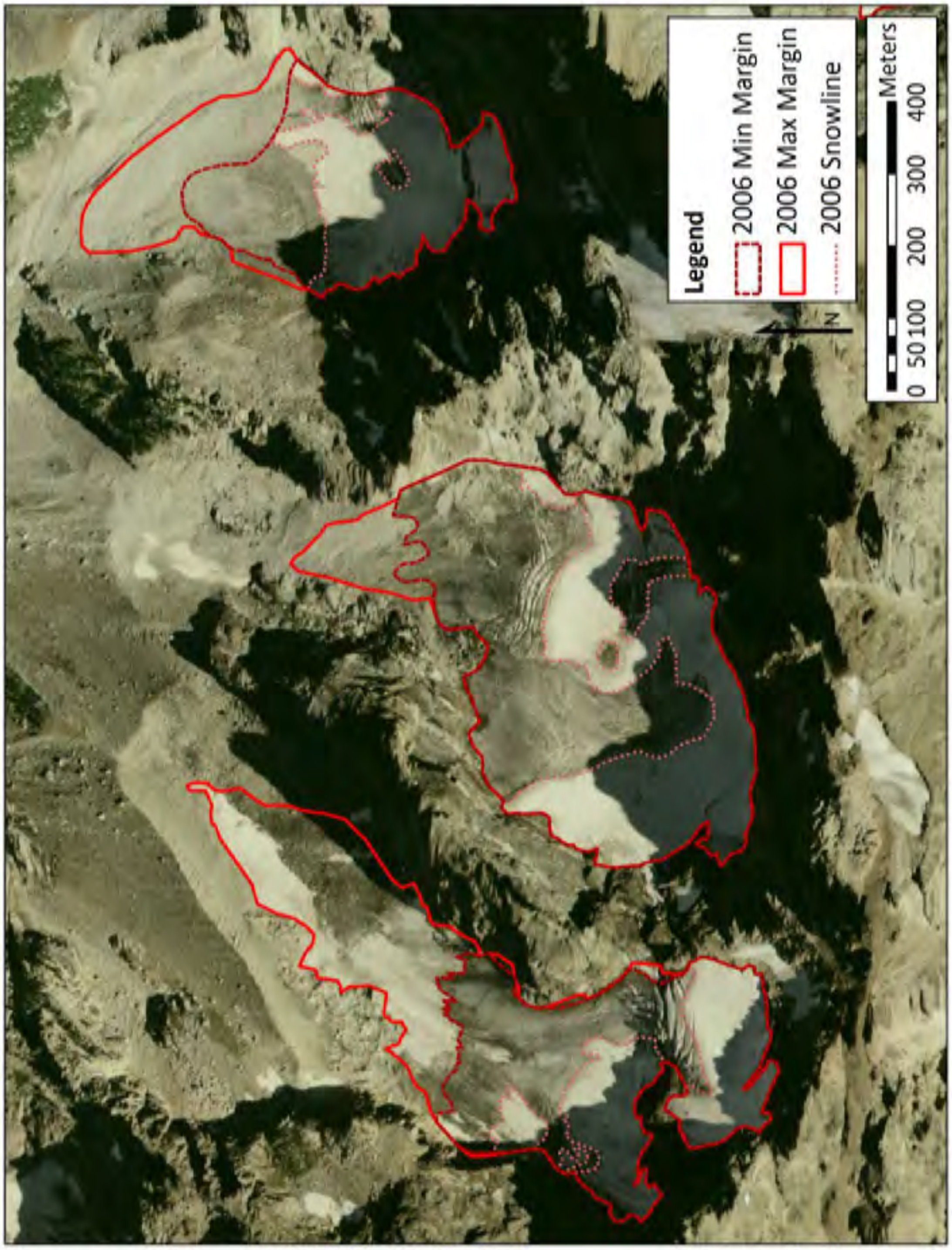

Figure 33. Triple Glaciers in 2006.

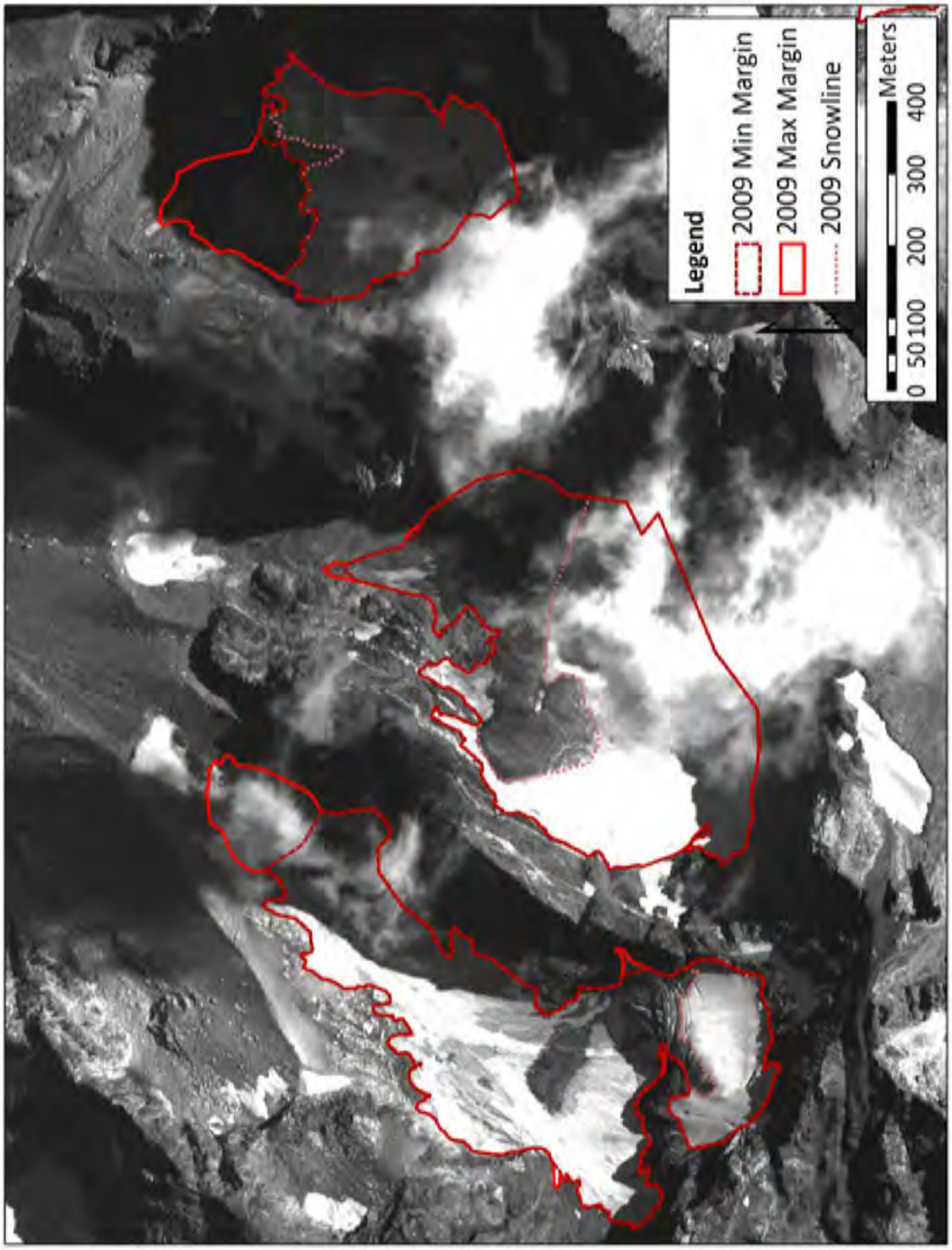

Figure 34. Triple Glaciers in 2009.

Appendix C: Pearson correlation coefficients and Partial least squares regression analysis

Pearson correlation coefficients

Partial Least Squares regression (PLS) determined the same dominant seasonal climatic variable as determined by Pearson correlation coefficients (PCC) for Falling Ice, Skillet, and the Triple Glaciers (Table 1). However, PLS determined the dominant annual seasonal climate variable was winter temperature at Schoolroom Glacier, instead of summer precipitation, as shown by PCC. Schoolroom Glacier likely is strongly influenced by wind-blown snow and this effect may confound simple glacier-climate relationships.

PCC comparisons of glacier area and temperature indicate that the strongest negative correlations were with spring and annual temperatures at Falling Ice Glacier. This result suggests that higher spring and annual temperatures lead to smaller glacier areas. If mean spring temperatures remain above freezing, they would contribute to glacier loss through ablation. Conversely, spring temperatures occasionally dip below freezing and, if coincident with precipitating storms, would contribute to increasing glacier mass.

Falling Ice Glacier is strongly correlated with spring and annual temperature as the area changes of the glacier are generally linear. We suggest that smaller temperature variability seems to force this glacier, which has limited area variability. Annual temperatures at Schoolroom Glacier tended to straddle 0°C while temperatures at Mt. Moran tended to remain below freezing until 1998, after which they remained above freezing until 2009.

The two statistical analyses did not agree on the strongest climatic variable for Schoolroom Glacier. PCC shows a weak positive correlation with summer precipitation whereas PLS determined the strongest variable was winter temperature closely followed by summer precipitation. This suggests that precipitation in the summer is still important. These two climatic variables occur in opposite seasons to produce typical annual glacier area fluctuations. That is, glacier area increases in winter as cooler temperatures allow more accumulation than ablation to occur. Additionally, warmer winter temperatures associated with storms could provide heavier, more water-rich snow. Alternatively, as summer precipitation decreases, glacier area decreases. However, this issue may not be directly related to less precipitation as much as it may be related to less cloudiness or shade from direct sun (Rupper and Roe, 2008).

Schoolroom Glacier is heavily influenced by wind. Schoolroom Glacier is located just east of the watershed divide for the Teton Range and just below a trail pass aptly named Hurricane Pass. This pass is often windy with high gusts. A high plain is located to the southwest and upwind of the glacier. It is highly likely that snow deposited on this plain and further upwind is redeposited onto the glacier, and may be a primary factor for the continued existence and area fluctuations of this clean-ice glacier.

The strongest PCC climate – ice area relationships with the remaining four glaciers are with different seasonal precipitation variables. Skillet Glacier and West Triple Glacier exhibited the strongest PCCs with spring precipitation, which was confirmed by PLS. Winter and summer precipitation were the strongest climatic variables for East and Middle Triple Glaciers, respectively. Spring precipitation, especially when it falls as snow, can lengthen the glacial accumulation season and thus shorten the ablation season.

Spring precipitation may also correlate with cloudiness, which will also reduce ablation. As mentioned earlier, orographic precipitation can contribute larger amounts of mass to these glaciers. Higher precipitation in any season is often accompanied by more storminess and thus more clouds can provide both shade from shortwave radiation and retain reflected longwave radiation (Rupper and Roe, 2008). The former situation would retard ablation and the latter would not. Records of air pressure would help to constrain this factor.

Table 1. Strongest Pearson correlation coefficients for seasonal climate variables and Teton glaciers.

	Strong		**Weak**
Schoolroom	Summer P	Spring P	Spring T
correlation	0.510	0.502	-0.486
p-value	0.132	0.139	0.154
Falling Ice	Spring T	Annual T	Summer T
correlation	-0.984	-0.878	-0.799
p-value	0.000	0.004	0.017
Skillet	Spring P	Summer P	Spring T
correlation	0.811	0.803	-0.798
p-value	0.008	0.009	0.010
East Triple	Summer P	Annual P	Spring T
correlation	0.687	0.688	-0.601
p-value	0.041	0.041	0.087
Middle Triple	Winter P	Annual P	Fall P
correlation	0.637	0.552	0.530
p-value	0.065	0.123	0.142
West Triple	Spring P	Spring T	Annual P
correlation	0.800	-0.705	0.607
p-value	0.010	0.034	0.083

Three-year Partial least squares regression analysis
Results

Figure A and Table A present partial least squares regression standardized regression coefficients of three-year moving averages of weather variables for Teton glaciers. Three of six glaciers correlate strongly with the three-year moving average of winter temperature, whereas the remaining three glaciers correlate most strongly with either winter or spring temperature or precipitation. Using annually averaged temperature and precipitation, all but East Triple Glacier correlates most strongly with temperature.

Discussion

The three-year moving average PLS results are different from those found with one water year (or three months from one water year) of weather data compared to a glacier observation from the end of the same water year. As for the three-year moving average analysis, winter temperature was the strongest factor at three glaciers. However, dominant annual weather influences do not agree between the three analyses. We find the dominant annual weather variable at the three-year moving average analysis is temperature at five of six glaciers.

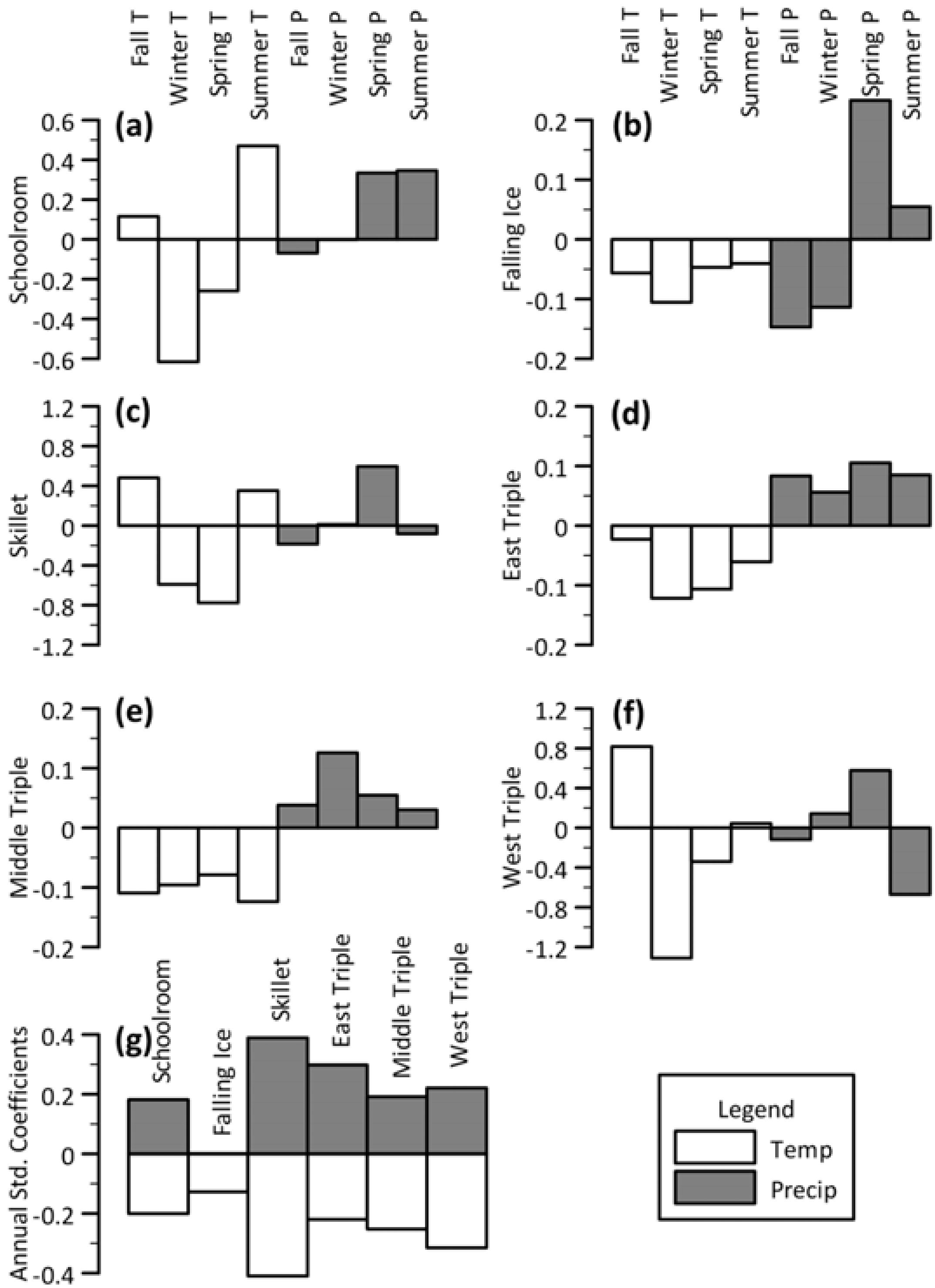

Figure A. Standardized regression coefficients of Teton glaciers with three-year moving averages of seasonal and (g) annual temperature and precipitation. Seasonal plots are for (a) Schoolroom, (b) Falling Ice, (c) Skillet, (d) East Triple, (e) Middle Triple, and (f) West Triple.

Table A. Highest ranked partial least squares regression standardized regression coefficients of three-year moving averages of weather variables for Teton glaciers.

Seasonal

rank	**School-room**	Std. coeff.	**Falling Ice**	Std. coeff.	**Skillet**	Std. coeff.	**East Triple**	Std. coeff.	**Middle Triple**	Std. coeff.	**West Triple**	Std. coeff.
1	Winter T	-0.616	Spring P	0.233	Spring T	-0.776	Winter T	-0.122	Winter P	0.126	Winter T	-1.310
2	Summer T*	0.470	Fall P*	-0.147	Spring P	0.596	Spring T	-0.106	Summer T	-0.124	Fall T*	0.819
3	Summer P	0.346	Winter P*	-0.114	Winter T	-0.590	Spring P	0.105	Fall T	-0.109	Summer P*	-0.670
	Spring P	0.335	Winter T	-0.105							Spring P	0.578
			Fall T	-0.056							Spring T	-0.339

Annual

rank	**School-room**	Std. coeff.	**Falling Ice**	Std. coeff.	**Skillet**	Std. coeff.	**East Triple**	Std. coeff.	**Middle Triple**	Std. coeff.	**West Triple**	Std. coeff.
1	Temp	-0.200	Temp	-0.127	Temp	-0.410	Precip	0.298	Temp	-0.252	Temp	-0.315
2	Precip	0.182	Precip	0.001	Precip	0.389	Temp	-0.220	Precip	0.192	Precip	0.221

* denotes opposite correlation than expected.

Partial least squares regression analysis

Results of Minitab (v. 16) output from partial least squares regression analysis in this study are displayed below.

Annual PLS results

Schoolroom Glacier (seasonally only)

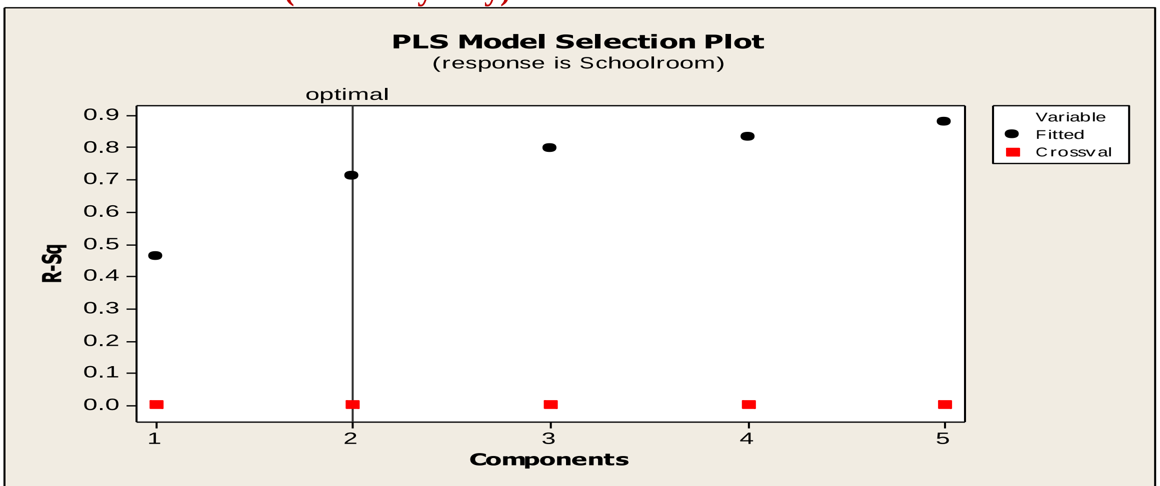

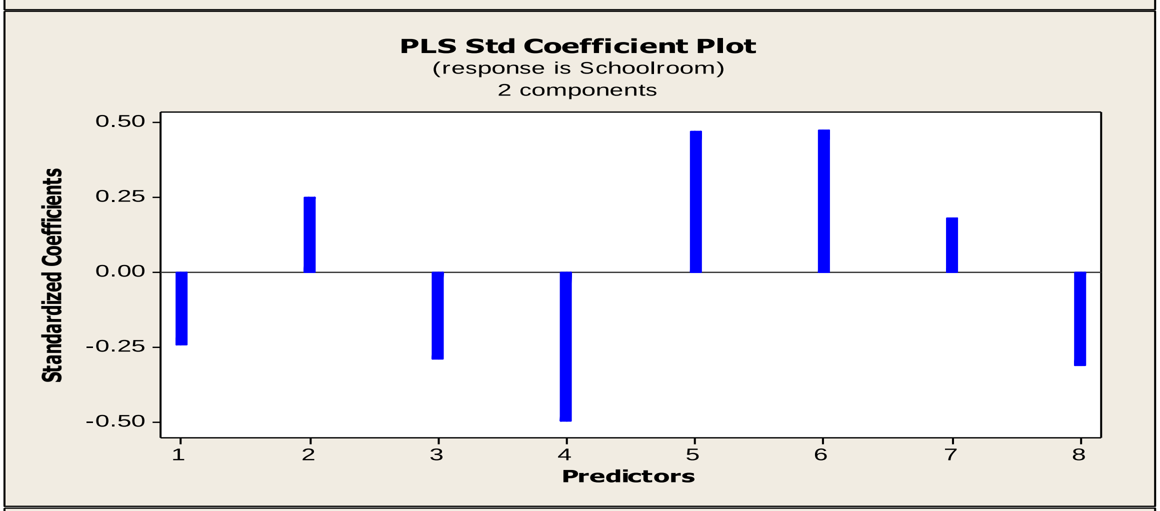

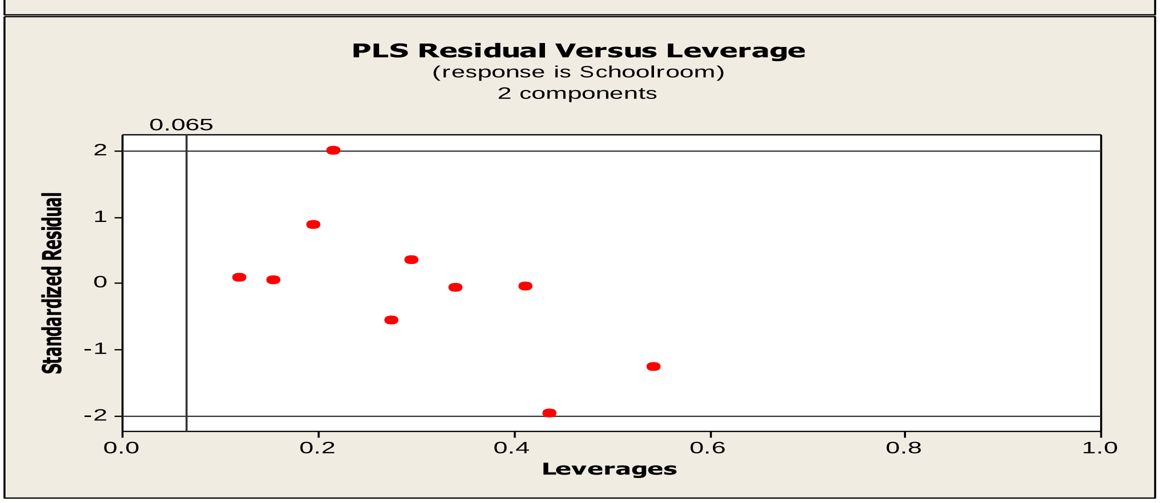

There are two outliers (1956 and 2001) on the residual versus leverage plot.

PLS Regression: Schoolroom versus SchSpT, SchSuT, SchFaT, SchWiT, SchSpP, ...

```
Method
Cross-validation                Leave-one-out
Components to evaluate          User specified
Number of components evaluated  5
Number of components selected   2

Analysis of Variance for Schoolroom
Source          DF         SS         MS     F      P
Regression       2  455246983  227623491  8.68  0.013
Residual Error   7  183557342   26222477
Total            9  638804325

Model Selection and Validation for Schoolroom
Components  X Variance      Error      R-Sq       PRESS  R-Sq (pred)
         1    0.259620  344334881  0.460970  1120318100            0
         2    0.434926  183557342  0.712655  1075387221            0
         3              128333541  0.799104  1403774143            0
         4              106022153  0.834030  1680213629            0
         5               78185022  0.877607  2385660912            0

Coefficients
          Schoolroom  standardized
Constant    -44299.4      0.000000
SchSpT       -1962.2     -0.241712
SchSuT        2467.7      0.250034
SchFaT       -2131.2     -0.291236
SchWiT       -3313.6     -0.495627
SchSpP          34.5      0.472910
SchSuP          43.5      0.474482
SchFaP           7.0      0.181715
SchWiP         -12.2     -0.309331
```

Falling Ice Glacier (seasonally only)

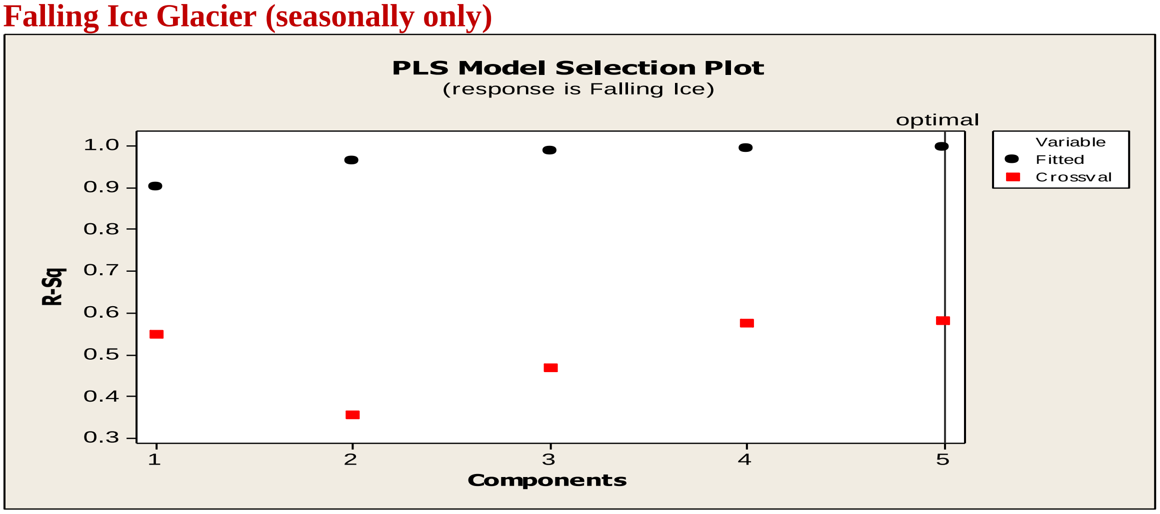

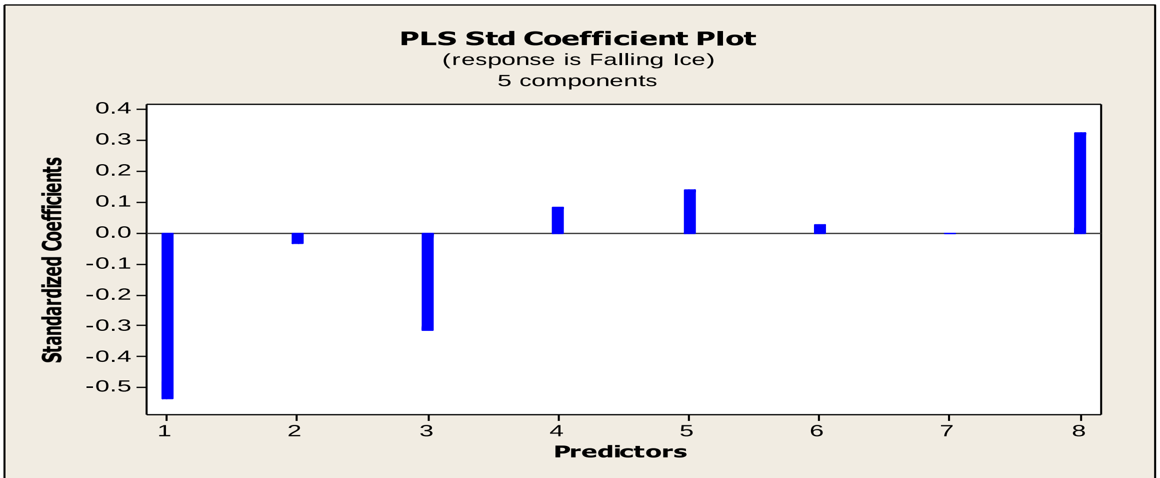

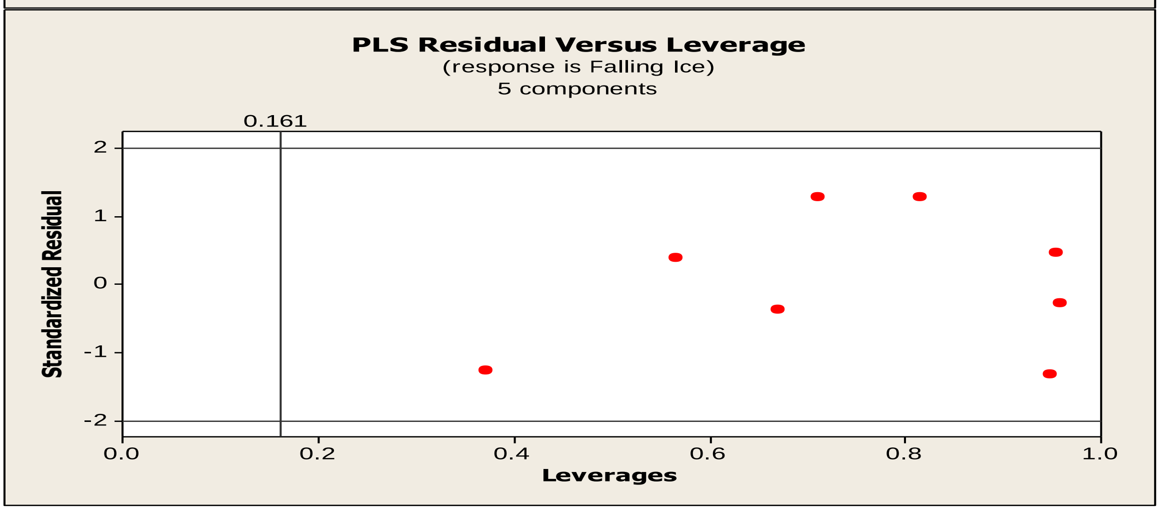

PLS Regression: Falling Ice versus SpT, SuT, FaT, WiT, SpP, SuP, FaP, WiP

Method

Cross-validation	Leave-one-out
Components to evaluate	User specified
Number of components evaluated	5
Number of components selected	5

Analysis of Variance for Falling Ice

Source	DF	SS	MS	F	P
Regression	5	142707525	28541505	128.57	0.008
Residual Error	2	443980	221990		
Total	7	143151504			

Model Selection and Validation for Falling Ice

Components	X Variance	Error	R-Sq	PRESS	R-Sq (pred)
1	0.522870	14042842	0.901902	64721158	0.547883
2	0.676353	5154767	0.963991	92297322	0.355247
3	0.807488	1574137	0.989004	75908043	0.469736
4	0.900893	794899	0.994447	60843738	0.574970
5	0.958724	443980	0.996899	60109731	0.580097

Coefficients

	Falling Ice	Falling Ice standardized
Constant	130865	0.000000
SpT	-2433	-0.537398
SuT	-164	-0.031714

```
FaT          -825     -0.314538
WiT           180      0.083526
SpP             5      0.137782
SuP             1      0.025679
FaP            -0     -0.000053
WiP             7      0.324517
```

Skillet Glacier (seasonally only)

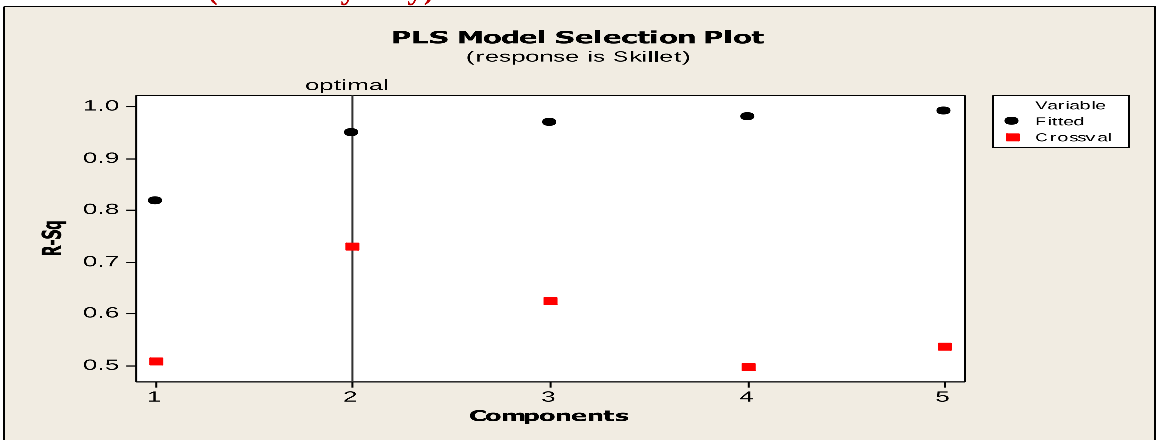

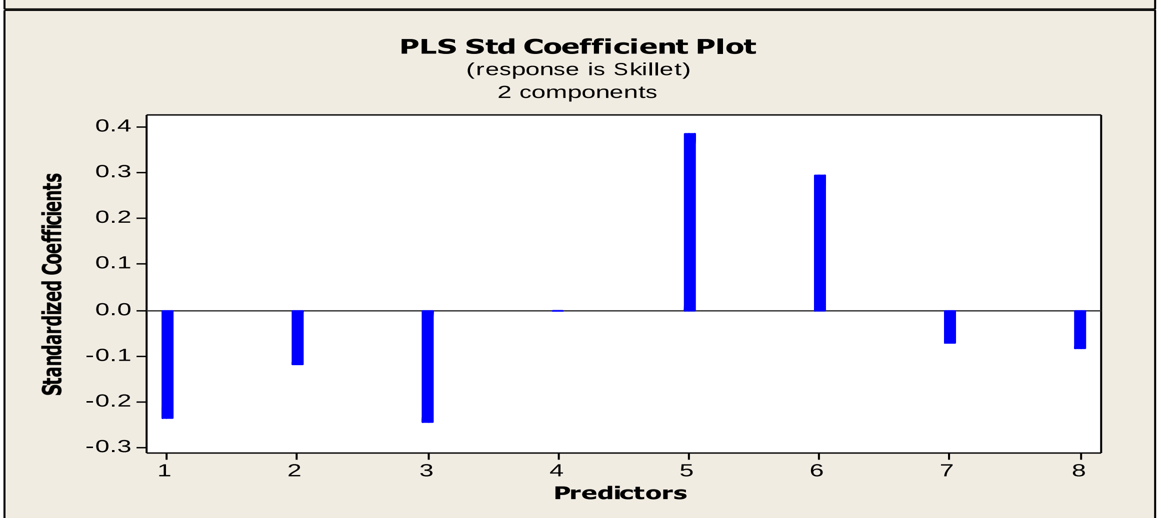

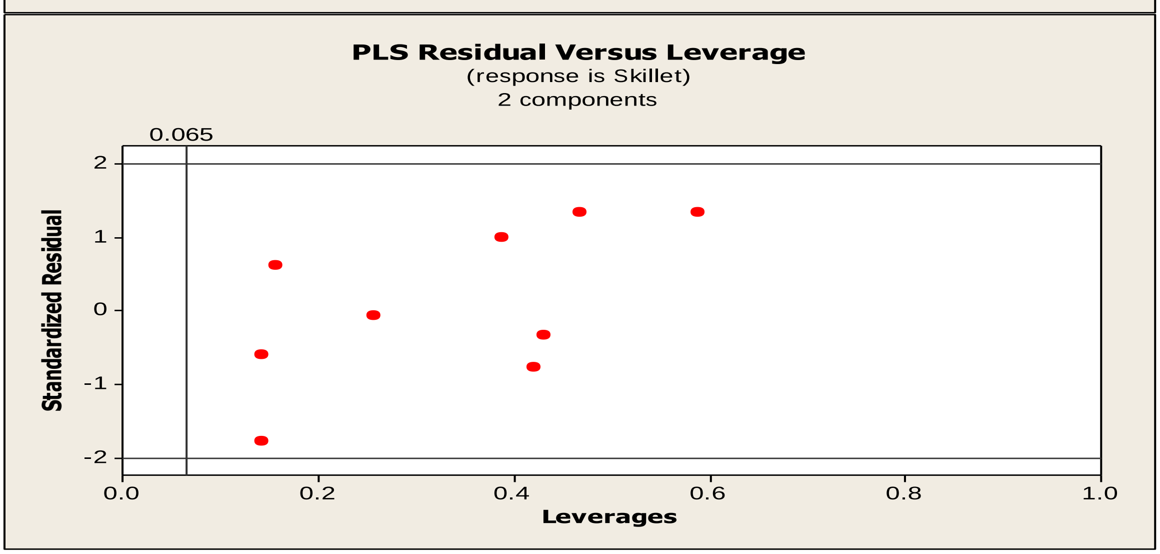

PLS Regression: Skillet versus SpT, SuT, FaT, WiT, SpP, SuP, FaP, WiP

```
Method
Cross-validation                Leave-one-out
Components to evaluate          User specified
Number of components evaluated  5
Number of components selected   2

Analysis of Variance for Skillet
Source          DF          SS         MS      F      P
Regression       2  1178815193  589407596  56.34  0.000
Residual Error   6    62765217   10460869
Total            8  1241580409

Model Selection and Validation for Skillet
Components  X Variance      Error      R-Sq      PRESS  R-Sq (pred)
         1    0.478869  226330789  0.817708  611788596     0.507250
         2    0.749646   62765217  0.949447  334691958     0.730431
         3               39463696  0.968215  467233043     0.623679
         4               25182189  0.979718  624068471     0.497360
         5                9825791  0.992086  576921834     0.535333

Coefficients
                       Skillet
          Skillet  standardized
Constant   119933      0.000000
SpT         -2958     -0.236304
SuT         -1611     -0.119858
FaT         -1887     -0.244379
WiT           -16     -0.002738
SpP            42      0.386665
SuP            29      0.294902
FaP            -4     -0.071289
WiP            -5     -0.083957
```

East Triple Glacier (seasonally only)

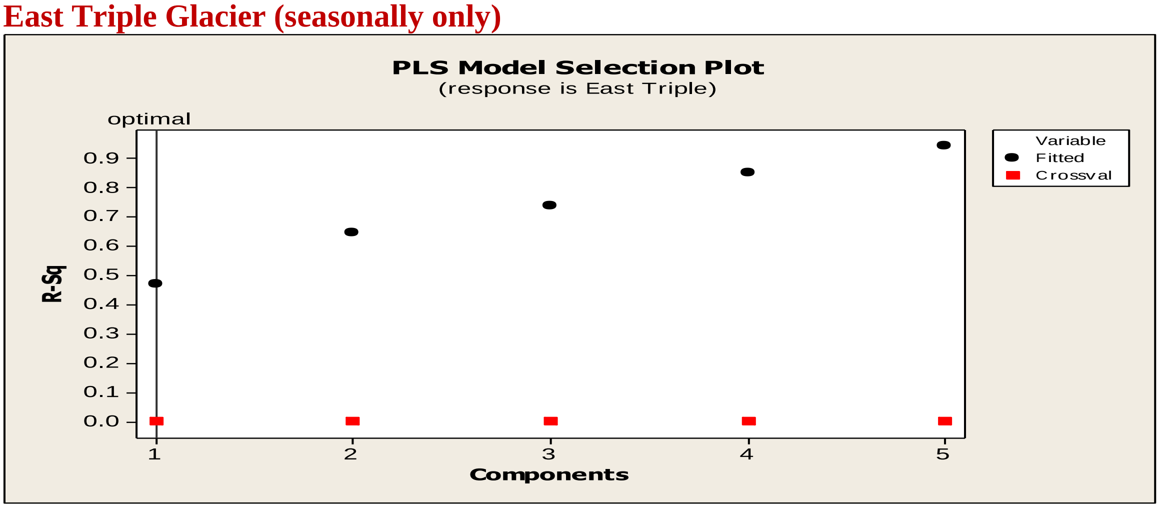

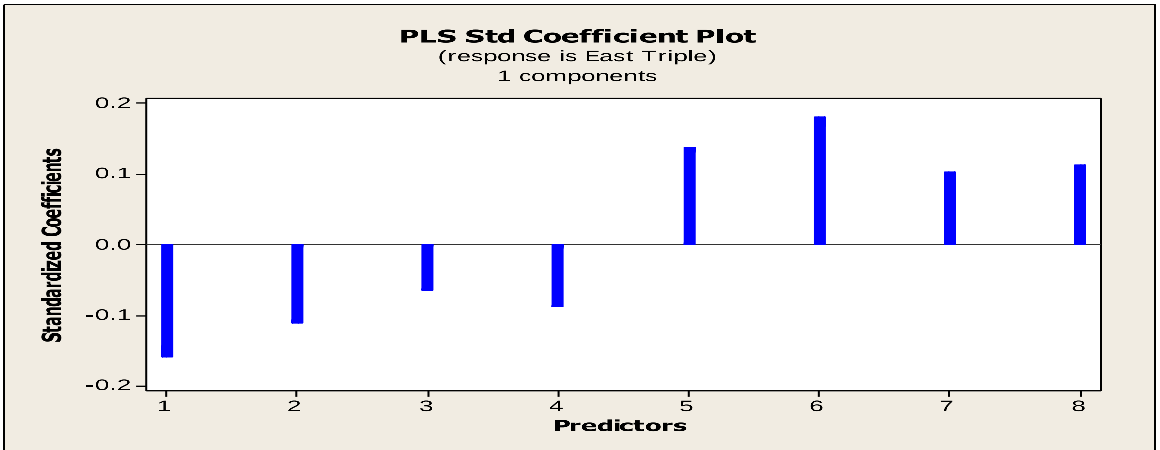

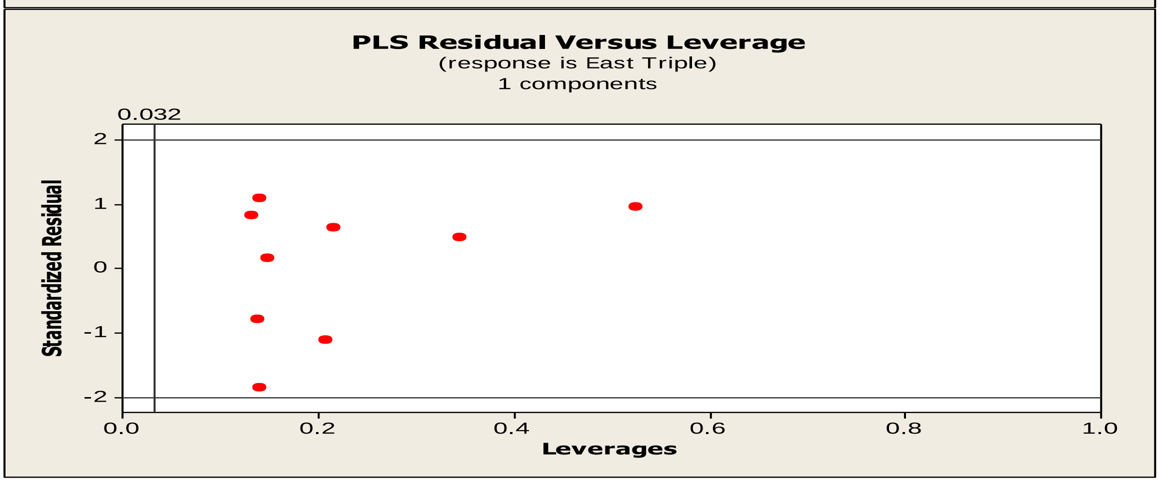

PLS Regression: East Triple versus SpT, SuT, FaT, WiT, SpP, SuP, FaP, WiP

Method

Cross-validation	Leave-one-out
Components to evaluate	User specified
Number of components evaluated	5
Number of components selected	1

Analysis of Variance for East Triple

Source	DF	SS	MS	F	P
Regression	1	1503089679	1503089679	6.25	0.041
Residual Error	7	1684334827	240619261		
Total	8	3187424506			

Model Selection and Validation for East Triple

Components	X Variance	Error	R-Sq	PRESS	R-Sq (pred)
1	0.512076	1684334827	0.471569	3.30305E+09	0
2		1123683654	0.647463	7.10024E+09	0
3		837725339	0.737178	9.26848E+09	0
4		473823619	0.851346	1.10950E+10	0
5		187630311	0.941134	1.14127E+10	0

Coefficients

	East Triple	East Triple standardized
Constant	78682.9	0.000000
SpT	-3174.8	-0.158295
SuT	-2403.1	-0.111555
FaT	-794.5	-0.064232
WiT	-833.2	-0.086878

SpP	24.2	0.137492
SuP	28.7	0.180855
FaP	9.5	0.103026
WiP	10.0	0.112972

Middle Triple Glacier (seasonally only)

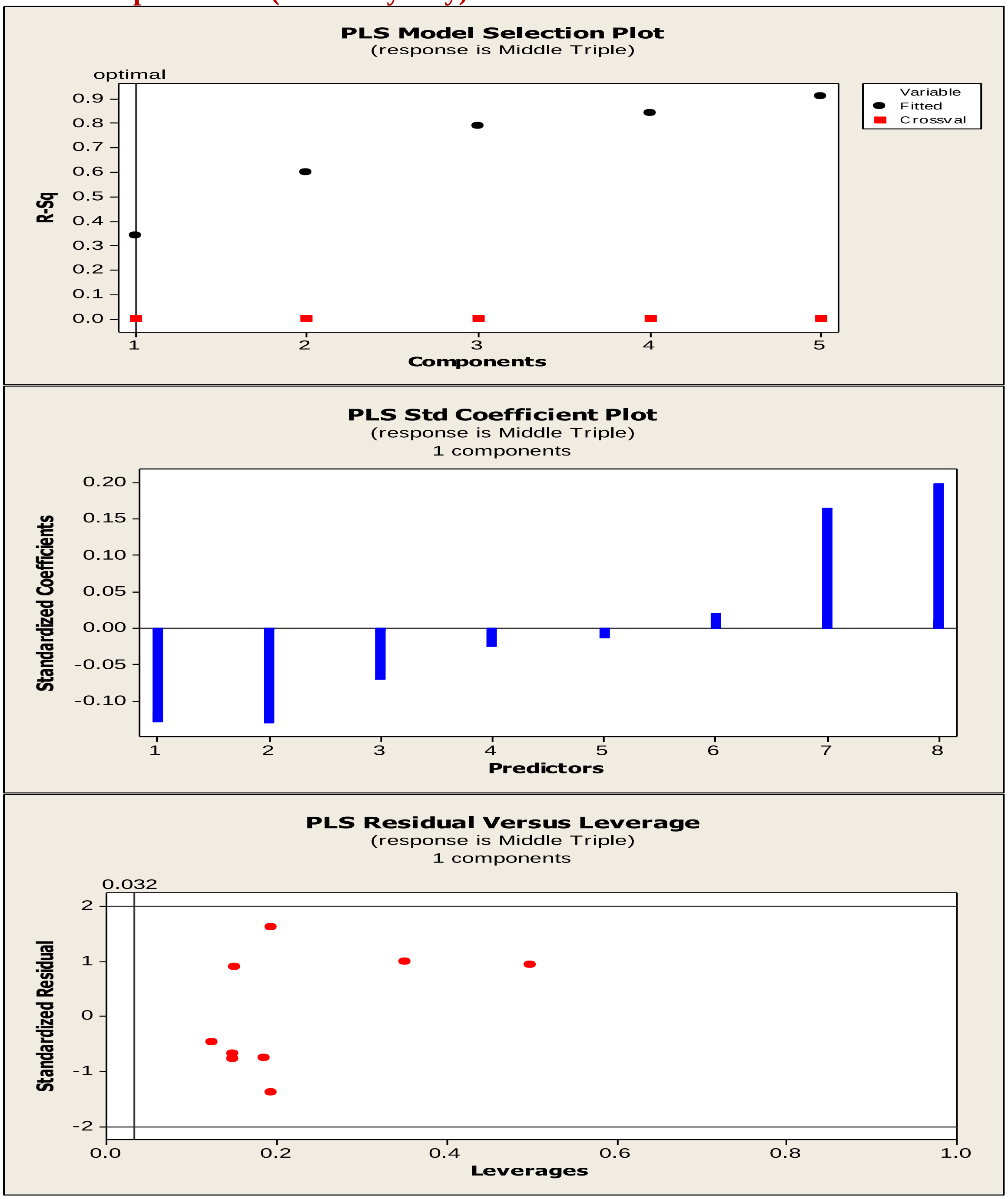

PLS Regression: Middle Triple versus SpT, SuT, FaT, WiT, SpP, SuP, FaP, WiP

```
Method
Cross-validation                Leave-one-out
Components to evaluate          User specified
Number of components evaluated  5
Number of components selected   1
```

Analysis of Variance for Middle Triple

Source	DF	SS	MS	F	P
Regression	1	329761396	329761396	3.63	0.098
Residual Error	7	635085202	90726457		
Total	8	964846598			

Model Selection and Validation for Middle Triple

Components	X Variance	Error	R-Sq	PRESS	R-Sq (pred)
1	0.489417	635085202	0.341776	1470166043	0
2		384952049	0.601023	1627951949	0
3		202172761	0.790461	1892686572	0
4		153083408	0.841339	2047869767	0
5		88545069	0.908229	2312423675	0

Coefficients

	Middle Triple	Middle Triple standardized
Constant	196020	0.000000
SpT	-1429	-0.129465
SuT	-1535	-0.129548
FaT	-481	-0.070730
WiT	-131	-0.024752
SpP	-1	-0.012482
SuP	2	0.020004
FaP	8	0.165300
WiP	10	0.198639

West Triple Glacier (seasonally only)

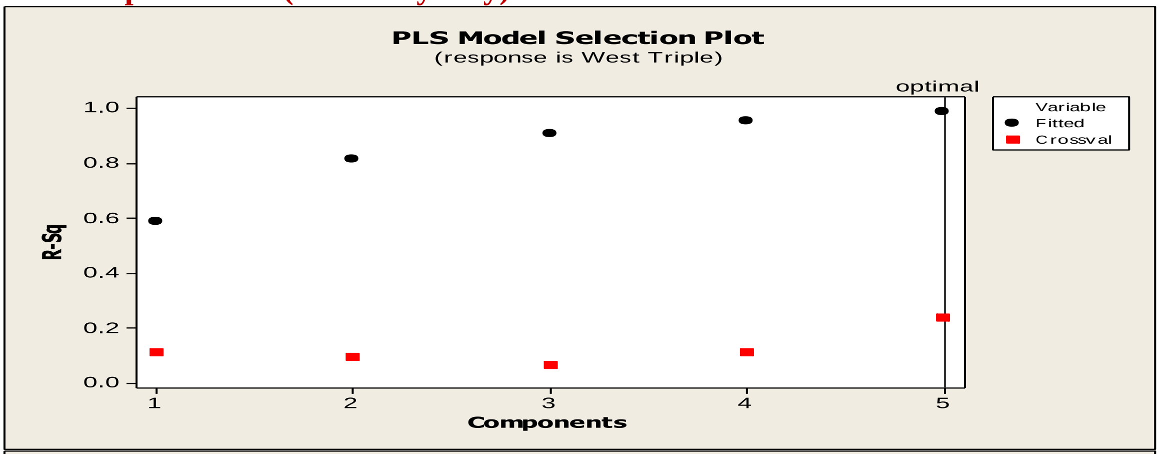

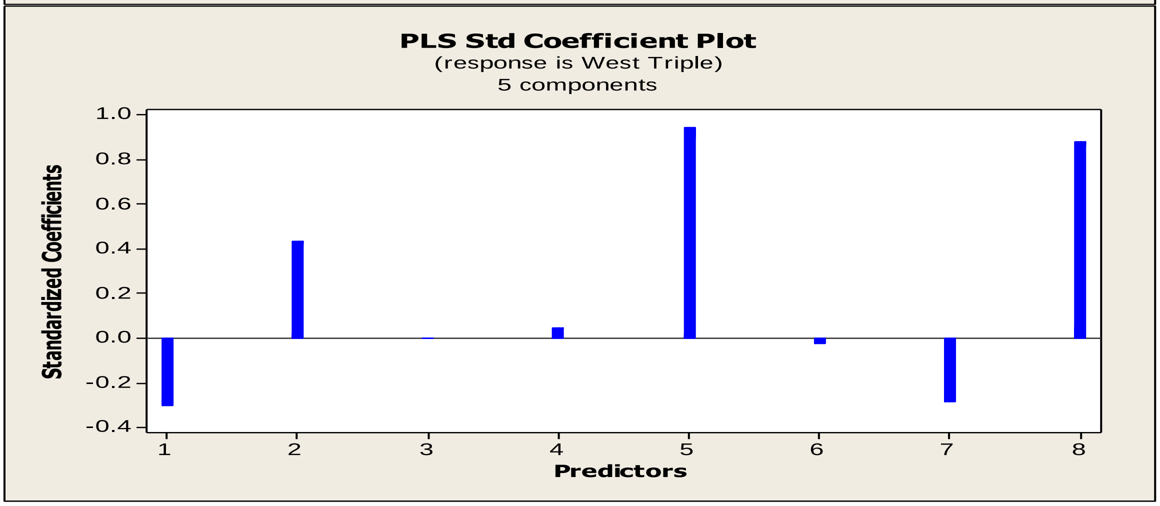

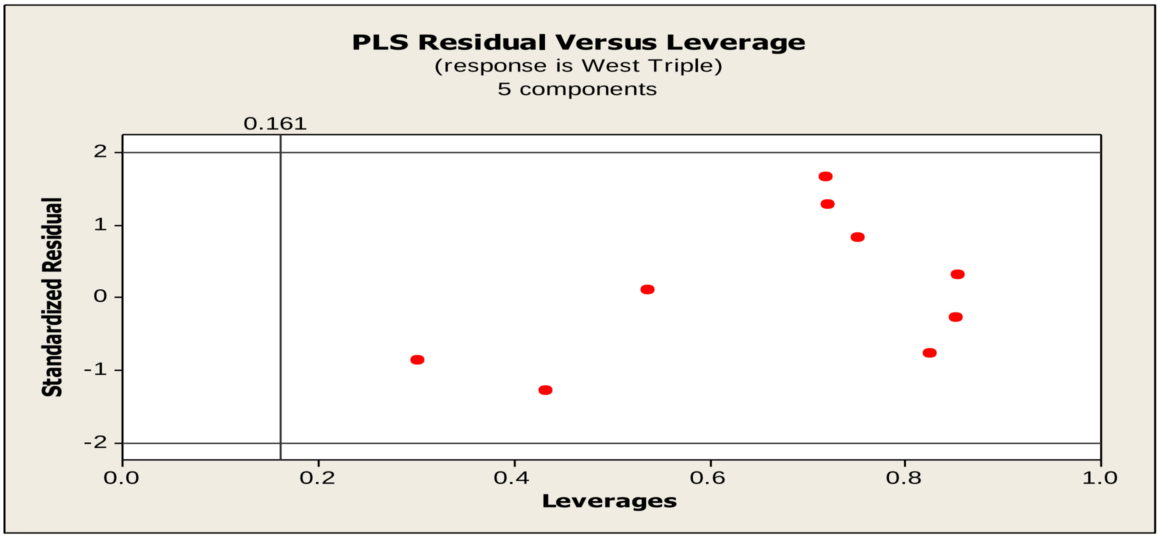

PLS Regression: West Triple versus SpT, SuT, FaT, WiT, SpP, SuP, FaP, WiP

Method

Cross-validation	Leave-one-out
Components to evaluate	User specified
Number of components evaluated	5
Number of components selected	5

Analysis of Variance for West Triple

Source	DF	SS	MS	F	P
Regression	5	1.47249E+10	2944977852	47.28	0.005
Residual Error	3	1.86883E+08	62294174		
Total	8	1.49118E+10			

Model Selection and Validation for West Triple

Components	X Variance	Error	R-Sq	PRESS	R-Sq (pred)
1	0.499107	6137463783	0.588415	1.32281E+10	0.112908
2	0.685065	2745663660	0.815873	1.34597E+10	0.097379
3	0.832718	1381924626	0.907327	1.39398E+10	0.065185
4	0.904693	651719511	0.956295	1.32583E+10	0.110887
5	0.923641	186882521	0.987467	1.13318E+10	0.240076

Coefficients

	West Triple	West Triple standardized
Constant	-194170	0.000000
SpT	-13214	-0.304603
SuT	20199	0.433510
FaT	-91	-0.003404
WiT	899	0.043346
SpP	360	0.945389
SuP	-8	-0.024057
FaP	-56	-0.283907
WiP	168	0.880846

Schoolroom Glacier (annually only)

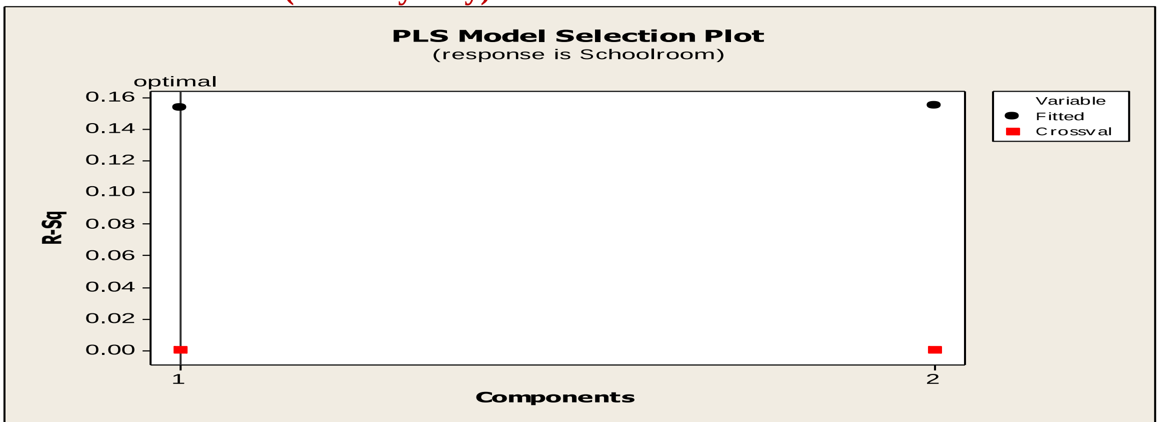

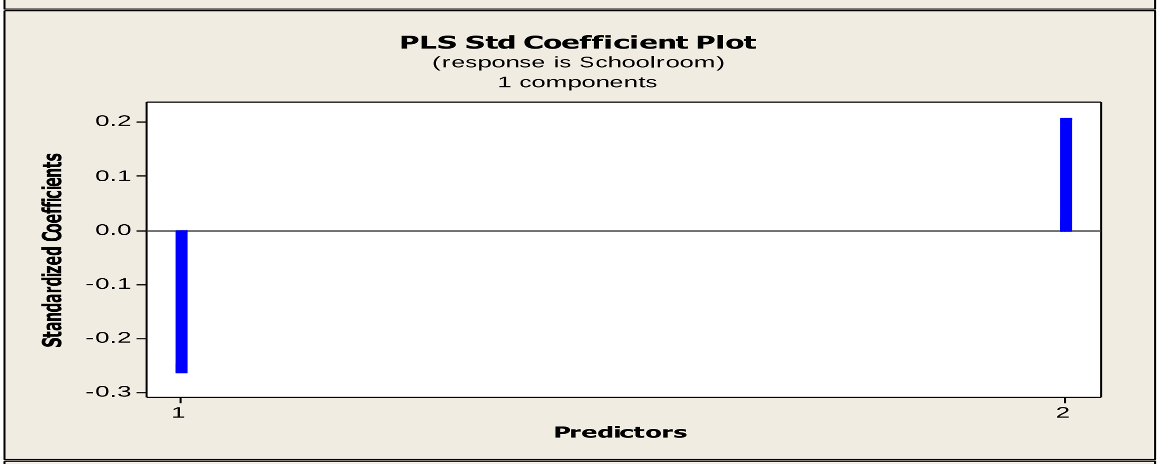

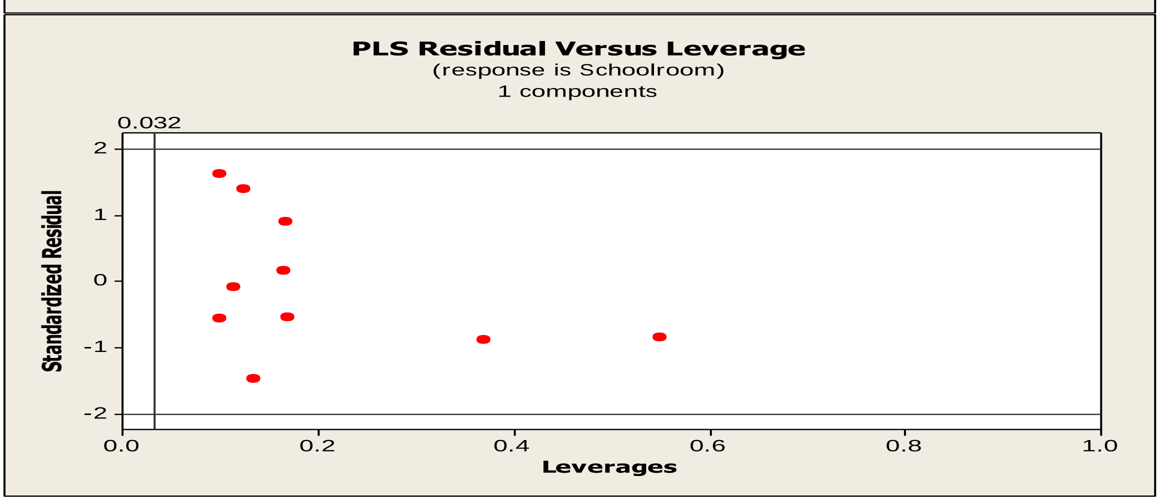

PLS Regression: Schoolroom versus SchAnT, SchAnP

Method

Cross-validation	Leave-one-out
Components to evaluate	Adjusted
Number of components evaluated	2
Number of components selected	1

Analysis of Variance for Schoolroom

Source	DF	SS	MS	F	P
Regression	1	97974867	97974867	1.45	0.263
Residual Error	8	540829458	67603682		
Total	9	638804325			

Model Selection and Validation for Schoolroom

Components	X Variance	Error	R-Sq	PRESS	R-Sq (pred)
1	0.682245	540829458	0.153372	919373053	0
2		540004061	0.154664	1026720855	0

Coefficients

	Schoolroom	Schoolroom standardized
Constant	20627.0	0.000000
SchAnT	-4339.6	-0.263556
SchAnP	4.2	0.208288

Falling Ice Glacier (annually only)

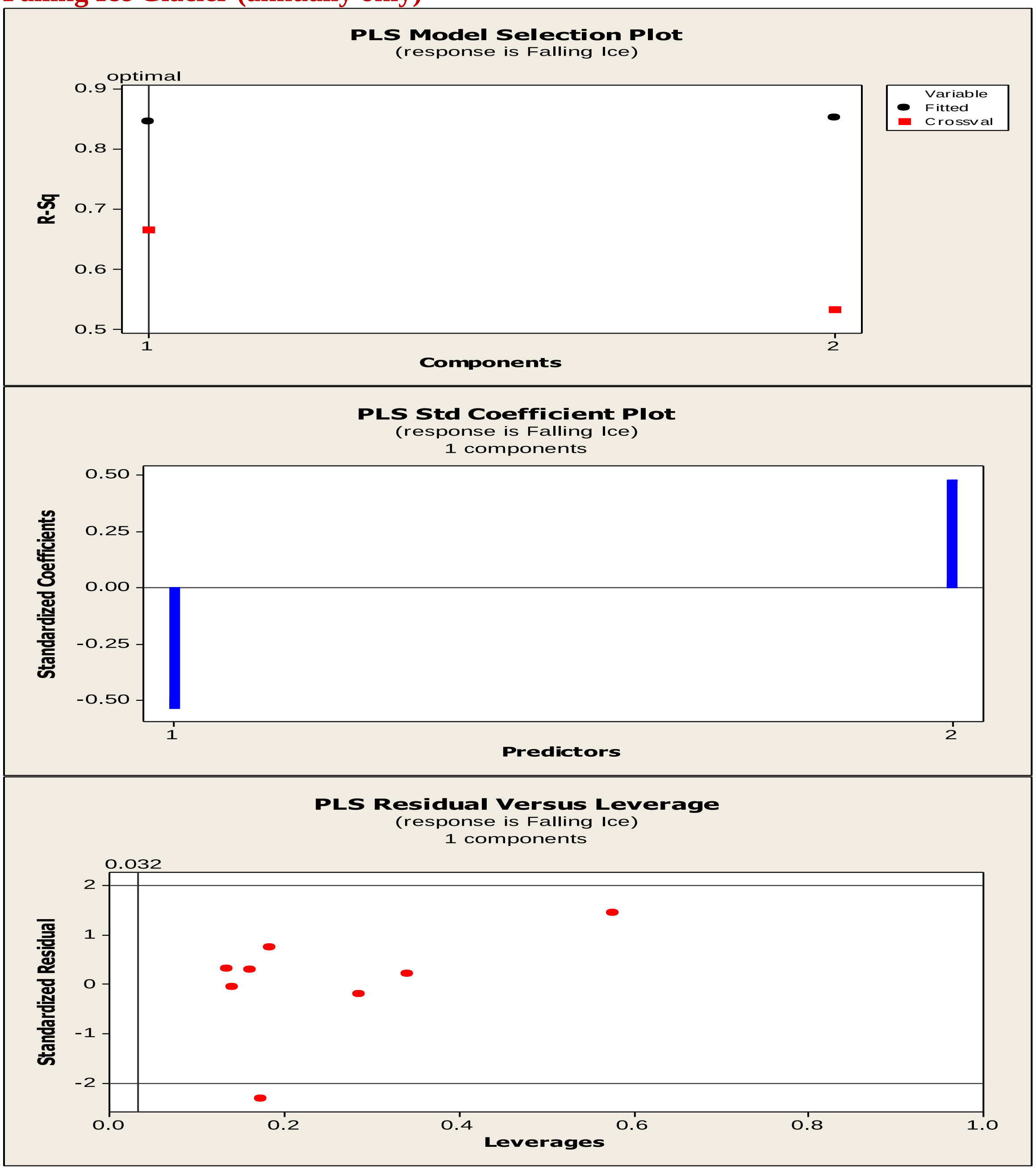

There is one outlier (2006) on the residual versus leverage plot.

PLS Regression: Falling Ice versus AnT, AnP

```
Method
Cross-validation                 Leave-one-out
Components to evaluate           Adjusted
Number of components evaluated   2
Number of components selected    1

Analysis of Variance for Falling Ice
Source          DF          SS          MS      F      P
Regression       1   121065019   121065019  32.89  0.001
Residual Error   6    22086485     3681081
Total            7   143151504

Model Selection and Validation for Falling Ice
Components  X Variance     Error      R-Sq     PRESS  R-Sq (pred)
         1    0.821326  22086485  0.845713  47875257     0.665562
         2              21019148  0.853169  66935876     0.532412

Coefficients
          Falling   Falling Ice
              Ice  standardized
Constant   123427      0.000000
AnT         -2066     -0.535464
AnP             5      0.478658
```

Skillet Glacier (annually only)

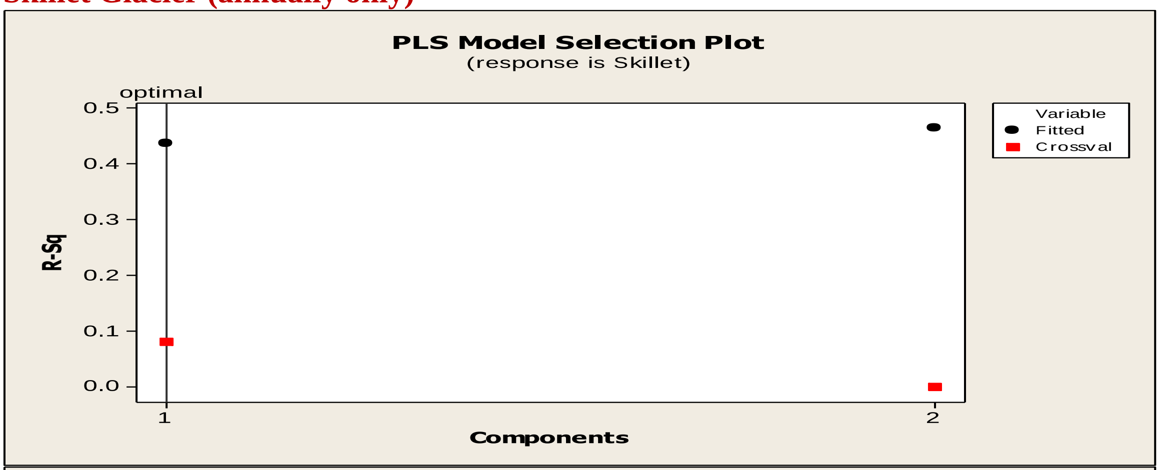

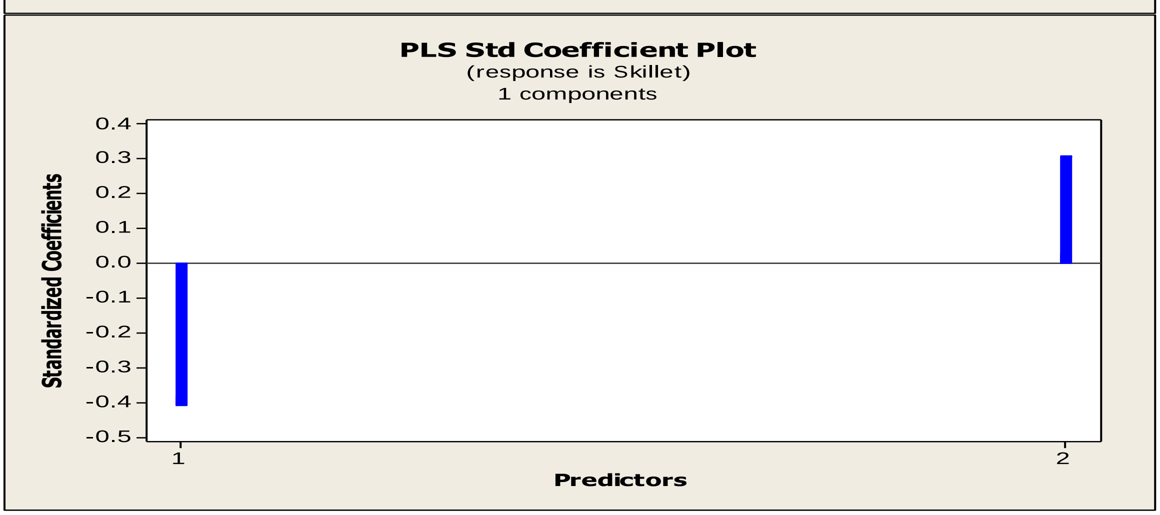

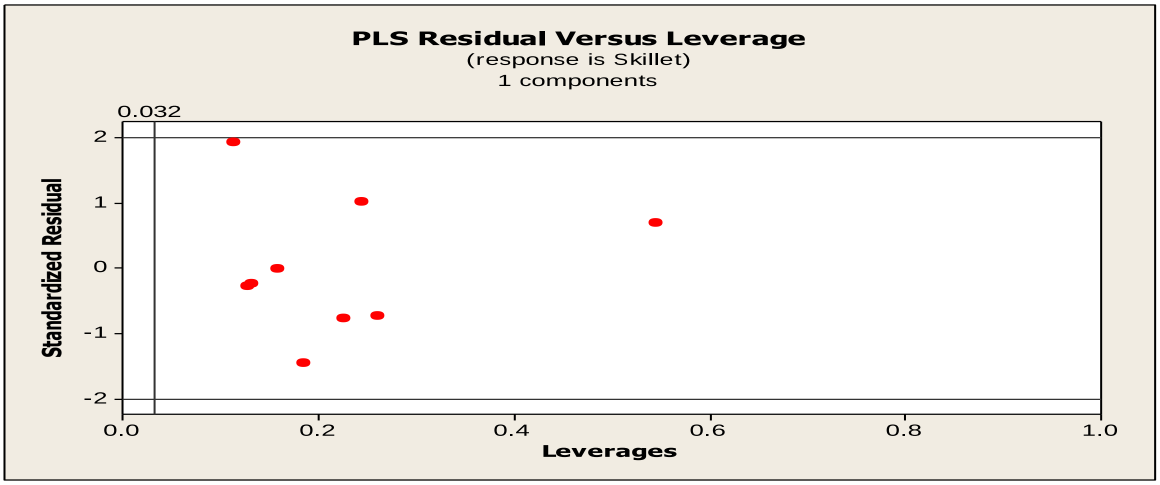

PLS Regression: Skillet versus AnT, AnP

Method

Cross-validation	Leave-one-out
Components to evaluate	Adjusted
Number of components evaluated	2
Number of components selected	1

Analysis of Variance for Skillet

Source	DF	SS	MS	F	P
Regression	1	541056154	541056154	5.41	0.053
Residual Error	7	700524255	100074894		
Total	8	1241580409			

Model Selection and Validation for Skillet

Components	X Variance	Error	R-Sq	PRESS	R-Sq (pred)
1	0.839349	700524255	0.435780	1141928807	0.0802619
2		665691888	0.463835	1406042254	0.0000000

Coefficients

	Skillet	Skillet standardized
Constant	109339	0.000000
AnT	-4426	-0.408680
AnP	8	0.309538

East Triple Glacier (annually only)

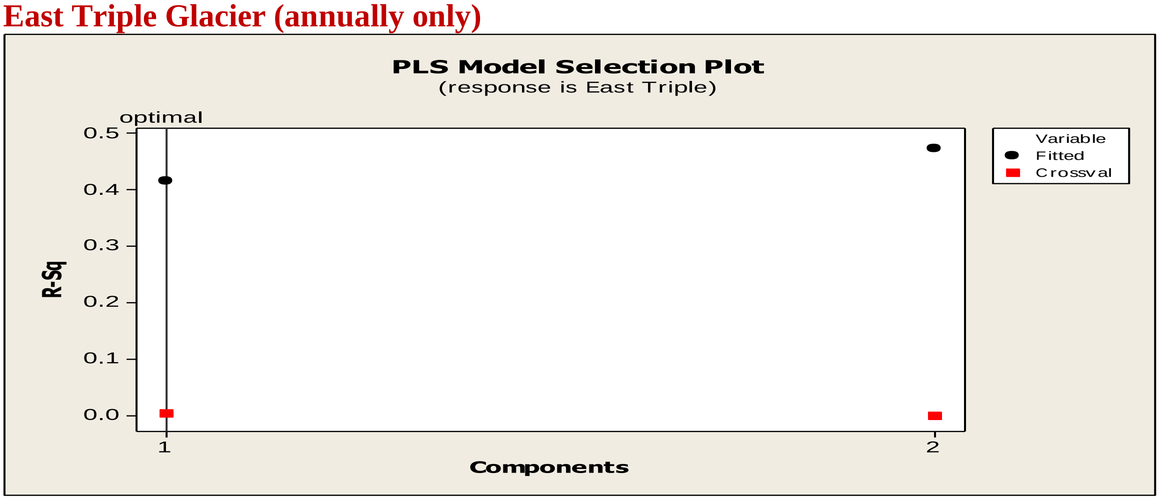

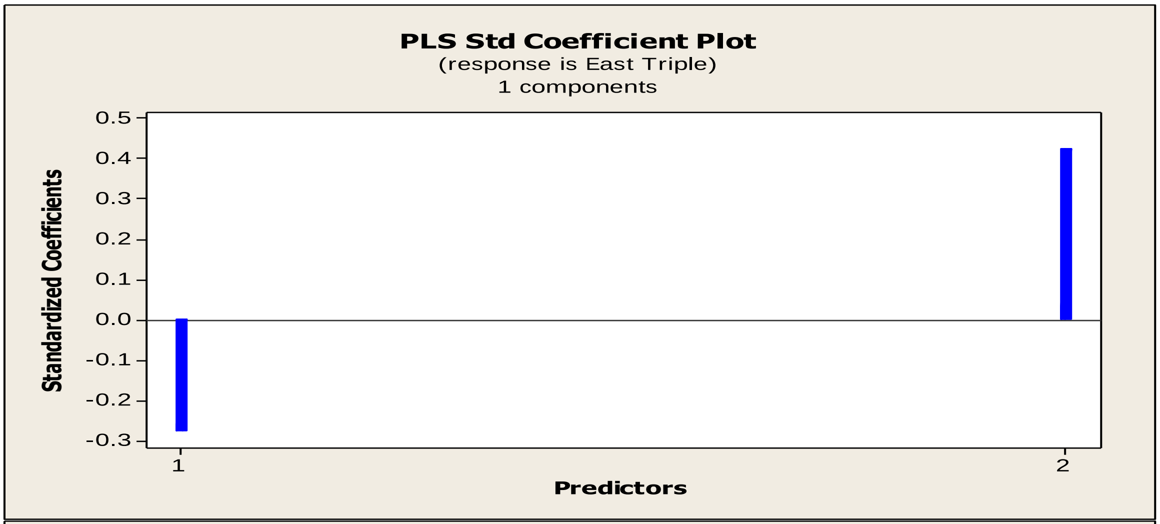

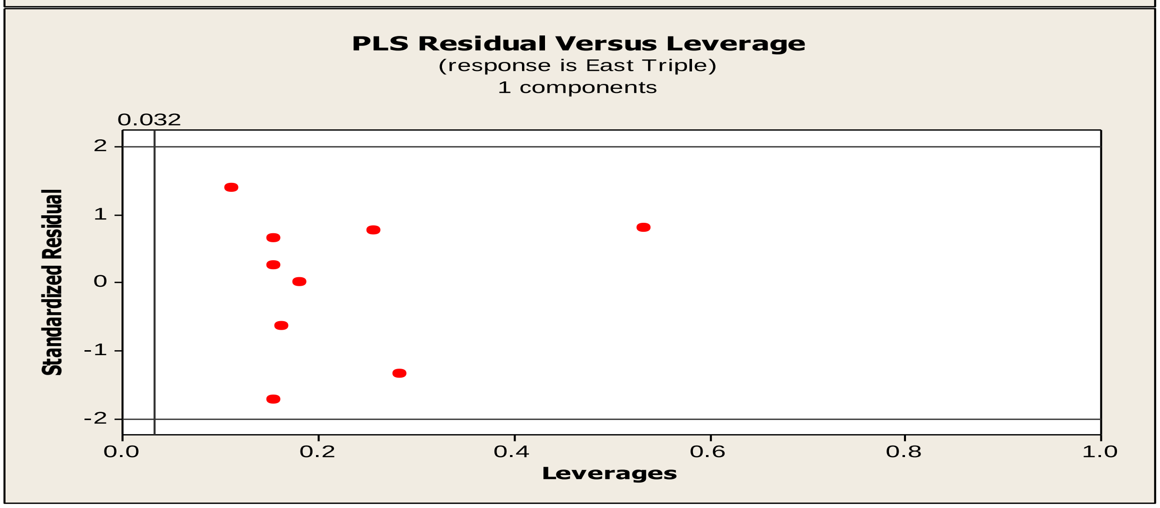

PLS Regression: East Triple versus AnT, AnP

Method

Cross-validation	Leave-one-out
Components to evaluate	Adjusted
Number of components evaluated	2
Number of components selected	1

Analysis of Variance for East Triple

Source	DF	SS	MS	F	P
Regression	1	1323812211	1323812211	4.97	0.061
Residual Error	7	1863612295	266230328		
Total	8	3187424506			

Model Selection and Validation for East Triple

Components	X Variance	Error	R-Sq	PRESS	R-Sq (pred)
1	0.836237	1863612295	0.415323	3176023466	0.0035769
2		1677823338	0.473612	3514938336	0.0000000

Coefficients

	East Triple	East Triple standardized
Constant	52791.3	0.000000
AnT	-4802.9	-0.276774
AnP	17.7	0.422780

Middle Triple Glacier (annually only)

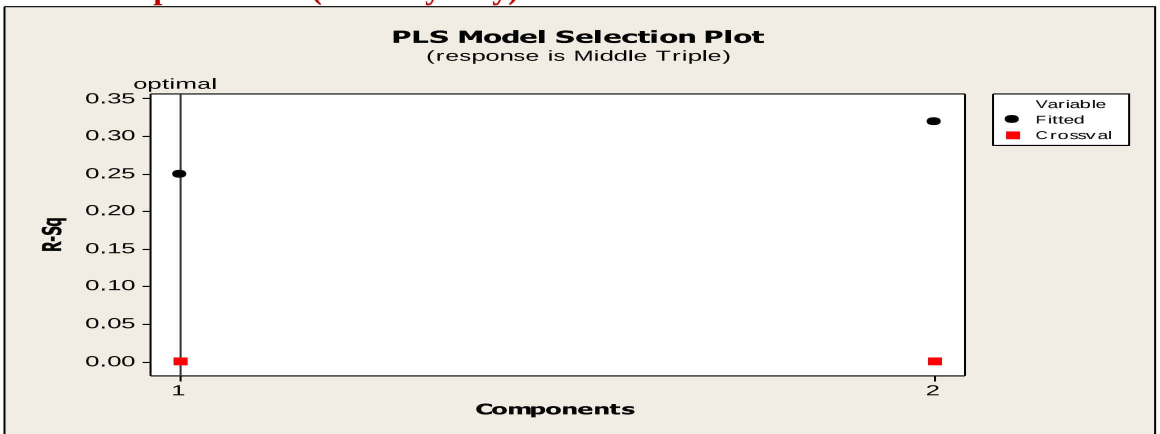

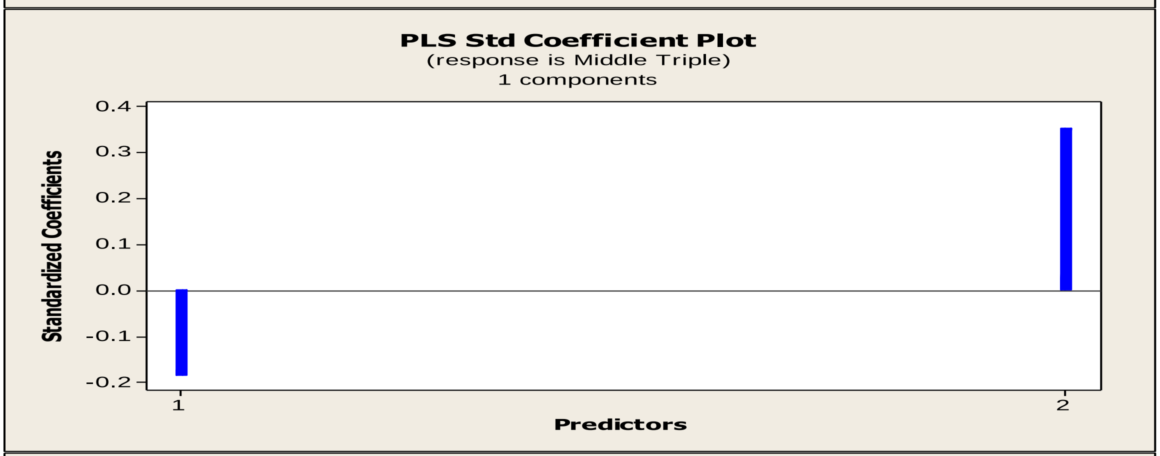

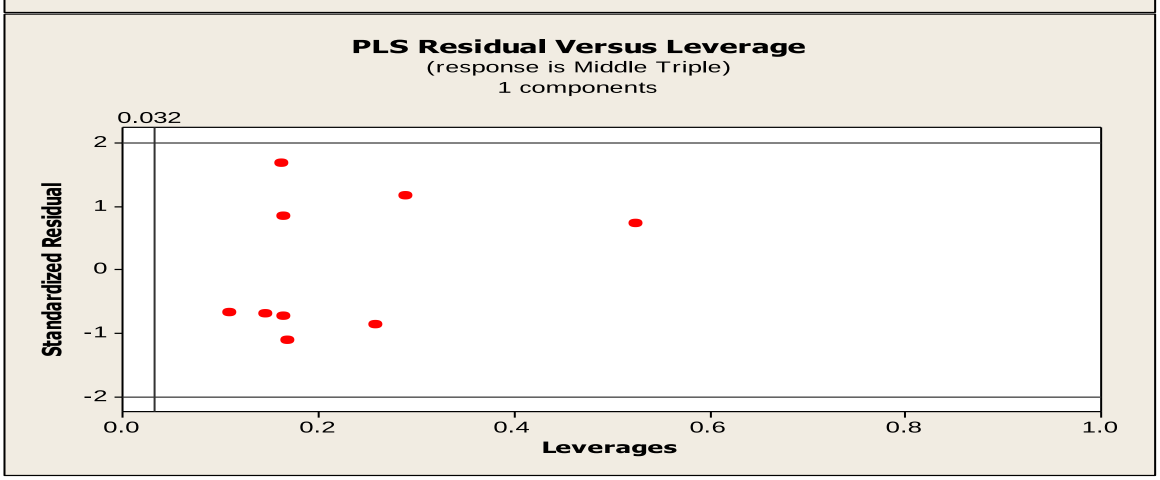

PLS Regression: Middle Triple versus AnT, AnP

```
Method
Cross-validation                 Leave-one-out
Components to evaluate           Adjusted
Number of components evaluated   2
Number of components selected    1

Analysis of Variance for Middle Triple
Source          DF         SS         MS     F      P
Regression       1  239939222  239939222  2.32  0.172
Residual Error   7  724907376  103558197
Total            8  964846598
```

```
Model Selection and Validation for Middle Triple
Components  X Variance      Error      R-Sq       PRESS  R-Sq (pred)
         1    0.829462  724907376  0.248681  1251763518            0
         2              656646363  0.319429  1573882546            0

Coefficients
          Middle  Middle Triple
          Triple   standardized
Constant  177924       0.000000
AnT        -1767      -0.185125
AnP            8       0.353478
```

West Triple Glacier (annually only)

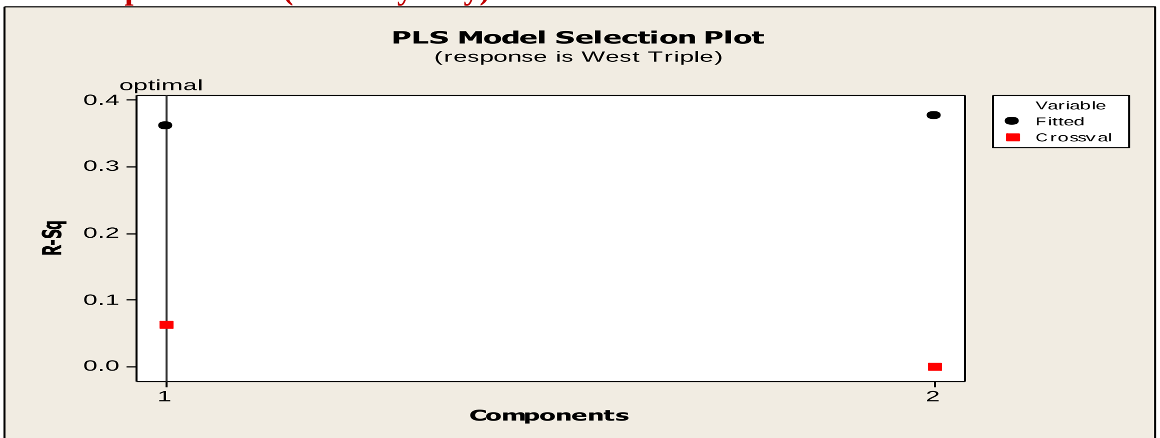

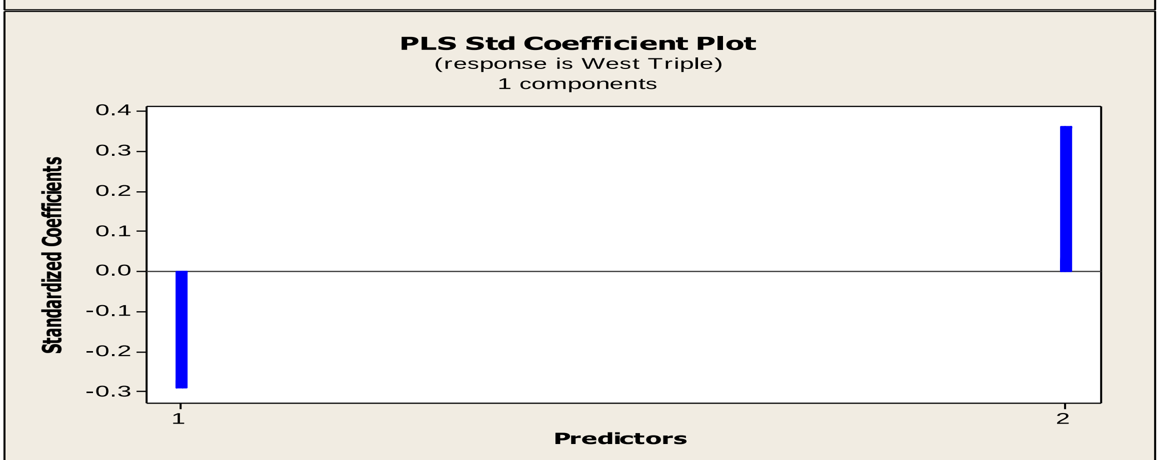

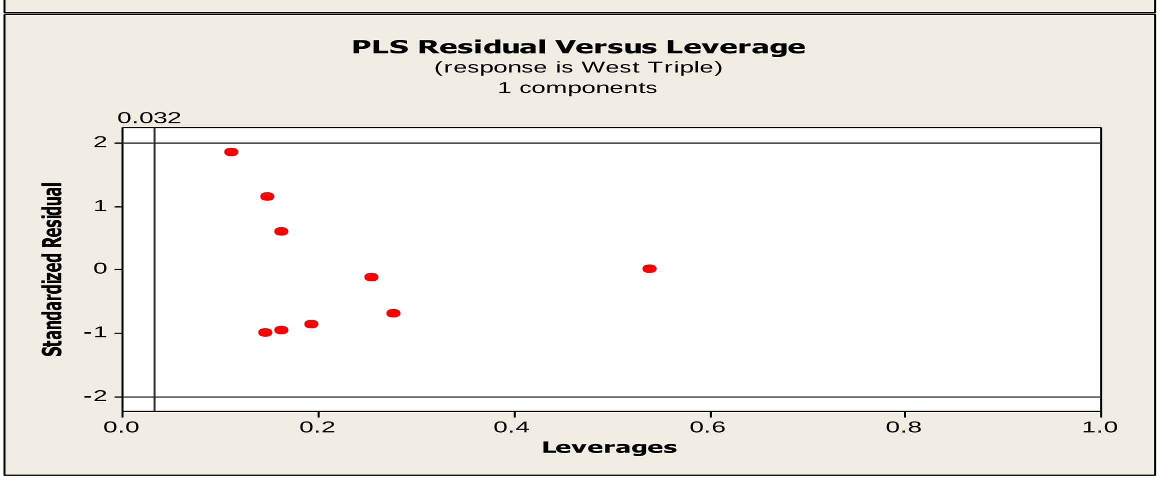

PLS Regression: West Triple versus AnT, AnP

Method

Cross-validation	Leave-one-out
Components to evaluate	Adjusted
Number of components evaluated	2
Number of components selected	1

Analysis of Variance for West Triple

Source	DF	SS	MS	F	P
Regression	1	5.39031E+09	5390308917	3.96	0.087
Residual Error	7	9.52146E+09	1360208981		
Total	8	1.49118E+10			

Model Selection and Validation for West Triple

Components	X Variance	Error	R-Sq	PRESS	R-Sq (pred)
1	0.840178	9521462866	0.361480	1.39727E+10	0.0629720
2		9289676087	0.377024	1.79401E+10	0.0000000

Coefficients

	West Triple	West Triple standardized
Constant	85900.9	0.000000
AnT	-10906.6	-0.290579
AnP	33.0	0.363950

Three year moving average PLS results

Schoolroom Glacier (three-year seasonally only)

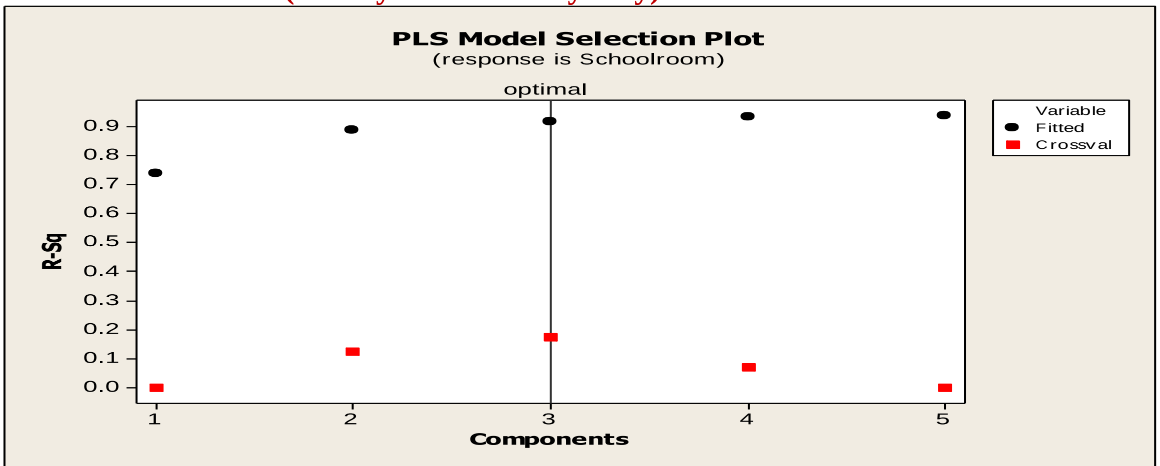

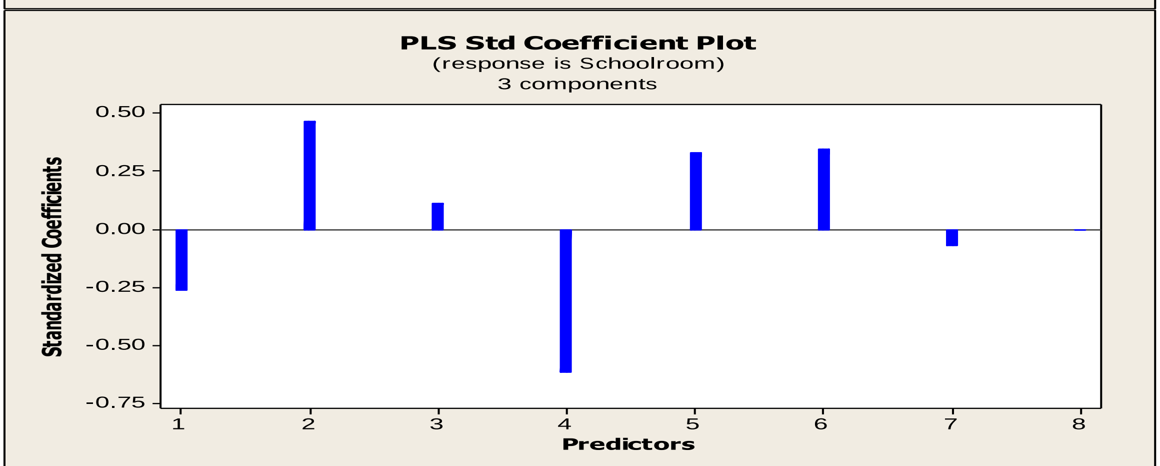

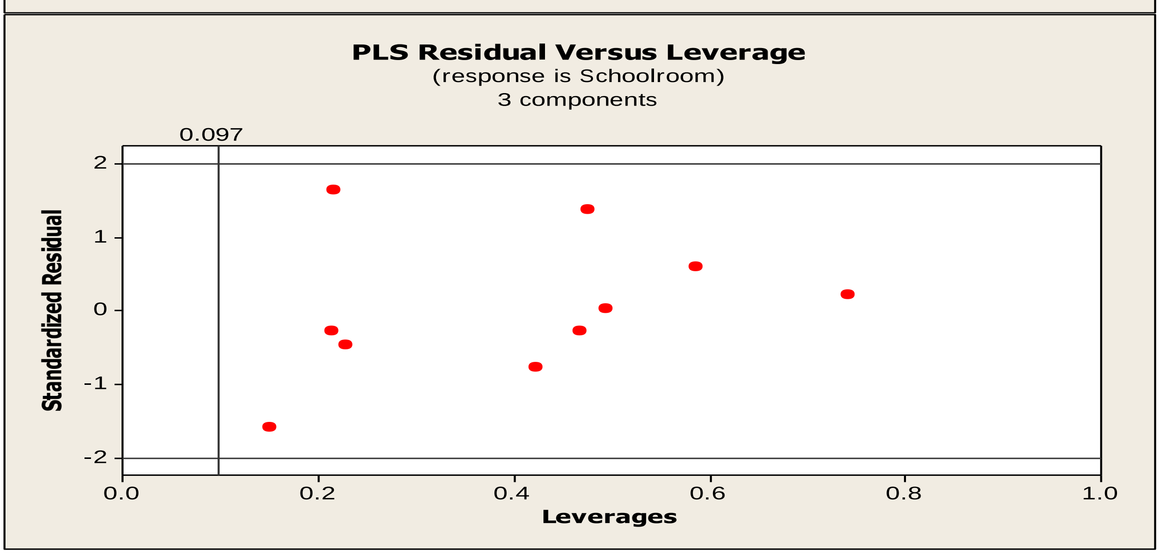

PLS Regression: Schoolroom versus SchSpT, SchSuT, SchFaT, SchWiT, SchSpP, ...

```
Method
Cross-validation               Leave-one-out
Components to evaluate         User specified
Number of components evaluated  5
```

```
Number of components selected    3
Analysis of Variance for Schoolroom
Source          DF          SS          MS       F       P
Regression       3   585001961   195000654   21.75   0.001
Residual Error   6    53802364     8967061
Total            9   638804325

Model Selection and Validation for Schoolroom
Components   X Variance      Error       R-Sq      PRESS   R-Sq (pred)
         1     0.227671  168101982   0.736849  729666455      0.000000
         2     0.429151   72195102   0.886984  559816380      0.123650
         3     0.635878   53802364   0.915776  528459155      0.172737
         4                44375970   0.930533  595455856      0.067859
         5                42108504   0.934082  938929802      0.000000

Coefficients
                         Schoolroom
             Schoolroom  standardized
Constant        -110577      0.000000
SchSpT            -2618     -0.258990
SchSuT             8889      0.470168
SchFaT             1333      0.115764
SchWiT            -6191     -0.615899
SchSpP            35124      0.334502
SchSuP            44684      0.346009
SchFaP            -3996     -0.068846
SchWiP              -52     -0.000953
```

Falling Ice Glacier (three-year seasonally only)

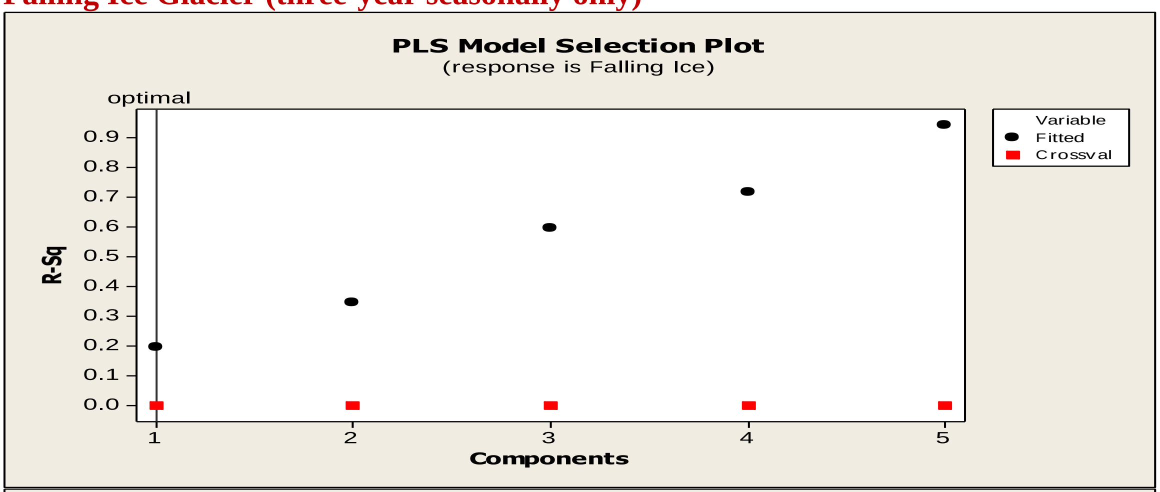

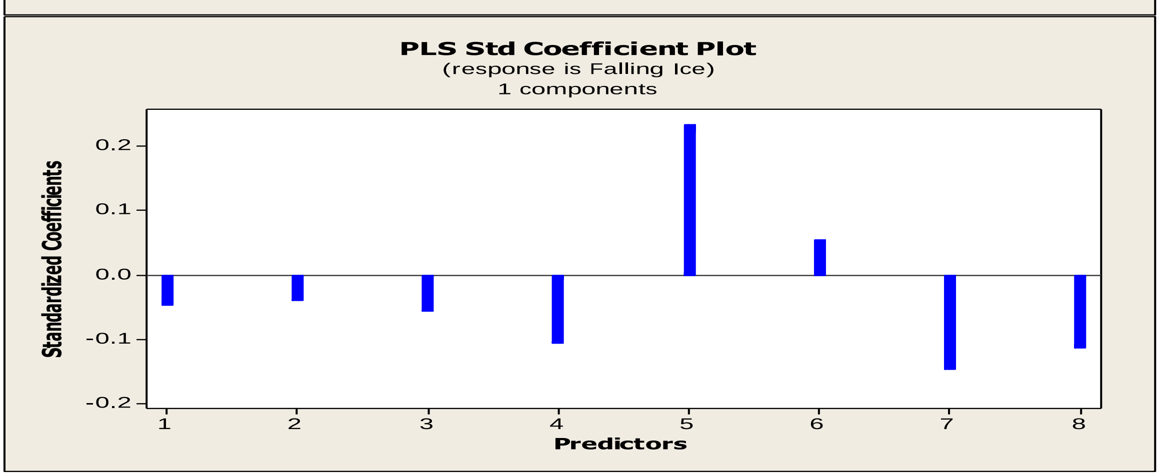

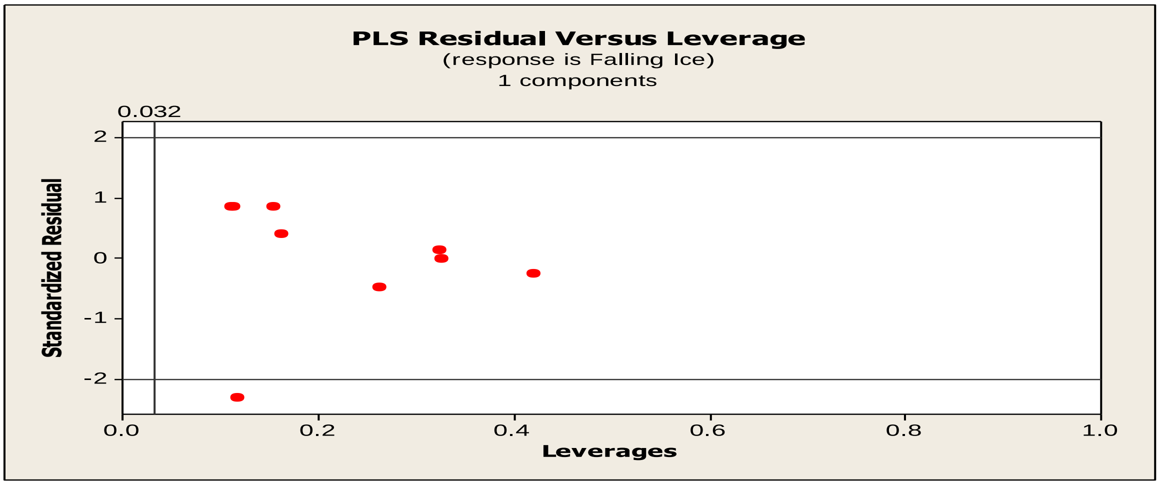

There is one outlier (1974) on the residual versus leverage plot.

PLS Regression: Falling Ice versus MMSpT, MMSuT, MMFaT, MMWiT, MMSpP, ...

```
Method
Cross-validation                  Leave-one-out
Components to evaluate            User specified
Number of components evaluated    5
Number of components selected     1

Analysis of Variance for Falling Ice
Source          DF         SS        MS     F      P
Regression       1   87030304  87030304  1.70  0.234
Residual Error   7  358542367  51220338
Total            8  445572671

Model Selection and Validation for Falling Ice
Components  X Variance      Error      R-Sq       PRESS  R-Sq (pred)
         1    0.443213  358542367  0.195322  1178151932            0
         2              292320660  0.343944  1581434610            0
         3              181249726  0.593221  2302286985            0
         4              127112052  0.714722  3151598876            0
         5               27388554  0.938532  3616102757            0

Coefficients
          Falling  Falling Ice
              Ice  standardized
Constant   131159      0.000000
MMSpT        -298     -0.046822
MMSuT        -305     -0.040235
MMFaT        -264     -0.056308
MMWiT        -398     -0.105419
MMSpP       14841      0.233253
MMSuP        3785      0.054802
MMFaP       -7312     -0.146933
```

Skillet Glacier (three-year seasonally only)

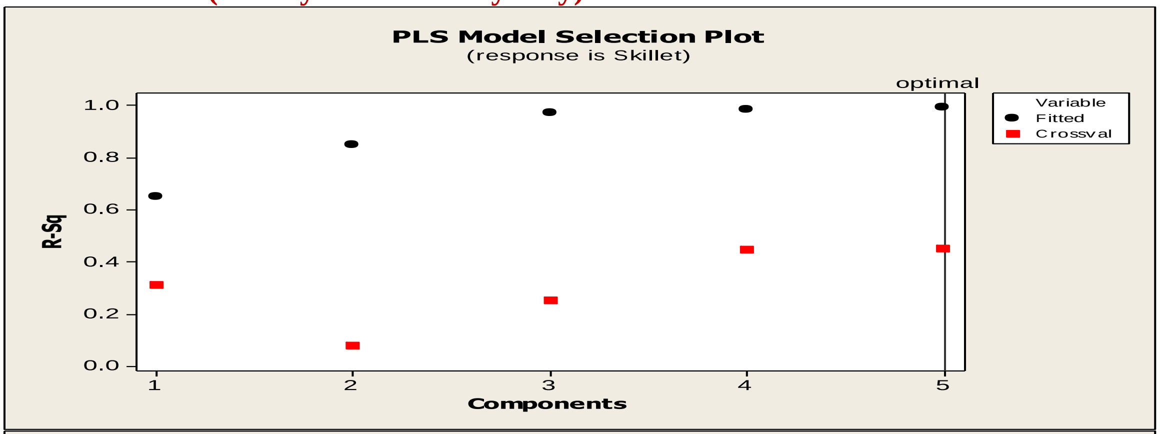

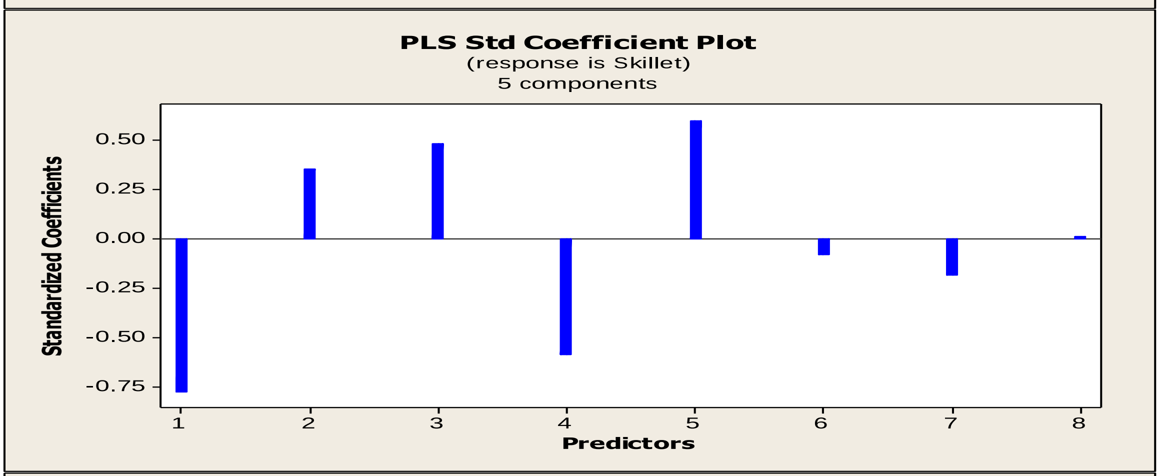

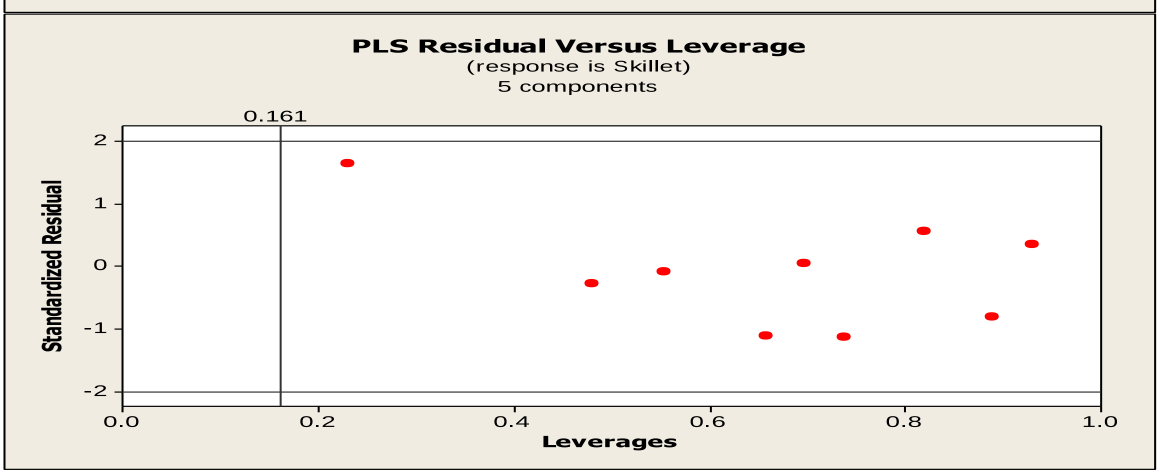

PLS Regression: Skillet versus MMSpT, MMSuT, MMFaT, MMWiT, MMSpP, MMSuP, ...

Method

Cross-validation	Leave-one-out
Components to evaluate	User specified
Number of components evaluated	5
Number of components selected	5

Analysis of Variance for Skillet

Source	DF	SS	MS	F	P
Regression	5	1233139010	246627802	87.65	0.002

```
Residual Error   3     8441399    2813800
Total            8  1241580409
Model Selection and Validation for Skillet
Components  X Variance      Error      R-Sq       PRESS  R-Sq (pred)
         1    0.651467  436116744  0.648741   852497692     0.313377
         2    0.769483  188033997  0.848553  1145290516     0.077554
         3    0.841640   36498585  0.970603   926489944     0.253782
         4    0.937480   21555203  0.982639   686463455     0.447105
         5    0.968213    8441399  0.993201   681380635     0.451199

Coefficients
                        Skillet
           Skillet  standardized
Constant   83007.8      0.000000
MMSpT      -8235.5     -0.775695
MMSuT       4467.5      0.352999
MMFaT       3767.3      0.481380
MMWiT      -3718.0     -0.589898
MMSpP      63321.6      0.596178
MMSuP      -9467.6     -0.082115
MMFaP     -15375.8     -0.185085
```

East Triple Glacier (three-year seasonally only)

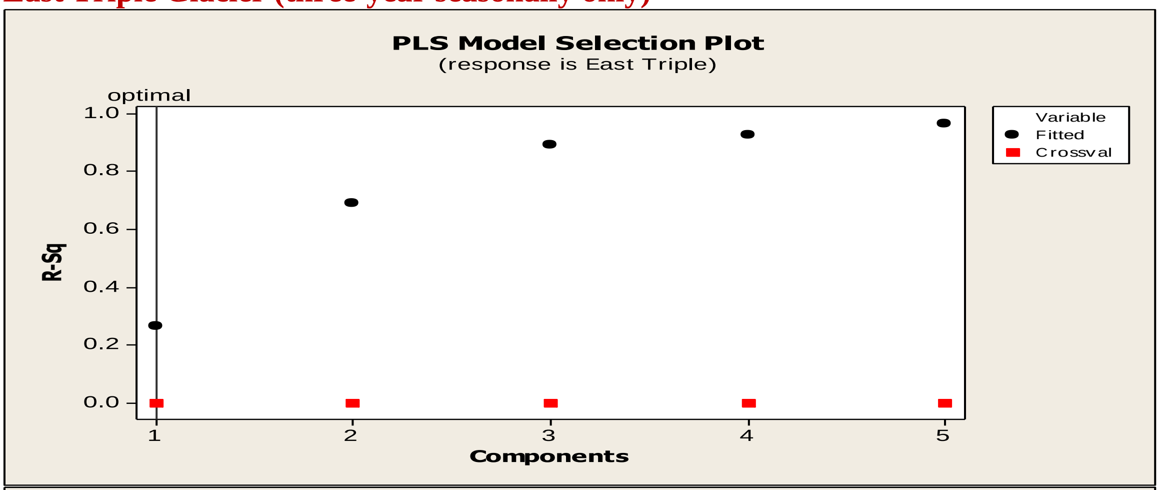

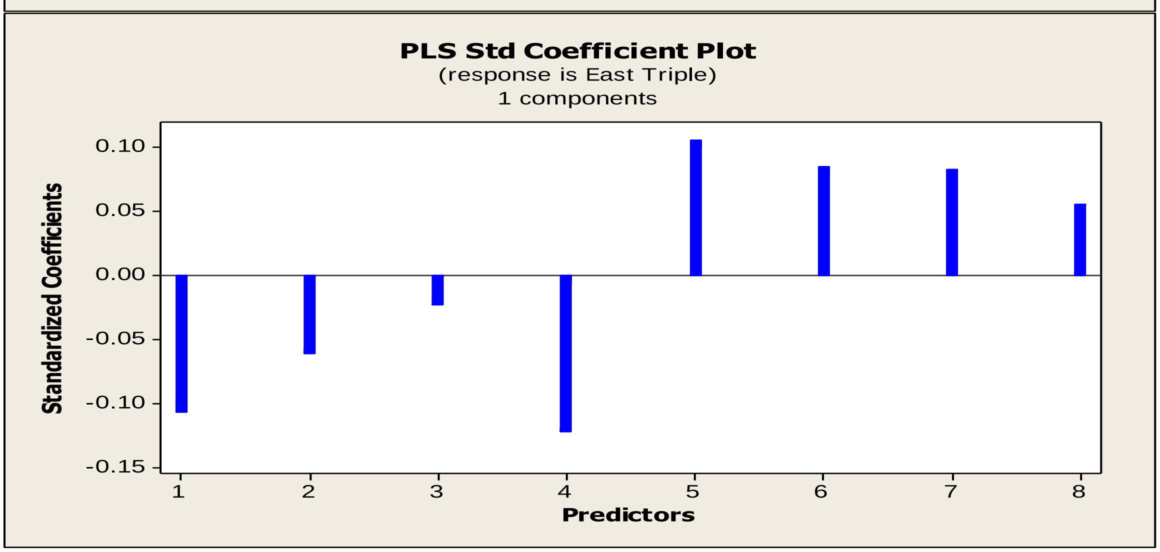

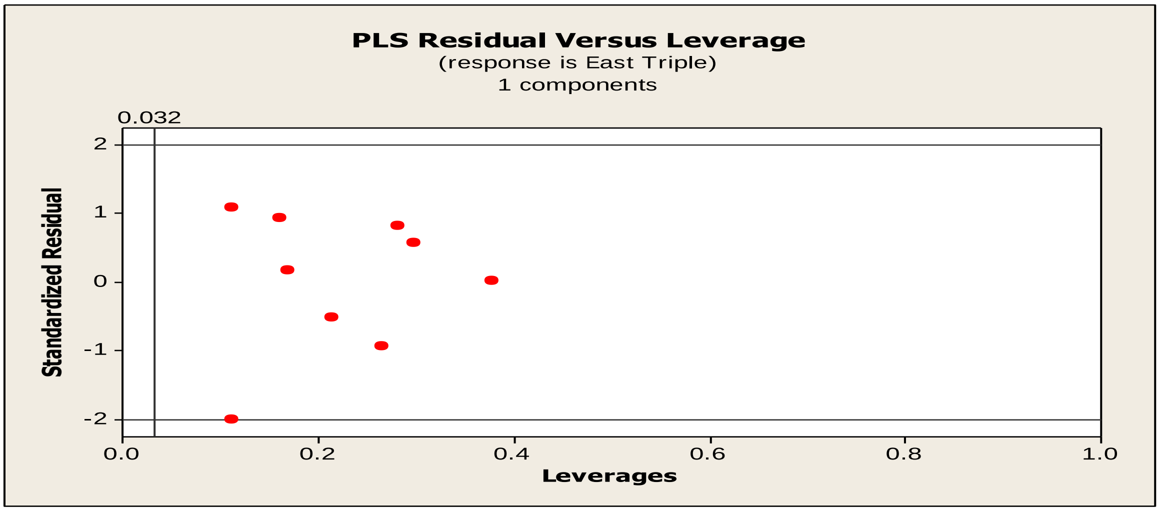

There is almost one outlier (1994) on the residual versus leverage plot.

PLS Regression: East Triple versus MMSpT, MMSuT, MMFaT, MMWiT, MMSpP, ...

Method

Cross-validation	Leave-one-out
Components to evaluate	User specified
Number of components evaluated	5
Number of components selected	1

Analysis of Variance for East Triple

Source	DF	SS	MS	F	P
Regression	1	839090514	839090514	2.50	0.158
Residual Error	7	2348333992	335476285		
Total	8	3187424506			

Model Selection and Validation for East Triple

Components	X Variance	Error	R-Sq	PRESS	R-Sq (pred)
1	0.646754	2348333992	0.263250	4190461280	0
2		986535163	0.690491	8326045128	0
3		344692216	0.891859	6673205449	0
4		235529227	0.926107	5211151075	0
5		109789932	0.965555	5725033520	0

Coefficients

	East Triple	East Triple standardized
Constant	67228.0	0.000000
MMSpT	-1810.7	-0.106443
MMSuT	-1227.9	-0.060554
MMFaT	-285.0	-0.022727
MMWiT	-1229.5	-0.121746
MMSpP	17937.9	0.105405
MMSuP	15707.6	0.085028
MMFaP	11109.9	0.083466

Middle Triple Glacier (three-year seasonally only)

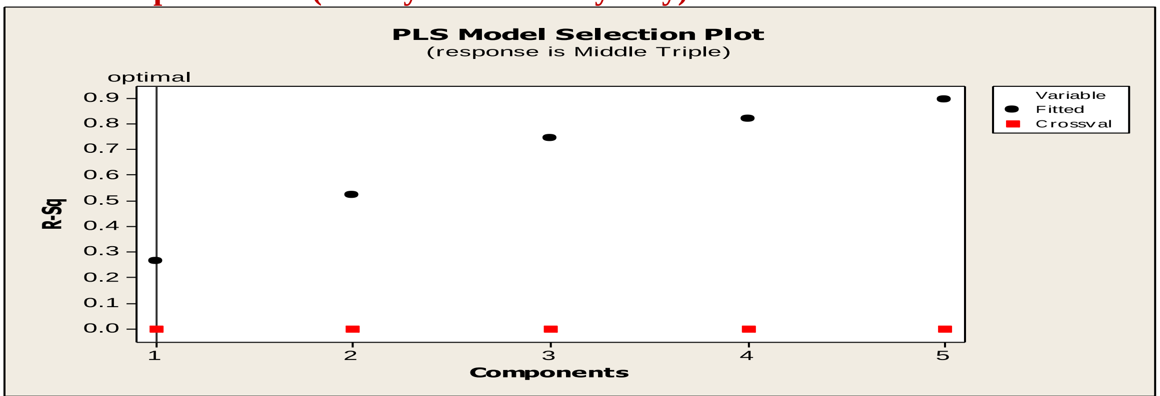

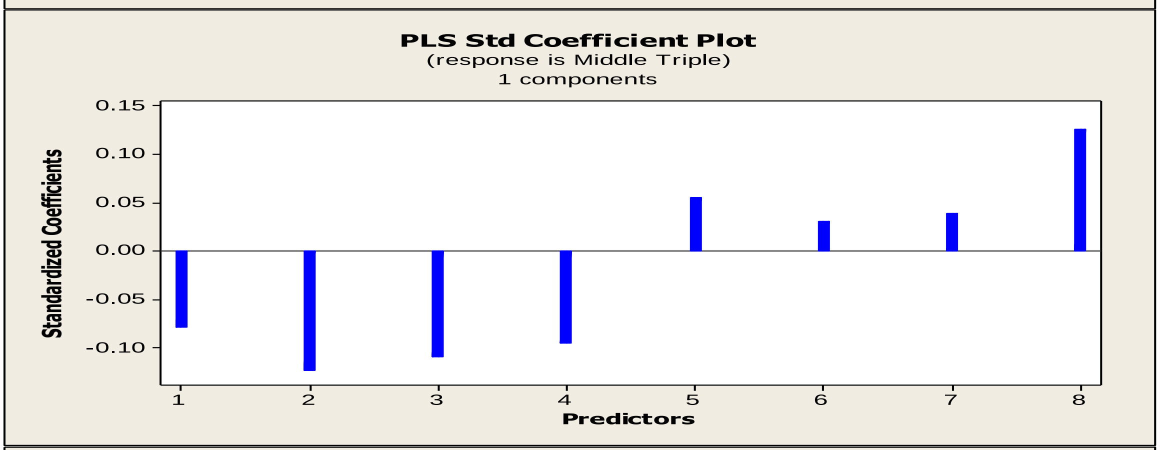

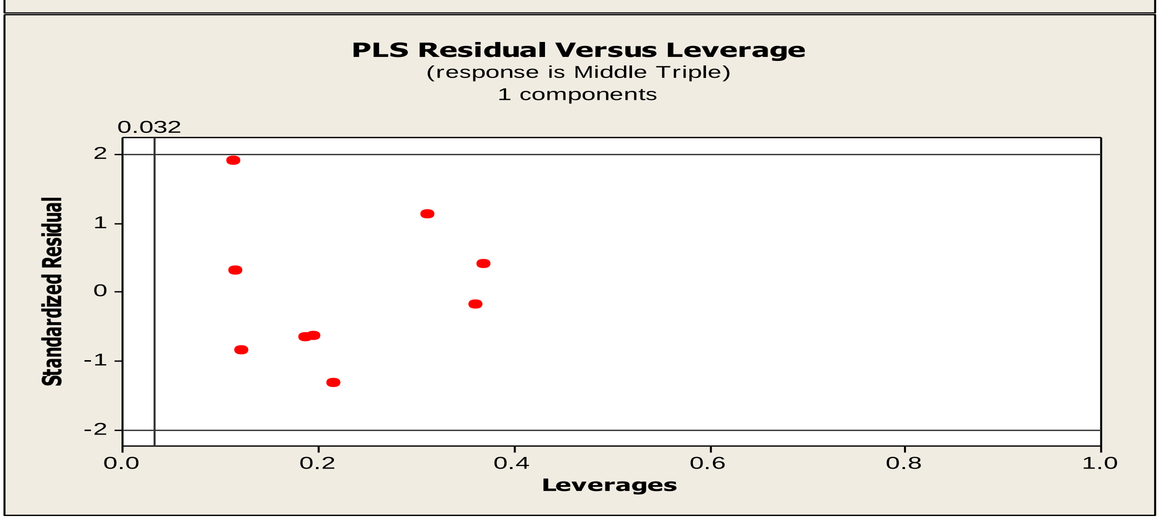

PLS Regression: Middle Triple versus MMSpT, MMSuT, MMFaT, MMWiT, MMSpP, ...

Method

Cross-validation	Leave-one-out
Components to evaluate	User specified
Number of components evaluated	5
Number of components selected	1

Analysis of Variance for Middle Triple

Source	DF	SS	MS	F	P
Regression	1	254119257	254119257	2.50	0.158
Residual Error	7	710727341	101532477		

```
Total              8  964846598
Model Selection and Validation for Middle Triple
Components  X Variance      Error     R-Sq       PRESS  R-Sq (pred)
         1    0.629105  710727341  0.263378  1236451362            0
         2              459992497  0.523248  1690136162            0
         3              245818226  0.745226  2240805768            0
         4              175223489  0.818392  2790117161            0
         5              103999435  0.892211  3489221350            0

Coefficients
           Middle  Middle Triple
           Triple   standardized
Constant   186270       0.000000
MMSpT        -737      -0.078762
MMSuT       -1380      -0.123669
MMFaT        -753      -0.109166
MMWiT        -531      -0.095652
MMSpP        5138       0.054873
MMSuP        3076       0.030269
MMFaP        2794       0.038147
MMWiP       14284       0.125924
```

West Triple Glacier (three-year seasonally only)

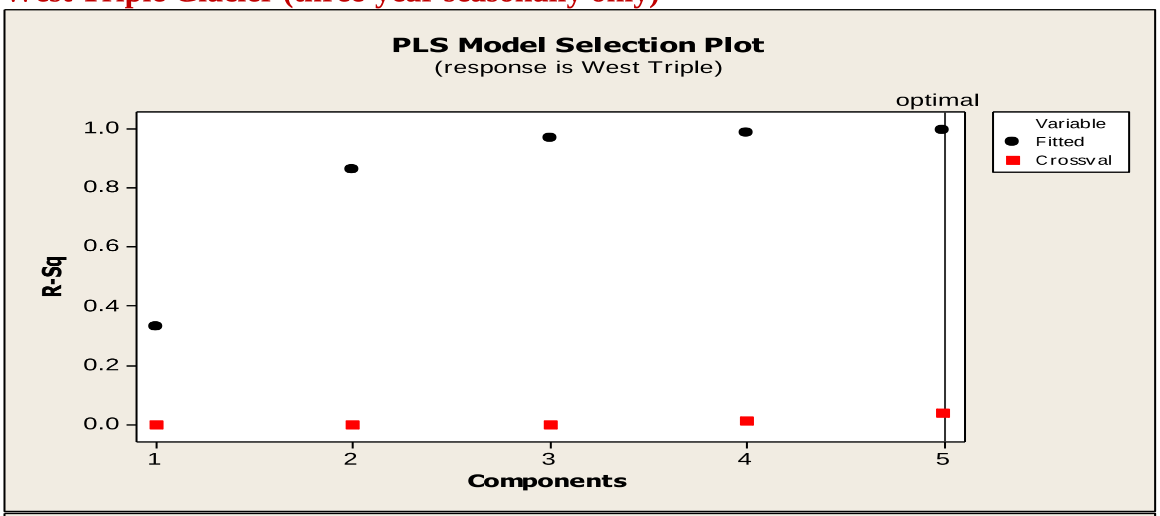

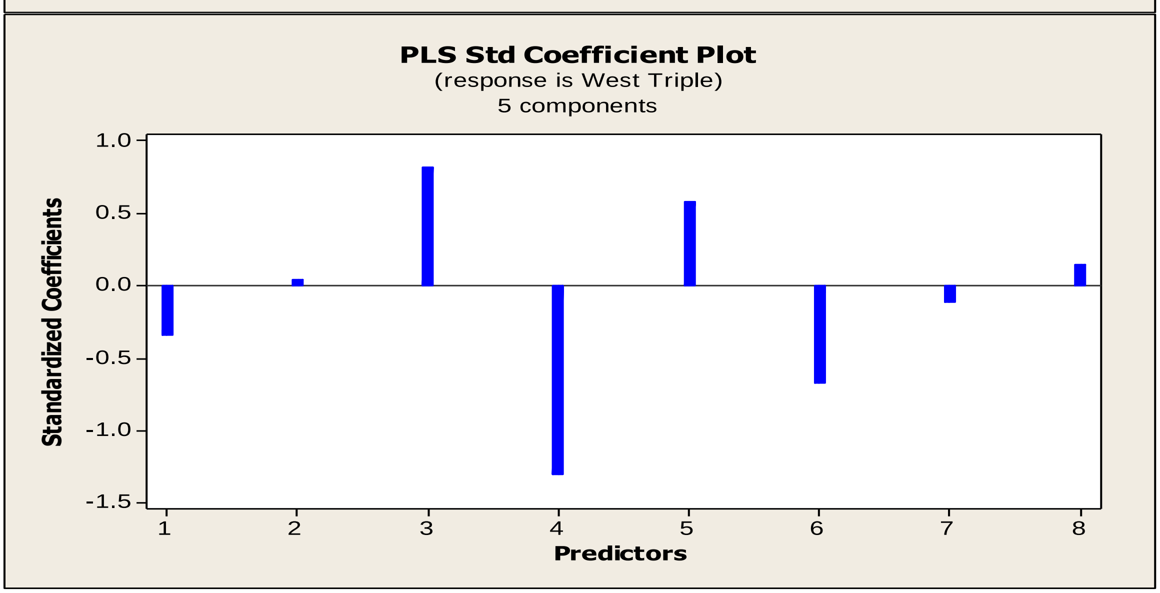

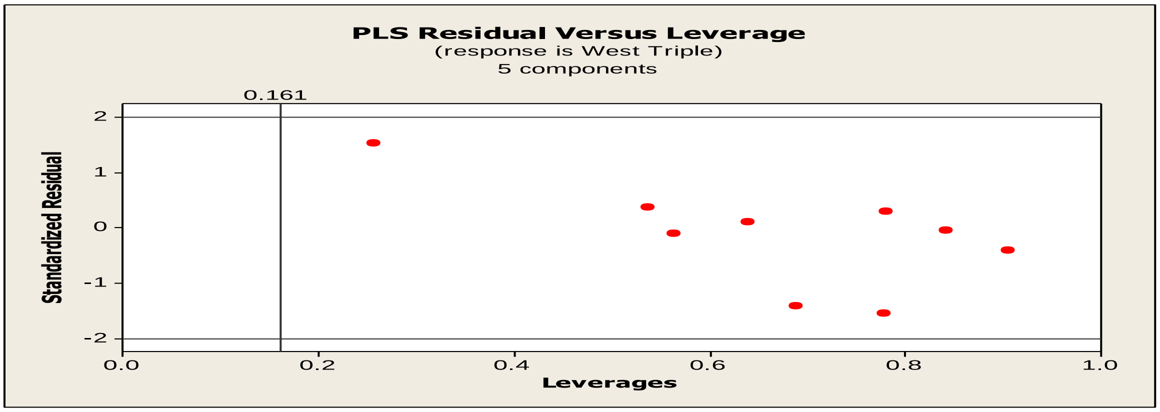

PLS Regression: West Triple versus MMSpT, MMSuT, MMFaT, MMWiT, MMSpP, ...

```
Method
Cross-validation                Leave-one-out
Components to evaluate          User specified
Number of components evaluated  5
Number of components selected   5

Analysis of Variance for West Triple
Source          DF          SS          MS       F      P
Regression       5  1.48625E+10  2972497746  180.94  0.001
Residual Error   3  4.92831E+07    16427685
Total            8  1.49118E+10

Model Selection and Validation for West Triple
Components  X Variance        Error      R-Sq        PRESS  R-Sq (pred)
         1    0.649470  1.00156E+10  0.328345  1.69952E+10    0.0000000
         2    0.714357  2.06763E+09  0.861342  2.81585E+10    0.0000000
         3    0.824615  4.56072E+08  0.969415  1.79771E+10    0.0000000
         4    0.924652  2.08616E+08  0.986010  1.47438E+10    0.0112640
         5    0.971809  4.92831E+07  0.996695  1.43389E+10    0.0384173

Coefficients
                       West Triple
          West Triple  standardized
Constant        17506       0.00000
MMSpT          -12477      -0.33909
MMSuT            1944       0.04433
MMFaT           22202       0.81860
MMWiT          -28611      -1.30987
MMSpP          212671       0.57777
MMSuP         -267588      -0.66969
MMFaP          -33735      -0.11718
```

Schoolroom Glacier (three-year annually only)

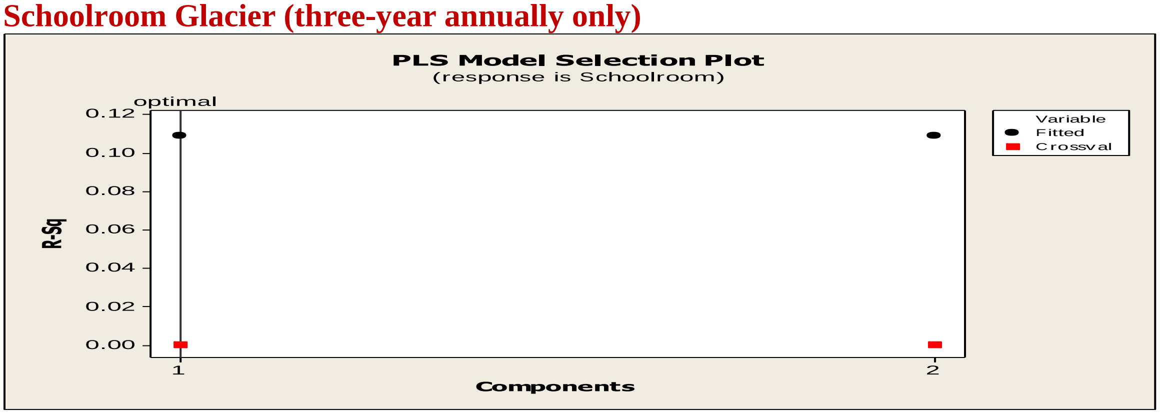

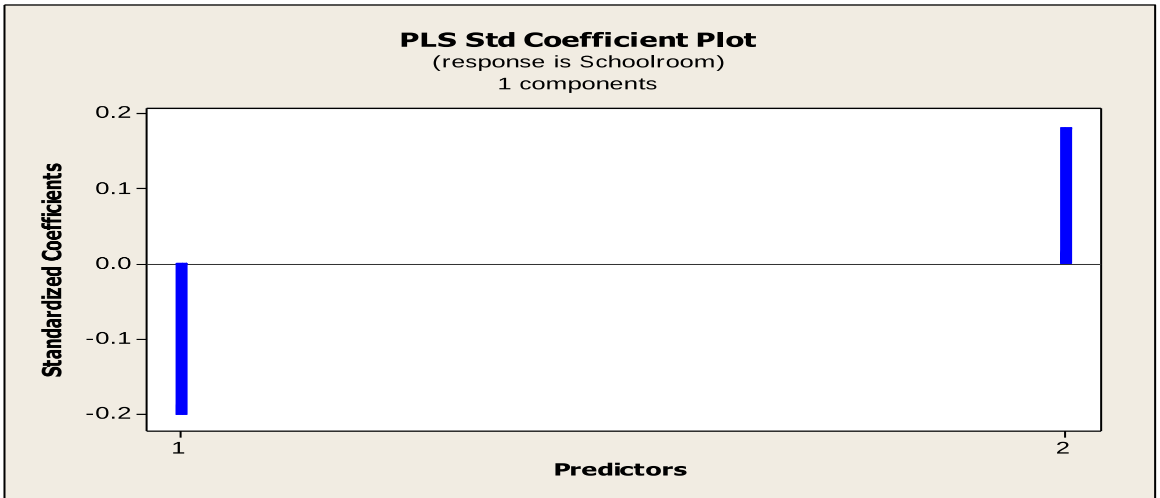

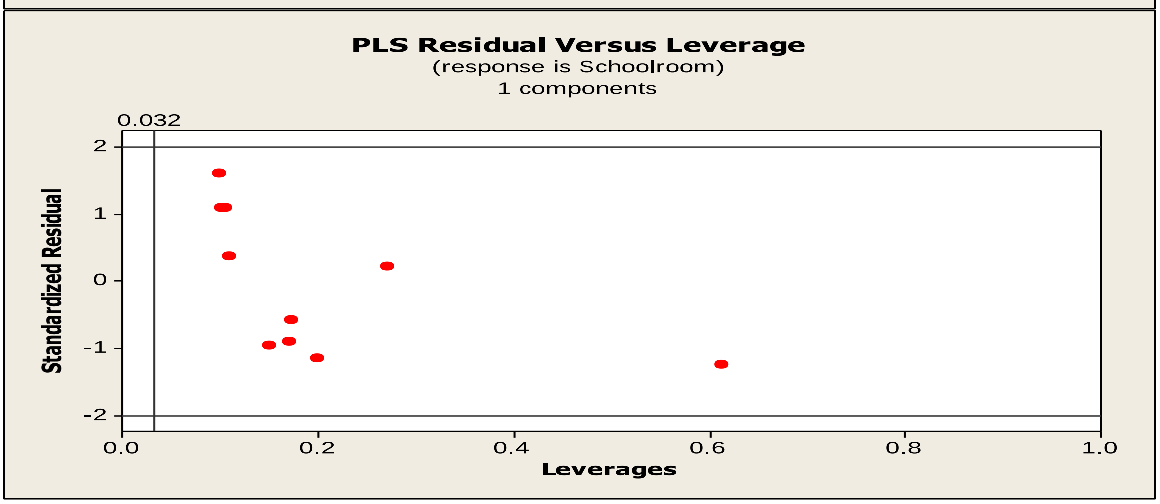

PLS Regression: Schoolroom versus SchAnT, SchAnP

```
Method
Cross-validation                 Leave-one-out
Components to evaluate           User specified
Number of components evaluated   2
Number of components selected    1

Analysis of Variance for Schoolroom
Source          DF         SS        MS     F      P
Regression       1   69492063  69492063  0.98  0.352
Residual Error   8  569312262  71164033
Total            9  638804325

Model Selection and Validation for Schoolroom
Components  X Variance      Error      R-Sq       PRESS  R-Sq (pred)
         1    0.743405  569312262  0.108785  1069727468            0
         2              569109955  0.109101  1409546476            0

Coefficients
                          Schoolroom
          Schoolroom    standardized
Constant     18710.2        0.000000
SchAnT       -4046.2       -0.200394
SchAnP        5412.0        0.181885
```

Falling Ice Glacier (three-year annually only)

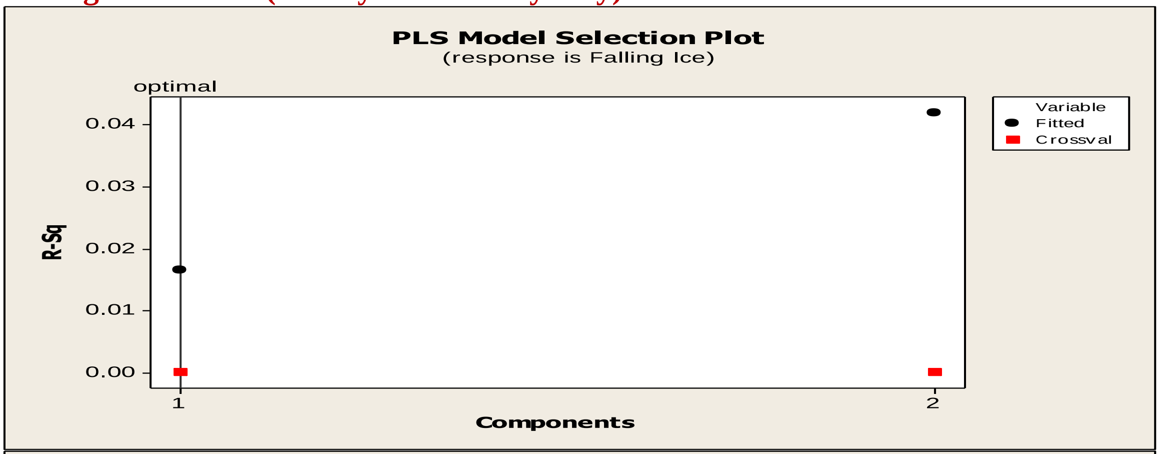

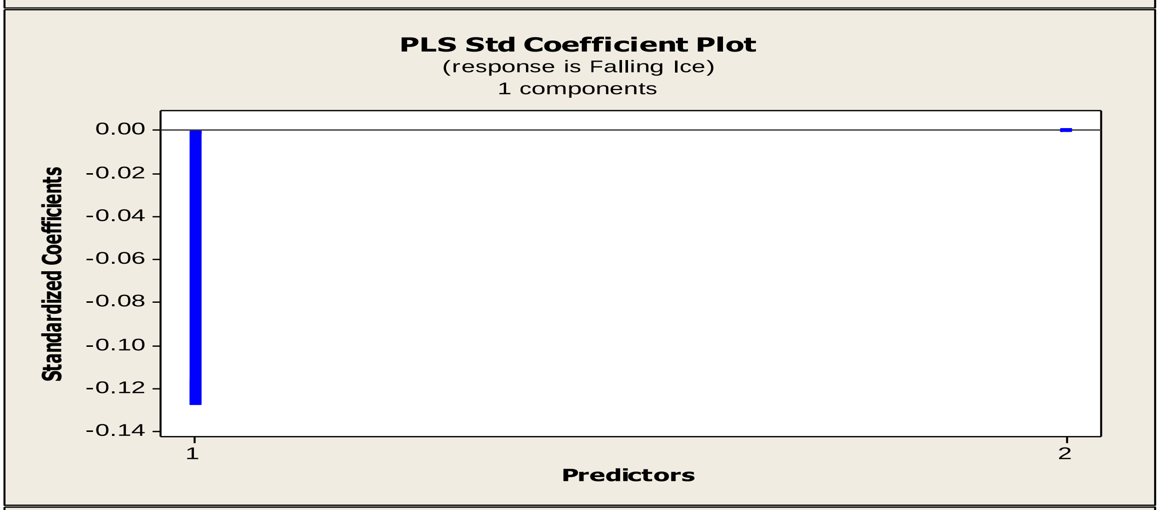

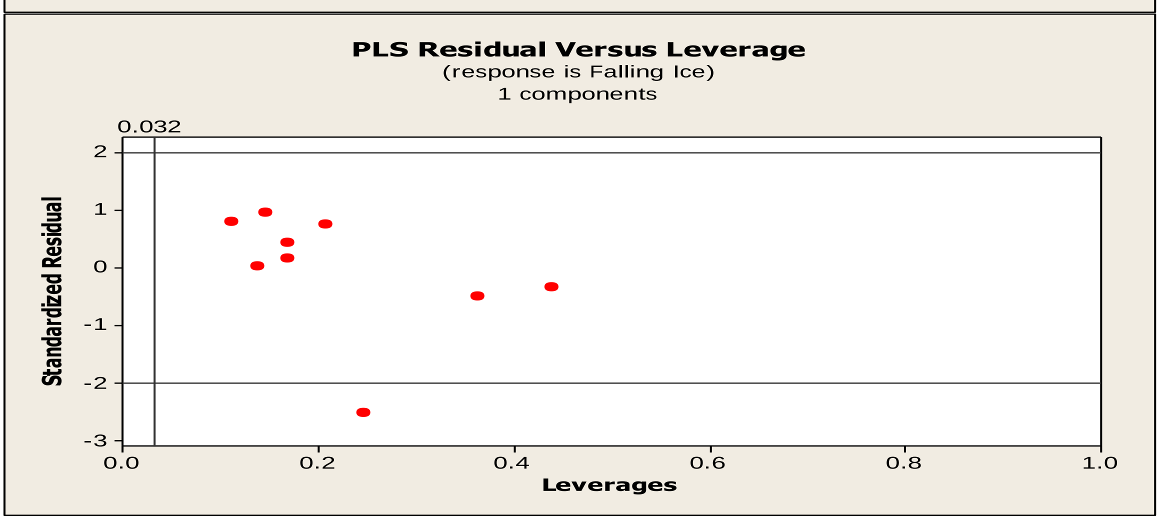

There is one outlier (1974) on the residual versus leverage plot.

PLS Regression: Falling Ice versus MMAnT, MMAnP

```
Method
Cross-validation                 Leave-one-out
Components to evaluate           User specified
Number of components evaluated   2
Number of components selected    1
```

```
Analysis of Variance for Falling Ice
Source           DF         SS         MS     F      P
Regression        1    7330895    7330895  0.12  0.742
Residual Error    7  438241776   62605968
Total             8  445572671

Model Selection and Validation for Falling Ice
Components  X Variance      Error       R-Sq       PRESS  R-Sq (pred)
         1    0.807136  438241776  0.0164527  1027930320            0
         2              426861638  0.0419932  1712022942            0

Coefficients
           Falling   Falling Ice
               Ice  standardized
Constant    130674      0.000000
MMAnT         -705     -0.127280
MMAnP           28      0.001264
```

Skillet Glacier (three-year annually only)

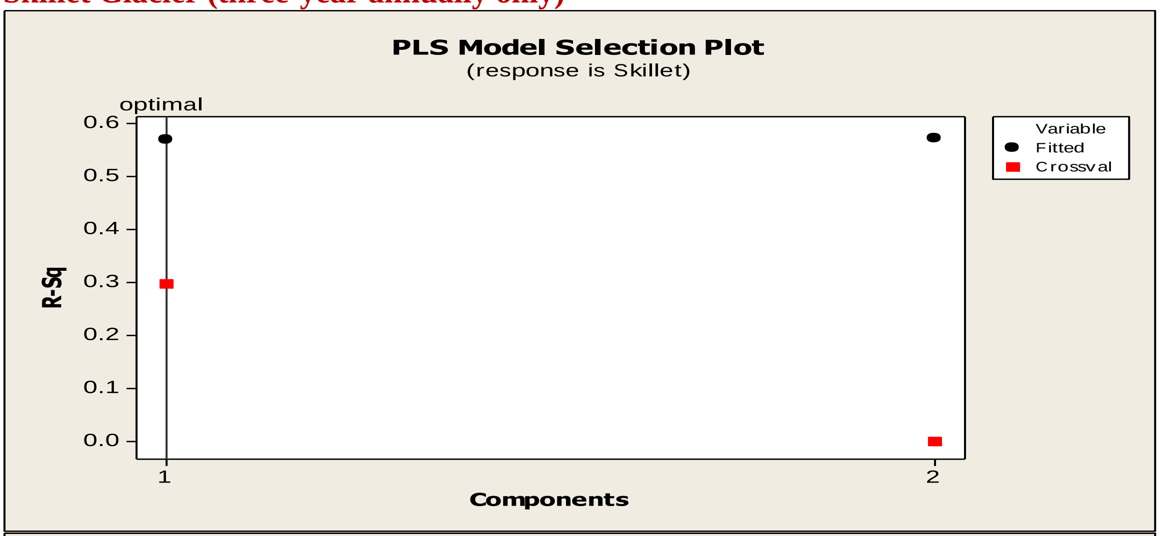

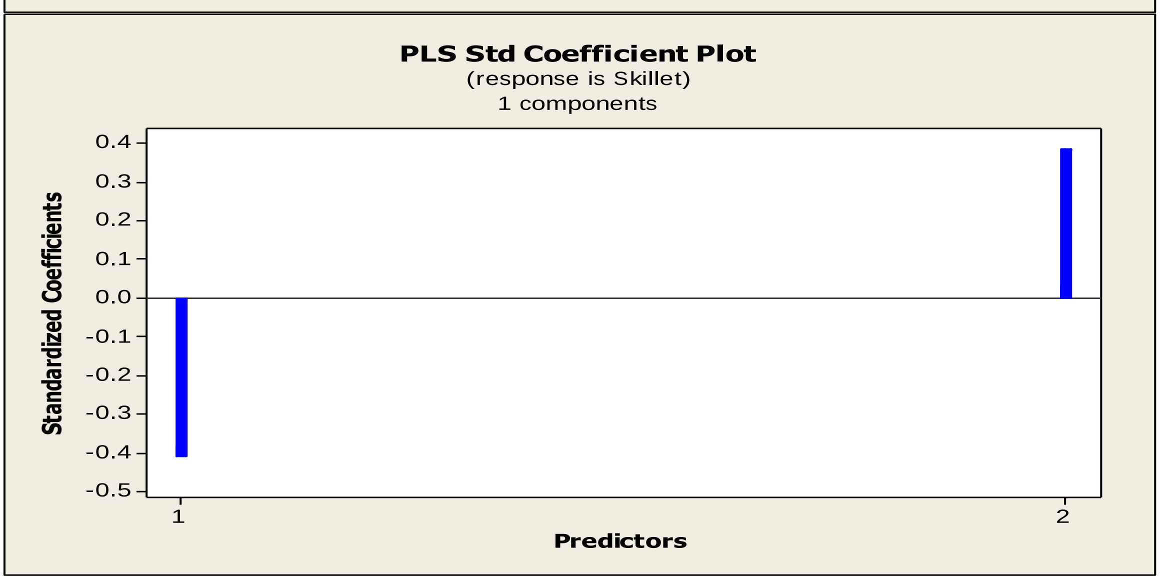

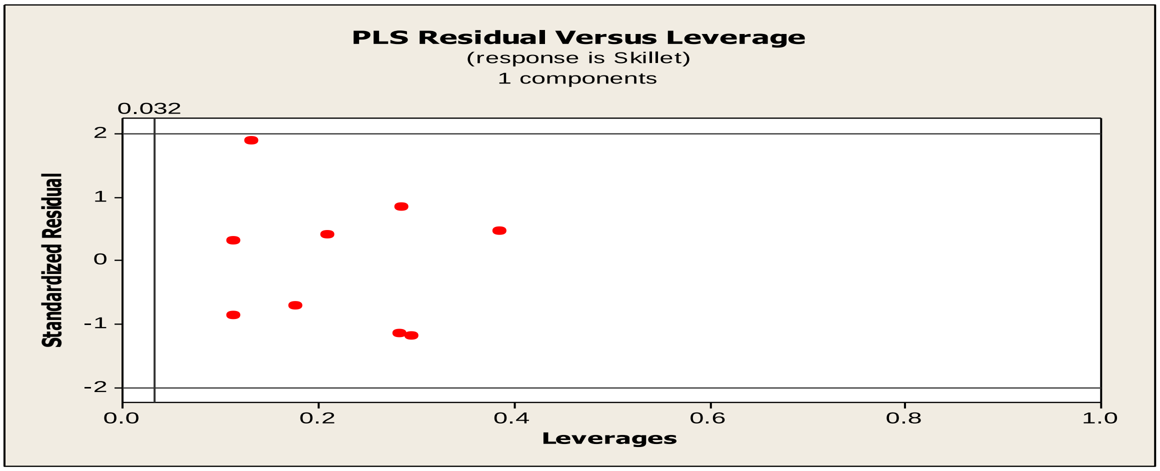

PLS Regression: Skillet versus MMAnT, MMAnP

Method

Cross-validation	Leave-one-out
Components to evaluate	User specified
Number of components evaluated	2
Number of components selected	1

Analysis of Variance for Skillet

Source	DF	SS	MS	F	P
Regression	1	704961654	704961654	9.20	0.019
Residual Error	7	536618755	76659822		
Total	8	1241580409			

Model Selection and Validation for Skillet

Components	X Variance	Error	R-Sq	PRESS	R-Sq (pred)
1	0.889905	536618755	0.567794	874289094	0.295826
2		533771564	0.570087	1534178183	0.000000

Coefficients

	Skillet	Skillet standardized
Constant	98619.2	0.000000
MMAnT	-3784.5	-0.409546
MMAnP	14269.2	0.389167

East Triple Glacier (three-year annually only)

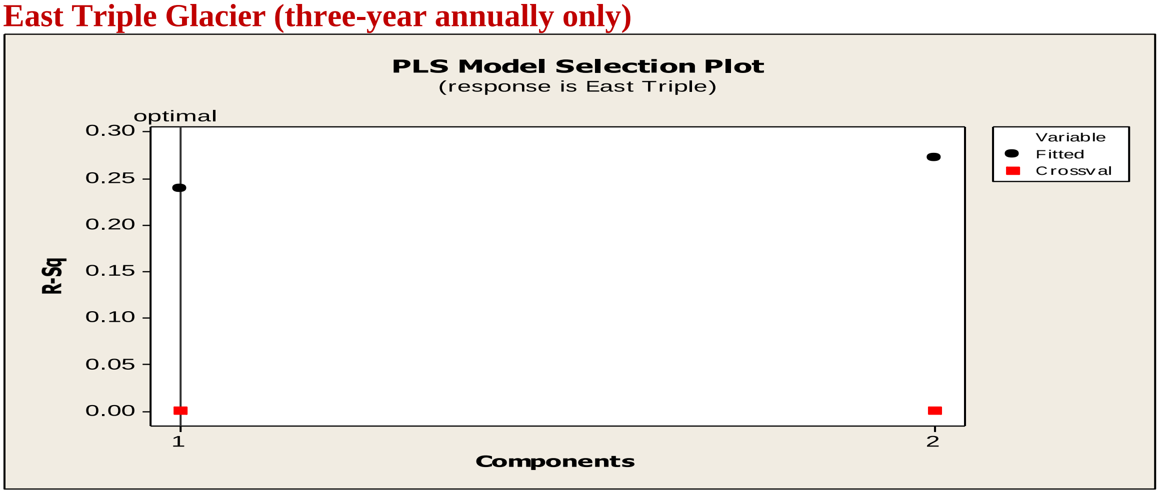

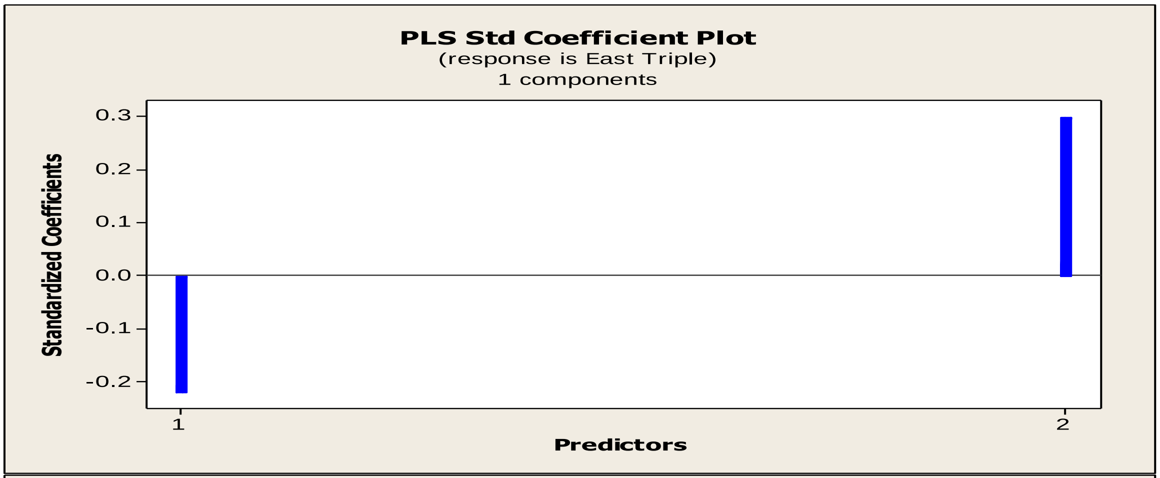

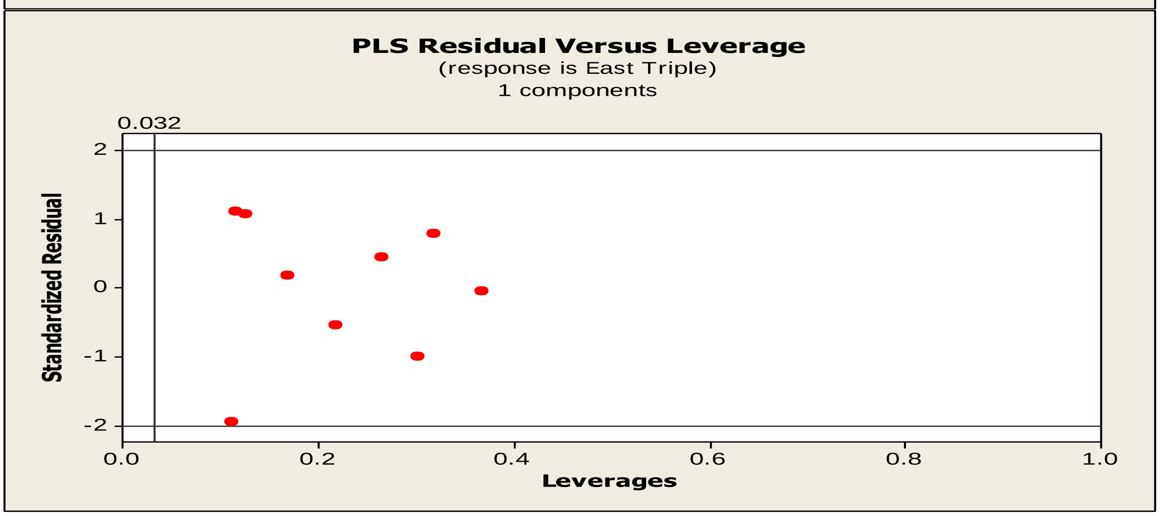

There is almost one outlier (1994) on the residual versus leverage plot.

PLS Regression: East Triple versus MMAnT, MMAnP

```
Method
Cross-validation                 Leave-one-out
Components to evaluate           User specified
Number of components evaluated   2
Number of components selected    1

Analysis of Variance for East Triple
Source          DF          SS          MS     F      P
Regression       1   763180785   763180785  2.20  0.181
Residual Error   7  2424243721   346320532
Total            8  3187424506

Model Selection and Validation for East Triple
Components  X Variance       Error      R-Sq       PRESS  R-Sq (pred)
         1    0.887742  2424243721  0.239435  3580844998            0
         2              2319432895  0.272318  4372045492            0

Coefficients
                           East Triple
          East Triple     standardized
Constant      54500.3         0.000000
MMAnT         -3251.1        -0.219576
MMAnP         17528.9         0.298372
```

Middle Triple Glacier (three-year annually only)

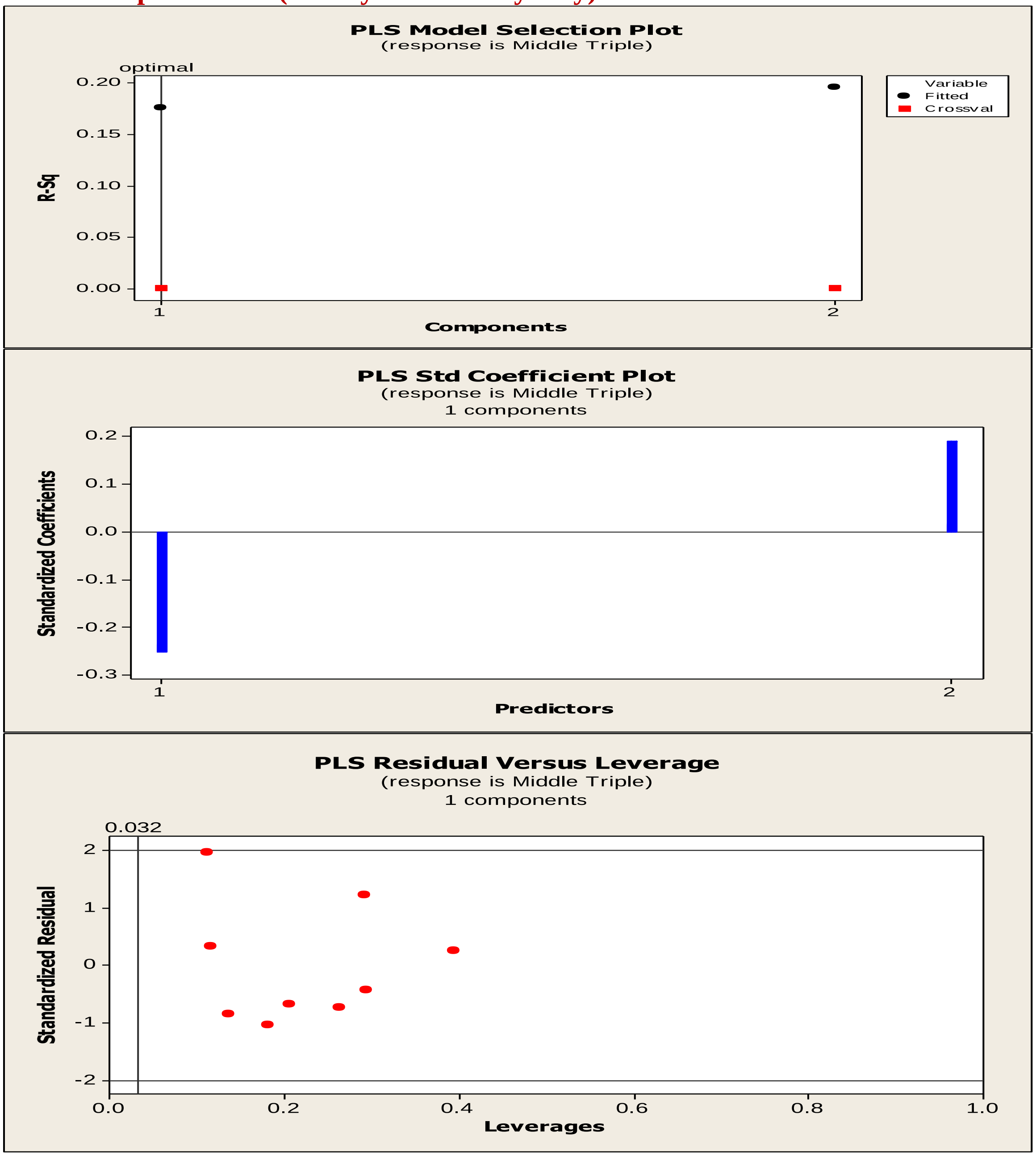

There is almost one outlier (1989) on the residual versus leverage plot.

PLS Regression: Middle Triple versus MMAnT, MMAnP

```
Method
Cross-validation                 Leave-one-out
Components to evaluate           User specified
Number of components evaluated   2
Number of components selected    1

Analysis of Variance for Middle Triple
Source          DF         SS         MS     F      P
Regression       1  169500426  169500426  1.49  0.261
Residual Error   7  795346172  113620882
```

```
Total              8  964846598
Model Selection and Validation for Middle Triple
Components  X Variance      Error     R-Sq       PRESS  R-Sq (pred)
         1    0.888174  795346172  0.175676  1228763322            0
         2              776425578  0.195286  1475456119            0

Coefficients
          Middle  Middle Triple
          Triple   standardized
Constant  181283       0.000000
MMAnT      -2054      -0.252190
MMAnP       6193       0.191591
```

West Triple Glacier (three-year annually only)

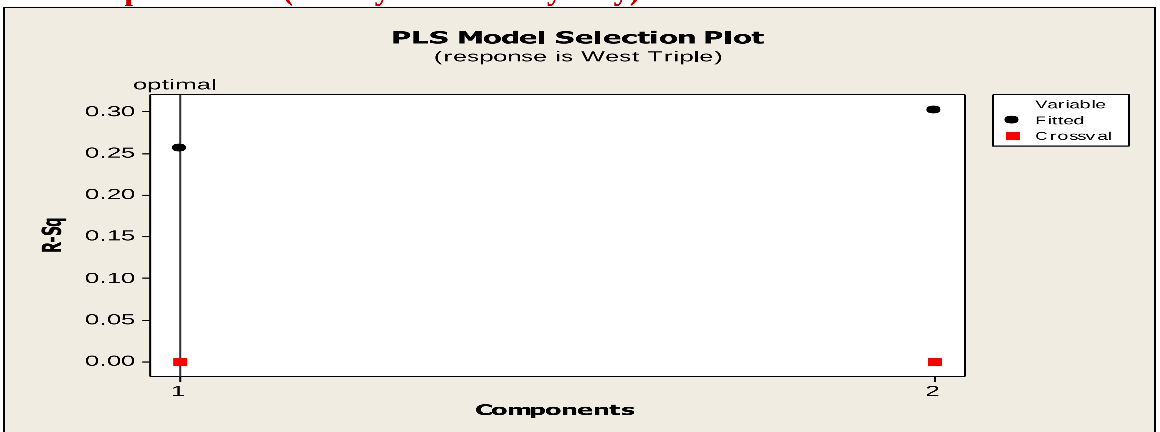

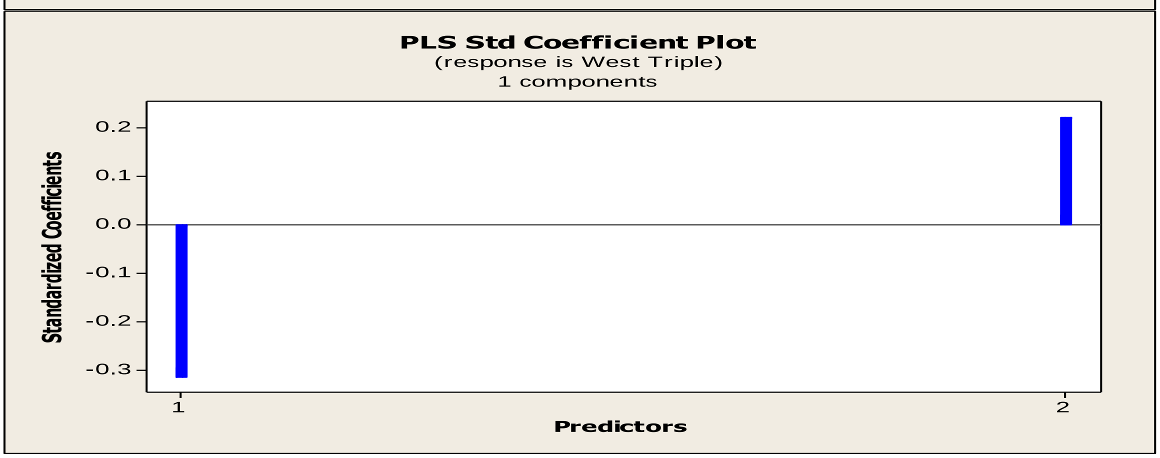

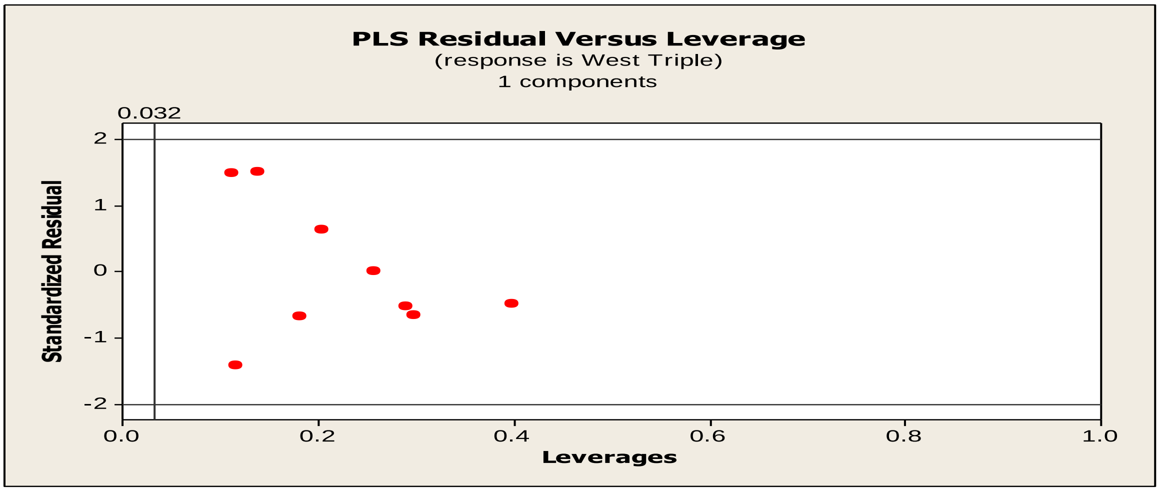

PLS Regression: West Triple versus MMAnT, MMAnP

```
Method
Cross-validation                Leave-one-out
Components to evaluate          User specified
Number of components evaluated  2
Number of components selected   1

Analysis of Variance for West Triple
Source          DF           SS          MS     F      P
Regression       1  3.82623E+09  3826234820  2.42  0.164
Residual Error   7  1.10855E+10  1583648138
Total            8  1.49118E+10

Model Selection and Validation for West Triple
Components  X Variance        Error      R-Sq        PRESS  R-Sq (pred)
         1    0.887037  1.10855E+10  0.256592  1.58536E+10            0
         2              1.04027E+10  0.302385  2.08234E+10            0

Coefficients
                          West Triple
          West Triple  standardized
Constant      95567.6      0.000000
MMAnT        -10080.6     -0.314777
MMAnP         28103.1      0.221163
```

Four year moving average PLS results

Schoolroom Glacier (four-year seasonally only)

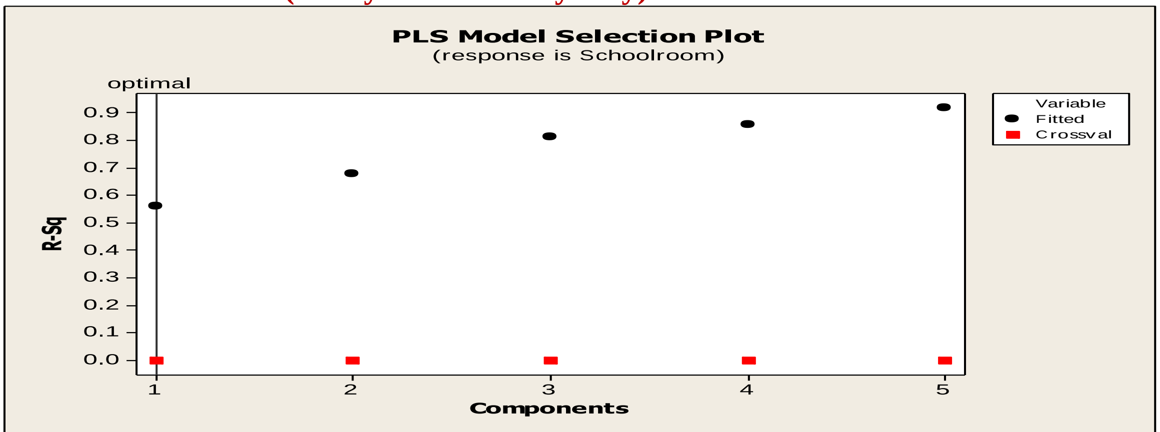

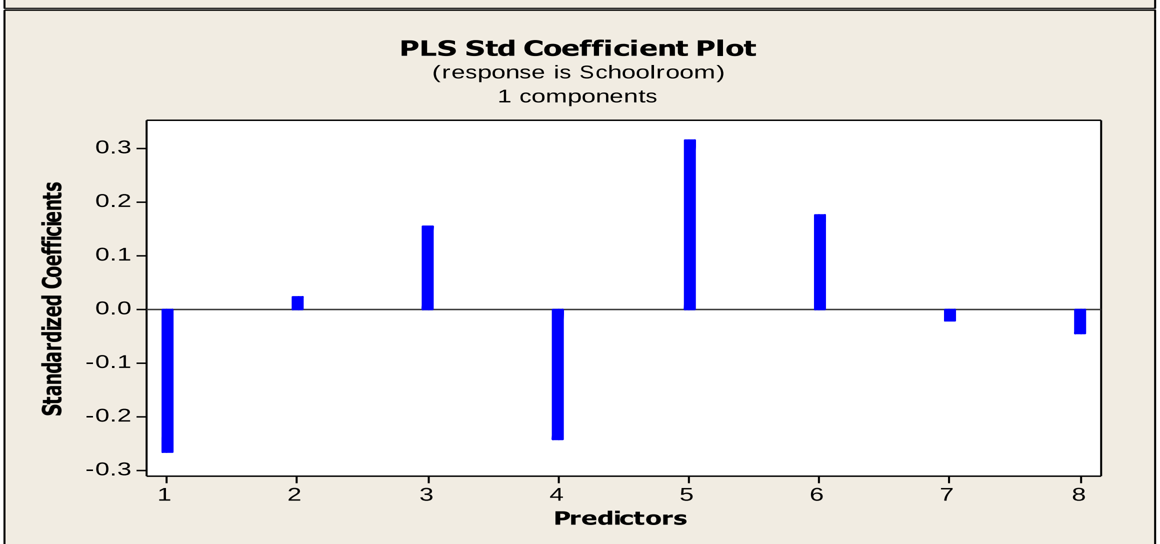

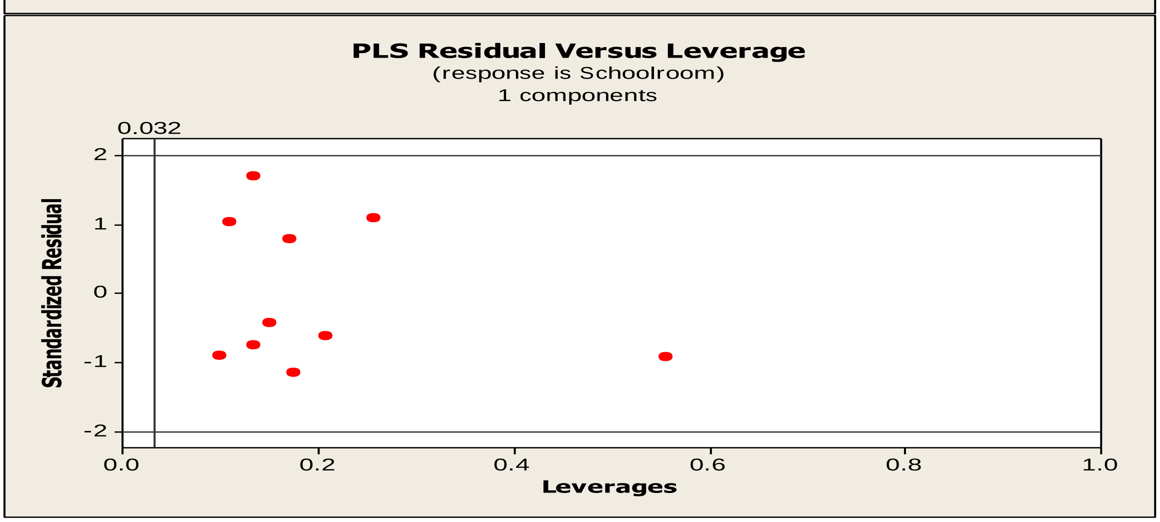

PLS Regression: Schoolroom versus SchSpT, SchSuT, SchFaT, SchWiT, SchSpP, ...

```
Method
Cross-validation              Leave-one-out
Components to evaluate        User specified
```

```
Number of components evaluated  5
Number of components selected   1
Analysis of Variance for Schoolroom
Source          DF         SS         MS      F      P
Regression       1  358226967  358226967  10.21  0.013
Residual Error   8  280577357   35072170
Total            9  638804325

Model Selection and Validation for Schoolroom
Components  X Variance      Error      R-Sq       PRESS  R-Sq (pred)
         1    0.275997  280577357  0.560777   820923599            0
         2              206341244  0.676988   964861672            0
         3              119613301  0.812754  1444688469            0
         4               90621303  0.858139  1493751918            0
         5               53991781  0.915480  1607293828            0

Coefficients
                          Schoolroom
           Schoolroom   standardized
Constant       9977.8       0.000000
SchSpT        -3097.2      -0.266678
SchSuT          435.5       0.023372
SchFaT         1880.2       0.154355
SchWiT        -2330.9      -0.242988
SchSpP        33740.8       0.316048
SchSuP        23384.8       0.175609
SchFaP        -1474.6      -0.021954
SchWiP        -2378.9      -0.044769
```

Falling Ice Glacier (four-year seasonally only)

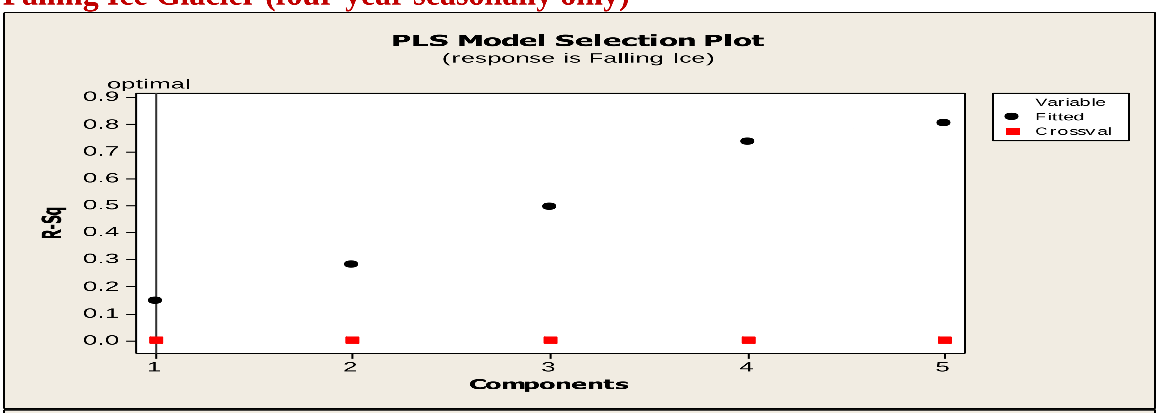

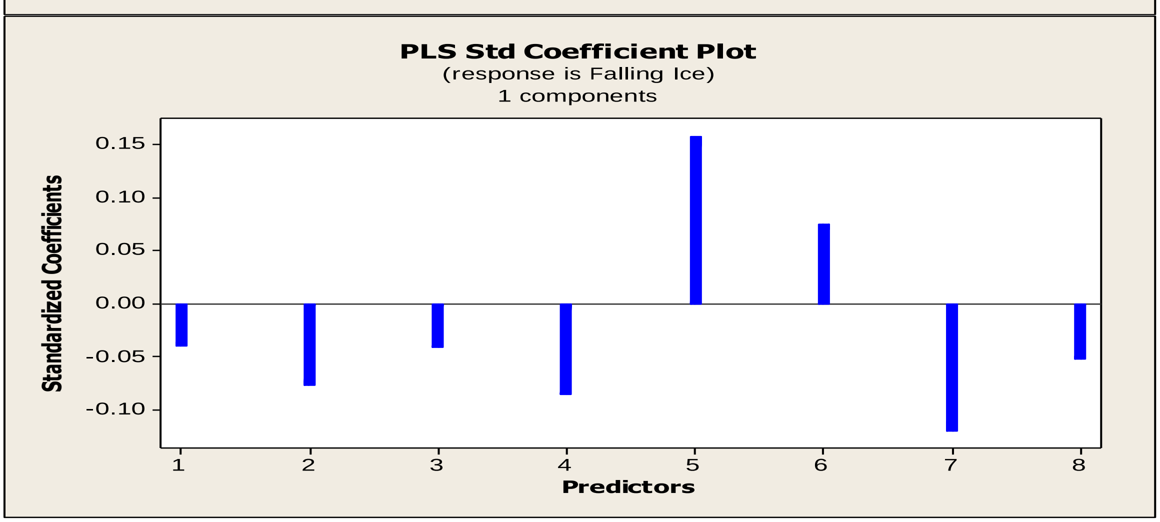

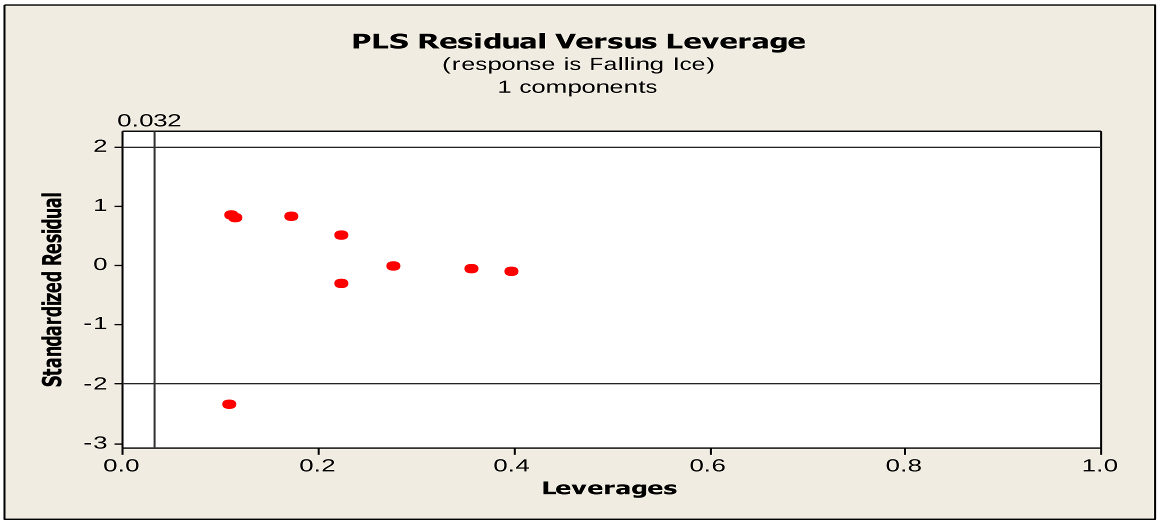

There is one outlier (1974) on the residual versus leverage plot.

PLS Regression: Falling Ice versus MMSpT, MMSuT, MMFaT, MMWiT, MMSpP, ...

```
Method
Cross-validation                Leave-one-out
Components to evaluate          User specified
Number of components evaluated  5
Number of components selected   1

Analysis of Variance for Falling Ice
Source          DF         SS        MS     F      P
Regression       1   65447220  65447220  1.21  0.309
Residual Error   7  380125451  54303636
Total            8  445572671

Model Selection and Validation for Falling Ice
Components  X Variance      Error      R-Sq       PRESS  R-Sq (pred)
         1    0.517770  380125451  0.146883   921349745         0
         2              319976297  0.281876  1687756915         0
         3              225175323  0.494638  2001570125         0
         4              118050790  0.735058  3565243250         0
         5               87093726  0.804535  4148332615         0
Coefficients
          Falling   Falling Ice
              Ice  standardized
Constant   133538      0.000000
MMSpT        -263     -0.040323
MMSuT        -510     -0.077481
MMFaT        -203     -0.041491
MMWiT        -317     -0.086025
MMSpP        9418      0.157790
MMSuP        5336      0.075016
MMFaP       -8158     -0.119677
MMWiP       -3624     -0.051582
```

Skillet Glacier (four-year seasonally only)

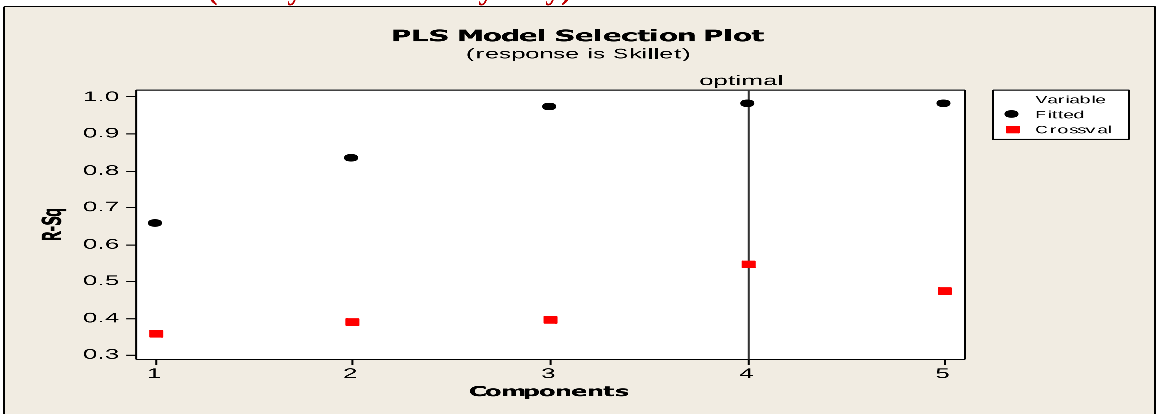

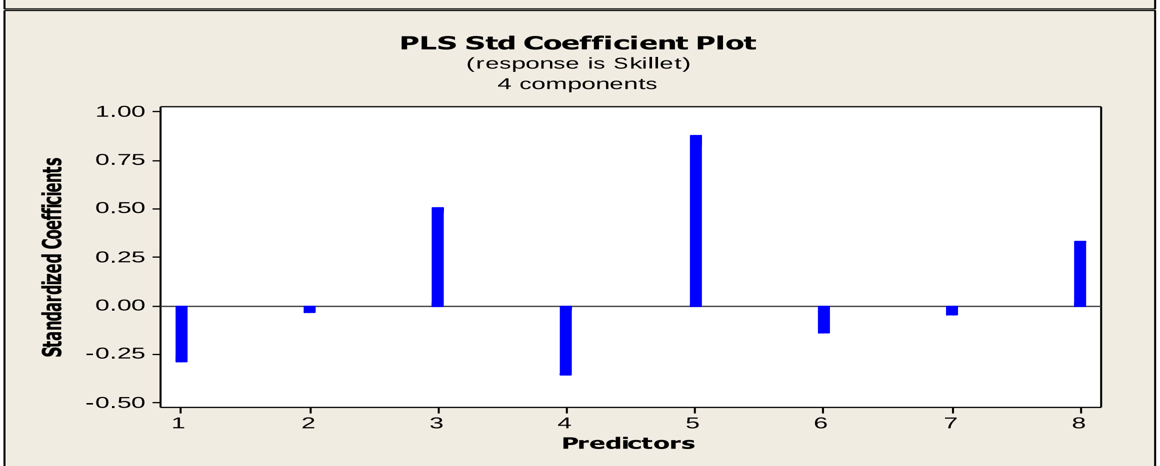

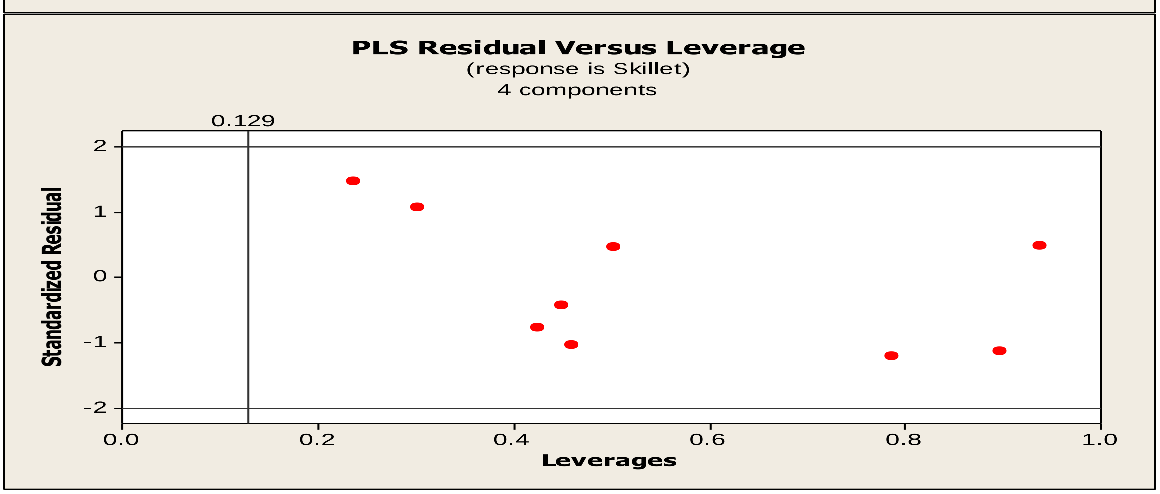

PLS Regression: Skillet versus MMSpT, MMSuT, MMFaT, MMWiT, MMSpP, MMSuP, ...

Method

Cross-validation	Leave-one-out
Components to evaluate	User specified
Number of components evaluated	5
Number of components selected	4

Analysis of Variance for Skillet

Source	DF	SS	MS	F	P
Regression	4	1216778459	304194615	49.06	0.001

```
Residual Error   4    24801950    6200488
Total            8  1241580409
Model Selection and Validation for Skillet
Components  X Variance       Error       R-Sq       PRESS  R-Sq (pred)
         1    0.675269   426964014   0.656112   799718502     0.355887
         2    0.825185   205828572   0.834221   758412070     0.389156
         3    0.888186    34103142   0.972532   750793662     0.395292
         4    0.909164    24801950   0.980024   564793828     0.545101
         5                23424971   0.981133   654418315     0.472915

Coefficients
                         Skillet
            Skillet  standardized
Constant    89186.6      0.000000
MMSpT       -3144.8     -0.288704
MMSuT        -355.3     -0.032364
MMFaT        4160.4      0.510481
MMWiT       -2211.9     -0.359493
MMSpP       87618.2      0.879389
MMSuP      -16529.0     -0.139198
MMFaP       -5289.8     -0.046488
MMWiP       39073.3      0.333169
```

East Triple Glacier (four-year seasonally only)

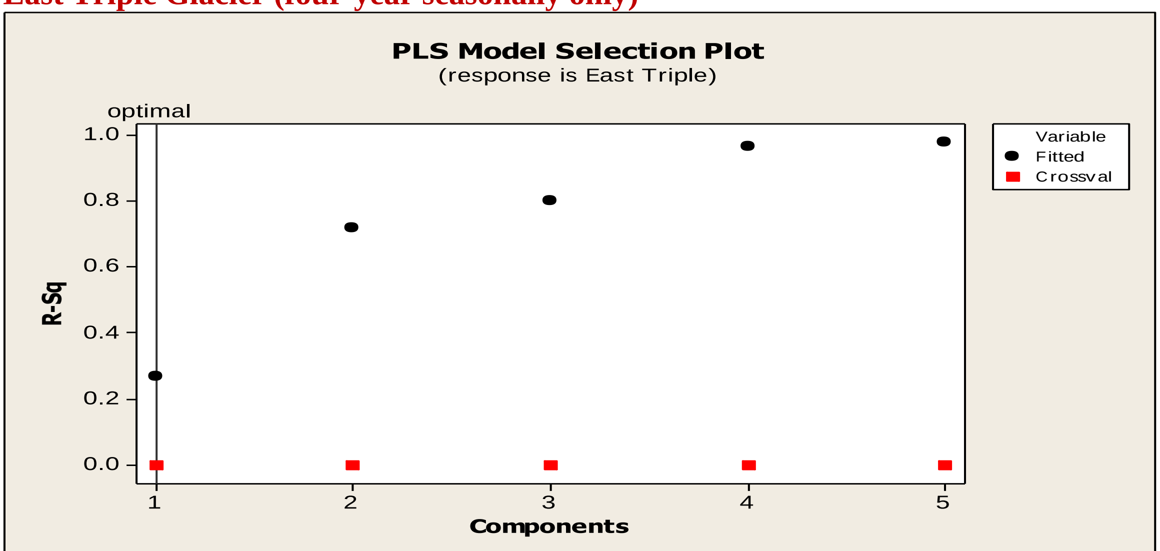

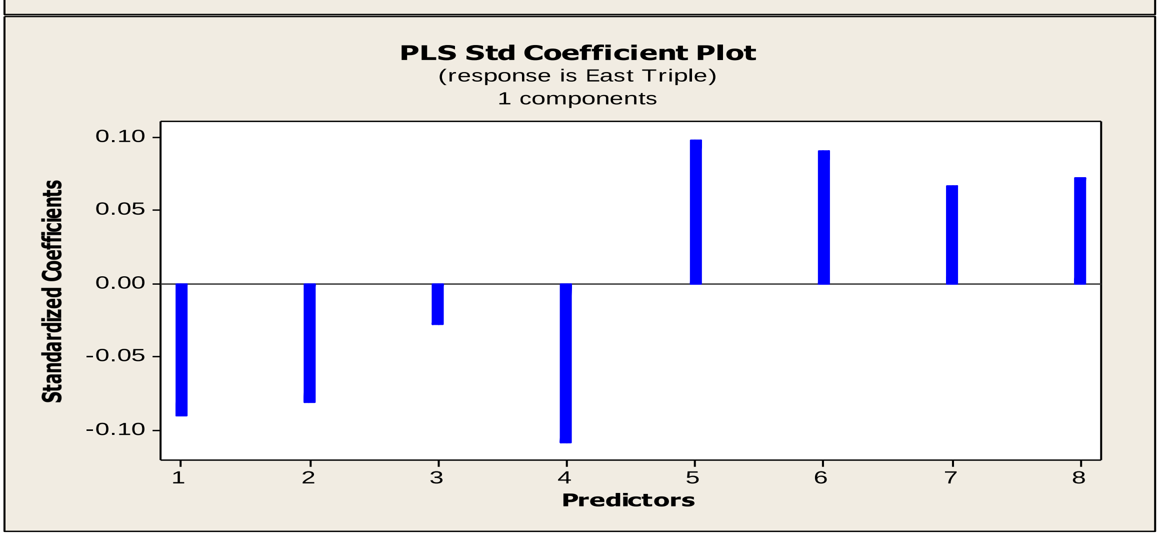

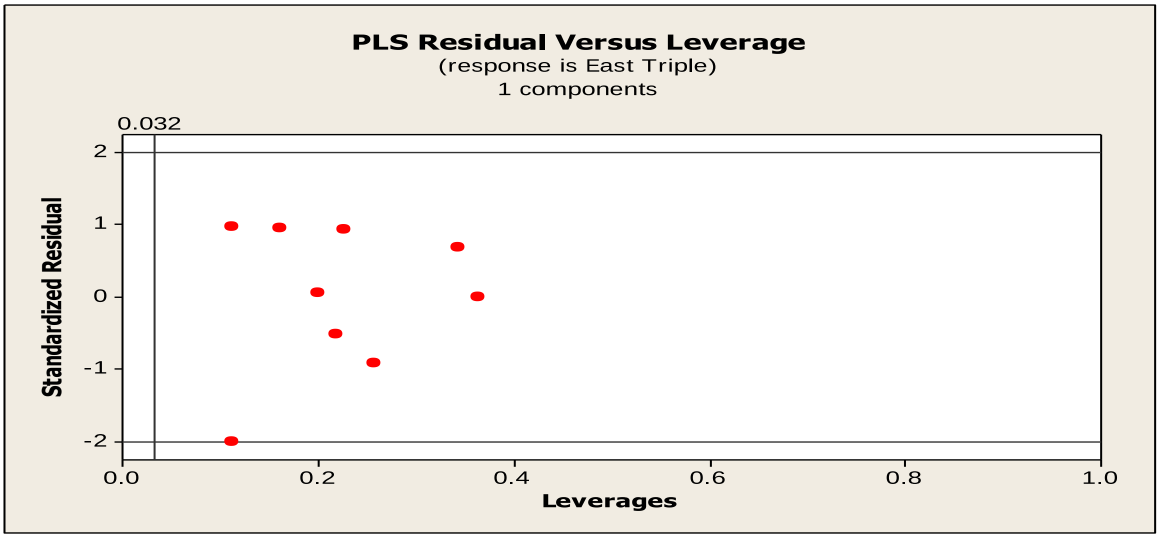

There is one outlier (1994) on the residual versus leverage plot.

PLS Regression: East Triple versus MMSpT, MMSuT, MMFaT, MMWiT, MMSpP, ...

Method

Cross-validation	Leave-one-out
Components to evaluate	User specified
Number of components evaluated	5
Number of components selected	1

Analysis of Variance for East Triple

Source	DF	SS	MS	F	P
Regression	1	848321165	848321165	2.54	0.155
Residual Error	7	2339103340	334157620		
Total	8	3187424506			

Model Selection and Validation for East Triple

Components	X Variance	Error	R-Sq	PRESS	R-Sq (pred)
1	0.675628	2339103340	0.266146	4.09193E+09	0
2		907155493	0.715395	8.78284E+09	0
3		631471188	0.801887	9.09871E+09	0
4		107038000	0.966419	1.04065E+10	0
5		78679594	0.975316	1.04086E+10	0

Coefficients

	East Triple	East Triple standardized
Constant	67192.5	0.000000
MMSpT	-1582.9	-0.090696
MMSuT	-1427.8	-0.081166
MMFaT	-363.5	-0.027836
MMWiT	-1069.0	-0.108438
MMSpP	15662.8	0.098112
MMSuP	17328.2	0.091077
MMFaP	12242.0	0.067146
MMWiP	13664.9	0.072721

Middle Triple Glacier (four-year seasonally only)

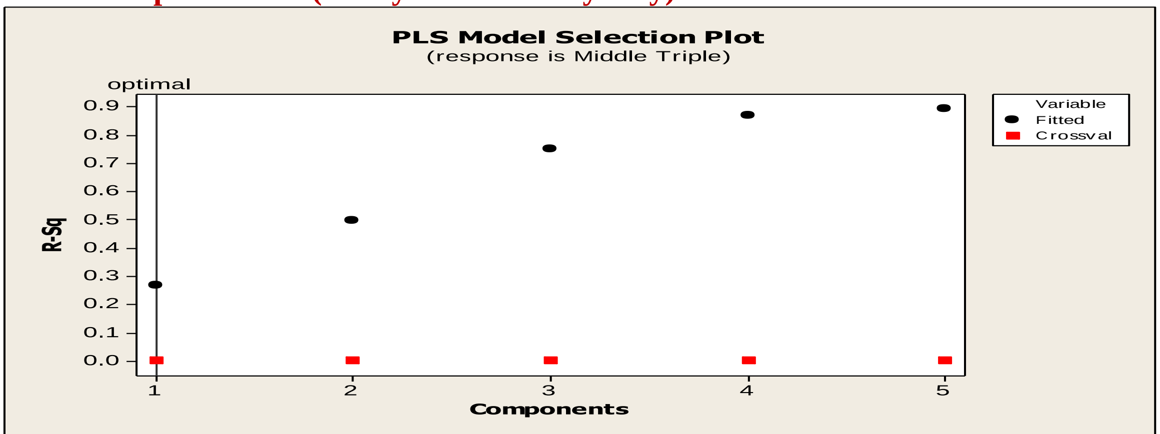

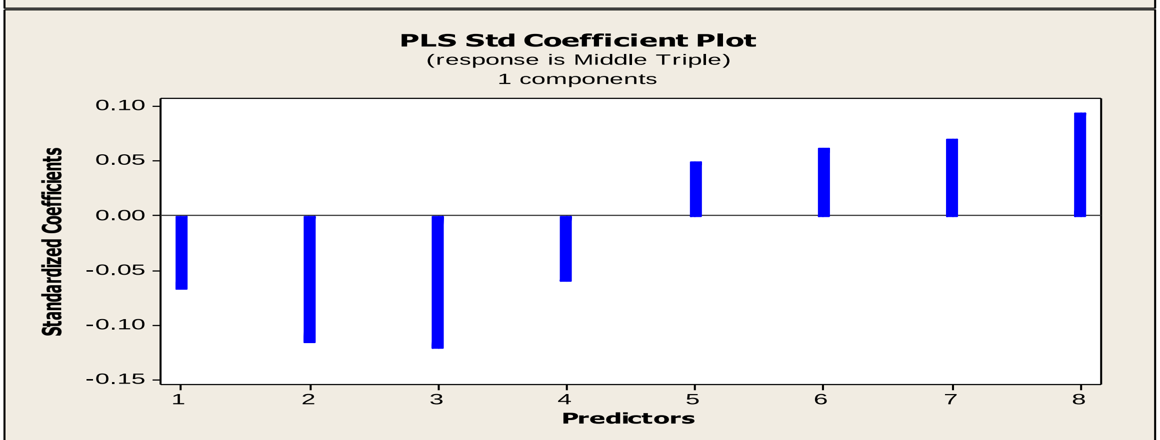

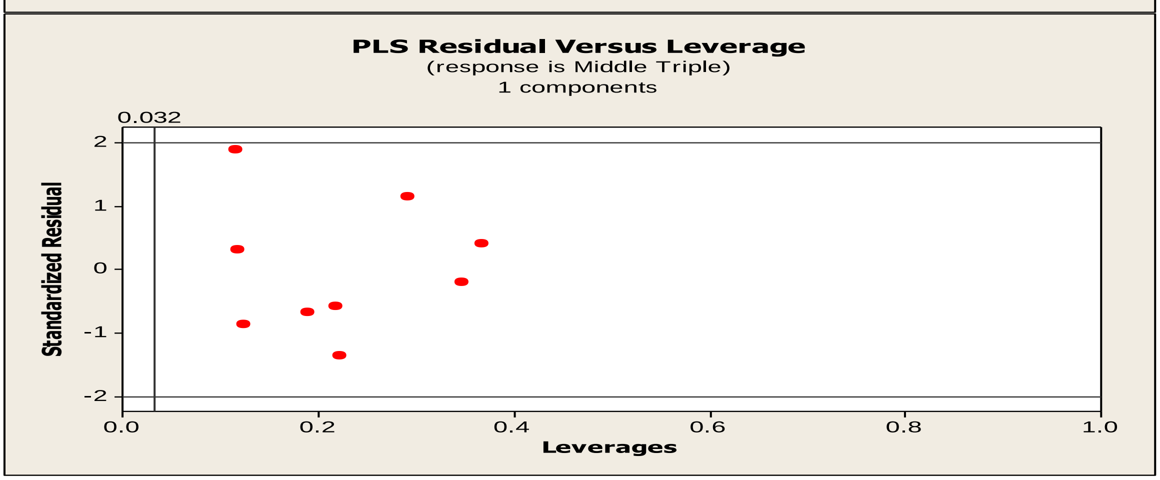

PLS Regression: Middle Triple versus MMSpT, MMSuT, MMFaT, MMWiT, MMSpP, ...

Method

Cross-validation	Leave-one-out
Components to evaluate	User specified
Number of components evaluated	5
Number of components selected	1

Analysis of Variance for Middle Triple

Source	DF	SS	MS	F	P
Regression	1	256967592	256967592	2.54	0.155
Residual Error	7	707879006	101125572		

Total	8	964846598			

Model Selection and Validation for Middle Triple

Components	X Variance	Error	R-Sq	PRESS	R-Sq (pred)
1	0.668021	707879006	0.266330	1225820955	0
2		483927714	0.498441	1882985963	0
3		242473110	0.748693	2156292602	0
4		124539904	0.870923	2069603987	0
5		105037092	0.891136	3397499799	0

Coefficients

	Middle Triple	Middle Triple standardized
Constant	183914	0.000000
MMSpT	-646	-0.067307
MMSuT	-1121	-0.115783
MMFaT	-867	-0.120691
MMWiT	-325	-0.059981
MMSpP	4373	0.049790
MMSuP	6517	0.062260
MMFaP	7069	0.070469
MMWiP	9703	0.093853

West Triple Glacier (four-year seasonally only)

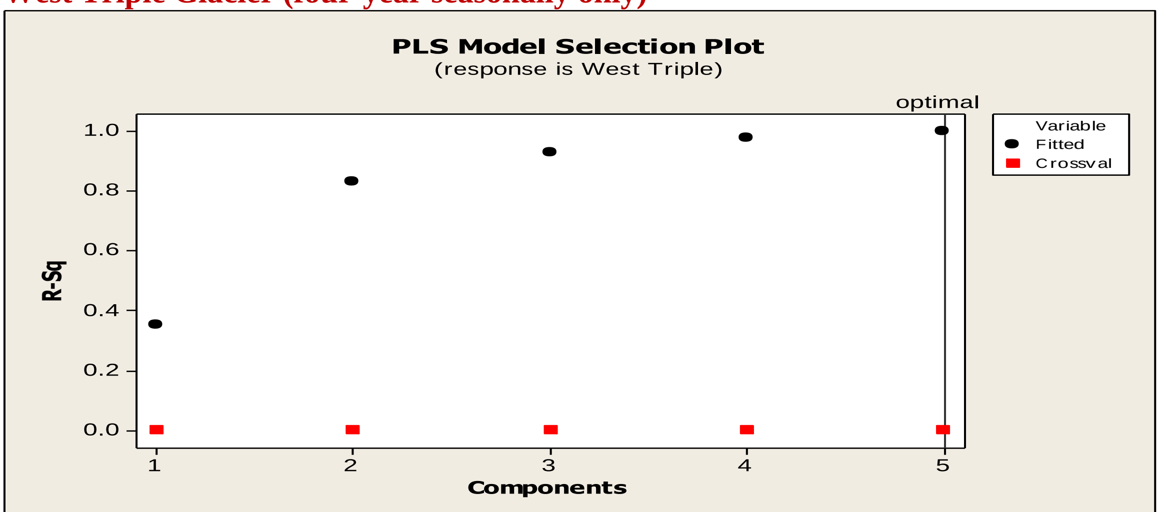

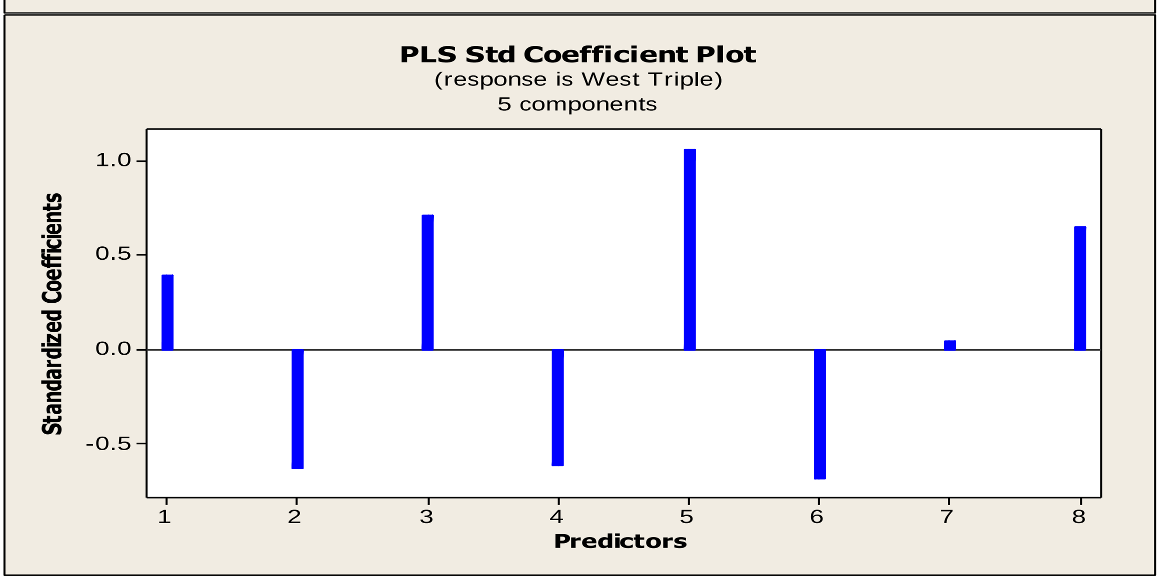

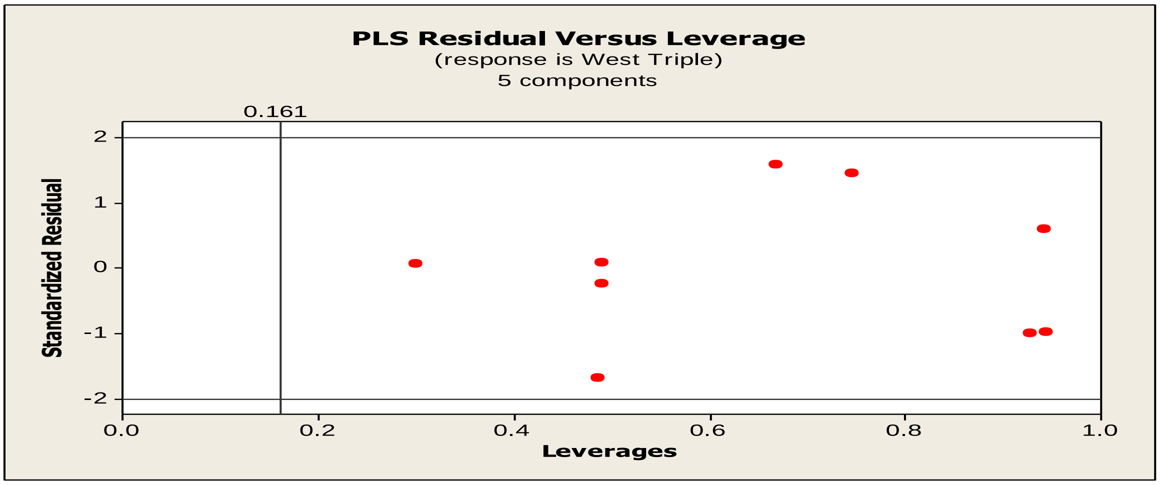

PLS Regression: West Triple versus MMSpT, MMSuT, MMFaT, MMWiT, MMSpP, ...

Method

Cross-validation	Leave-one-out
Components to evaluate	User specified
Number of components evaluated	5
Number of components selected	5

Analysis of Variance for West Triple

Source	DF	SS	MS	F	P
Regression	5	1.48602E+10	2972047018	173.01	0.001
Residual Error	3	5.15367E+07	17178898		
Total	8	1.49118E+10			

Model Selection and Validation for West Triple

Components	X Variance	Error	R-Sq	PRESS	R-Sq (pred)
1	0.674838	9650527670	0.352825	1.61576E+10	0
2	0.748852	2508689696	0.831764	2.57697E+10	0
3	0.887483	1092348106	0.926746	1.74975E+10	0
4	0.938307	379856685	0.974526	1.69741E+10	0
5	0.963002	51536694	0.996544	1.53016E+10	0

Coefficients

	West Triple	West Triple standardized
Constant	73578	0.00000
MMSpT	14781	0.39155
MMSuT	-23924	-0.62878
MMFaT	20141	0.71309
MMWiT	-13210	-0.61952
MMSpP	366126	1.06033
MMSuP	-280812	-0.68238
MMFaP	18023	0.04570
MMWiP	265184	0.65246

Schoolroom Glacier (four-year annually only)

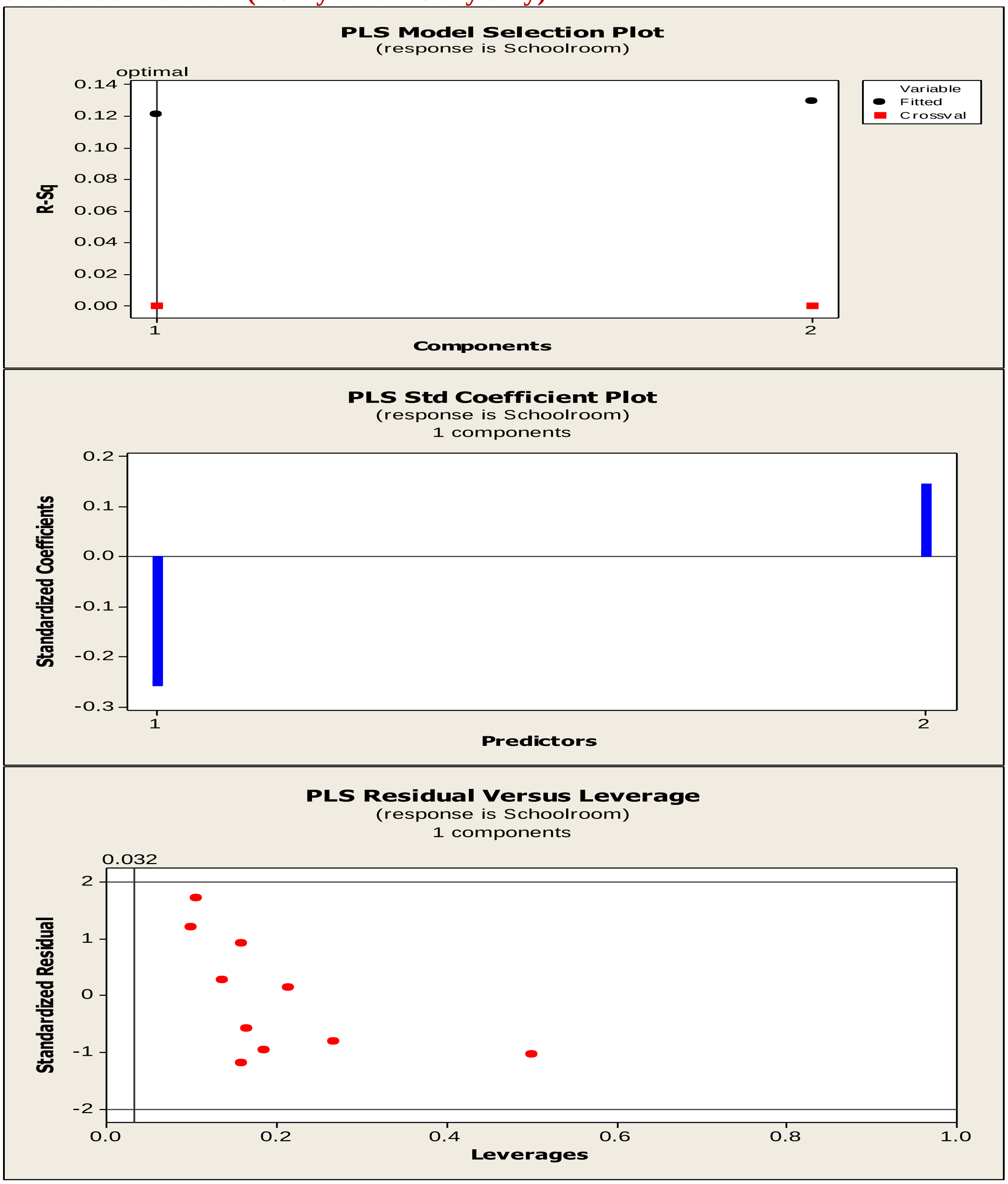

PLS Regression: Schoolroom versus SchAnT, SchAnP

```
Method
Cross-validation                  Leave-one-out
Components to evaluate            Adjusted
Number of components evaluated    2
Number of components selected     1

Analysis of Variance for Schoolroom
Source          DF          SS         MS     F       P
Regression       1    77383606   77383606  1.10   0.324
```

```
Residual Error    8  561420719  70177590
Total             9  638804325
Model Selection and Validation for Schoolroom
Components  X Variance      Error      R-Sq       PRESS  R-Sq (pred)
         1    0.712653  561420719  0.121138  1005916270            0
         2              556167166  0.129362  1212801927            0

Coefficients
                         Schoolroom
           Schoolroom  standardized
Constant      19720.7      0.000000
SchAnT        -5483.1     -0.257346
SchAnP         4839.2      0.145451
```

Falling Ice Glacier (four-year annually only)

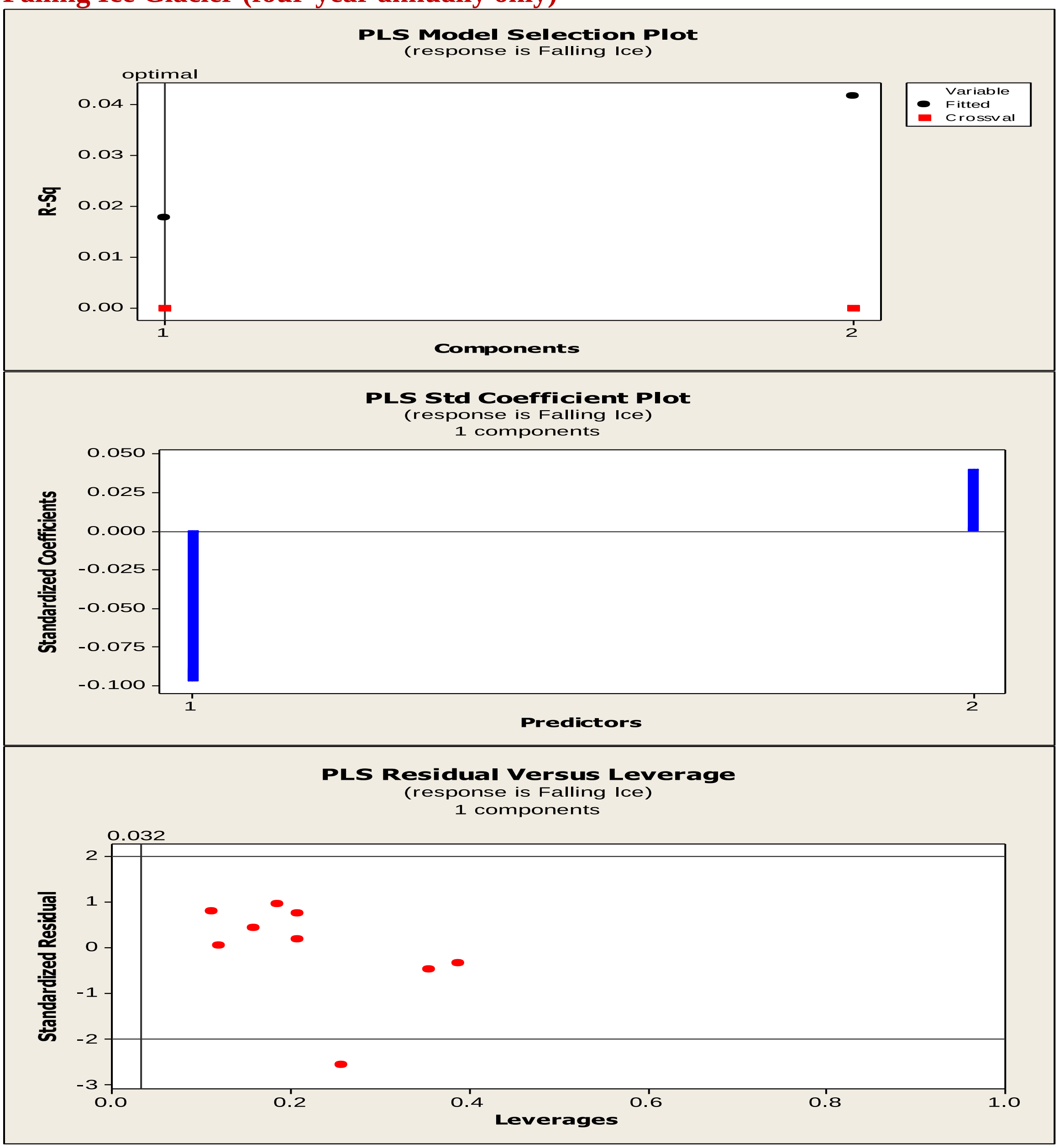

There is one outlier (1974) on the residual versus leverage plot.

PLS Regression: Falling Ice versus MMAnT, MMAnP

```
Method
Cross-validation                Leave-one-out
Components to evaluate          User specified
Number of components evaluated  2
Number of components selected   1

Analysis of Variance for Falling Ice
Source          DF         SS        MS     F      P
Regression       1    7853413   7853413  0.13  0.733
Residual Error   7  437719258  62531323
Total            8  445572671

Model Selection and Validation for Falling Ice
Components  X Variance      Error       R-Sq       PRESS  R-Sq (pred)
         1    0.915572  437719258  0.0176254   965835045            0
         2              426974221  0.0417406  1149908465            0

Coefficients
          Falling   Falling Ice
              Ice  standardized
Constant   129114     0.0000000
MMAnT        -530    -0.0970943
MMAnP         920     0.0398469
```

Skillet Glacier (four-year annually only)

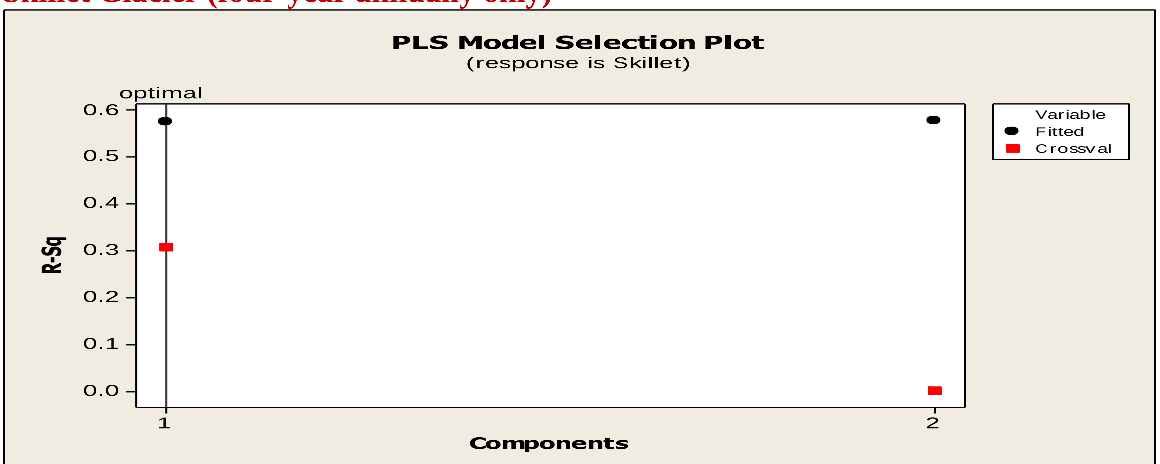

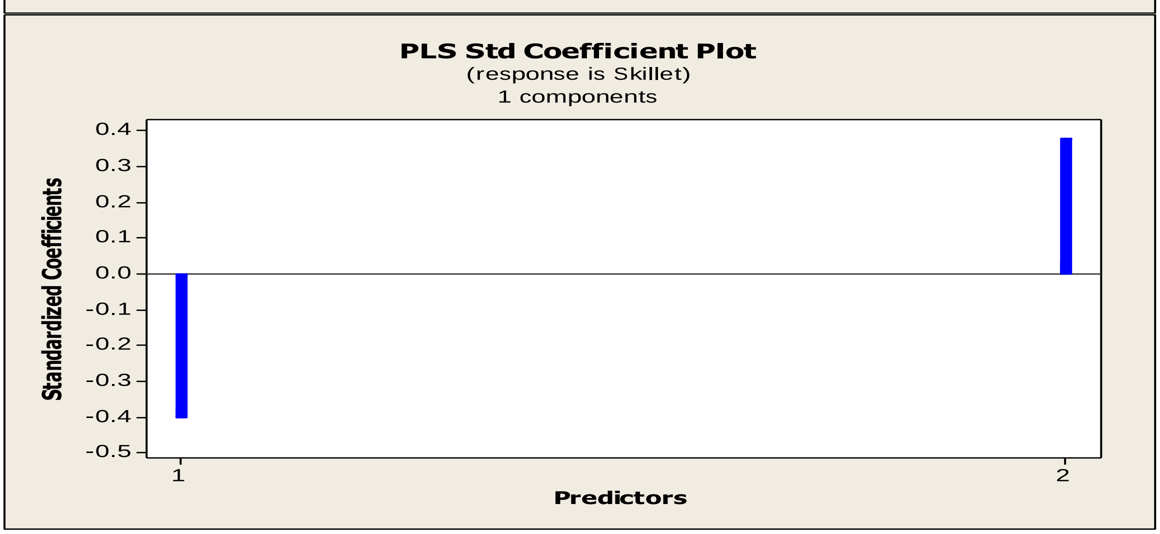

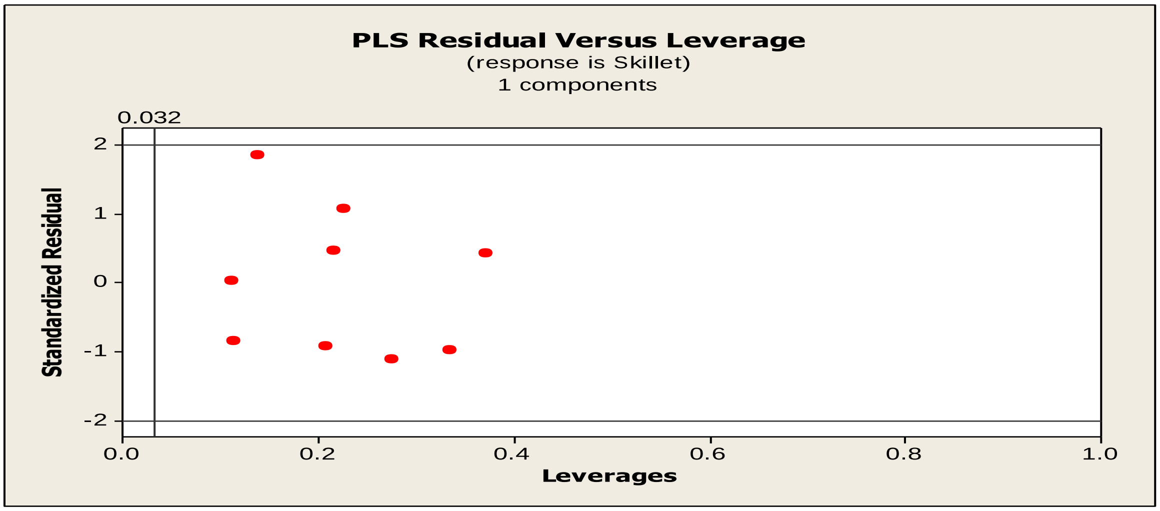

PLS Regression: Skillet versus MMAnT, MMAnP

Method

Cross-validation	Leave-one-out
Components to evaluate	User specified
Number of components evaluated	2
Number of components selected	1

Analysis of Variance for Skillet

Source	DF	SS	MS	F	P
Regression	1	713089452	713089452	9.45	0.018
Residual Error	7	528490957	75498708		
Total	8	1241580409			

Model Selection and Validation for Skillet

Components	X Variance	Error	R-Sq	PRESS	R-Sq (pred)
1	0.927095	528490957	0.574340	859397393	0.307820
2		522731010	0.578979	1563690334	0.000000

Coefficients

	Skillet	Skillet standardized
Constant	96929.3	0.000000
MMAnT	-3684.6	-0.404289
MMAnP	14749.8	0.382753

East Triple Glacier (four-year annually only)

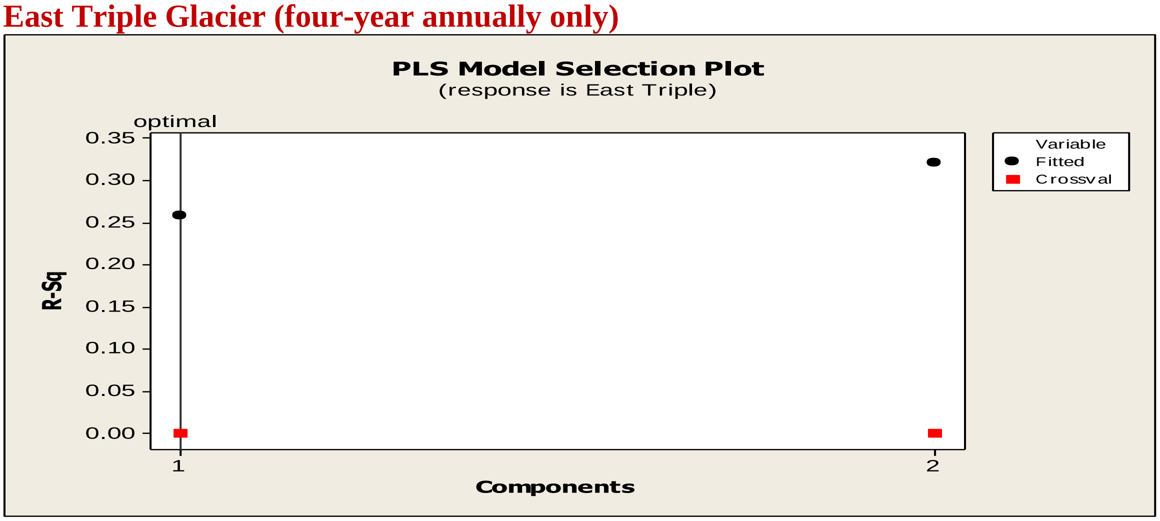

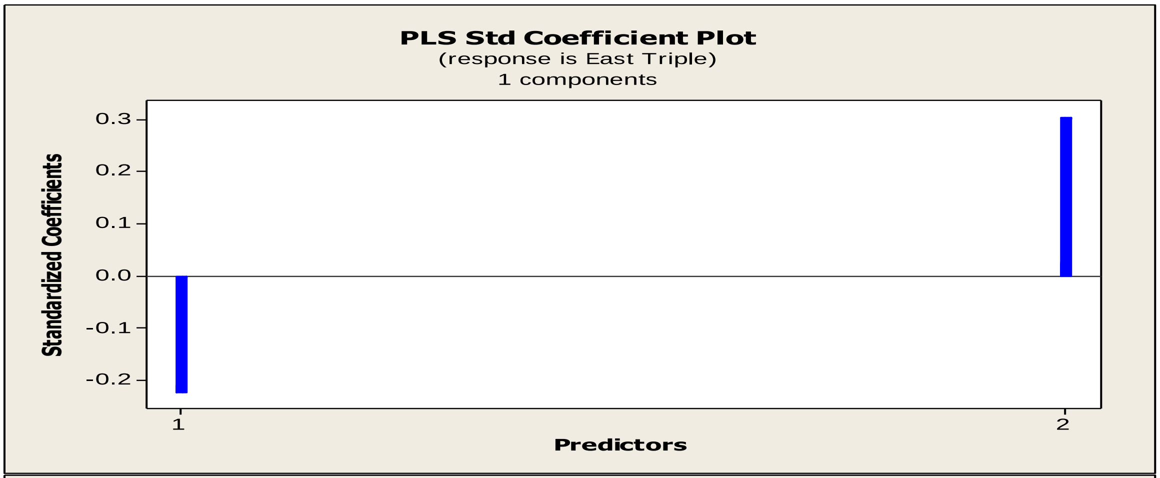

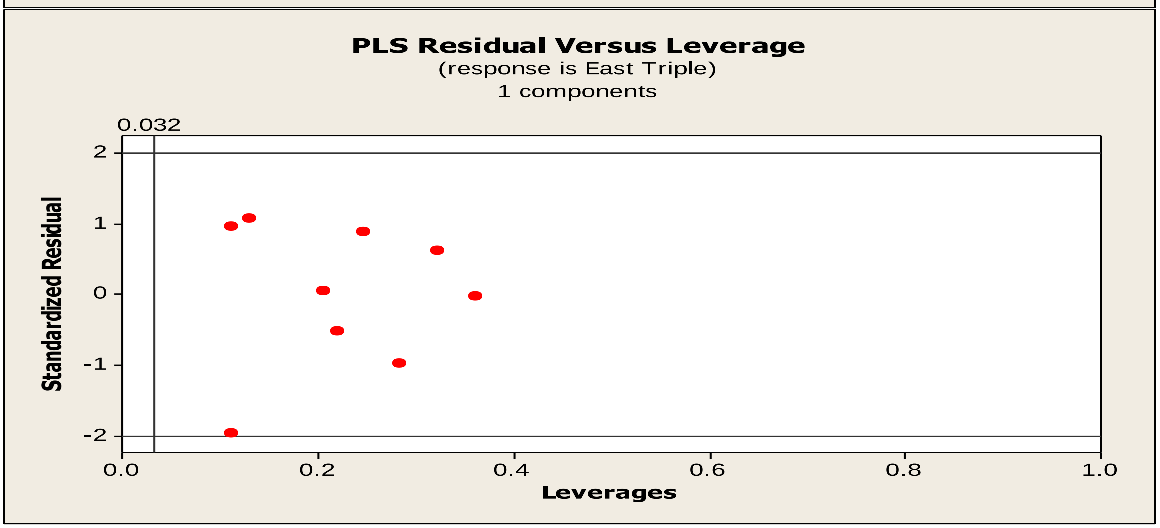

There is almost one outlier (1994) on the residual versus leverage plot.

PLS Regression: East Triple versus MMAnT, MMAnP

```
Method
Cross-validation                Leave-one-out
Components to evaluate          User specified
Number of components evaluated  2
Number of components selected   1

Analysis of Variance for East Triple
Source          DF          SS         MS     F      P
Regression       1   822258525  822258525  2.43  0.163
Residual Error   7  2365165980  337880854
Total            8  3187424506

Model Selection and Validation for East Triple
Components  X Variance       Error      R-Sq       PRESS  R-Sq (pred)
         1    0.925565  2365165980  0.257970  3494375411            0
         2              2165237519  0.320694  5091866928            0

Coefficients
                        East Triple
          East Triple  standardized
Constant      51217.3      0.000000
MMAnT         -3256.9     -0.223038
MMAnP         18767.8      0.303959
```

Middle Triple Glacier (four-year annually only)

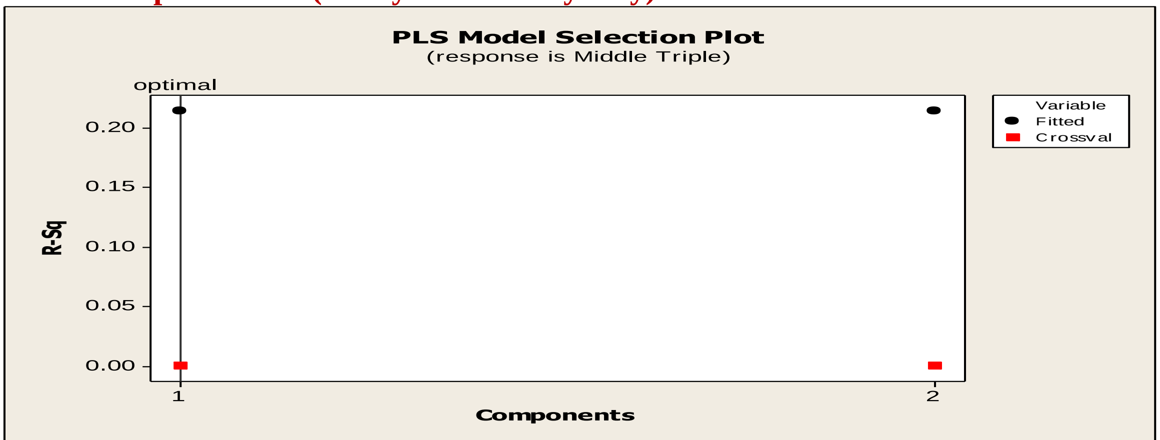

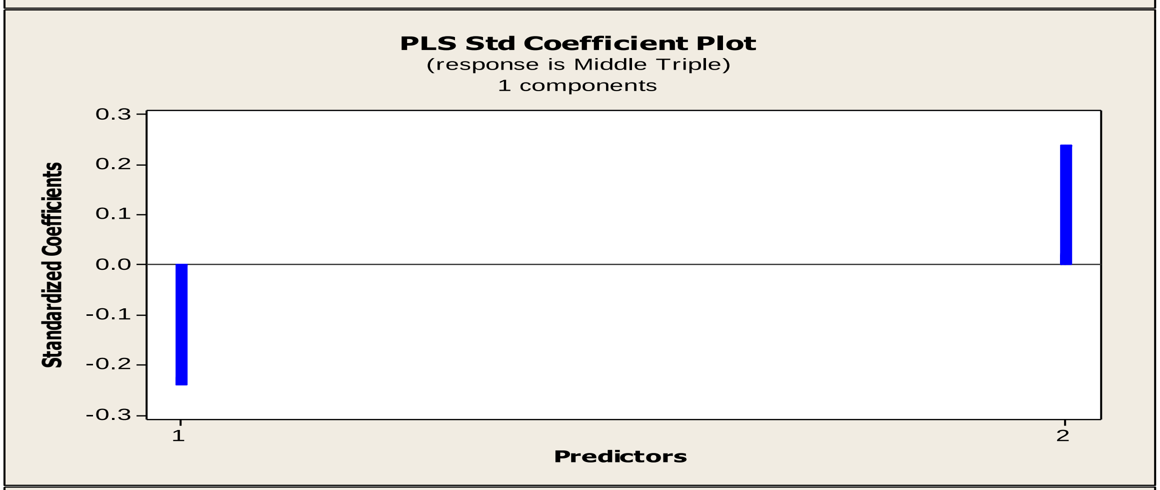

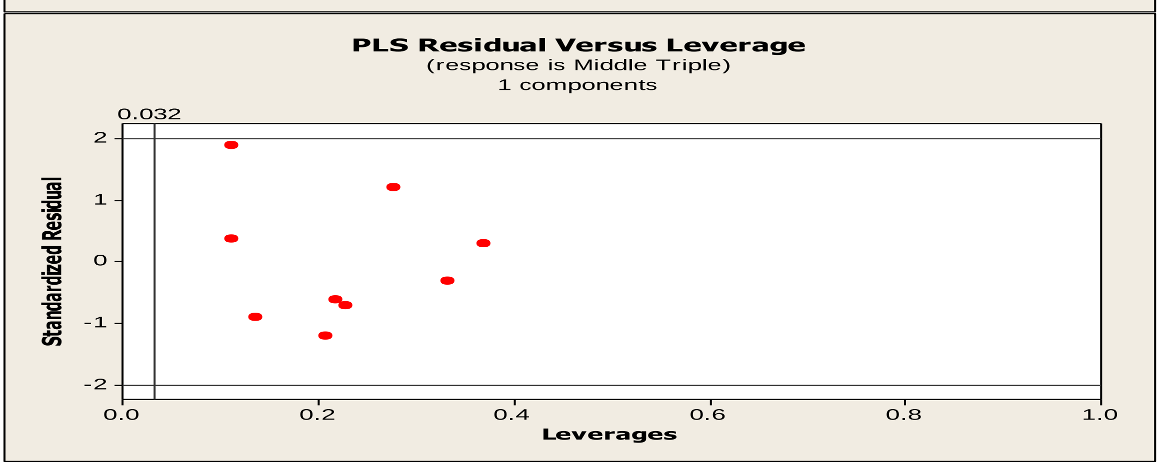

PLS Regression: Middle Triple versus MMAnT, MMAnP

Method

Cross-validation	Leave-one-out
Components to evaluate	User specified
Number of components evaluated	2
Number of components selected	1

Analysis of Variance for Middle Triple

Source	DF	SS	MS	F	P
Regression	1	206784470	206784470	1.91	0.210
Residual Error	7	758062128	108294590		

```
Total              8  964846598
Model Selection and Validation for Middle Triple
Components  X Variance      Error      R-Sq       PRESS  R-Sq (pred)
         1    0.927145  758062128  0.214318  1147685082            0
         2              758061392  0.214319  1457536742            0

Coefficients
          Middle  Middle Triple
          Triple   standardized
Constant  177295       0.000000
MMAnT      -1930      -0.240257
MMAnP       8171       0.240533
```

West Triple Glacier (four-year annually only)

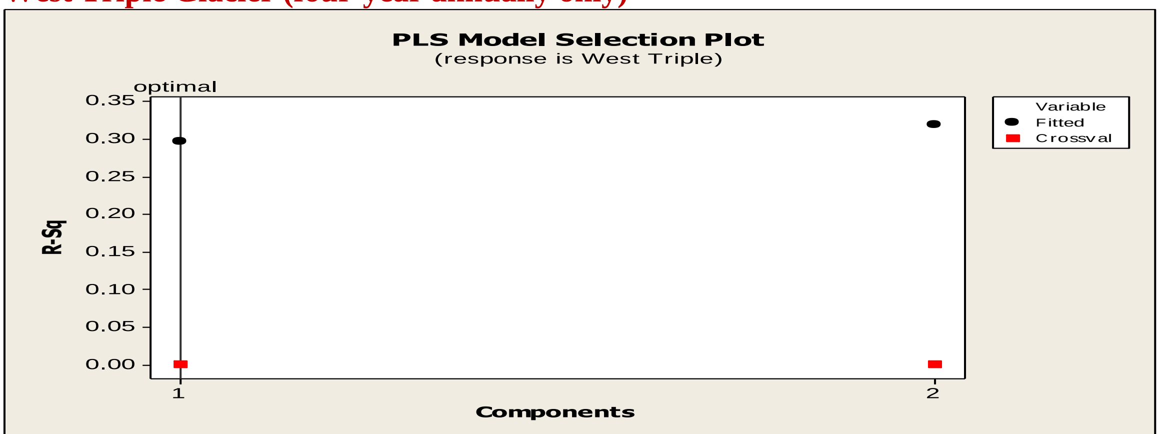

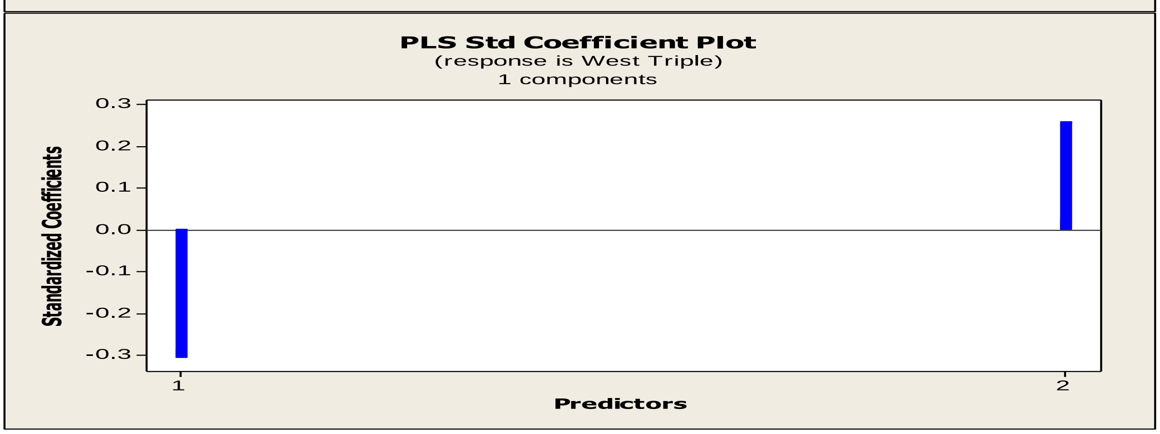

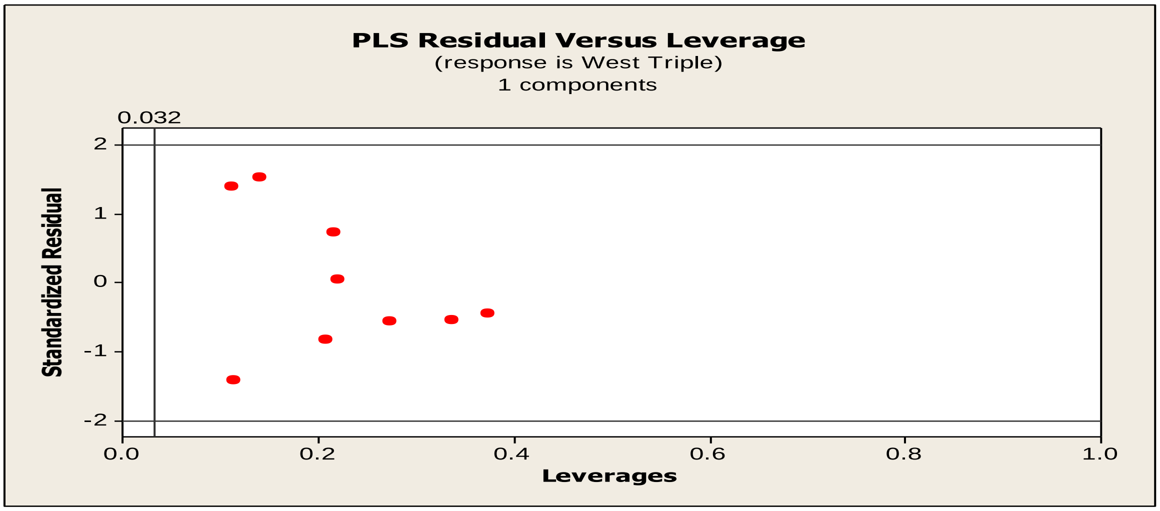

PLS Regression: West Triple versus MMAnT, MMAnP

Method

Cross-validation	Leave-one-out
Components to evaluate	User specified
Number of components evaluated	2
Number of components selected	1

Analysis of Variance for West Triple

Source	DF	SS	MS	F	P
Regression	1	4.41976E+09	4419755729	2.95	0.130
Residual Error	7	1.04920E+10	1498859436		
Total	8	1.49118E+10			

Model Selection and Validation for West Triple

Components	X Variance	Error	R-Sq	PRESS	R-Sq (pred)
1	0.926675	1.04920E+10	0.296394	1.51421E+10	0
2		1.01617E+10	0.318542	2.19844E+10	0

Coefficients

	West Triple	West Triple standardized
Constant	81909.9	0.000000
MMAnT	-9674.2	-0.306294
MMAnP	34583.5	0.258956

Appendix E: Seasonal meteorologic differences from mean (1956-2010)

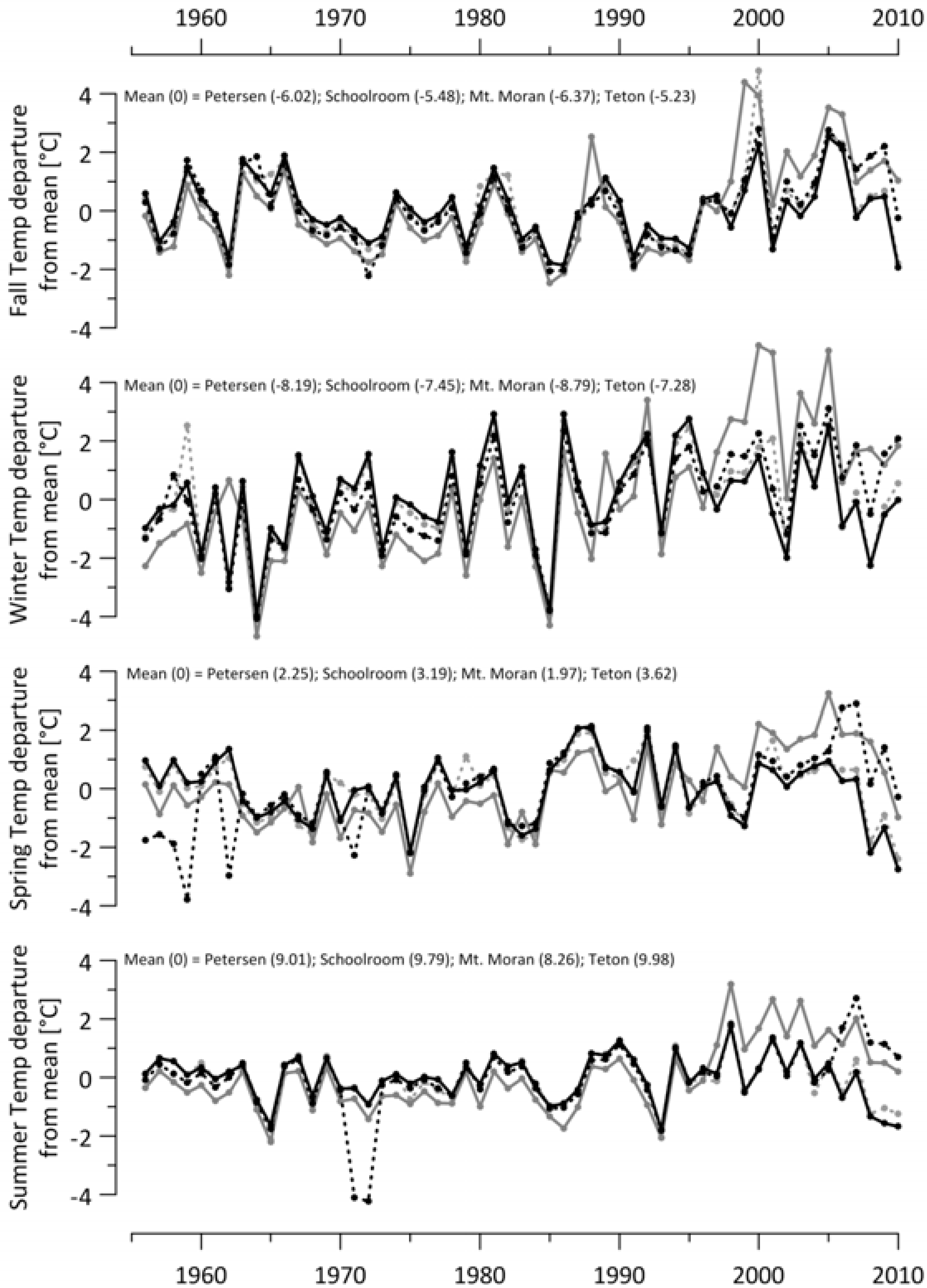

Appendix E: Figure 1. Seasonal temperature differences from mean (1956-2010) PRISM output at the Petersen (dotted black line), Schoolroom (black line), Mt. Moran (grey line), and Teton (dotted gray line) PRISM pixels.

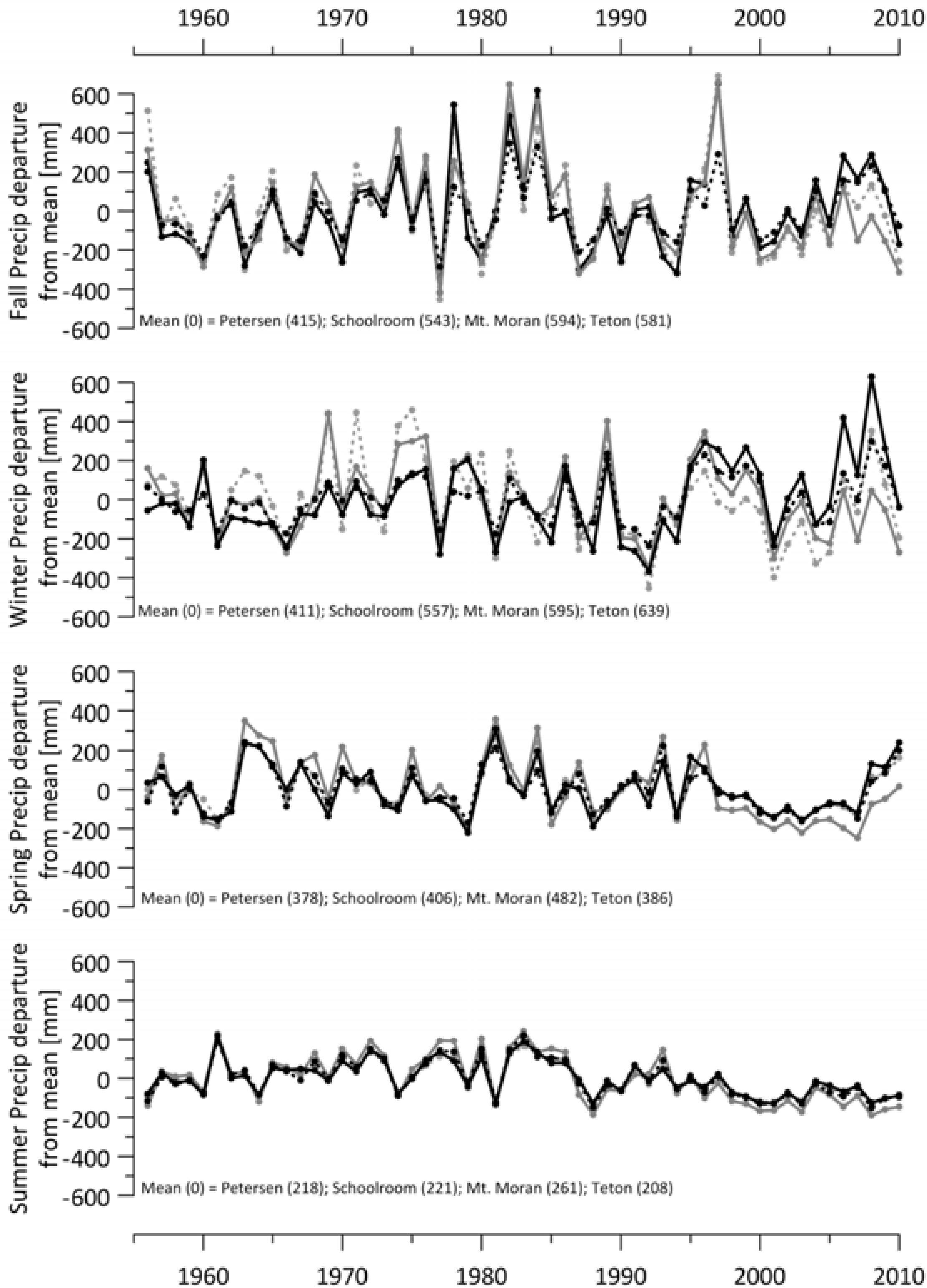

Appendix E: Figure 2. Seasonal precipitation differences from mean (1956-2010) PRISM output at the Petersen (dotted black line), Schoolroom (black line), Mt. Moran (grey line), and Teton (dotted gray line) PRISM pixels.